UNIVERSITY OF NOTTINGHAM

DEPARTMENT OF CIVIL ENGINEERING

THE GEOMETRICAL NON-LINEAR RESPONSE OF SOME PRE-TENSIONED CABLE STRUCTURES

by

ROBERT THEW, B.Sc.

Thesis submitted to the University of Nottingham for the degree of Doctor of Philosophy.

October 1982

ACKNOWLEDGEMENTS

I should like to thank Professor R. C. Coates for making available the facilities within the Civil Engineering Department which have enabled this research to be carried out and the technicians and members of staff for their help and advice.

Thanks are also due to the Science Research Council for providing a research studentship and Miss Joanna Guest for typing this thesis.

Above all I should like to thank Professor R. C. Coates and Mr. C. Snell, my two supervisors, for their guidance and support throughout this project and my wife Dianne for her patience and constant encouragement.

TABLE OF CONTENTS

ABSTRACT

A geometrical non-linear analysis of pre-tensioned cable structures is presented. Fully consistent methods of analysis are developed from earlier work involving minimum energy search techniques. The descent direction in the iterative process is determined by the method of conjugate gradients. The algorithm is suitable for both cable trusses and cable net structures and can include the effect of fully flexible boundaries. Convergence is obtained for all of the structural forms investigated for loadings up to the point where significant instability in the structure caused by member slackening occurs. An initial linear approximate analysis is shown to be of computational value as an initial starting point for the iterative process.

Economic form finding routines are also presented including the flexible boundary case which are of general value.

Two and three dimensional cable model experiments are devised to provide data for comparison with the theoretical analysis. The three dimensional net is constructed with fully flexible boundaries to provide a stringent test for the theory. Suitable measurement techniques are developed to record cable tensions and nodal deflections. Reservations of other writers about the vibrating wire method of tension measurement are overcome by a rigorous treatment of the theoretical analysis and a careful development of a demountable vibrating wire gauge.

Comparison between experimental and theoretical results gives generally good agreement particularly for the non-symmetrical load cases which exhibit the greatest degree of non-linear behaviour.

NOMENCLATURE

Unless explicitly stated otherwise the following notation has been used throughout this work.

A	Cross sectional area
e	extension
E	Young's Modulus of elasticity
f	frequency of vibration
$\underset{\sim}{F}_{ij}$	component tensile forces of member ij acting at joint i
$\underset{\sim}{g}$	gradient vector
G	shear modulus
h	scaling constants
H_x, H_y	horizontal components of tension
I	second moment of area
J	polar second moment of area
k	member stiffness matrix
K	structure stiffness matrix
L_o	unstressed member length
L	pretensioned member length
$L + \Delta L$	member length after loading
M	bending moment
m	mass per unit length
n	number of members at a joint
N	number of degrees of freedom
$\underset{\sim}{P}_i$	load vector at joint i
$\underset{\sim}{r}_i = (x,y,z)^T_i$	position vector of joint i

$\underset{\sim}{R}$ residual out of balance force

S steplength along descent direction

t temperature

$T, T+\Delta T$ member tensions

$\underset{\sim}{u}_i = (u,v,w)^T_i$ displacement vector at joint i

U total elastic potential energy

V total potential energy of applied loads

$\underset{\sim}{y}_i$ descent vector at joint i

W total potential energy of structure

X,Y,Z global coordinate directions

α coefficient of thermal expansion

ρ density

μ strain function

$\underset{\sim}{u}$ column matrix of all component displacements

u_i element of $\underset{\sim}{u}$

$\underset{\sim}{v}$ column matix of all component descent directions

v_i element of $\underset{\sim}{v}$

$\delta\underset{\sim}{r}$ change in $\underset{\sim}{r}$ along a member

$\delta\underset{\sim}{u}$ change in $\underset{\sim}{u}$ along a member

INTRODUCTION

The geometrical non-linear response of two and three dimensional pretensioned cable structures is investigated.

Chapter 1 briefly describes the development and use of tension structures in engineering and introduces the inherent problems of their analysis. The three basic elements of cable structures, i.e. single cables, cable trusses and cable nets are defined and structural examples of their use presented.

The geometrical non-linear problem has been recognised by many previous authors and three different algorithms for its solution are given. Iterative methods involving a minimum energy search technique were found to warrant further study and these are developed in Chapter 2.

In Chapter 2 a fully consistent set of equilibrium equations is presented and the minimum energy search technique is carefully developed to include all relevant terms. A number of search techniques are employed, the most successful being the scaled conjugate gradients method. Economic methods of form finding (or initialisation) are developed for the particular structural examples investigated later. The effect of flexible boundaries is included in the form finding algorithm.

The general method of calculation is illustrated by the analysis of a number of two and three dimensional pretensioned cable structures. As further verification of the algorithm, two pretensioned cable model experiments are developed together with the necessary measurement techniques which are detailed in Chapter 3.

The vibrating wire method of tension measurement is developed from earlier work and given a full analytical treatment. Previous deflection measurement techniques are discounted as either too costly or limited in scope (i.e. vertical deflections only) therefore a both economic and accurate photographic method is presented.

The detailed design and construction of a pretensioned cable truss and prestressed cable net experiment are described in Chapters 4 and 5 respectively. A comparison of the practical results with the predicted theoretical results is also included.

The implications of these results and the comparison with predicted theoretical analysis is discussed in Chapter 6 where topics for further research are also introduced.

CHAPTER 1

THE DEVELOPMENT OF CABLE STRUCTURES

1.0 Historical Review

The use of tension cables by man dates back into antiquity. The probable first uses were for providing shelter in the construction of tents and aiding transport in sailing craft and in rope bridges.

Unlike those building elements whose predominant stresses are in bending and compression major tension structures have not appeared until modern times. The first substantial suspension bridges appeared after the beginning of the 19th Century (1.1). The first suspended roofs appeared later, for example the pavillions constructed in 1896 at Nijny-Novgorod, Russia, are generally regarded as the first engineering surface structures in which roof membrane and structure form one unit.

With conventional structures dead loads predominate so that all wind loadings are subsidiary to the analysis. For all light weight structures, which can exhibit little damping to their natural frequency of vibration, a much more careful analysis of the wind uplift forces and possible dynamic effects must be carried out with reasonable accuracy.

With a number of notable exceptions such as the Rayleigh Arena in the early 1950's the general development of tension structures was not possible until the advent of widely available and relatively cheap electronic computers in the 1960's.

Roof structures were developed by Jowerth (1.2), for example the Ice Rink in Stockholm spanning 83 m, using pretensioned cable trusses

for the principal load bearing members.

Notable space net structures have included the Munich Olympic Stadium Roof in 1972 and the Tokyo Olympic Swimming Pool. A report by Tsuboi and Kawaguchi (1.3) details the design, construction, analysis and model testing of the Tokyo structure.

More recently a new form of composite structure has been developed , incorporating tension and rigid frame elements, known as 'masted structures' (1.4). These consist of tension assisted beams suspended on ties hung from masts. Such structures are not investigated in this thesis but they present no insurmountable difficulties in the analysis or design.

It is hoped that this work will encourage the use of cable structures in the future by adding to the understanding of their design and analysis and by encouraging and extending the availability of analytical methods.

1.1 Classification of Cable Structures

Complex examples of possible shape of suspension systems have been presented by Otto (1.5). However it is convenient to consider each structure as a combination of one or more of the following elements:

a) single cables

b) cable trusses (Fig. 1.1)

c) cable nets

Single cables are commonly found in structures and are of interest to engineers working in several fields, the design of suspension bridges, suspended roofs, transmission lines and ship mooring cables are but a few examples.

FIG 1.1

TYPES OF CABLE STRUCTURE

(i) SINGLE CABLES

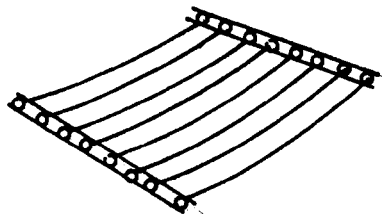

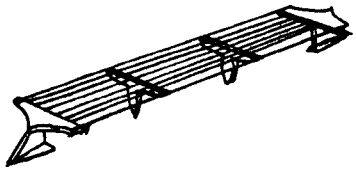

(ii) CABLE TRUSSES

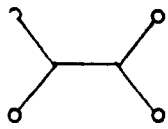

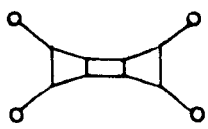

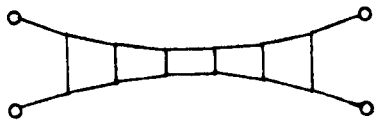

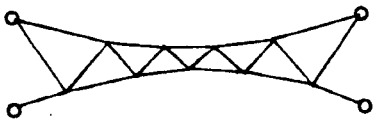

(iii) CABLE NETS

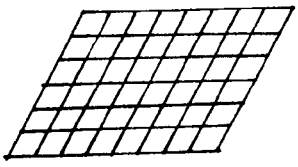

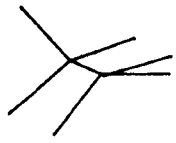

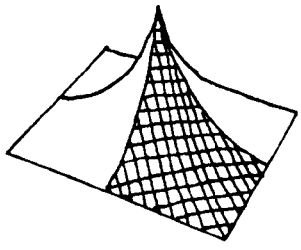

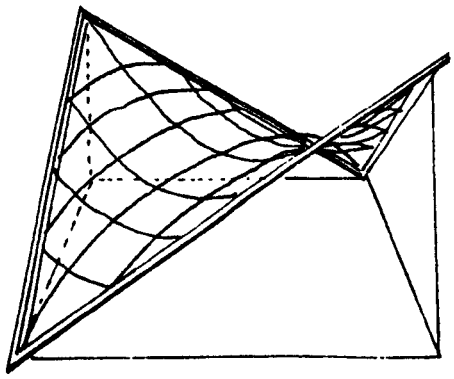

A single weightless cable has no tension and therefore no stiffness against deformation. It becomes stiff if prestressed against some more rigid constraint or by the action of dead loads, which would include the self weight.

The simplest single cable structure consists of a number of parallel cables supporting roof panels as at the Dulles International Airport Passenger Terminal (Fig. 1.2). In this example additional stiffness was obtained by making the concrete infill panels take compression. The concrete panels spanning approximately 3.05 m were placed between cables spanning between towers 61 m apart. A temporary uniform load was placed over the roof area increasing the cable tensions. In situ concrete was then placed between the concrete units and once it had reached the required strength the temporary load was removed to give a prestressed roof of composite construction.

Recent developments have been towards prestressing the cables by forces other than gravity. For acceptably small deflections under wind action structural stiffness is required. It has been recognised that this stiffness depends on increased cable tensioning and with the trend towards lighter weight structures forms other than the single cable have been explored.

In this way pretensioned cable girders and trusses are two-dimensional structural elements which have been used to form three-dimensional roof structures with acceptable properties.

It is with three-dimensional pretensioned net structures however where the greatest scope for large span light weight structures lies. Those net structures which rely on dead weight for pretensioning form single curvature or synclastic surfaces whilst those relying solely

FIG 1.2

SINGLY CURVED SINGLE LAYER CABLE SUSPENDED ROOF

eg DULLES AIRPORT TERMINAL

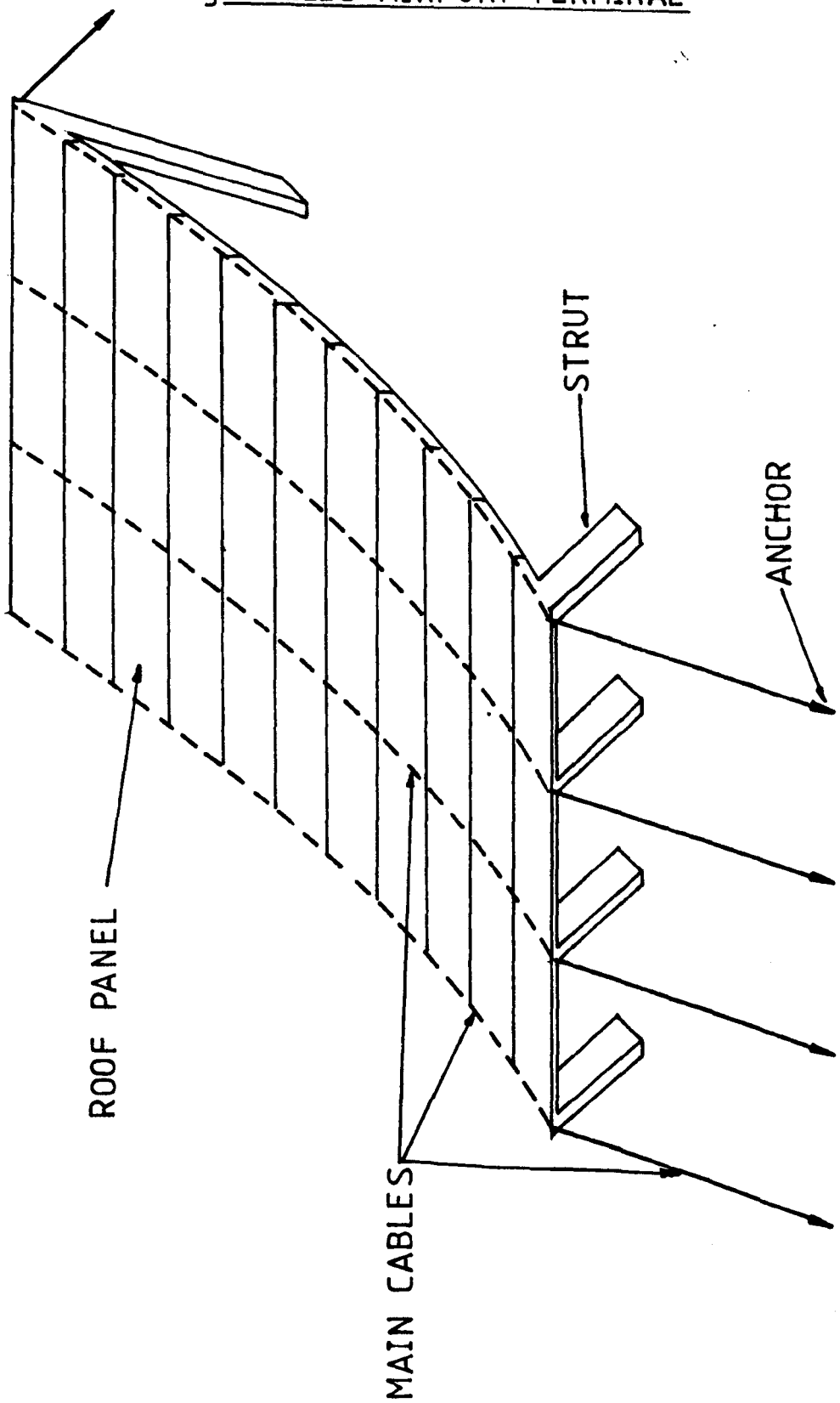

on cable forces for stiffness must form double curvature or anticlastic surfaces. (Fig. 1.3).

The form of the cable net structure is influenced by the type of boundary fixings which may be fixed anchorage points, boundary members acting in bending, boundary members acting in compression, or any combination of these as illustrated in Fig. 1.4.

1.2. Analysis of Cable Structures

Cable structures give rise to problems not normally encountered in more conventional structures. They rely upon pretensioning of their members for structural stiffness and can exhibit significant deflection when subject to load. This change in geometry can lead to a different structural stiffness and hence a geometrical non-linear response to load. The difference is illustrated by comparing the lateral loading of a simply supported beam and a single cable fixed between two supports (Fig. 1.5). For the beam there is the well known linear response relation between P and δ whereas for the single cable the relation is more complex

$$\delta = \frac{PL}{4AE}\left(\frac{L}{e} + 1\right) \qquad (1.1)$$

where e is the elastic extension of the member. The stiffness of the structure is now a function of the applied load P.

The method of analysis must therefore take this geometrical non-linearity into account and a classical linear theory of structural analysis cannot be used. Methods for the discrete analysis of cable structures have only become available since the advent of electronic computers, due to the large number of calculations involved for even a modest structure.

FIG 1.3

THREE DIMENSIONAL CABLE NET SURFACES

(i)SYNCLASTIC

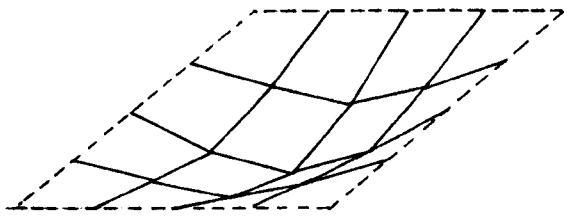

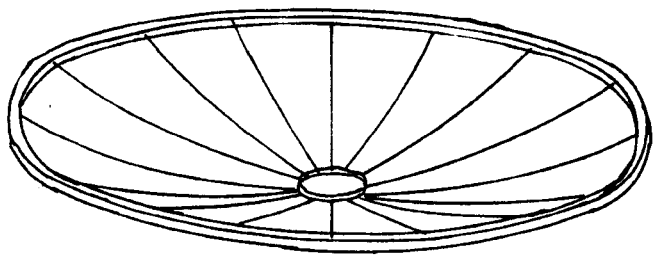

(ii)ANTICLASTIC

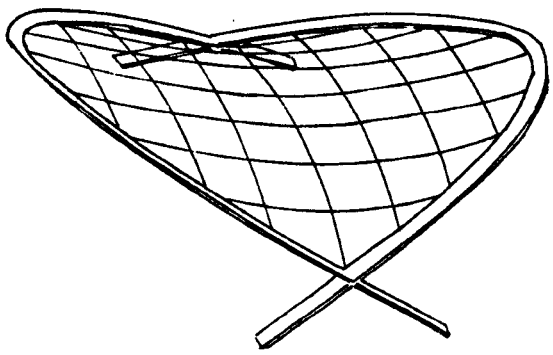

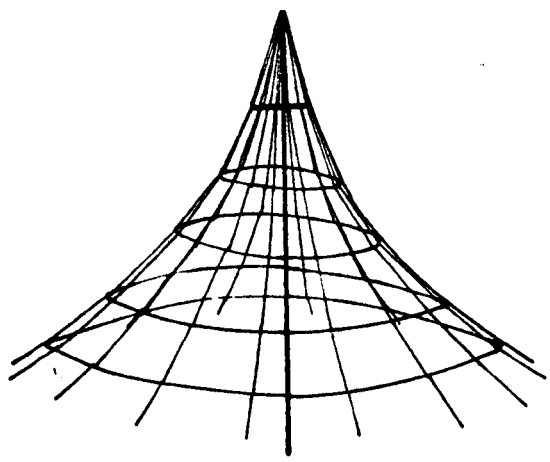

FIG 1.4

TYPES OF CABLE NET BOUNDARY

i) FIXED ANCHORAGE POINTS

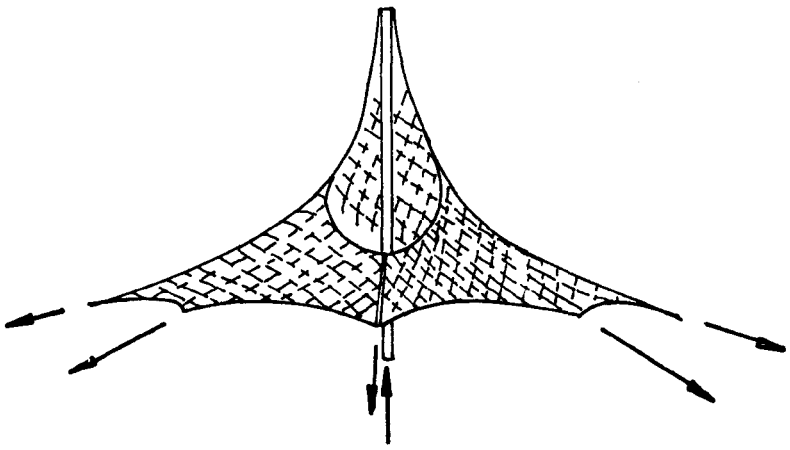

ii) BOUNDARY MEMBERS IN BENDING

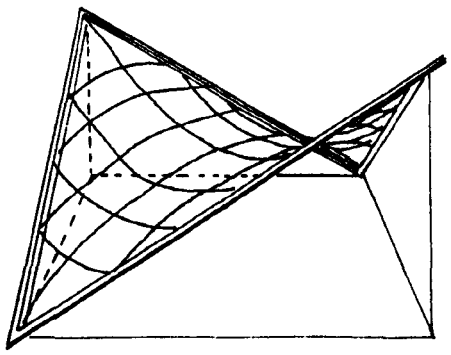

iii) BOUNDARY MEMBERS IN COMPRESSION

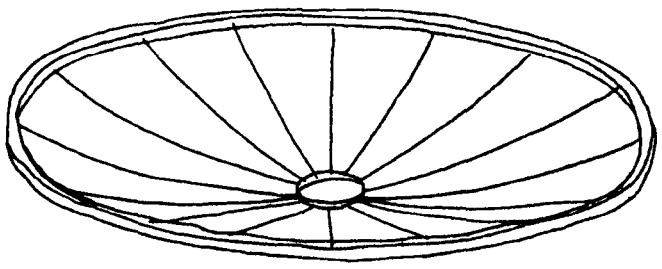

FIG 1.5

COMPARISON BETWEEN LATERAL LOADING TO A BEAM AND A CABLE

i) BEAM

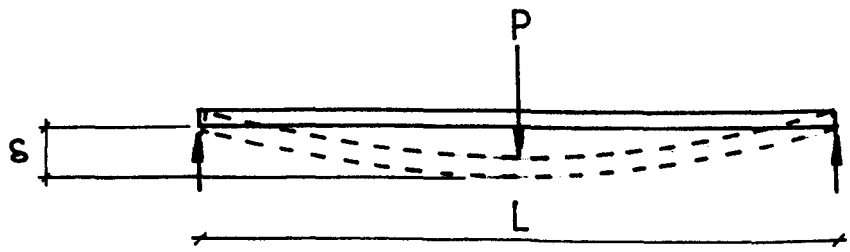

$$\delta = \frac{PL^3}{48EI}$$

ii) CABLE

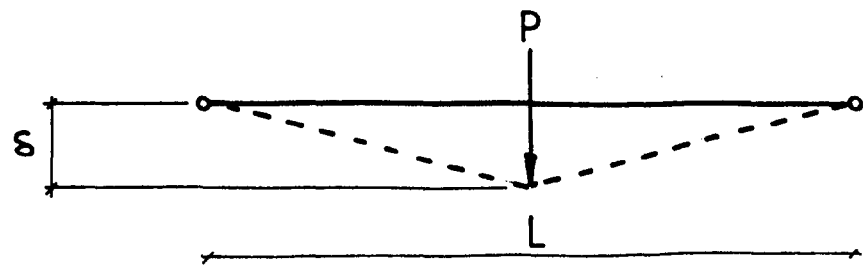

$$\delta = \frac{PL}{4AE}\left(\frac{L}{e}+1\right)$$

e is the elastic extension of the cable

Before about 1960 analysis therefore concentrated upon replacing the actual cable system by an equivalent continuous system. This is an inherently inaccurate method of analysis due to the necessary approximations involved. This thesis therefore confines itself to a reveiw of the discrete methods of analysis available.

(i) Displacement and stiffness methods

An early attempt at a general discrete analysis of prestressed nets was presented by Siev (1.6). Assuming a linear displacement response a set of equations of the form

$$\underset{\sim}{P} = (K + G)\,\underset{\sim}{u} \qquad (1.2)$$

were developed, $\underset{\sim}{P}$ is the vector of applied loads and $\underset{\sim}{u}$ the vector of nodal displacements. K is the classical stiffness matrix and G the geometrical stiffness matrix caused by the initial prestress force. Using the above equation an initial estimate of the displacement vector $\underset{\sim}{u}$ can be determined. Residual forces at each node are calculated and treated as an out of balance force in the next stage of the iterative process. For small degrees of non-linearity the stiffness matrix is assumed constant throughout the iteration process. This is known as the simplified Newton-Raphson method. With those linear assumptions no attempt has been made to determine whether the algorithm still converges to the correct solution.

A second iterative method is proposed by Siev where after each cycle of iteration the stiffness matrices are updated using the latest displacement values. The theoretical development is presented without worked examples and there is no discussion of convergence criteria to determine when the iterative procedure should be terminated.

Møllmann and Mortenson (1.7) have encountered convergence difficulties using the Siev method and have often had to use incremental loadings to obtain results. Møllmann (1.8) continued the development of the displacement method to include general flexural members in space subject to bending and torsional as well as direct stresses.

(ii) Relaxation methods

An entirely different approach to the non-linear analysis is provided by relaxation methods where the static analysis problem is transformed into a dynamic one. The loads are applied suddenly to the system and the equations of motion of the joints, with high fictitious damping, are used to determine the equilibrium position.

Barnes (1.9) has successfully used the method of dynamic relaxation, as proposed for structural analysis by Day (1.10) and Otter (1.11), in the analysis of tension networks. The basis of the method is to trace step by step for a central difference of time the dynamic behaviour of the structure from when it was first loaded. The governing equation of motion is of the form

$$\underset{\sim}{R}_i^t = M_i \cdot \underset{\sim}{\dot{V}}_i^t + K_i \underset{\sim}{V}_i^t \qquad (1.3)$$

where

$\underset{\sim}{R}_i^t$ is the residual force at node "i" at time t

M_i is the mass at node "i"

K_i is the damping constant at node "i".

$\underset{\sim}{V}_i^t$ and $\underset{\sim}{\dot{V}}_i^t$ are respectively the velocity and acceleration of node "i" at time t.

The examples given appear to be limited to structures with fixed boundaries and no reference to elastic boundary structures is given.

Convergence is only assured by using a high fictitious damping constant and a small enough time interval. Both of these constants must be determined before the analysis can proceed. Barnes has produced upper and lower limits for the time interval Δt but a trial run is required to obtain the optimum damping constant. It is not known whether the damping constant is dependent upon the applied loading but from observations of the models described later it is thought that may be the case.

Provided the damping constant was below the critical damping Barnes was able to obtain useful dynamic information regarding the cable structure, from the static analysis, which is a valuable extra. Barnes has extended his analysis to include the effects of cladding panels upon the net structure and also possible non-linear material behaviour, however no attempt has been made to include the effects of a flexible boundary structure. Variations in the boundary conditions which would clearly alter the response to wave reflection would be expected to modify the way in which the damping constant and time interval determines the rate of convergence.

(iii) Energy Methods

A third, and in its execution essentially different method is now presented. Energy methods (or descent methods) are concerned with finding the minimum of an N-dimensional energy surface, and hence the equilibrium configuration of a structure, by moving in a series of descent directions. They have been extensively analysed as a numerical and analytical process and considerable understanding of these exists for large linear systems and for small perturbations (1.12).

Application of the method to the specific non-linear forms that arise in cable structures is due to Buchholdt (1.13). The development of the equations of equilibrium is discussed in detail in Chapter 2. Advantages of the method are that it requires considerably less storage space than the displacement method described earlier and can continue to give computational results where the Newton-Raphson method fails due to singularity of the stiffness matrix.

In conformity with experience elsewhere Buchholdt later changes from the steepest descent to the conjugate gradients method (1.14) in the search for the minimum energy configuration and was more successful in obtaining convergence. Even with conjugate gradients he reports difficulties in some cases which he overcame by a scaling method described in Chapter 2.

1.3 The Development of Model Analysis Techniques

The use of models to determine structural behaviour is as well established as the modern scientific study of deformation.

Model analysis is not always intended to verify a theoretical analysis but may also be undertaken when theoretical analysis is impractical (1.15, 1.16). The work intends to use model analysis in the former of the above roles.

The following review limits itself to an appraisal of those models which have influenced the design and construction of the cable truss and cable net experiment described later.

(i) Two-dimensional models

Among other early experimental papers on two-dimensional model analysis, work is described by Krishna (1.17) on a plane pretensioned

FIG 1.6

CABLE TRUSS EXPERIMENT BY KRISHNA

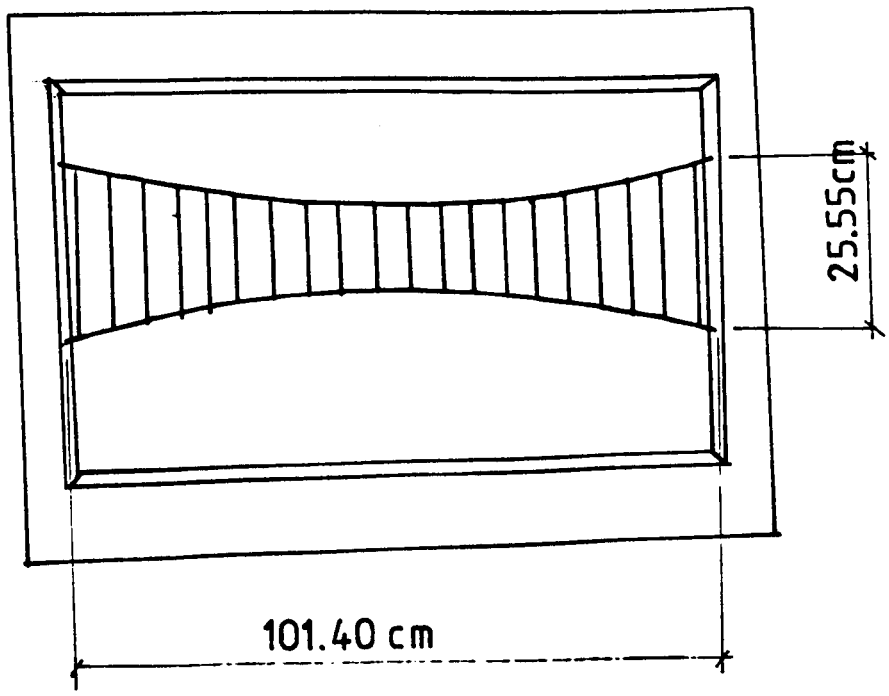

structure of 1.02 m span (Fig. 1.6) constructed from stainless steel wire. The structure was supported by a rigid steel frame and the wires pretensioned by dead weight and calibrated springs. The wires were joined by fusion welding after pretensioning. No comment was made by Krishna of the effect of fusion welding on the pretension forces. In view of the high local temperatures involved in welding it seems unwise to assume that no change had occurred. The model was subject to gravity loads, changes in the hanger forces were measured using the vibrating wire method (discussed in detail in Chapter 3) and vertical deflections of joints were measured using a travelling microscope. It is shown later that horizontal deflections are also significant particularly for non-symmetrical loading cases where marked non-linear behaviour is exhibited. No attempt though by Krishna appears to have been made to measure these deflections.

Of other experimental papers (1.18, 1.19) that by Buchholt (1.20) is the best documented, describing a two-dimensional cable girder experiment. Buchholdt tensioned the two main cables against five compressive struts rather than tensile hangers (Fig. 1.7), the advantage being that only one support point was needed at each end of the model. The model spanning 2.74 m was contained in a rigid frame. Set against this is the need for compressive members between the pretensioning cables which have to be designed against buckling. With one support only at each end of the model there is no restraint against out of plane displacements so the two-dimensional girder is less attractive for building up into a three-dimensional cable system. Horizontal reactions were measured at one end only of the girder and no attempt was made to measure internal forces. Again only the vertical deflections at the nodes were measured in this case with dial gauges attached by threads to the nodes.

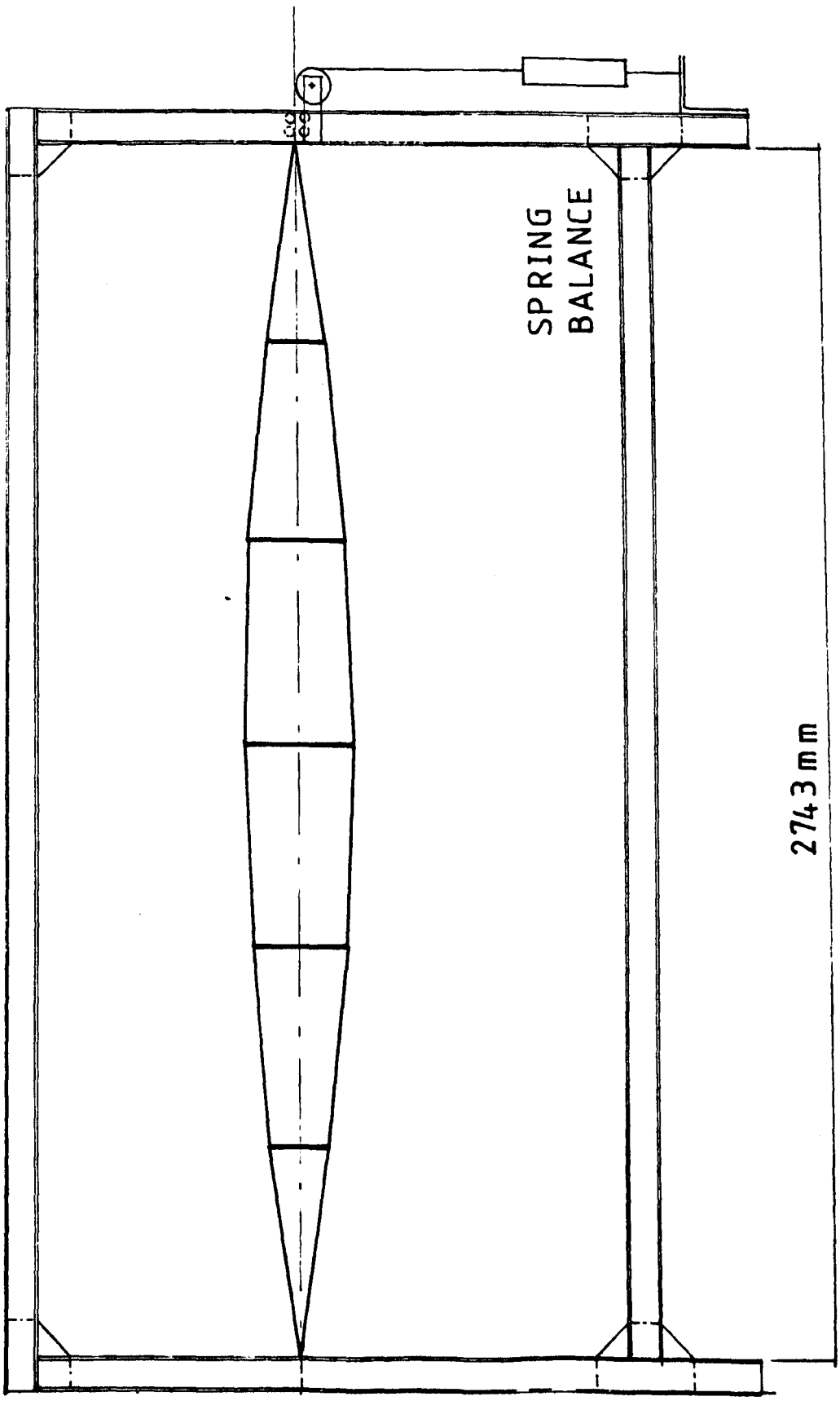

FIG 1.7

PRETENSION CABLE EXPERIMENT BY BUCHHOLDT

(ii) Three-dimensional models

The majority of published work on three-dimensional net experiments, designed to verify theoretical analysis has concerned two types of net, prestressed flat nets and prestressed saddle shaped nets. In flat nets all of the cable elements are in one plane thus considerably simplifying the initial prestress calculation but providing only a limited test to any general deformation theory.

Foster and Beaufait (1.21) experimented on a model cable net panel roof structure. The model (Fig. 1.8) consisted of a 1.52 m square compression frame, assumed to be rigid, with four cables at 0.304 m centres spanning in orthogonal directions to form a grid. An anchor system allowed for horizontal adjustment in the pretensioning which was by means of an anchor bolt around which the wire was wrapped. The wire being tensioned by the application of a known torque to the bolt. Instrumentation was only available to determine the tension in half of the cables therefore the initial prestress condition could only be found to a limited accuracy. In the design of the model cable net experiment described in Chapter 5 care was taken to have available the tension at each of the cable support points during the initial pretensioning operation. Flat nets have also been investigated by Buchholdt et al (1.22).

Tests on saddle shaped nets have included work by Siev (1.23) who investigated the behaviour of a hyperbolic parabaloid shape net (Fig. 1.9). The model was fixed at four anchorage points forming a 2 m x 2 m square in plan with a height difference of 0.635 m between diagonal corners. Main cables between the anchorage points provided support for a cable grid. Excessive sectional dimensions were used for the frame to give

FIG 1.8

CABLE NET EXPERIMENT BY FOSTER AND BEAUFAIT

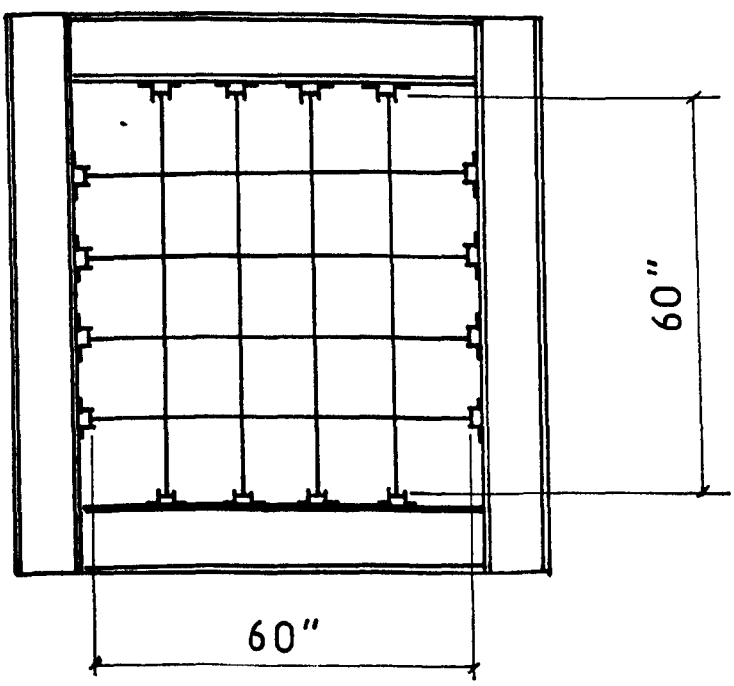

PLAN

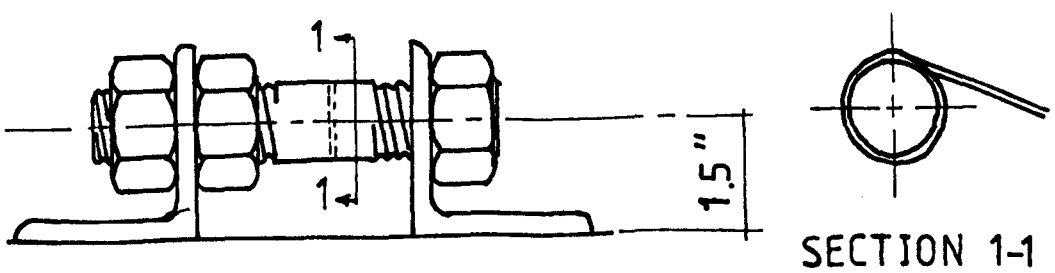

CABLE END CONNECTION

SECTION 1-1

FIG 1.9

CABLE NET EXPERIMENT BY SIEV

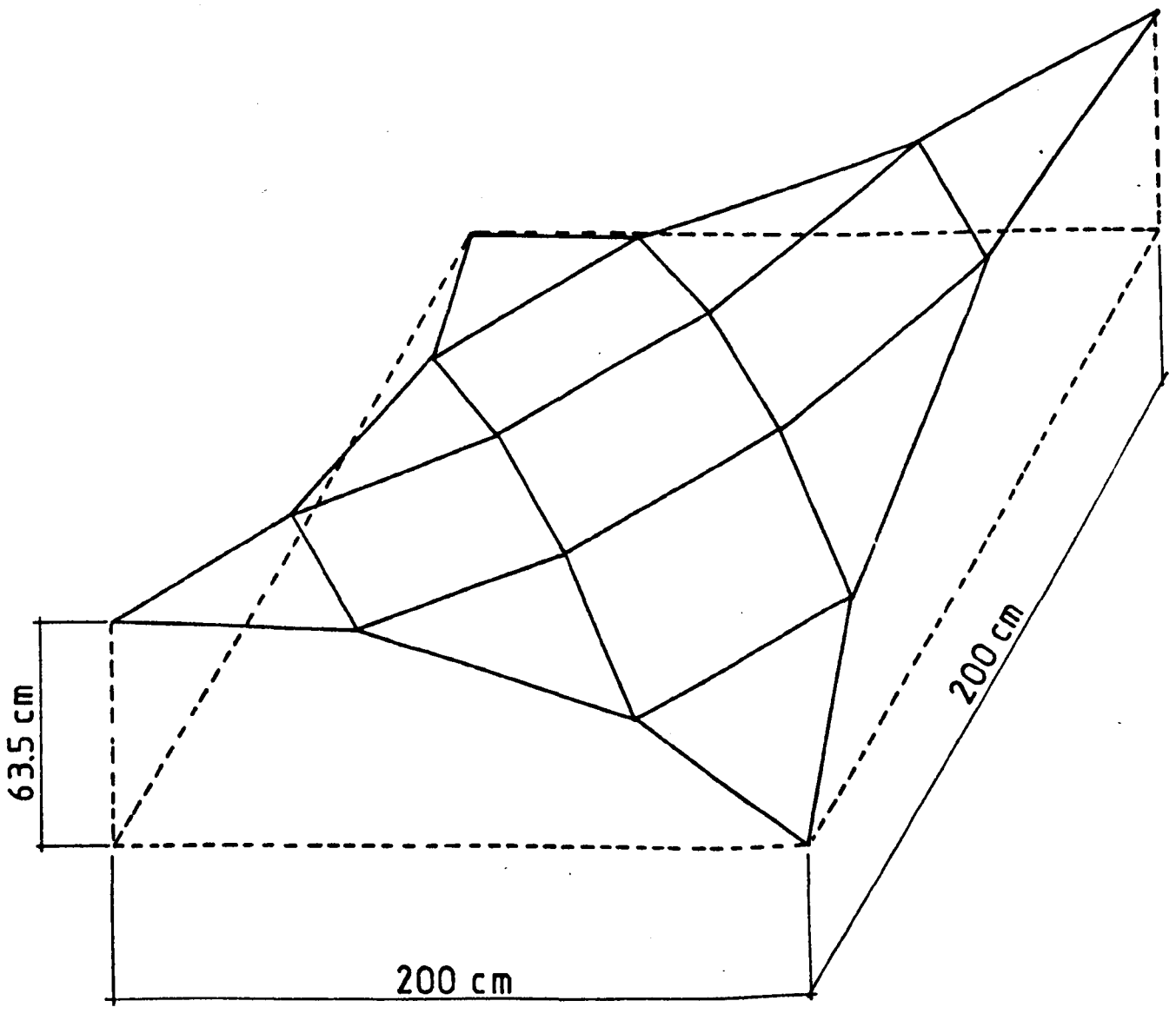

GENERAL ARRANGEMENT

extremely high stiffness and minimum deflection at the supports. No indication is given though if there is any movement of supports during prestressing or loading of the net. Vertical deflections of joints were measured using an optical level to an accuracy of 0.1 mm. Horizontal deflections were not measured. Tension in the wires was measured using a dynamometer introduced along the length of the wire and the initial prestress forces were found to be within 3.5% of the required values.

A hyperbolic paraboloid shaped net has also been investigated by Krishna and Agarwal (1.24). The model (Fig. 1.10) was 3.66 m square in plan with rigid straight edge beams constructed from rolled steel channel sections. Solid light, tension steel wires were used to represent stranded cables. The wires were anchored against mild steel blocks welded to the outside of the beams, the angle of the blocks was arranged so that the wire passed through the beam and the block without producing a kink in it. This form of anchorage outside of the boundary beam has been developed for use in the cable net experiment described later.

Forces in the wires were measured by light weight dynamometers and deflections using dial gauges. The initial prestress forces were within $\pm$ 2.7% of the stipulated values.

Barnes (1.9) has experimented on a similar shaped net to that used by Siev but with a larger number of cable members.

The use of hyperbolic parabaloid nets in model analysis is understandably popular due to the ease with which the initial prestress condition can be determined. However it is felt that concentration on this form has provided a less than rigorous test of the fully developed

FIG 1.10

CABLE NET EXPERIMENT BY KRISHNA AND AGARWAL

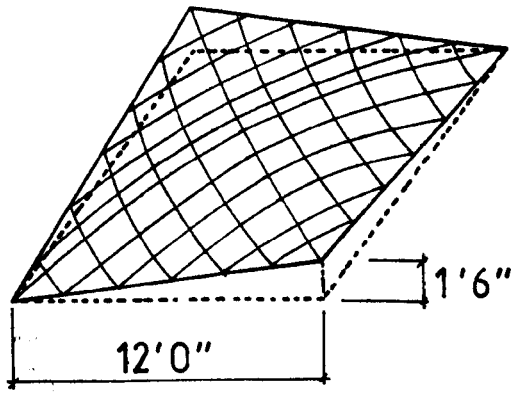

GENERAL ARRANGEMENT

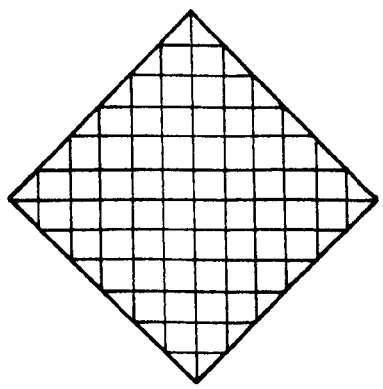

PLAN

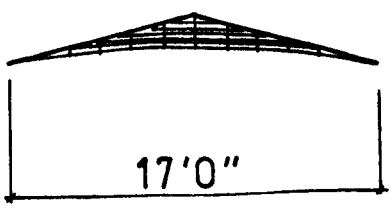

ELEVATION

non-linear theory. Therefore there is a considerable need for a more rigorous experimental test for the non-linear response and to this end a prestressed net with fully flexible curved boundaries was developed as described in Chapter 5.

CHAPTER 2

ANALYSIS OF CABLE STRUCTURES

2.0 Introduction

The problems and special features of tension structures, for example large deflections and stiffness due to prestress have been mentioned in Chapter 1.

For this type of structure or structural mechanism full account must be taken of the change in the geometry of the structure in its analysis. This leads to a non-linear form of the equilibrium equations which cannot be solved by the classical linear theory of structural analysis.

The following rigorous theory has been developed to take account of this non-linearity, and to provide methods for the solution of the non-linear equations so formed.

2.1 Equilibrium of a Cable System

To develop the following equations consider a set of nodes in equilibrium connected by a series of members. A node occurs where two or more members join. The relation between the number of nodes to members required for equilibrium in two-dimensional structures has been considered by Buchholdt (2.1) and more generally by Vilnay (2.2).

The equilibrium of the whole system is investigated by considering the equilibrium of its component parts, i.e. the members and nodes. The initial state of the system may be caused by pretensioning or by

the application of an initial dead load. Cable structures rely almost entirely upon direct tension in tension members for their strength and stiffness. This thesis follows other authors in neglecting any strain energy from bending action in the cables. Consider then the equilibrium of a tension member in space capable of transmitting direct tensile forces only.

2.2 Elongation of a Tension Member in Space

Consider a simple tension member "ij" defined by position vectors $\underset{\sim}{r}_i$, $\underset{\sim}{r}_j$ having end displacements $\underset{\sim}{u}_i$, $\underset{\sim}{u}_j$. Fig. (2.1) shows

In the initial prestressed state

$$L_{ij}^2 = (\underset{\sim}{r}_j - \underset{\sim}{r}_i).(\underset{\sim}{r}_j - \underset{\sim}{r}_i) \tag{2.1}$$

After loading

$$(L_{ij} + \Delta L_{ij})^2 = ((\underset{\sim}{r}_j - \underset{\sim}{r}_i) + (\underset{\sim}{u}_j - \underset{\sim}{u}_i)).((\underset{\sim}{r}_j - \underset{\sim}{r}_i) + (\underset{\sim}{u}_j - \underset{\sim}{u}_i)) \tag{2.2}$$

For shortness introduce the notation

$$\delta\underset{\sim}{r} = (\underset{\sim}{r}_j - \underset{\sim}{r}_i) \tag{2.3}$$

$$\delta\underset{\sim}{u} = (\underset{\sim}{u}_j - \underset{\sim}{u}_i) \tag{2.4}$$

and omit subscripts ij

Equation (2.1) becomes $L^2 = \delta\underset{\sim}{r} \cdot \delta\underset{\sim}{r}$ (2.5)

and (2.2) becomes $(L + \Delta L)^2 = (\delta\underset{\sim}{r} + \delta\underset{\sim}{u}).(\delta\underset{\sim}{r} + \delta\underset{\sim}{u})$ (2.6)

FIG 2.1

EQUILIBRIUM OF A GENERAL TENSION MEMBER

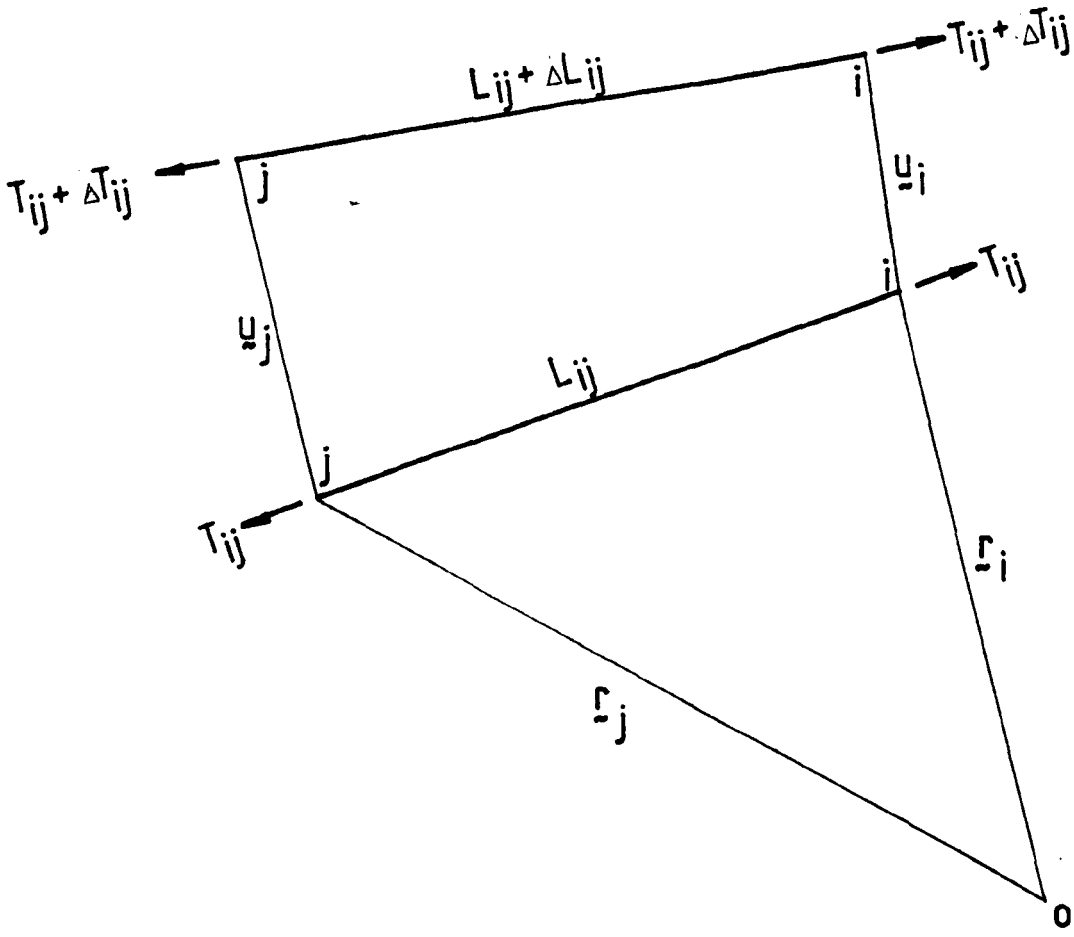

Combining equations (2.5) and (2.6) gives

$$\Delta L^2 + 2L\Delta L = 2\,\delta\underset{\sim}{r}.\delta\underset{\sim}{u} + \delta\underset{\sim}{u}^2 \qquad (2.7)$$

Dividing (2.7) by L^2 and rearranging gives a quadratic in $(\frac{\Delta L}{L})$

$$(\frac{\Delta L}{L})^2 + 2(\frac{\Delta L}{L}) - (2\,\frac{\delta r.\delta u}{L^2} + \frac{\delta u^2}{L^2}) = 0 \qquad (2.8)$$

Solution of the quadratic gives

$$\frac{\Delta L}{L} = -1 + (1 + 2\,\frac{\delta r.\delta u}{L^2} + \frac{\delta u^2}{L^2})^{\frac{1}{2}} \qquad (2.9)$$

Define the strain function $\mu = 2\,\frac{\delta r.\delta u}{L^2} + \frac{\delta u^2}{L^2}$ (2.10)

Then $\frac{\Delta L}{L}$ simplifies to the form

$$\frac{\Delta L}{L} = -1 + (1 + \mu)^{\frac{1}{2}} \qquad (2.11)$$

Previous papers for example Buchholdt (2.1) have neglected the $(\frac{\Delta L}{L})^2$ term in equation (2.8) which gives

$\frac{\Delta L}{L} = \frac{\delta r.\delta u}{L^2} + \frac{\delta u^2}{2L^2}$ which corresponds to the first order expansion of equation (2.11).

The above formula is a general one and has made no assumptions regarding the material properties of the structure. All necessary terms are carried through the analysis so that consistent approximations can be made at a later stage.

2.3 Equilibrium of a Pinned Joint in Space

Consider the equilibrium at some general pinned joint "i" connected by members to joints "j,k,l,..." and subjected to load $\underset{\sim}{P}_i$. Fig. (2.2) shows the position of the joint in equilibrium before and after the application of load $\underset{\sim}{P}_i$.

Introduce $\{F_{in_x} \quad F_{in_y} \quad F_{in_z}\}^T = \underset{\sim}{F}_{in}$

which are the component forces of member force T_{in}

i.e. $$\underset{\sim}{F}_{in} = T_{in} \frac{\delta \underset{\sim}{r}_{in}}{L_{in}} \quad \text{where } n = j,k,l,... \tag{2.12}$$

Consider the joint "i" in its initial prestressed condition before the application of load $\underset{\sim}{P}_i$.

The equilibrium equation can be written as

$$\sum \underset{\sim}{F}_{in} = 0 \tag{2.13}$$

$n = j,k,l.$

Combining equations (2.12) and (2.13) gives

$$\sum \underset{\sim}{T}_{in} \frac{\delta \underset{\sim}{r}_{in}}{L_{in}} = 0 \tag{2.14}$$

$n = j,k,l,$

Now consider the joint equilibrium after the application of load $\underset{\sim}{P}_i$ at joint "i"

$$\sum \underset{\sim}{F}_{in} + \Delta \underset{\sim}{F}_{in} + \underset{\sim}{P}_i = 0 \tag{2.15}$$

$n = j,k,l,$

FIG 2.2

EQUILIBRIUM OF A GENERAL PINNED JOINT

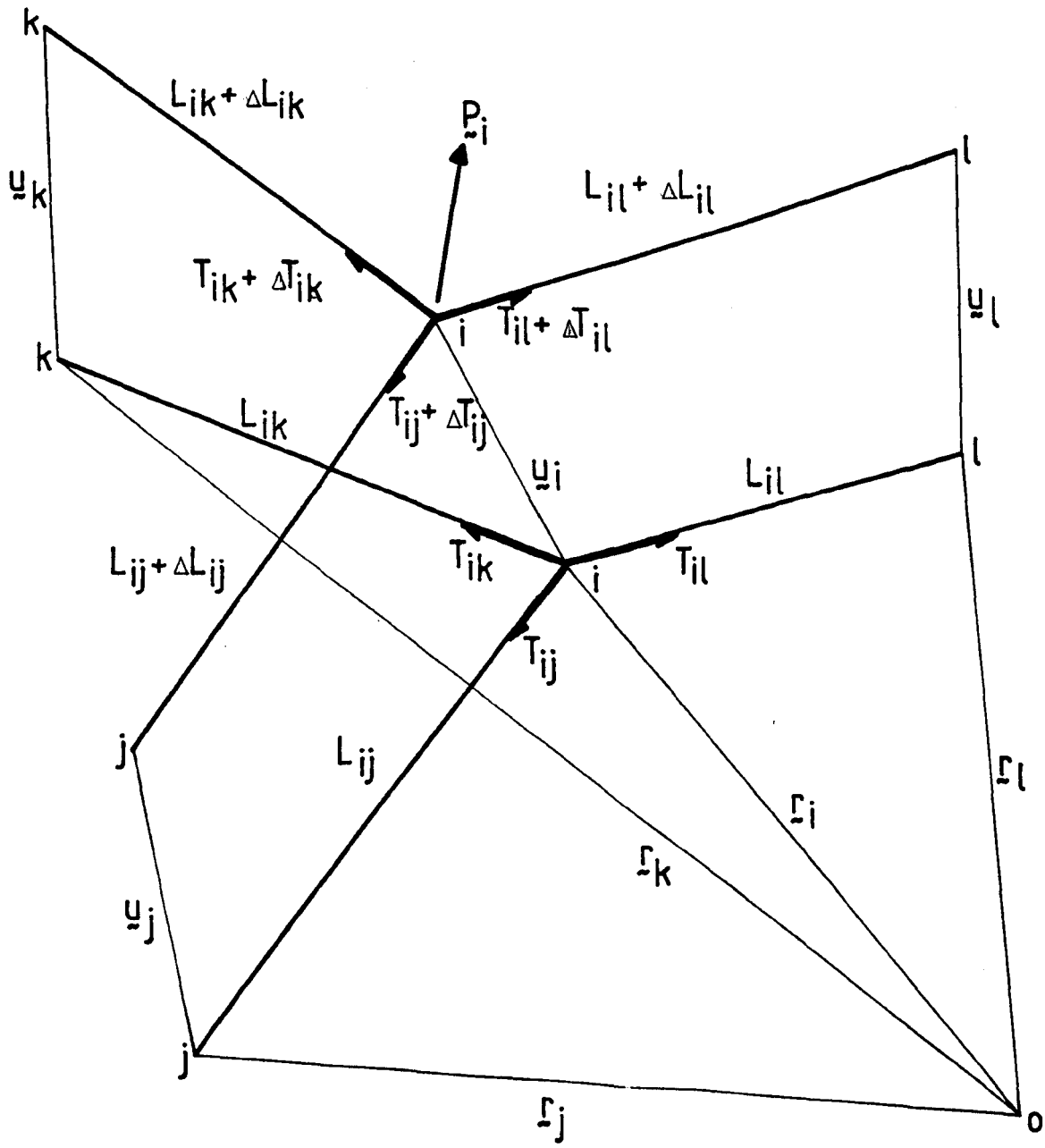

where $\underset{\sim}{F}_{in} + \Delta\underset{\sim}{F}_{in}$ are now the component forces of member force $T_{in} + \Delta T_{in}$

$$\text{i.e. } \underset{\sim}{F}_{in} + \Delta\underset{\sim}{F}_{in} = (T_{in} + \Delta T_{in}) \frac{(\delta\underset{\sim}{r}_{in} + \delta\underset{\sim}{u}_{in})}{L_{in} + \Delta L_{in}} \qquad (2.16)$$

where $\frac{(\delta\underset{\sim}{r}_{in} + \delta\underset{\sim}{u}_{in})}{L_{in} + \Delta L_{in}}$ is the vector of direction cosines for the deflected member "i,n."

Combining equations (2.15) and (2.16) and again omitting subscripts for shortness gives

$$\sum_{\substack{\text{All members at} \\ \text{joint i}}} \frac{(T + \Delta T)\ (\delta\underset{\sim}{r} + \delta\underset{\sim}{u})}{L + \Delta L} + \underset{\sim}{P}_i = 0 \qquad (2.17)$$

$(L + \Delta L)^{-1}$ can be written as $\frac{1}{L}\left(1 + \frac{\Delta L}{L}\right)^{-1}$

Substituting the strain function μ from equation (2.10) for $\frac{\Delta L}{L}$ gives

$$(L + \Delta L)^{-1} = \frac{1}{L}(1 + \mu)^{-\frac{1}{2}} \qquad (2.18)$$

Substituting for $(L + \Delta L)^{-1}$ in (2.17) gives

$$\sum_{\substack{\text{All members} \\ \text{at joint i}}} \frac{(T + \Delta T)(\delta\underset{\sim}{r} + \delta\underset{\sim}{u})\quad (1 + \mu)^{-\frac{1}{2}}}{L} + \underset{\sim}{P}_i = 0 \qquad (2.19)$$

We now seek ΔT in terms of the strain function μ. Let the unstressed length of the member be L_o.

At the initial prestress $L = L_o + e$. (2.20)

Where e is the extension of the member due to prestress force T.

The large displacement effects are a 'geometrical' cause of a non-linear relation between nodal force and nodal displacement components.

In addition there is the possibility of non-linear material behaviour. This thesis concentrates solely on the former which is considered to be of fundamental importance to the behaviour of cable structures, whereas for considerable forces the material stress/strain relation is a linear one.

Assuming then the member to be linearly elastic the extension can be written as

$$e = \frac{TL_o}{EA} \tag{2.21}$$

Substituting for e in equation (2.20) gives

$$L = L_o + \frac{TL_o}{EA} = L_o \left(1 + \frac{T}{EA}\right) \tag{2.22}$$

Now

$$\Delta T = \frac{EA\,\Delta L}{L_o} = \frac{EA\,\Delta L\,(1 + \frac{T}{EA})}{L} = \frac{\Delta L}{L}(EA + T) \tag{2.23}$$

Substituting for $\frac{\Delta L}{L}$ in terms of the strain function μ gives

$$\Delta T = -(EA + T) + (EA + T)\,(1 + \mu)^{\frac{1}{2}} \tag{2.24}$$

Substituting for ΔT in equation (2.19) and simplifying gives

$$\sum_{\text{All members at joint "i"}} \frac{(\delta\underset{\sim}{r} + \delta\underset{\sim}{u})}{L} (T + EA\,(1 - (1 + \mu)^{-\frac{1}{2}})) + \underset{\sim}{P}_i = 0 \qquad (2.25)$$

The $(1 - (1 + \mu)^{-\frac{1}{2}})$ term in equation (2.25) is now expanded to give the equilibrium equation in terms of one unknown $\delta\underset{\sim}{u}$. Since $\delta\underset{\sim}{u}$ is of a small order compared with $\delta\underset{\sim}{r}$ terms of the power of δu^4 and above have been neglected.

$$(1 - (1 + \mu)^{-\frac{1}{2}}) = (1 - (1 - \frac{\mu}{2} + \frac{3\mu^2}{8} - \frac{5\mu^3}{16} + \frac{35\mu^4}{128} \ \ldots) \qquad (2.26)$$

Where $\mu = \dfrac{2(\delta r.\ \delta u)}{L^2} + \dfrac{\delta u^2}{L^2}$

$$\mu^2 = \frac{4(\delta r.\delta u)^2}{L^4} + \frac{4(\delta r.\delta u)\ \delta u^2}{L^4} + 0(\delta u^4)$$

$$\mu^3 = \frac{8(\delta r.\delta u)^3}{L^6} + 0(\delta u^4) \qquad (2.27)$$

Substituting for $1 - (1 + \mu)^{-\frac{1}{2}}$ in equation (2.27) gives

$$1 - (1 + \mu)^{-\frac{1}{2}} = \frac{\delta r.\delta u}{L^2} + \frac{\delta u^2}{2L^2} - \frac{3(\delta r.\delta u)^2}{2L^4} - \frac{3(\delta r.\delta u)\ \delta u^2}{2L^4} + \frac{5(\delta r.\delta u)^3}{2L^6} \qquad (2.28)$$

Substituting for $1 - (1 + \mu)^{-\frac{1}{2}}$ in equation (2.25) and expanding gives the following terms in powers of $\delta\underset{\sim}{u}$.

$$\text{Zero power } \frac{T}{L}\,\delta\underset{\sim}{r} + \underset{\sim}{P}_i$$

$$\text{First power } \frac{T}{L}\,\delta\underset{\sim}{u} + \frac{EA(\delta r.\delta u)}{L^3}\,\delta\underset{\sim}{r}$$

$$\text{Second power } \frac{EA(\delta r.\delta u)}{L^3}\,\delta\underset{\sim}{u} + \frac{EA(\delta u^2)}{2L^3}\,\delta\underset{\sim}{r} - \frac{3EA(\delta r.\delta u)^2}{2L^5}\,\delta\underset{\sim}{r}$$

$$\text{Third power } \frac{EA(\delta u^2)}{2L^3}\,\delta\underset{\sim}{u} - \frac{3EA(\delta r.\delta u)^2}{2L^5}\,\delta\underset{\sim}{u} - \frac{3EA(\delta r.\delta u)}{2L^5}\,\delta u^2\,\delta\underset{\sim}{r}$$

$$+ \frac{5EA(\delta r.\delta u)^3}{2L^7}\,\delta\underset{\sim}{r} \qquad (2.29)$$

The degree of non-linearity in the response of a cable structure can be assessed by comparison with the first order stiffness which is modified by the pretension. This is the tensegrity concept as described by Vilnay[2.2], where for most net like structures without the "tension terms" there would be no structural integrity.

Although earlier workers have stressed the importance of non-linear response they appear to have argued this without explicitly defining what the linear response would be. This is now developed in a uniform manner.

2.4 First Order Stiffness Analysis

Taking just the zero and first order terms of the equilibrium equation (2.29) gives linear equation in terms of $\delta\underset{\sim}{u}$

$$\sum_{\substack{\text{All members}\\ \text{at joint i}}} \left(\frac{T}{L}\,\delta\underset{\sim}{r} + \frac{T}{L}\,\delta\underset{\sim}{u} + \frac{EA(\delta r.\delta u)}{L^3}\,\delta\underset{\sim}{r} \right) + \underset{\sim}{P}_i = 0 \qquad (2.30)$$

From equation (2.14) it is seen that the first term in (2.30)

$$\sum \frac{T}{L}\,\delta\underset{\sim}{r} = 0 \quad \text{which leaves}$$

$$\underset{\sim}{P}_i = \sum_{\substack{\text{All members}\\ \text{at joint i}}} -\frac{T}{L}\,\delta\underset{\sim}{u} \qquad -\frac{EA(\delta r.\delta u)}{L^3}\,\delta\underset{\sim}{r} \tag{2.31}$$

We are seeking to express equation (2.31) in the form $\underset{\sim}{P}_i = K\underset{\sim}{u}_i$.

For simplicity consider just one member, joining points 1 and 2.

$$\delta\underset{\sim}{u} = ((u_2 - u_1),\ (v_2 - v_1),\ (w_2 - w_1))^T$$

$$\therefore\ -\frac{T}{L}\,\delta\underset{\sim}{u} = \left[\begin{array}{ccc:ccc} T/L & & & -T/L & & \\ & T/L & & & -T/L & \\ & & T/L & & & -T/L \\ \hdashline -T/L & & & T/L & & \\ & -T/L & & & T/L & \\ & & -T/L & & & T/L \end{array}\right] \left\{\begin{array}{c} u \\ v \\ w \end{array}\right\}_1 \left\{\begin{array}{c} u \\ v \\ w \end{array}\right\}_2 \tag{2.32}$$

Expanding the $\frac{-EA(\delta r.\delta u)}{L^3}\,\delta\underset{\sim}{r}$ term

$$\frac{-EA(\delta r.\delta u)}{L^3}\,\delta\underset{\sim}{r} = \frac{-EA}{L^3}\,(\delta x.\delta u + \delta y.\delta v + \delta z.\delta w)\,(\delta x\underset{\sim}{i} + \delta y\underset{\sim}{j} + \delta z\underset{\sim}{k})$$

By inspection we have

$$\frac{EA}{L}\left[\begin{array}{ccc|ccc} \left(\frac{\delta x}{L}\right)^2 & \frac{\delta x.\delta y}{L^2} & \frac{\delta x.\delta z}{L^2} & -k_{11} & -k_{12} & -k_{13} \\ \frac{\delta y.\delta x}{L^2} & \frac{\delta y^2}{L^2} & \frac{\delta y \delta z}{L^2} & -k_{21} & -k_{22} & -k_{23} \\ \frac{\delta z.\delta x}{L^2} & \frac{\delta z.\delta y}{L^2} & \frac{\delta z^2}{L^2} & -k_{31} & -k_{32} & -k_{33} \\ \hline K_{21} = K_{12} & & & K_{22} = K_{11} & & \end{array}\right]\begin{array}{c} u \\ v \\ w \\ \hline u \\ v \\ w \end{array}\begin{array}{l} 1 \\ \\ \\ \\ 2 \end{array} \qquad (2.33)$$

Combining (2.32) and (2.33) gives

$$K_{11} = \frac{EA}{L}\begin{bmatrix} \left(\frac{T}{EA} + \frac{\delta x^2}{L^2}\right) & \frac{\delta x.\delta y}{L^2} & \frac{\delta x.\delta z}{L^2} \\ \frac{\delta y.\delta x}{L^2} & \left(\frac{T}{EA} + \frac{\delta y^2}{L^2}\right) & \frac{\delta y.\delta z}{L^2} \\ \frac{\delta z.\delta x}{L^2} & \frac{\delta z.\delta y}{L^2} & \left(\frac{T}{EA} + \frac{\delta z^2}{L^2}\right) \end{bmatrix} \qquad (2.34)$$

$K_{22} = K_{11}$, $K_{21} = K_{12} = -K_{11}$, which agrees with other different derivations of the linear problem (1.6). Previous work on the general non-linear behaviour of cable structures has not seen the value of extracting this first order relationship between $\underset{\sim}{P}_i$ and $\underset{\sim}{u}_i$. It is shown later that this has value in computation.

2.5 The Effect of Temperature Changes on the Deformation of Cable Structures

Cable structures are liable to temperature changes and to differential temperature changes. It is not part of this thesis to analyse temperature dependent cable forces, but the basic relationships need to be examined to see in what manner they effect the non-linear analysis.

Let the coefficient of thermal expansion of the cable material be given by α and the change in temperature be Δt.

At the initial prestress member length

$$L = L_o(1 + \frac{T}{EA})$$

After the application of load $\underset{\sim}{P}$ and a temperature change Δt the change in member tension T is given by ΔT and the change in length L by ΔL, where

$$L + \Delta L = L_o(1 + \frac{T + \Delta T}{EA}) + L_o \alpha \Delta t \qquad (2.35)$$

$$\Delta L = \frac{L \Delta T}{(1 + \frac{T}{EA})EA} + \frac{L \quad \alpha \quad \Delta t}{(1 + \frac{T}{EA})} \qquad (2.36)$$

Which rearranging gives

$$\Delta T = \frac{\Delta L}{L}(T + EA) - EA\alpha\,\Delta t$$

$$= -(EA + T) - EA\,\alpha\,\Delta t + (EA + T)(1 + \mu)^{\frac{1}{2}} \qquad (2.37)$$

where μ is the strain function.

Substituting for ΔT into the equilibrium equation (2.25) gives

$$\sum_{j=1 \text{ to } n}\left\{\frac{(\delta\underset{\sim}{r} + \delta\underset{\sim}{u})}{L}\left[\frac{(EA + T) - EA(1 + \alpha\,\Delta t)(1 + \mu)^{-\frac{1}{2}}}{L}\right]\right\} + \underset{\sim}{P}_i = 0 \qquad (2.38)$$

for $i=1$ to $N/3$

The expansion of (2.38) above is equivalent to the expansion of (2.25) except that T is replaced by $T - EA\alpha\,\Delta t$ and EA is replaced by $EA(1 + \alpha\,\Delta t)$. The incorporation of a uniform temperature change is therefore quite straight forward. With fixed boundaries an increase in temperature would decrease all of the pretensions. For structures with flexible boundaries a similar analysis would be needed for the elements of the boundary structure.

2.6 Total Potential Energy of a Tension Structure

The equilibrium of a cable system is now looked at from the point of energy considerations. Minimisation of the total energy is a valued form of problem formulation. In its execution a knowledge of energy gradients is required. It is shown that the equilibrium equation (2.25) developed earlier can be obtained explicitly in terms of the energy gradient.

Let the total potential energy of a cable system be given by W where

$$W = U + V \tag{2.39}$$

U is the internal elastic potential or strain energy of the system and V is the potential energy of the external applied loads. When the system is in equilibrium the gradient of the total potential energy is zero

$$\frac{\partial W}{\partial u_i} = \frac{\partial U}{\partial u_i} + \frac{\partial V}{\partial u_i} = 0 \tag{2.40}$$

Where $i : 1$ to N and u_i is any element of the column matrix $\underset{\sim}{u}$ containing all the nodal displacement components

Consider one member in its deformed state where the force in a representative member is $T + \Delta T$ and its elongation is ΔL. The increment in strain energy ∂U in the limit is given by

$$\partial U = (T + \Delta T)\,\partial(\Delta L) = (T+\Delta T)\,\partial L \tag{2.41}$$

The symbol ∂ denotes partial differentiation with respect to one of the degrees of freedom u_i. The terms in (2.41) involve $\delta\underset{\sim}{u}$.

Expressions are now sought for $\frac{\partial U}{\partial u_i}$ and $\frac{\partial V}{\partial u_i}$ in terms of the relative displacement vector $\delta\underset{\sim}{u}$ which involve u_i.

$$\frac{\partial U}{\partial u_i} = \sum_{j=1 \text{ to } n} \frac{\partial U}{\partial(\delta u_j)} = \sum_{j=1 \text{ to } n} \frac{\partial U}{\partial L}\,\frac{\partial L}{\partial(\delta u_j)} \tag{2.42}$$

Where for example if u_i is an x component displacement (δu_j) is also the x component of the relative displacement (2.43)

$$\frac{\partial U}{\partial u_i} = \sum_{j=1 \text{ to } n} (T + \Delta T)\,\frac{\partial L}{\partial(\delta u_j)}$$

We now seek an expression for $\frac{\partial L}{\partial(\delta u_j)}$

From equations (2.10) and (2.11)

$$\Delta L = -L + L(1 + \mu)^{\frac{1}{2}} \quad \text{where } \mu = \frac{2\delta r.\delta u}{L^2} + \frac{\delta u^2}{L^2}$$

$$\frac{\partial L}{\partial(\delta u_j)} = \frac{\partial L}{\partial \mu} \cdot \frac{\partial \mu}{\partial(\delta u_j)} \tag{2.44}$$

Under differentiation of the scalar products $(\delta \underline{r}.\delta \underline{y})$ and $(\delta \underline{y}.\delta \underline{y})$ of two vectors with respect to u_i for node i or δu_j for member j the term ℓ^* arrises

$$\frac{\partial L}{\partial \mu} = \frac{L}{2}(1 + \mu)^{-\frac{1}{2}}, \quad \frac{\partial \mu}{\partial(\delta u_j)} = \frac{\ell^*}{L^2}$$

$$\therefore \frac{\partial L}{\partial(\delta u_j)} = \frac{\ell^*}{L}(1 + \mu)^{-\frac{1}{2}} \tag{2.45}$$

Where ℓ^* is the component of $\delta \underline{r} + \delta \underline{y}$ for member j appropiate to the parameter being varied eg When u_i is an x displacement ℓ^* takes the x component.

Substituting for $\frac{\partial L}{\partial(\delta u_j)}$ in (2.43) gives

$$\frac{\partial U}{\partial u_i} = \sum_{j=1 \text{ to } n} (T + \Delta T)\left(\frac{\ell^*}{L}\right)(1 + \mu)^{-\frac{1}{2}} \tag{2.46}$$

For constant loading

$$V = -P_i \, u_i \tag{2.47}$$

$$\frac{\partial V}{\partial u_i} = -P_i \tag{2.48}$$

Where P_i is an element of the nodal load column matrix corresponding to the element of displacement matrix u_i.

The potential energy gradient with respect to any element of the nodal displacement column matrix $\underline{u}$ is given by

$$\frac{\partial W}{\partial u_i} = \sum_{j=1 \text{ to } n} (T + \delta T)\left(\frac{\ell^*}{L}\right)(1 + \mu)^{-\frac{1}{2}} - P_i \tag{2.49}$$

By inspection it is seen that equation (2.49) is directly equivalent to the equilibrium equation (2.19), for any component direction.

2.7 Gradient Methods of Analysis

We now seek a method for the solution of the full equilibrium equation. For an arbitrary set of relative joint displacements $\delta \underset{\sim}{u}_{j(0)}$ let the residual out of balance force at the joint "i" be given by $\underset{\sim}{R}_i$.

$$\text{where } \underset{\sim}{R}_i = - \sum_{j=1 \text{ to } n} \left\{ \frac{(\delta \underset{\sim}{r} + \delta \underset{\sim}{u}_{(0)})}{L} (T + EA(1 - (1 + \mu)^{-\frac{1}{2}})) \right\} - \underset{\sim}{P}_i \tag{2.50}$$

For each component direction and corresponding node

$$\frac{\partial W}{\partial u_i} = R_i \tag{2.51}$$

The iterative process can be described by reference to the first step. Suffices 0,1 denote initial and corrected estimates. The relative vector displacement of the ends of each member j are given by

$$\delta \underset{\sim}{u}_{j(1)} = \delta \underset{\sim}{u}_{j(0)} + S_{(0)} \delta \underset{\sim}{v}_{j(0)} \tag{2.52}$$

where $S_{(0)}$ is a scalar step length along the unit vector $\delta \underset{\sim}{v}_{j(0)}$. $\underset{\sim}{v}_i$ defines the descent direction along which the ith node moves in minimizing the total energy. Depending on the choise of algorithm $\underset{\sim}{v}_i$ need not be a unit vector, δv_j the relative descent vector for member j also has an arbitrary amplitude.

At equilibrium the total potential energy of the system is at a minimum.

$$\text{i.e.} \quad \frac{dW}{dS} = 0$$

$$\frac{dW}{dS} = \sum_{i=1 \text{ to } N} \frac{\partial W}{\partial u_i} \frac{du_i}{dS} \tag{2.53}$$

$$u_i(1) = u_i(0) + S(0).v_i(0)$$

$$\frac{du_i}{dS} = v_i \tag{2.54}$$

$$\therefore \quad \frac{dW}{dS} = - \sum_{i=1 \text{ to } N} R_i \cdot v_i = 0 \qquad (2.55)$$

The solution of the equation (2.55) gives the step length S along the unit vector $\underset{\sim}{v}_i$ required to give a minimum potential energy in that direction.

$\frac{dW}{dS}$ can be obtained by replacing δu_j by $\delta u_j + S\delta v_j$ in the equilibrium equation (2.29) and summing for all degrees of freedom. After some reduction we obtain

$$\frac{dW}{dS} = \sum_{\text{All members}} \frac{T}{L}(\delta r.\delta v) + \sum_{\text{All nodes}} \underset{\sim}{P}_i \cdot \underset{\sim}{v}_i$$

$$\sum_{\text{All members}} + \Big[\frac{EA}{L^3}(\delta r.\ (\delta u + S\delta v))(\delta r.\delta v) + \frac{T}{L}(\delta u + S\delta v).\delta v$$

$$+ \frac{EA}{2L^3}(\delta u + S\delta v)^2(\delta r.\delta v) + \frac{EA}{L^3}(\delta r.(\delta u + S\delta v)(\delta u + S\delta v).\delta v)$$

$$- \frac{3EA}{2L^5}(\delta r.(\delta u + S\delta v))^2(\delta r.\delta v)$$

$$+ \frac{EA}{2L^3}(\delta u + S\delta v)^2((\delta u + S\delta v).\delta v)$$

$$- \frac{3EA}{2L^5}(\delta r.(\delta u + S\delta v))^2(\delta u + S\delta v).\delta v$$

$$- \frac{3EA}{2L^5}(\delta r.(\delta u + S\delta v))(\delta u + S\delta v)^2(\delta r.\delta v)$$

$$+ \frac{5EA}{2L^5}(\delta r.(\delta u + S\delta v))^3(\delta r.\delta v) \Big] \qquad (2.56)$$

Where all the bracketed terms are scalar products of the relative vectors $\delta \underset{\sim}{r}_j$, $\delta \underset{\sim}{u}_j$ and $\delta \underset{\sim}{v}_j$

Expanding (2.56) and collecting terms in powers of S gives $\frac{dW}{dS}$ in terms of a cubic in S.

$$\frac{dW}{dS} = C_1 S^3 + C_2 S^2 + C_3 S + C_4 = 0 \qquad (2.57)$$

where

$$C_4 = \sum_{\text{All members}} \left[\frac{T}{L} ((\delta r.\delta v) + (\delta u.\delta v)) \right.$$

$$+ \frac{EA}{L^3} (((\delta r.\delta v) + (\ell u.\delta v))((\delta r.\delta u) + \frac{\delta u^2}{2}))$$

$$- \frac{3EA}{2L^5} ((\delta r.\delta u)((\delta r.\delta u)((\delta r.\delta v) + (\delta u.\delta v)) + \delta u^2(\delta r.\delta v)))$$

$$\left. + \frac{5EA}{2L^7} (\delta r.\delta u)^3(\delta r.\delta v) \right] + \sum_{\text{All nodes}} \underline{P}_i . \underline{v}_i \qquad (2.58)i$$

$$C_3 = \sum_{\text{All members}} \left[\frac{T}{L} \delta v^2 \right.$$

$$+ \frac{EA}{L^3} ((\delta r.\delta v) + (\delta u.\delta v))^2 + \delta v^2(\delta r.\delta u + \frac{\delta u^2}{2}))$$

$$- \frac{3EA}{2L^5} ((\delta r.\delta v)^2\ 2((\delta r.\delta u + \frac{\delta u^2}{2}) + (\delta r.\delta u)((\delta r.\delta u)\ \delta v^2 + 4(\delta r.\delta v)$$

$$(\delta u.\delta v)))$$

$$\left. + \frac{5EA}{2L^7} (3(\delta r.\delta u)^2\ (\delta r.\delta v)^2) \right] \qquad (2.58)ii$$

$$C_2 = \sum_{\text{All members}} \left[\frac{3EA}{2L^3} (\delta v^2((\delta r.\delta v) + (\delta u.\delta v))) \right.$$

$$\left. - \frac{3EA}{2L^5} ((\delta r.\delta v)((\delta r.\delta v)^2 + 3(\delta r.\delta v)(\delta u.\delta v) + 3(\delta r.\delta u)(\delta v^2))) \right]$$

$$(2.58)iii$$

$$C_1 = \sum_{\text{All members}} \left[\frac{EA}{2L^3} (\delta v^2)^2 \right.$$

$$\left. - \frac{3EA}{L^5} (\delta r.\delta v)^2\ \delta v^2 + \frac{5EA}{2L^7} (\delta r.\delta v)^4 \right] \qquad (2.58)iv$$

The corresponding terms C_1, C_2, C_3, C_4 from the analysis by Buchholdt (2.1) are

$$C_4 \sum_{\text{All members}} \left[\frac{T}{L} ((\delta r.\delta v) + (\delta u.\delta v)) + \frac{EA}{L^3} (((\delta r.\delta v) + (\delta u.\delta v))((\delta r.\delta u) + \frac{\delta u^2}{2})) \right] + \sum_{\text{All nodes}} \underset{\sim}{P}_i . \underset{\sim}{v}_i \qquad (2.59)\text{i}$$

$$C_3 \sum_{\text{All members}} \left[\frac{T}{L} \delta v^2 + \frac{EA}{L^3} (((\delta r.\delta v) + (\delta u.\delta v))^2 + \delta v^2((\delta r.\delta u) + \frac{\delta u^2}{2})) \right] \qquad (2.59)\text{ii}$$

$$C_2 \sum_{\text{All members}} \left[\frac{3EA}{2L^3} (\delta v^2((\delta r.\delta v) + (\delta u.\delta v))) \right] \qquad (2.59)\text{iii}$$

$$C_1 \sum_{\text{All members}} \left[\frac{EA}{2L^2} (\delta v^2)^2 \right] \qquad (2.59)\text{iv}$$

It can be seen from the above that Buchholdt has neglected higher order terms for $\delta \underset{\sim}{u}$ too early in his analysis (see equation 2.11) and the set of constants C_1, C_2, C_3, C_4 used in the cubic equation of S are inconsistent approximations in the order of small quantities retained.

The smallest positive root of S in the cubic equation (2.57) gives the value of the step length along $\underset{\sim}{v}_i$.

Methods are now discussed to determine the descent direction $\underset{\sim}{v}_i$.

2.8 Method of Steepest Descent

The method of steepest descent (2.3) is an iterative method for the solution of non-linear equations. It was used by Buchholdt (2.1) for the solution of the non-linear equations arising from the analysis of cable structures. The following is an outline of the

steepest descent method used by Buchholdt.

The gradient vector $\frac{\partial W}{\partial \underset{\sim}{u}_i} = \underset{\sim}{R}_i$ represents the out of balance force for the displacement vector $\underset{\sim}{u}_i$ in the direction of greatest increase in the total potential, where W is the scalar potential energy as a function of the N-dimensional space determined by the variables u_i, i = 1 - N.

At the K_{th} cycle of the iteration process the displacement vector is $\underset{\sim}{u}_{(K)}$. The norm of the out of balance force is given by

$$|R|_{(K)} = [(\frac{\partial W}{\partial u_{(K)}})^T (\frac{\partial W}{\partial u_{(K)}})]^{\frac{1}{2}} \qquad (2.60)$$

Dividing the gradient vector by $-|R|$ gives a unit vector $\underset{\sim}{v}_{(K)}$ in the direction of steepest descent of the potential energy. A distance S is moved along $\underset{\sim}{v}_{(K)}$ until the minimum value of the potential in this direction is found. The next displacement vector is given by

$$\underset{\sim}{u}(K + 1) = \underset{\sim}{u}_{(K)} + S\, \underset{\sim}{v}_{(K)} \qquad (2.61)$$

A simple representation of the surface of equal potential can be provided (Fig. 2.3) if N is 2. The shape of the potential illustrates some of the features of the method. Fig. 2.3 also assumes a very simple form of the function behaviour.

The directions of each successive descent are orthogonal and do not take into account any change in the shape of the potential function. For large N convergence is not always achieved and even with second order surfaces the example of a long narrow "valley" shows that most initial choices produce a long slow iteration although for such a simple form convergence is assured.

FIG 2.3

REPRESENTATIONOF SURFACE OF EQUAL POTENTIAL

(By Buchholdt)

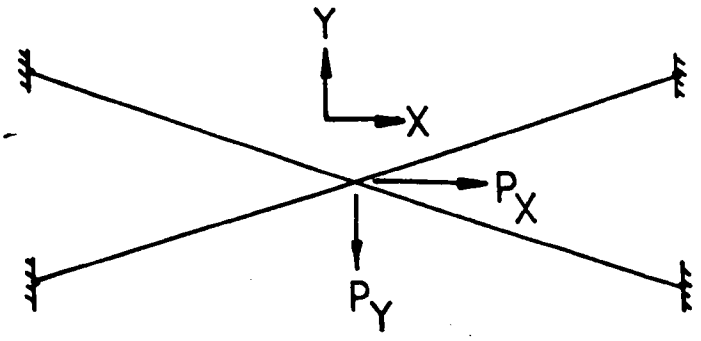

$W = W_{MINIMUM}$

$\frac{\partial W}{\partial u} = 0$

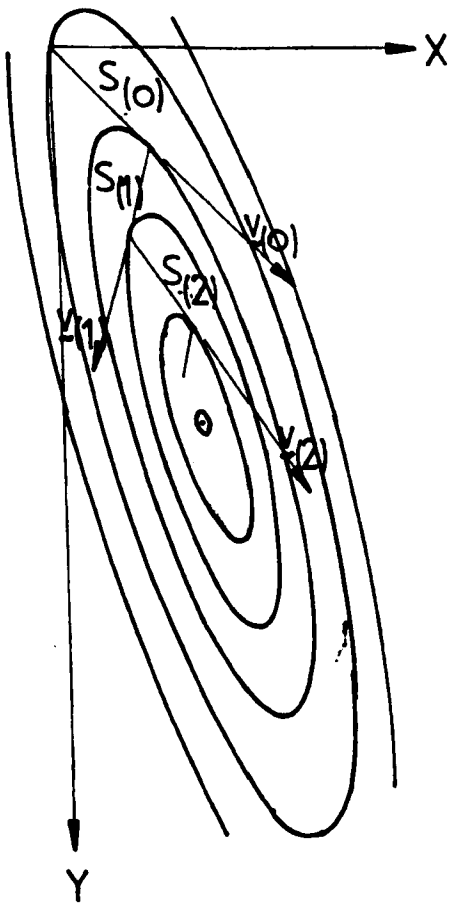

With the many degrees of freedom in even a modest structure and fourth order polynomial expressions for the potential gradient it is easy to obtain examples of a non converging sequence of steps. Earlier authors have recognised this effect.

2.9 Method of Conjugate Gradients

The conjugate gradients method was developed for the solution of linear simultaneous equations by Hestenes and Stiefel (2.4). The method is an iterative one involving a large number of repetitive calculations, so it has only become practicable since the advent of the electronic computer. The method has the advantage of being simple and requiring a minimum of computer storage space.

The algorithm as used by Hesteres and Stiefel for the solution of a set of linear equations $\underset{\sim}{P} = A\underset{\sim}{u}$ can be given as follows.

For an arbitrary $\underset{\sim}{u}_{(0)}$

$$\underset{\sim}{v}_{(0)} = \underset{\sim}{R}_{(0)} = \underset{\sim}{P} - A\underset{\sim}{u}_{(0)} \qquad (2.62)\text{i}$$

$$S_{(i)} = \frac{|R_{(i)}|^2}{(\underset{\sim}{v}_{(i)}, A\underset{\sim}{v}_{(i)})} \qquad (2.62)\text{ii}$$

$$\underset{\sim}{u}_{(i+1)} = \underset{\sim}{u}_{(i)} + S_{(i)}\,\underset{\sim}{v}_{(i)} \qquad (2.62)\text{iii}$$

$$\underset{\sim}{R}_{(i+1)} = \underset{\sim}{R}_{(i)} - S_{(i)}\,A\underset{\sim}{v}_{(i)} \qquad (2.62)\text{iv}$$

$$\underset{\sim}{v}_{(i+1)} = \underset{\sim}{R}_{(i+1)} + \frac{|R_{(i+1)}|^2}{|R_{(i)}|^2}\,\underset{\sim}{v}_{(i)} \qquad (2.62)\text{v}$$

Proof of convergence required that 'A') should be a symmetric and positive definate matrix.

Having chosen as estimate $\underset{\sim}{u}_{(0)}$ of the solution $\underset{\sim}{h}$, the initial step is to calculate the residual $\underset{\sim}{R}_{(0)}$ and the direction $\underset{\sim}{y}_{(0)}$ by equation (2.62)i. Then, having determined an estimate $\underset{\sim}{u}_{(i)}$ of $\underset{\sim}{h}$, the residual $\underset{\sim}{R}_{(i)}$ and the direction $\underset{\sim}{y}_{(i)}$, to compute $\underset{\sim}{u}_{(i+1)}$, $\underset{\sim}{R}_{(i+1)}$ and $\underset{\sim}{y}_{(i+1)}$ by equations (2.62)ii to (2.62)v successively.

Hestenes and Stiefel show that for a set of linear simultaneous equations the maximum number of iterations required for a solution apart from rounding is N, where N is the number of variables. They also show that the residuals $R_{(0)}$, $R_{(i)}$... are mutually orthogonal

$$\text{i.e.} \quad (R_{(i)} \cdot R_{(j)}) = 0 \qquad (i \neq j)$$

and the direction vectors $v_{(0)}$, $v_{(i)}$... are mutually conjugate

$$(v_{(i)} \cdot Av_{(j)}) = 0 \qquad (i \neq j)$$

Fletcher and Reeves (2.5) used the conjugate gradients method for a solution of functions of several variables. The basic algorithm was the same as for Hestenes and Stiefel except that the residual vector $\underset{\sim}{R}_{(i)}$ is replaced by a gradient vector $\underset{\sim}{g}_{(i)}$. By this means the method was shown to be quadratically convergent for successive linear searches when using any set of A conjugate directions.

Fletcher and Reeves also point out the inherent advantage of conjugate gradients over the steepest descent method, in that each new direction of search is calculated as part of each iteration cycle, thus avoiding the oscillatory behaviour characteristic of the steepest descent method.

2.10 Form Finding of Cable Structures

In the fabrication and forming of the initial unloaded shape of a cable structure there are two parameters which can be controlled during construction. They are the length and pretension force in each cable segment. For an economical structure these are chosen so far is as possible to evenly distribute stresses through the structure. The initialisation or form finding is therefore an essential requirement before the non-linear analysis can be performed.

In order that the non-linear analysis of cable structures be carried out the form of the structure in its initial unloaded state is required. This is also important practically as node positions and lengths of members are essential before fabrication of a model or full size structure can begin.

Published work (2.6) did not meet the requirements for a simple economical process to achieve the form of the model studies being considered. A general algorithm for the initial shape determination or form finding of cable structures is therefore not presented.

Methods involving linear equations for specific types of structure were developed for the form finding of cable structures. These methods have no bearing on the performance of the analysis of loaded cable systems presented earlier but have been chosen for ease of computation and for their suitability in the analysis of the model studies.

Form finding two dimensional structures

For a cable truss structure consisting of pretension cables joined by vertical members a simple graphical method (Fig. 2.4) can be used to determine the initial shape and prestress forces.

It is assumed that the structure is pin jointed, statically determinate and that the members are straight between joints. This method has been used to determine the initial shape required for the experimental cable truss structure investigated in Chapter 4. Values for the horizontal component of force in the pretension cables and the vertical hanger forces are prescribed (note the hanger forces need not be equal). The tension in the pretensioning cables can be measured directly on lines 01, 02, 03 etc. If the hangers are equally spaced horizontally then the length of each segment of the pretensioning cables can also be found by scaling the forces.

Form finding three dimensional structures

In the form finding of three dimensional structures the assumptions are, as for two dimensional structures, that the joints are pinned, the members are straight between joints and that the bending stresses in the cable are ignored. For convenience the cables are chosen to be orthogonal in plan.

The form finding can be expressed as a boundary value problem and solved by the method of finite differences. An orthogonal net gives the valuable simplification that the horizontal component of tension will be constant in both x and y directions.

Consider a general node and its four nearest neighbours (Fig. 2.5). The x and y coordinates of each node and the x, y and z

FIG 2.4

GRAPHICAL METHOD TO DETERMINE INITIAL SHAPE AND PRESTRESS FORCE IN CABLE TRUSSES WITH VERTICAL HANGERS

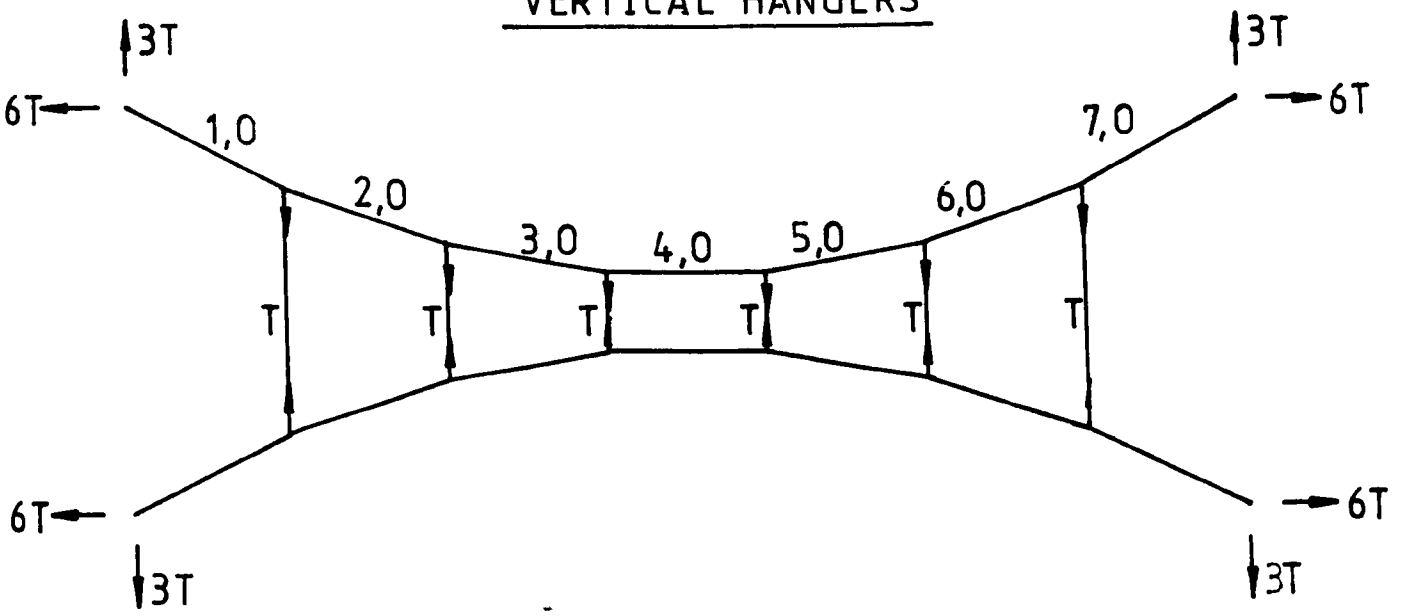

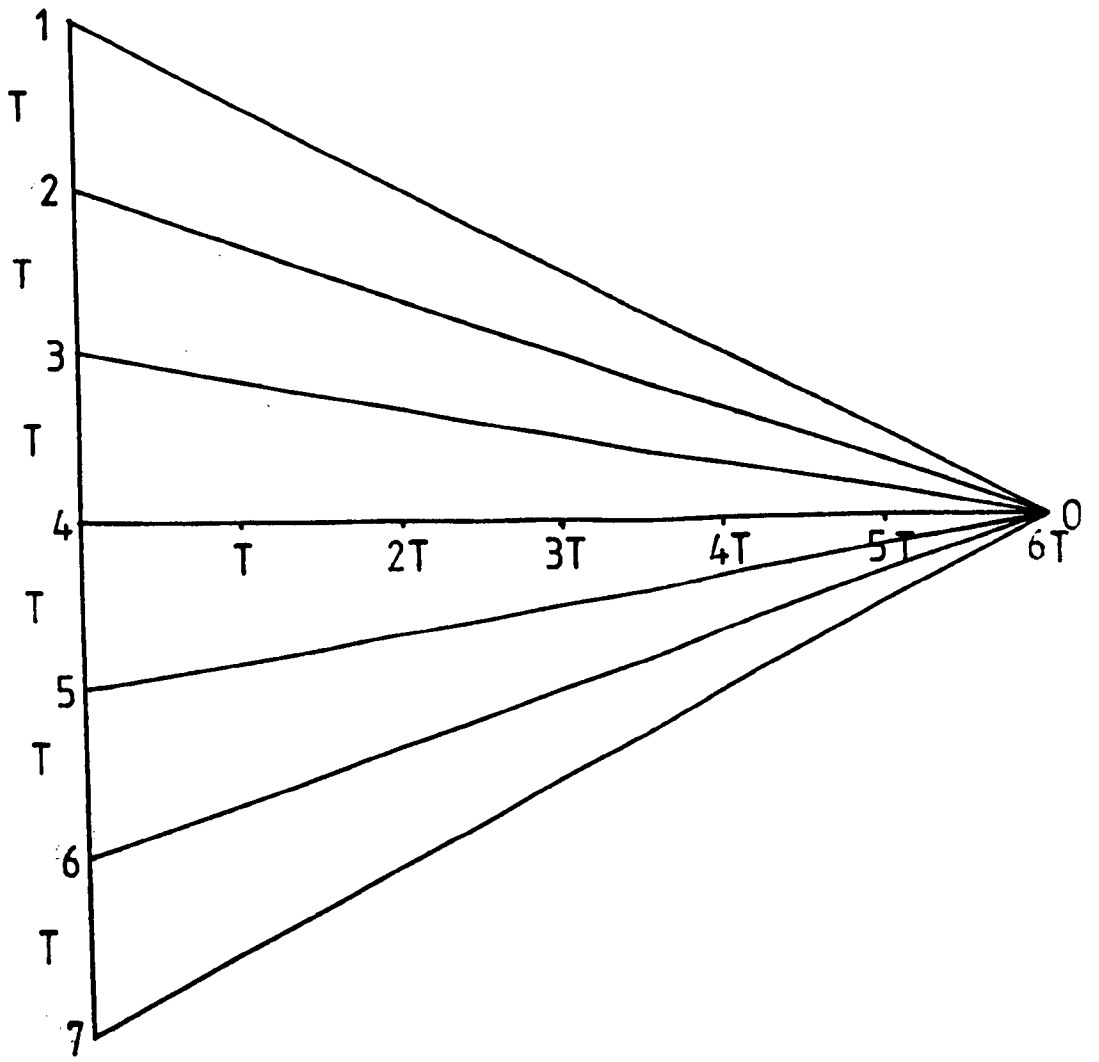

FIG 2.5

A GENERAL NODE IN AN ORTHOGONAL NET

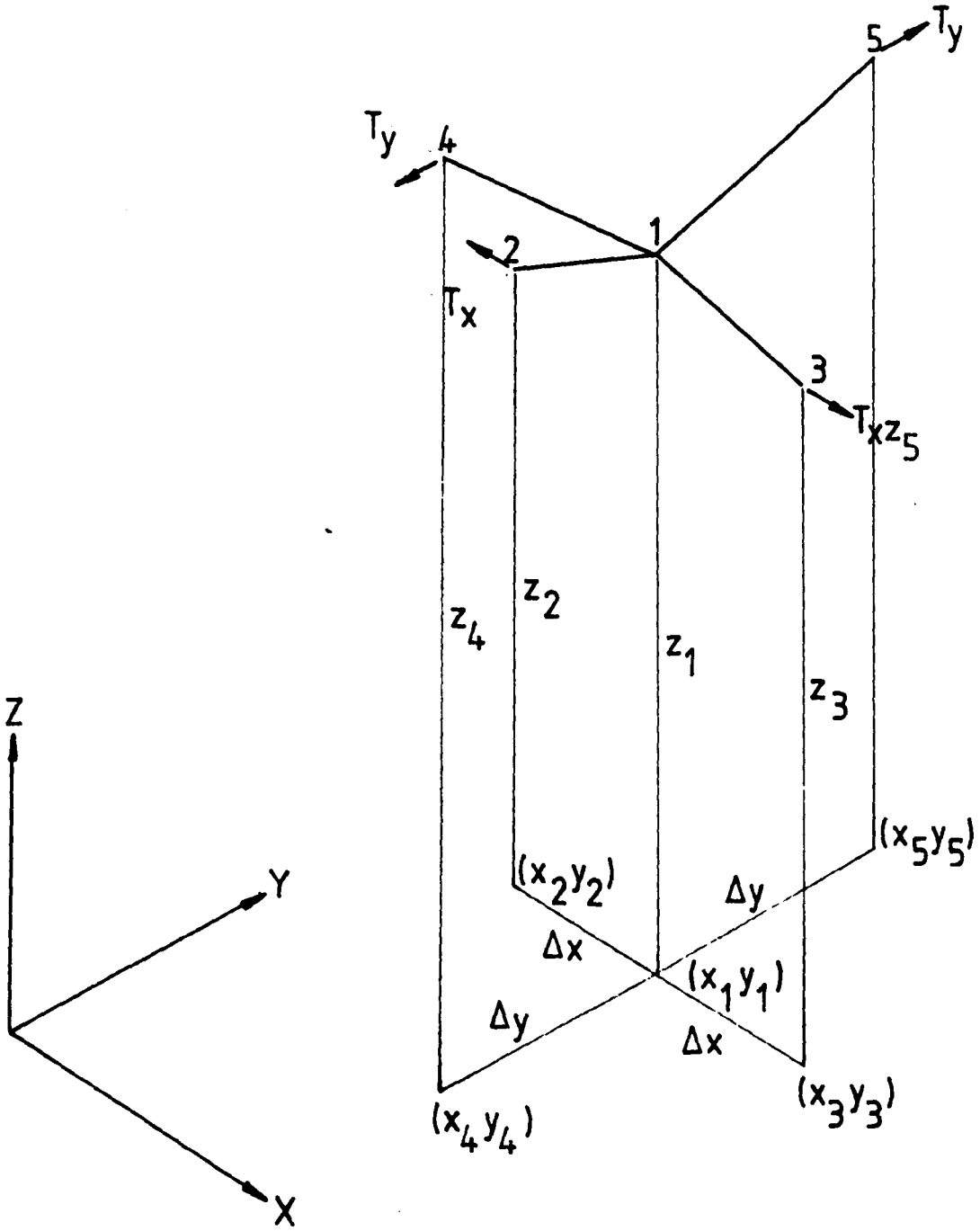

coordinates of the boundary nodes together with the horizontal component of tension in each member are prescribed. The unknown quantities are the z coordinates of each 'free' node and member tensions.

Resolving the cable forces vertically at nodes 1 we obtain the equation

$$\frac{(z_1 - z_2)}{L_{1,2}} T_{1,2} + \frac{(z_1 - z_3)}{L_{1,3}} T_{1,3} + \frac{(z_1 - z_4)}{L_{1,4}} T_{1,4} + \frac{(z_1 - z_5)}{L_{1,5}} T_{1,5} = 0$$

or in suffix notation $\sum_j \frac{T_{ij}\,\delta z_{ij}}{L_{ij}} = 0$ (2.63)

If the net is orthogonal then $\frac{T_{1,2}}{L_{1,2}} = \frac{T_{1,3}}{L_{1,3}} = \frac{T_x}{\Delta_x}$ and $\frac{T_{1,4}}{L_{1,4}} = -\frac{T_{1,5}}{L_{1,5}} = \frac{T_y}{\Delta_y}$ where T_x and T_y are the horizontal components of the member tensions in the x and y directions respectively.

Equation (2.63) becomes

$$2\left\{\frac{T_x}{\Delta_x} + \frac{T_y}{\Delta_y}\right\} z_1 - \frac{T_x}{\Delta_x} z_2 - \frac{T_x}{\Delta_x} z_3 - \frac{T_y}{\Delta_y} z_4 - \frac{T_y}{\Delta_y} z_5 = 0$$

This operation is then carried out at each node in turn and the equations expressed in matrix form.

$$[A][z] = [0] \qquad (2.64)$$

where $a_{ii} = 2\left\{\frac{T_x}{\Delta_x} + \frac{T_y}{\Delta_y}\right\}$, $a_{ij} = -\frac{T_x}{\Delta_x}$ or $-\frac{T_y}{\Delta_y}$

Without introducing boundary conditions there are an infinite number of solutions for z in the above equation.

So that the equilibrium equation can become determinate consider the general boundary node and its four nearest neighbours (Fig. 2.6). Resolving forces vertically at node 1 and collecting terms gives.

$$\left[\frac{T_{1,2}}{L_{1,2}}+\frac{T_{1,3}}{L_{1,3}}+\frac{T_{1,4}}{L_{1,4}}+\frac{T_{1,5}}{L_{1,5}}\right] z_1 - \frac{T_{1,2}}{L_{1,2}} z_2 - \frac{T_{1,5}}{L_{1,5}} z_5 = \frac{T_{1,3}}{L_{1,3}} z_3 + \frac{T_{1,4}}{L_{1,4}} z_4 \qquad (2.65)$$

In matrix form we have

$$[\,A\,]\;[\,z\,] \;=\; [\,b\,] \qquad (2.66)$$

Let the number of 'free' nodes be n and the number of fixed ones be nf ordered sequentially

Then $b_j = 0$ where $j \leq n$

$$b_j = \frac{T_{ij}}{\Delta x_{ij}} z_j \quad \text{where} \quad j > n \leq n + nf.$$

A computer program based on the above theory was written for the shape determination of cable structures with fixed boundaries, a flow chart for the program is shown in Fig. 2.7.

2.11 Cable Structures with Flexible Boundaries

Practical cable structures rely on an anchorage or a series of stiff members to resist the tensile forces in the cable members. In the simplest case the boundary member can be thought of as a series of fixed points. The cable structure can then be analysed using the theory already developed. More generally however the boundary member is flexible (i.e. a ring beam) which deflects when subject to load.

FIG 2.6

A BOUNDARY NODE IN AN ORTHOGONAL NET

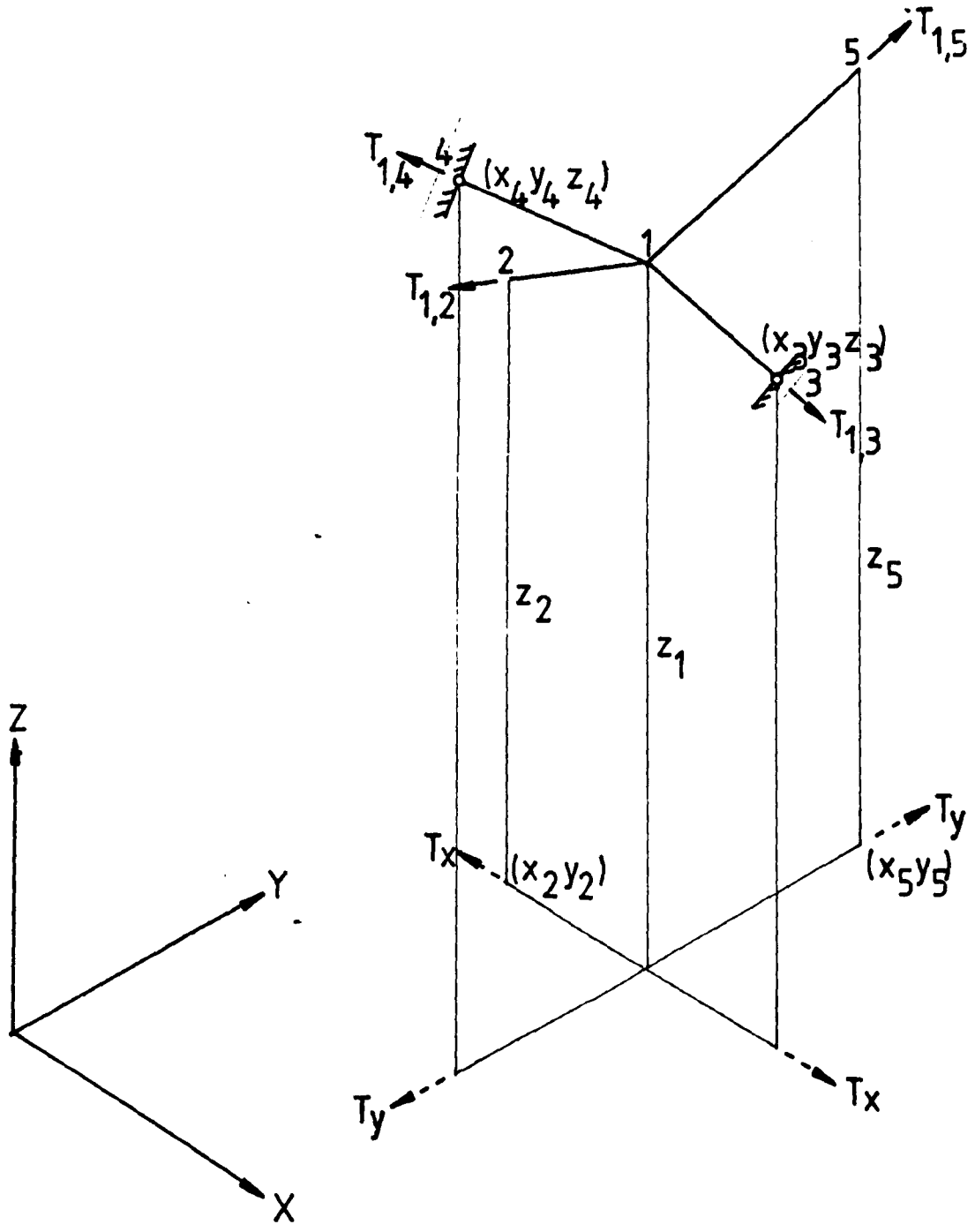

FIXED BOUNDARY POINT

FIG 2.7

FLOW CHART FOR SHAPE DETERMINATION OF CABLE STRUCTURES WITH FIXED BOUNDARIES

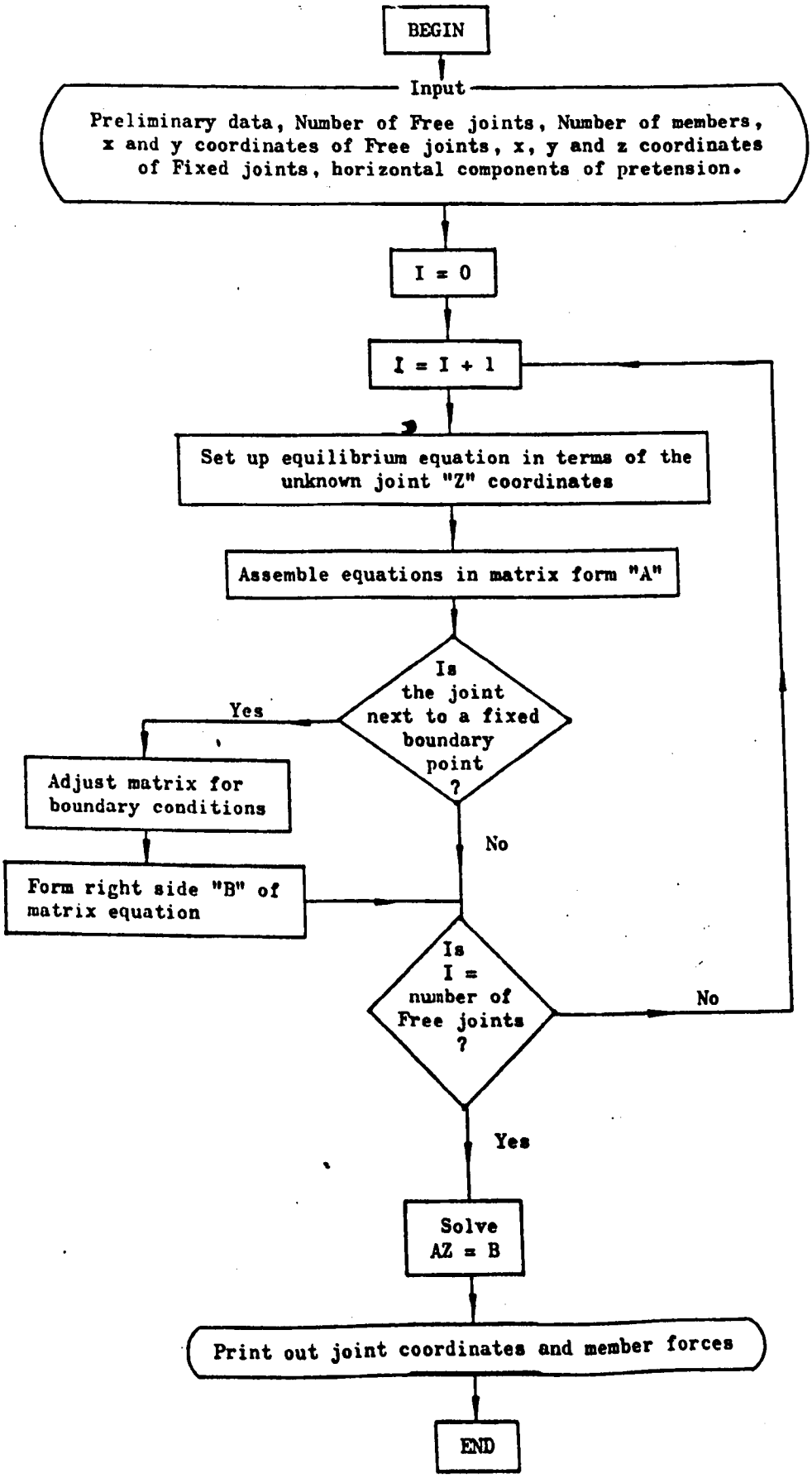

The boundary members must be able to resist axial forces as well as general bending action.

The boundary is considered to be made up of a series of beam elements (Fig. 2.8). Node positions occur whenever there are changes in section properties, anchorage points for cable members or changes in direction along the boundary member. Curved members can be approximated accurately by a series of chords.

The analysis of the boundary member follows the generally accepted stiffness approach (2.7). The member stiffness matrices are formed for the beam elements and transformed to form the structural stiffness matrix for the complete boundary (Appendix 2.1).

It was expected that there would be a standard ICL package available to analyse the edge beam, however it was found that the 'frame' analysis package was not a general three dimensional analysis. It assumed that the member v-v axis remained parallel to the global XY plane. This is not the case for many cable structures and in particular for the simple ring beam used in the model analysis. A computer program was therefore written for the general three dimensional case (Fig. 2.9). Use was made in the program of the banded nature of the stiffness matrix to reduce the computer storage requirements. For the example of a boundary consisting of a series of beam elements the minimum computer storage requirement for the stiffness matrix is $12 \times 6\ n_b$ where n_b is the number of boundary nodes labelled consecutively.

The analysis of boundary and cable net are now combined in a two stage iterative process. As a first step the boundary is assumed fixed in its initial equilibrium position and the loaded cable

FIG 2.8

BEAM ELEMENTS OF BOUNDARY MEMBER

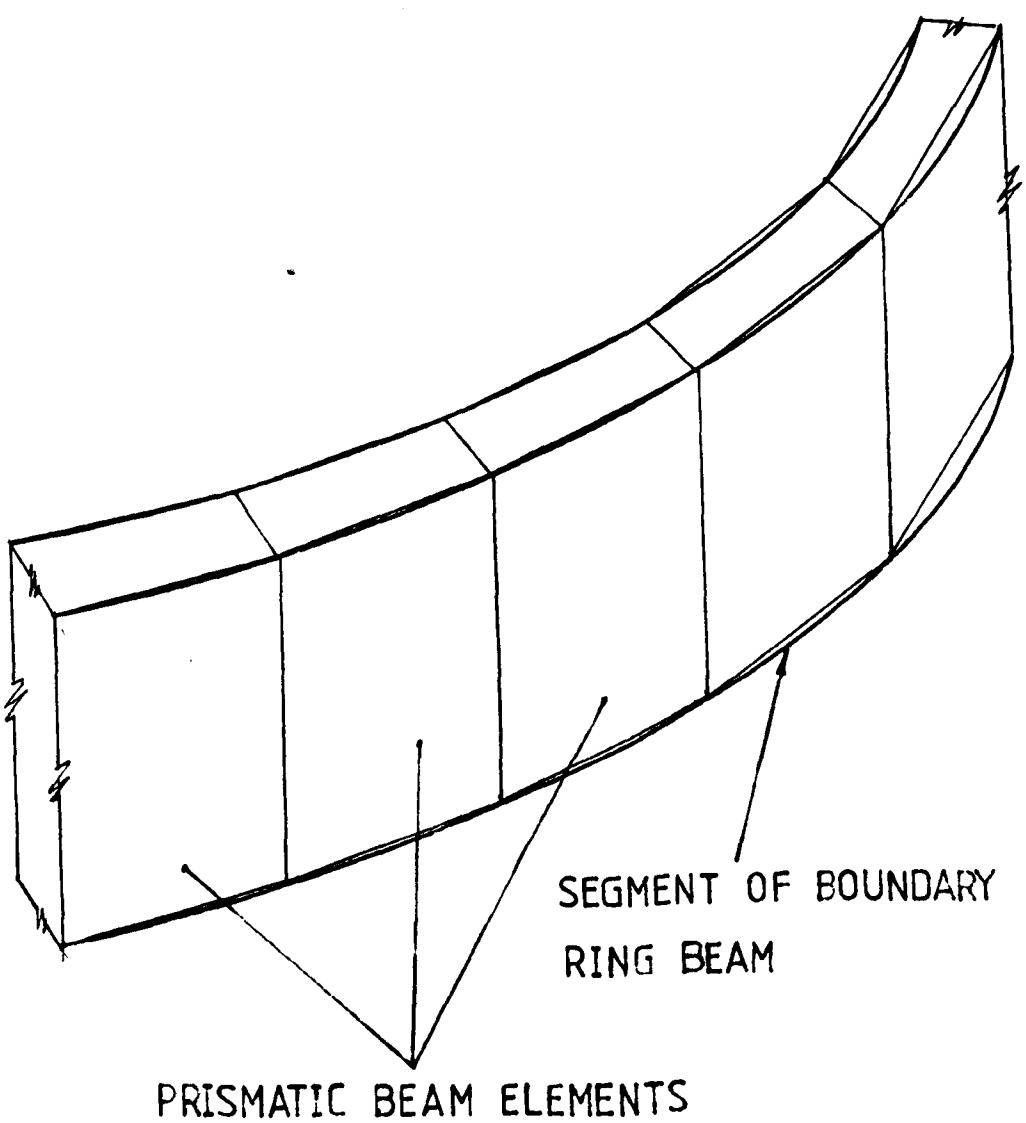

FIG 2.9

FLOW CHART FOR THE ANALYSIS OF CABLE STRUCTURES WITH FLEXIBLE BOUNDARIES

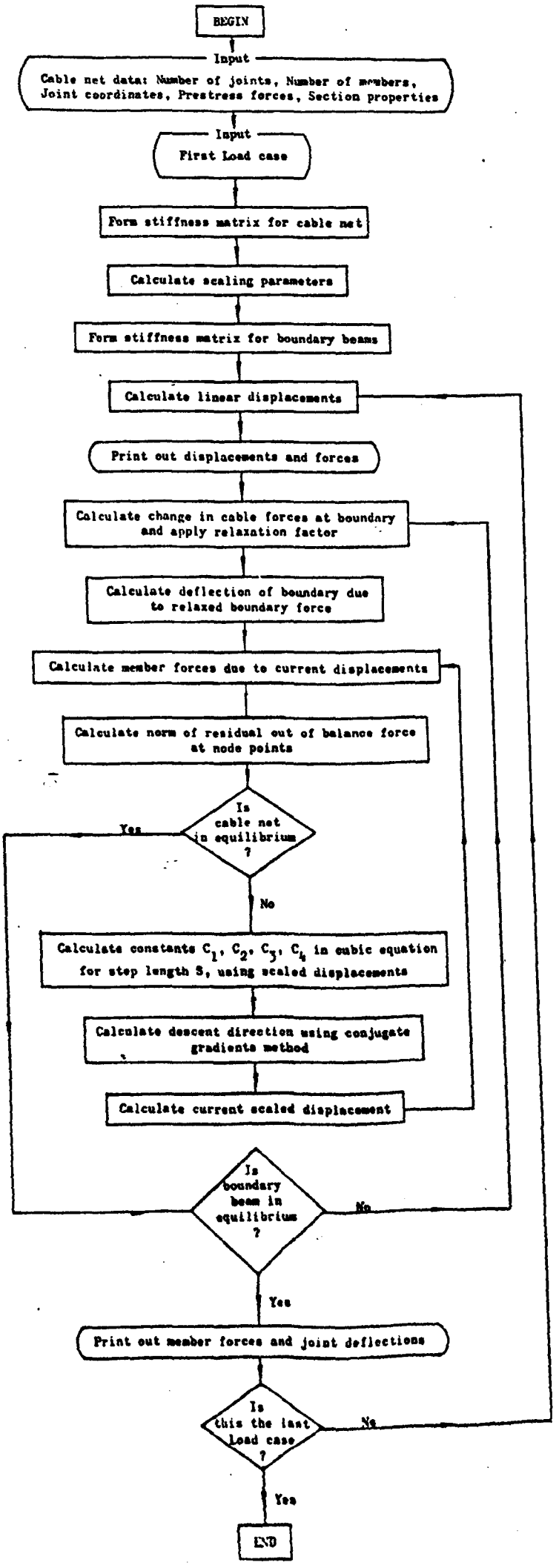

structure is analysed. The resulting change in the forces acting on the boundary are then applied to the boundary member and the new boundary position found. The cable net is then analysed for this new boundary position and the process repeated until the change in the member forces between successive iterations is less than a prescribed tolerance.

Consideration was given to a single analysis combining cable and boundary members to avoid the second stage of the iteration. The two components behave so differently in the analysis that the conclusion was reached that they should be handled separately and this was confirmed in subsequent calculation.

2.12 Method of Calculation

The two commonly available general methods of solution for the non-linear equilibrium equations developed earlier are by minimisation of the total potential energy using iterative techniques and by successive linear approximations. The incremental method was considered to be expensive in terms of computing time and storage requirements, also the nearness to the final solution is difficult to measure.

Conflicting evidence (2.8) on the effectiveness of the two most widely used methods, steepest descent (S.D.) and conjugate gradients (C.G.) is apparent in the literature. A comparative study was therefore carried out starting with two very simple two dimensional truss structures (Fig. 2.10). For the simplest structure little difference was found in the rates of convergence (Fig. 2.11). The norm of the out of balance forces $|R|$ (Equation 2.60) is used as

FIG 2.10

TWO SIMPLE PRETENSIONED TRUSS STRUCTURES

TRUSS 1

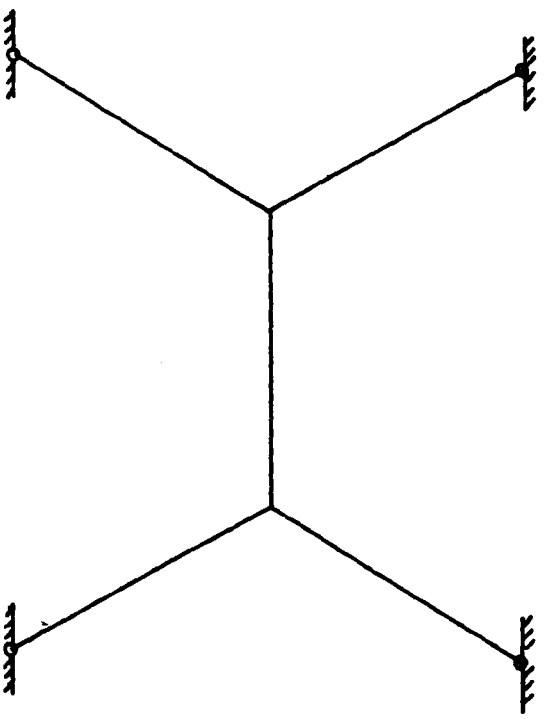

TRUSS 2

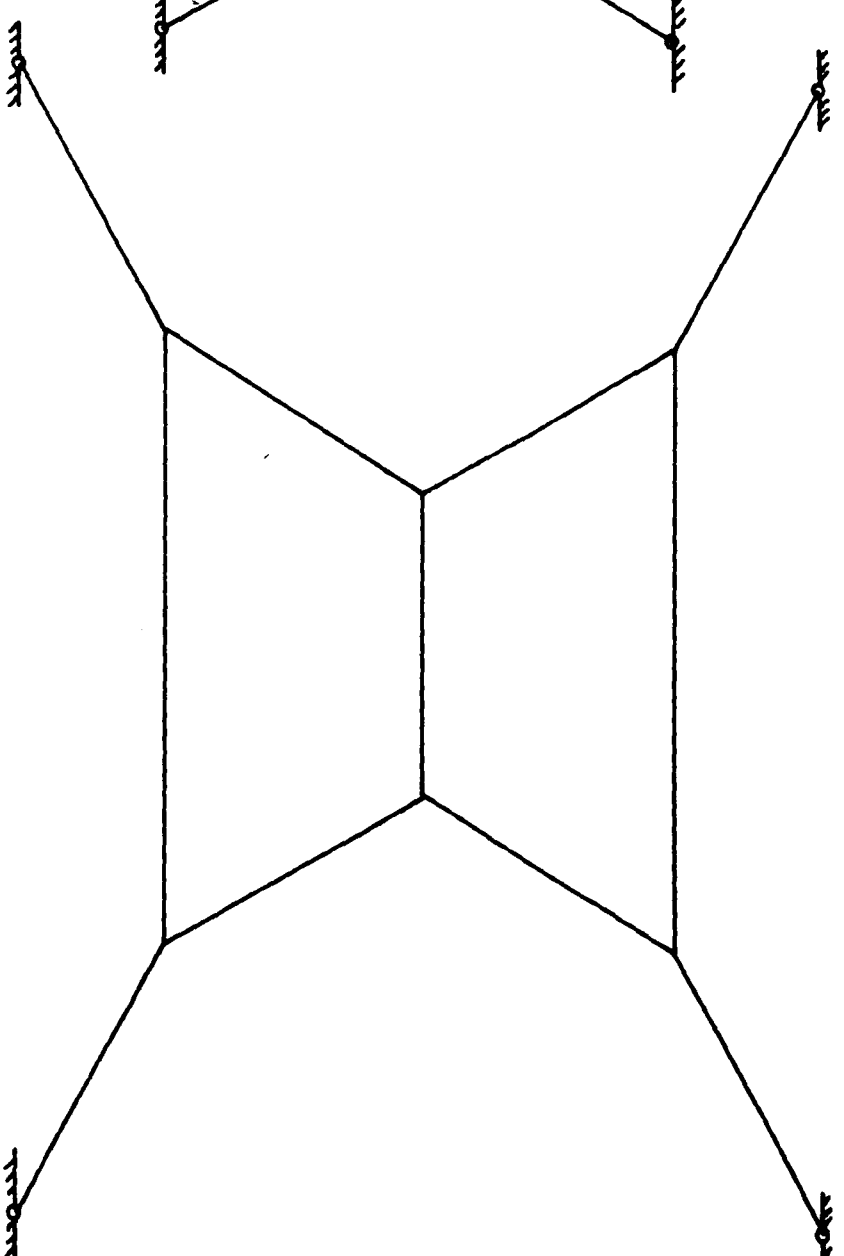

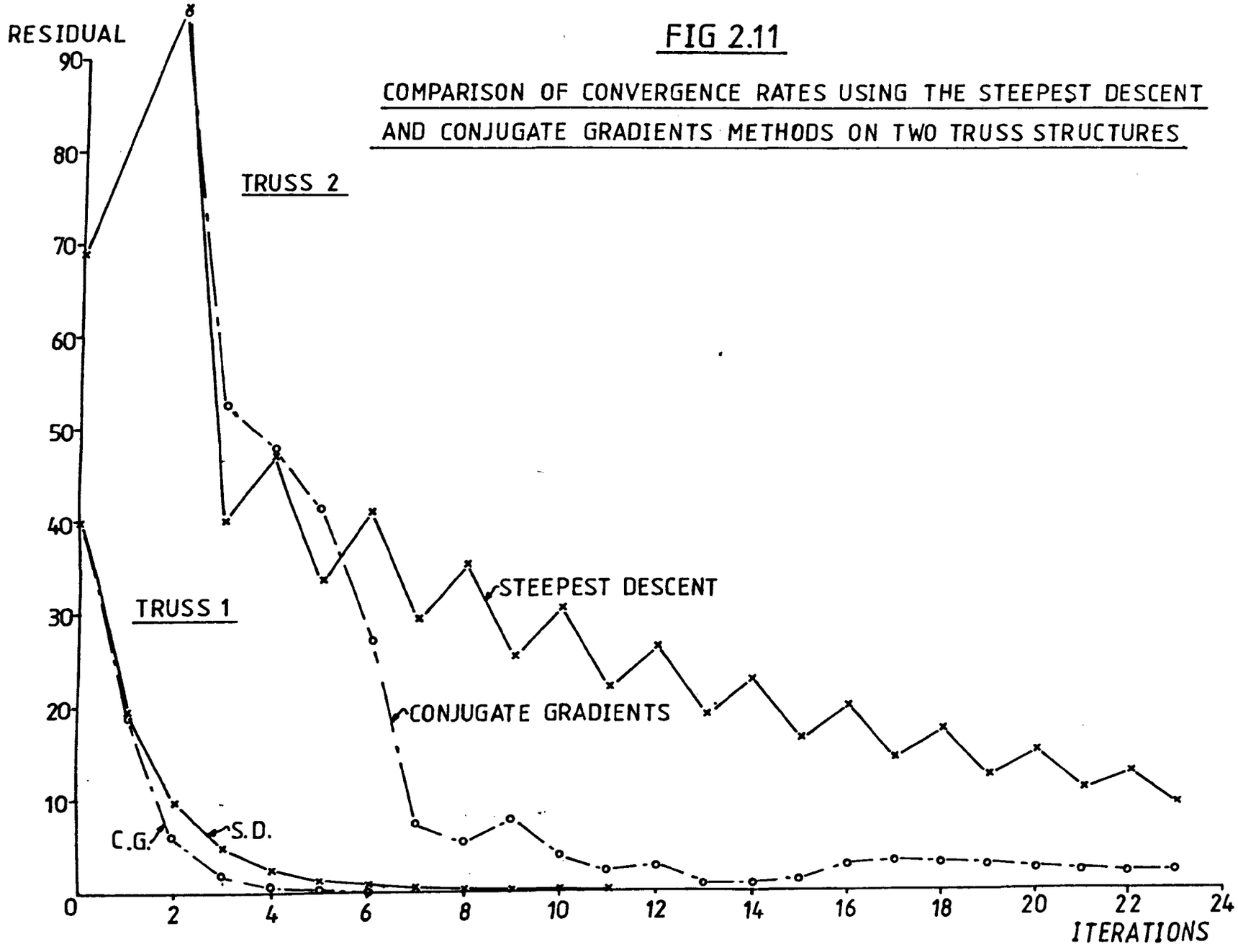

FIG 2.11

COMPARISON OF CONVERGENCE RATES USING THE STEEPEST DESCENT AND CONJUGATE GRADIENTS METHODS ON TWO TRUSS STRUCTURES

a measure of the rate of convergence. The value of $|R| \rightarrow 0$ indicates a well behaved convergence.

With increased number of g degrees of freedom for the second structure the oscillation nature of the (S.D.) method becomes apparent in Fig. (2.12) which shows the deflected position of the joints after each cycle of iteration.

For structures with a larger number of degrees of freedom an output of deflected positions after each cycle of iteration is not practicable, thus increasing the importance of using $|R|$ as a measure of the degree of convergence. The relation between $|R|$ and actual member forces is investigated by carrying out an analysis to different limits of $|R|$, and comparing the values of deflection and tension in the members, (Fig. 2.13).

The S.D. method was discounted as the rate of convergence is considerably less than that for the C.G. method. An oscillatory behaviour is also noted in the C.G. method with the increase in the number of degrees of freedom. It is possible to think of a 'wave of deflections' moving along the structure. The number of iterations per cycle of oscillations of the norm $|R|$ corresponds to the number of degrees of freedom in the structure, (Fig. 2.14). This behaviour is due to the ill-conditioned nature of the 2D problem, where the principal stresses occur horizontally and the principal deflections are vertical.

Two solutions were proposed to overcome the difficulty of ill-conditioning. The first was to introduce a relaxation factor of between 0.1 and 0.9 times the steplength in the descent direction. Buchholdt and McMillan (2.9) used a relaxation factor to improve the converg-

FIG 212

DEFLECTED POSITION OF TRUSS JOINTS AFTER EACH CYCLE OF ITERATION USING THE STEEPEST DESCENT METHOD

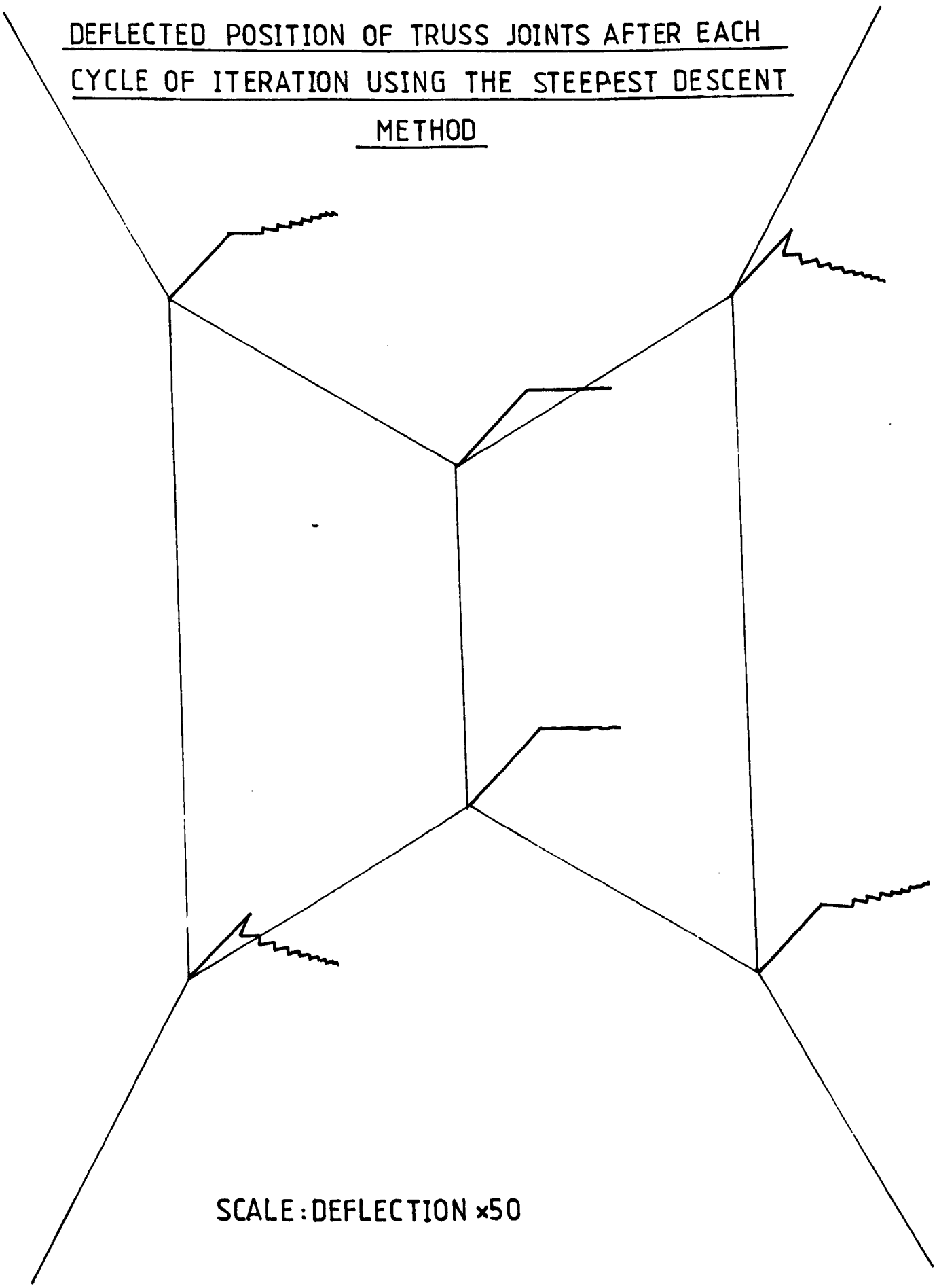

SCALE : DEFLECTION ×50

FIG 2.13

CABLE TRUSS* MEMBER FORCES AND JOINT DEFLECTIONS FOR ANALYSIS CARRIED OUT TO DIFFERENT LIMITS OF R

MEMBER NUMBER	MEMBER FORCE (N)			
	LINEAR	R<0.05 (15 ITERATIONS)	R<0.0001 (90 ITERATIONS)	R<0.000001 (162 ITERATIONS)
1	25.278	36.920	36.499	36.506
2	410.59	405.01	405.74	405.72
3	17.938	18.058	18.375	18.376
4	25.166	37.114	36.240	36.236
5	406.88	400.55	401.87	401.85
6	18.000	18.413	18.399	18.400
7	25.128	37.458	36.022	36.040
8	403.87	397.97	398.81	398.79
9	17.997	18.330	18.438	18.435
10	25.103	37.211	35.894	35.912
11	401.71	394.65	396.58	396.57
12	18.001	18.355	18.404	18.406
13	25.104	38.322	35.852	35.847
14	400.39	393.46	395.20	395.23
15	17.999	18.464	18.423	18.424
16	25.105	38.369	35.840	35.827
17	399.95	392.75	394.74	394.77
18	17.999	18.464	18.423	18.424

JOINT NUMBER	VERTICAL DEFLECTION (mm)			
	LINEAR	R<0.05	R<0.0001	R<0.000001
1	3.7826	3.8193	4.1179	4.1178
2	3.3832	3.4145	3.6977	3.6976
3	6.7360	6.4114	6.6522	6.6504
4	6.4114	6.0716	6.3132	6.3113
5	8.9003	8.5099	8.5294	8.5269
6	8.6342	8.2344	8.2505	8.2481
7	10.604	9.9570	9.8792	9.8806
8	10.376	9.9721	9.6415	9.6429
9	11.370	10.692	10.522	10.524
10	11.162	10.473	10.304	10.306
11	11.370	10.692	10.522	10.524

LOAD = 16.85 N/JOINT

*FOR DIAGRAM OF TRUSS SEE FIG 4.3 p.102

FIG 2.14

GRAPH OF RESIDUAL FORCE AGAINST ITERATION NUMBER FOR THE CONJUGATE GRADIENTS METHOD

For model truss Fig 4.3

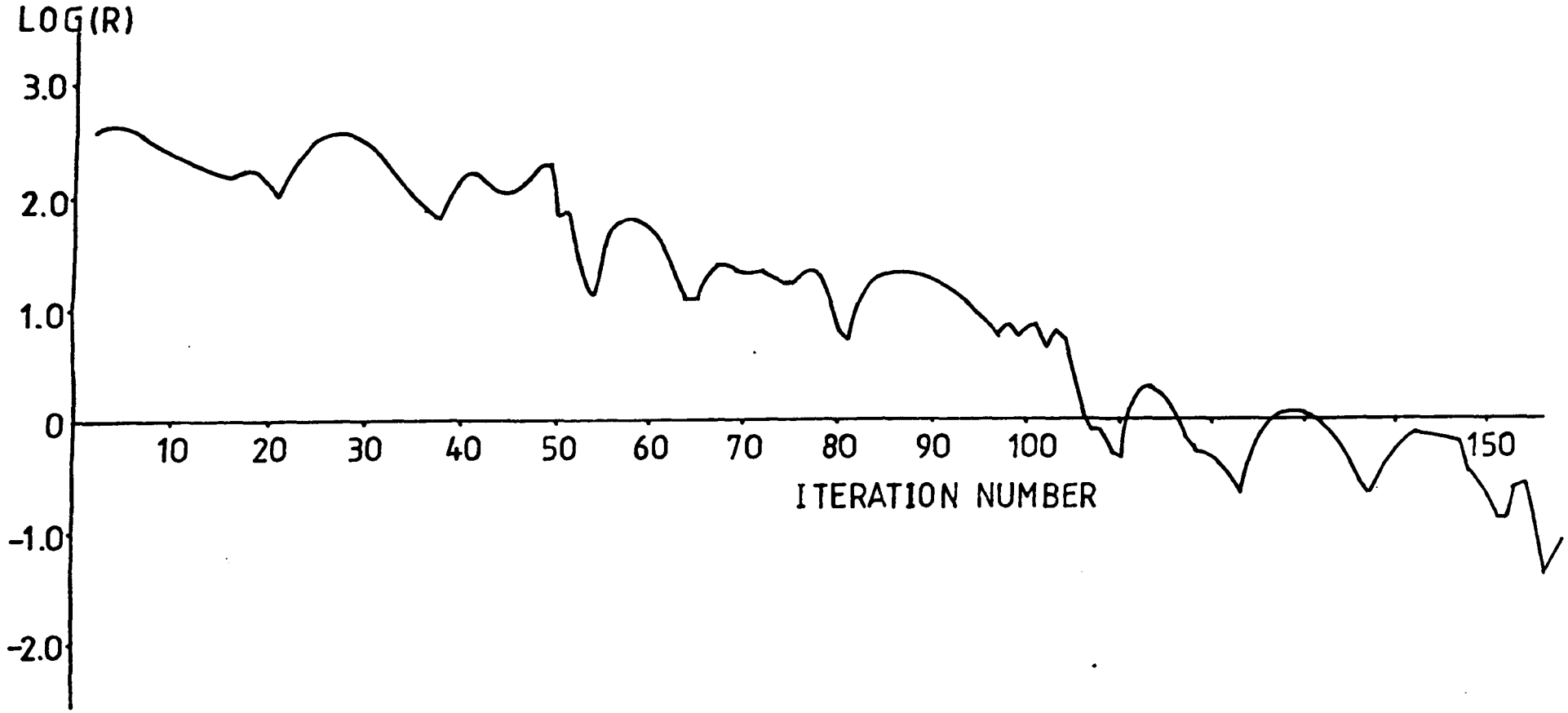

ence rate of the steepest descent method but did not apply it to the conjugate gradients method. No convenient way could be found to predict the optimum relaxation factor, other than by trial and error so the second solution of scaling was introduced.

The object of scaling is to lessen the effect of ill-conditioning by changing the shape of the potential energy surface. In a simple way this can be thought of as widening the narrow valleys of the two dimensional potential surface considered earlier, (Fig. 2.3).

Scaling is applied to the nodal deflections

$$\underset{\sim}{u}_i = h_i \, \underset{\sim}{u}^s_i \qquad (2.67)$$

where h_i is the scaling factor and $\underset{\sim}{u}^s_i$ the scaled deflection. If this substitution is carried through the analysis described earlier (equations 2.50-2.58) then the scaled gradient vector

$$\frac{\partial W}{\partial \underset{\sim}{u}^s} = h \, \frac{\partial W}{\partial \underset{\sim}{u}} \qquad (2.68)$$

and the scaled descent direction

$$\underset{\sim}{v}^s_i = h_i \, \underset{\sim}{v}_I \qquad (2.69)$$

The steplength S along the descent direction is calculated as before using equation (2.57) and the next scaled displacement vector in the iteration process is given by

$$\underset{\sim}{u}^s(K+1) = \underset{\sim}{u}^s(K) + S \, \underset{\sim}{v}^s(K) \qquad (2.70)$$

When the required limit for the residual out of balance force has been reached then the actual nodal displacements are found by

substitution in equation (2.67). The difficulty now arises in choosing the values for h_i the set of scaling constants. In common with other authors is was found that by choosing $h_i = \frac{1}{\sqrt{K_{ii}}}$, where K_{ii} is the diagonal term in the linear stiffness matrix, that satisfactory results were obtained.

As mentioned earlier considerable advantage was found in using the linear approximation analysis as a starting point for the iterative solution; this advantage does not appear to have been used by previous authors. Fig. 2.15 illustrates the comparative convergence rates obtained for the different iterative methods used.

FIG 2.15

COMPARATIVE CONVERGENCE RATES FOR DIFFERENT ITERATIVE METHODS

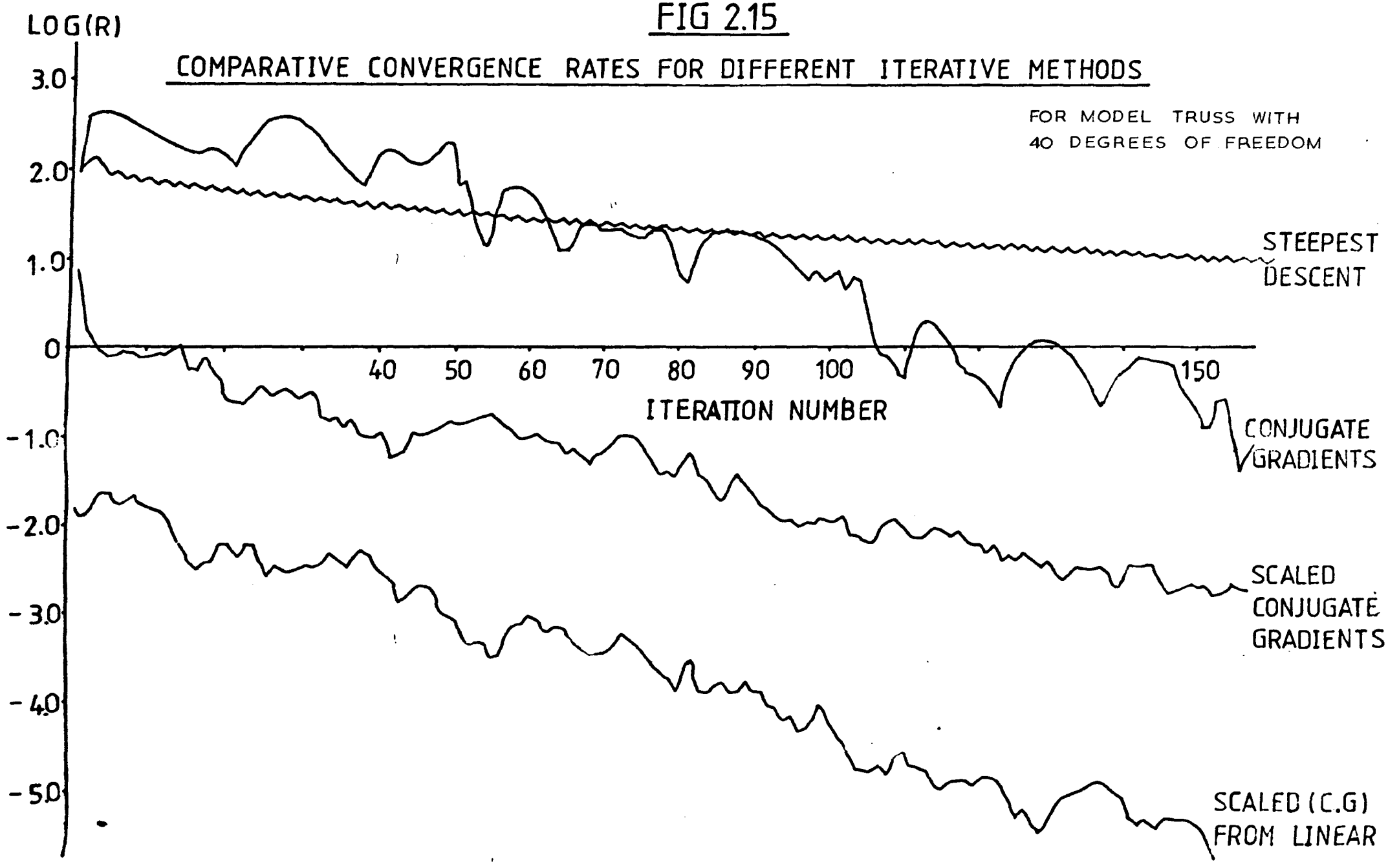

CHAPTER 3

MEASUREMENT METHODS USED IN MODEL ANALYSIS

3.0 Introduction

In this chapter the measurement techniques used in the model analysis described in Chapters 4 and 5 are introduced; particular attention is given to the methods used for the measurement of member forces and nodal displacements in cable structures. The main requirements for the measurement methods were that they were precise, easily repeatable and did not affect the value of the variable they were seeking to measure.

The purpose of this model analysis was to primarily provide data on the behaviour of cable structures subject to load. The models were required to display non-linear behaviour for comparison with the refined non-linear theoretical analysis presented in Chapter 2.

Models are not intended to be exact replicas of any full sized structure but to represent the type of behaviour exhibited by practical cable structures. Where the need to provide data comes into conflict with the representation of a practical cable structure, the data is given precedence, for example in the case of nodal displacements. In practical structures displacements are kept to a minimum so that the fabric of the building is not affected, i.e. roof finishes where excessive deflections may cause leakage or ponding, whereas in model structures large displacements are desirable to reduce the error factor in the measured result.

3.1 Tension Measurement in Cables

The main requirement for a tension measuring device in a cable structure is to measure the tension force in a cable accurately without affecting the force in the cable or the behaviour of the structure as a whole. For this reason the introduction of a dynamometer along the length of the cable was disregarded as this would necessarily impose a load on the cable and alter the stiffness along its length.

The possibility of attaching an electrical resistance strain gauge directly onto the cable was discounted due to the small diameter of the cable.

The two methods which were investigated involved attaching a device to the wire which was independently supported thus imparting a minimum of force to the wire.

The first method investigated involved clamping a known length of wire and applying a known lateral displacement at the mid-point along its length thus inducing a bending moment in the clamping device (Fig. 3.1). This bending moment was measured by electrical resistance strain gauges and by calibration the tension in the wire could be found from the bending moment. The same principal has been applied in practise in the design of overload devices on crane cables. Difficulty was found in practice due to the friction effects at the clamped supports which affected the tension in the wire by up to 7%.

The second method of tension measurements using the vibrational characteristic of the wire is now considered in more detail.

FIG 3.1

MEASUREMENT OF CABLE TENSION BY INDUCING BENDING IN A STEEL BAR

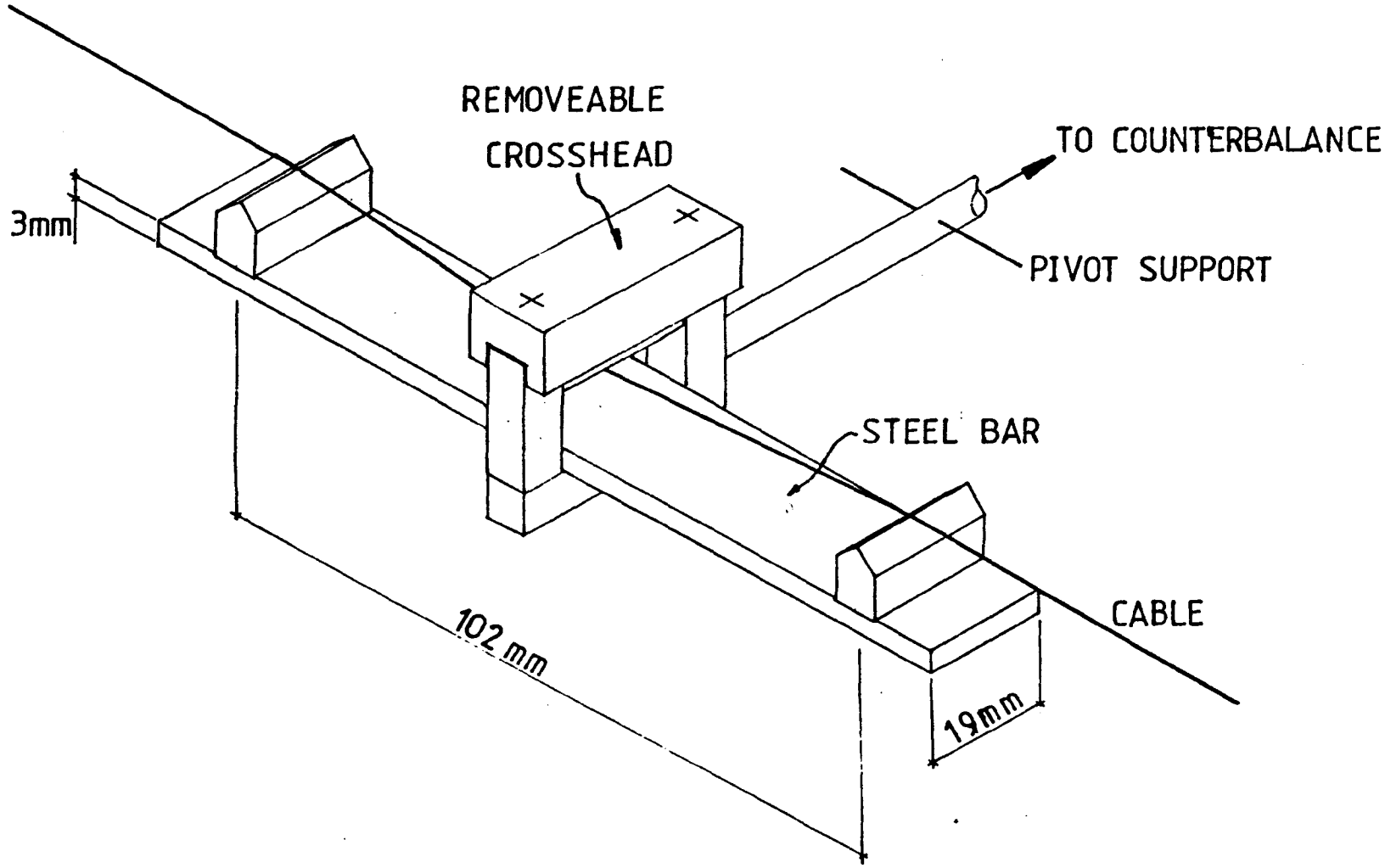

3.2 The Vibrating Wire Method of Tension Measurement

The versatility of the vibrating wire technique has been shown by previous experimenters with wire models for use in tension measurement on cable nets and trusses (3.1, 3.2). The technique has also been used to measure long term strains in concrete with gauges implanted in the mass of the concrete or mounted on the surface (3.3, 3.4).

The method makes use of the relation between the tension in a known length of wire and its natural frequency of vibration. All vibrating wire devices require a means of plucking the wire so that it vibrates at its natural frequency and a method of measuring the frequency thus induced. A single device can be used to combine both of the above functions.

A pulse of current passed through an electromagnetic coil placed between the two ends of the wire will act as a plucking device, provided that the wire is magnetic. The vibrating wire then induces an oscillating voltage, in the same coil, the frequency of which can be measured by an electric counting instrument.

When Nooshin and Butterworth (3.2) investigated the behaviour of a prestressed cable roof model, the tensions in the prestressing and suspension cables were measured using a vibrating wire transducer. Clamps determined the length of wire to be vibrated. The voltage induced in the plucking coil was passed to a counting instrument which recorded the period of 100 oscillations.

The relation between tension and frequency for a vibrating string is of the form

$$f = \frac{1}{2L}\sqrt{\frac{T}{m}} \qquad (3.1)$$

where L = length of vibrating string

m = mass/unit length of string

T = tension

The above relation holds for a uniform filament which has no flexural rigidity. Although Nooshin and Butterworth claim that for stranded cable the above relation is followed very closely it is not thought sufficiently accurate for this work. The stiffness of the wire was found to be significant.

With their transducer design Nooshin and Butterworth obtained an accuracy of 2% in the range 50N - 1000N for a 1.32 mm diameter cable.

The vibrating wire method has also been used to measure tensions in two dimensional pretensioned cable structures. Krishna (3.1) carried out experimental work on a plane pretensioned cable structure of 1.02 m span made of single strand stainless steel wire. The vibrating wire method was used as a strain measuring device fulfilling the two major requirements.

(i) The device should not alter the force or stiffness in the wire.

(ii) It should show no drift with time and should respond only to changes in force.

Krishna relates tension to frequency by the formula

$$f = \frac{1}{2L^2}\sqrt{a^2 x^2 + \frac{TL^2}{m}} \qquad (3.2)$$

where $a^2 = \frac{EI}{m}$ EI is the wire stiffness.

It can be shown that the above formula corrects for flexural stiffness but assumes perfectly pinned ends.

Krishna encountered difficulty in plucking the stainless steel wire so in order to make the wire locally magnetic in the region of the coil a 0.1 mm diameter soft steel wire was wound round the hanger wire. Due to the local increase in the mass of the wire from the presence of the soft steel wire and because of the fixity at the ends of the wire due to clamping Krishna abandoned the theoretical relationship in favour of a separate calibration for every wire. This is a considerable limitation since separate calibration must be carried out for any change in gauge length or diameter of the vibrating wire. Methods were obtained to avoid this experimental disadvantage.

Krishna found that for a gauge length of less than 90 mm the vibrations in the wire could not be sustained long enough to record them. A gauge length of 95.5 mm was therefore adopted. An accuracy of 1% is claimed for the typical value of 5.4Nin the 0.25 mm diameter wire.

Both Krishna, and, Nooshin and Butterworth, have shown the feasibility of the vibrating wire method and that accurate results can be obtained. Previous vibrating wire theory though has been somewhat over simplified and has failed to predict the frequency of vibration for given tensions in the wire. Experimenters in the past have relied on calibration curves to obtain a relation between the tension in the wire and its natural frequency of vibration.

3.3 Design of Vibrating Wire Gauge

To identify the problems of excitation and maintenance of an adequate vibration in wires, tests were conducted on single and multistrand cables using a commercially available coil. With the chosen wires the tests proved satisfactory for all of the experimental requirements provided certain precautions were taken:

i) The gauge length of wire to be vibrated must be appropriate for the wire thickness and tension to be measured. For convenience of working a standard length of 229 mm was chosen for all of the experimental work. Fig. 3.2 illustrates the range of response for different thicknesses and gauge lengths of wire.

ii) Consistency of end fixing for each new clamp position is important. The end clamps were provided with guides to give a precise location between the top and bottom clamping surfaces. Differences in frequency between encastré and pinned ends can be as much as 15%.

iii) Independent support and the use of a counterbalance ensured that a minimum of force was transmitted to the wire due to the self wt. of the gauge.

iv) The distance between the electromagnetic coil and the wire is important : too small a gap and the coil interferes with the vibrating wire, too large a gap prevents the coil plucking the wire. A gap of 2 mm was suitable for the wires used. The upper surface of the wire end clamp was fixed in position ensuring that the distance between the electromagnetic coil and the wire remained constant for different thicknesses of wire.

FIG 3.2

RANGE OF RESPONSE FOR VIBRATING WIRE GAUGE

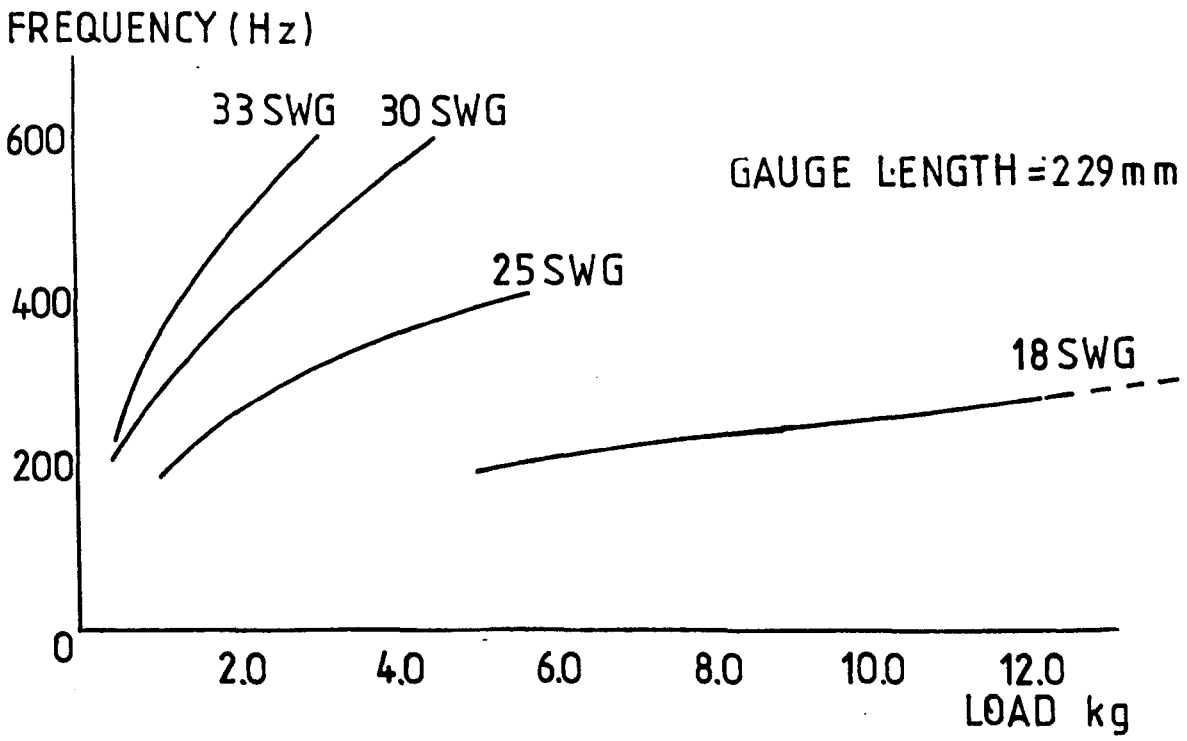

With the above criteria in mind a vibrating wire gauge (Fig. 3.3) was constructed.

3.4 Period Timing Device

A very adequate measuring system was commercially available supplied by Deakin Phillips Electronics Ltd. The 'strain measuring unit' model RRL/P/S is designed for use with a wide range of vibrating wire type strain gauges. The coil used in the vibrating wire gauge described above was taken from one of the purpose built gauges. A direct reading in microseconds is displayed where the least significant figure is in tens of microseconds. The plucking pulse amplitude can be preset by altering the plucking voltage in the coil from 3 to 60 volts.

3.5 Procedure

When using the gauge the plucking voltage was increased until the pulse was able to sustain the vibrations in the wire long enough to count 100 cycles of vibration and produce a readily repeatable result. The procedure adopted when taking a reading was to clamp and release the wire three times and on each occasion to repeat the plucking of the wire so that consistent readings could be taken.

3.6 Vibrating Wire Theory

To obviate the need for calibration of each wire individually the theoretical analysis of taut stiff strings with encastré and simply supported ends was carried out. This derivation of the natural frequency has not been published elsewhere and is given in

FIG 3.3

VIBRATING WIRE GAUGE

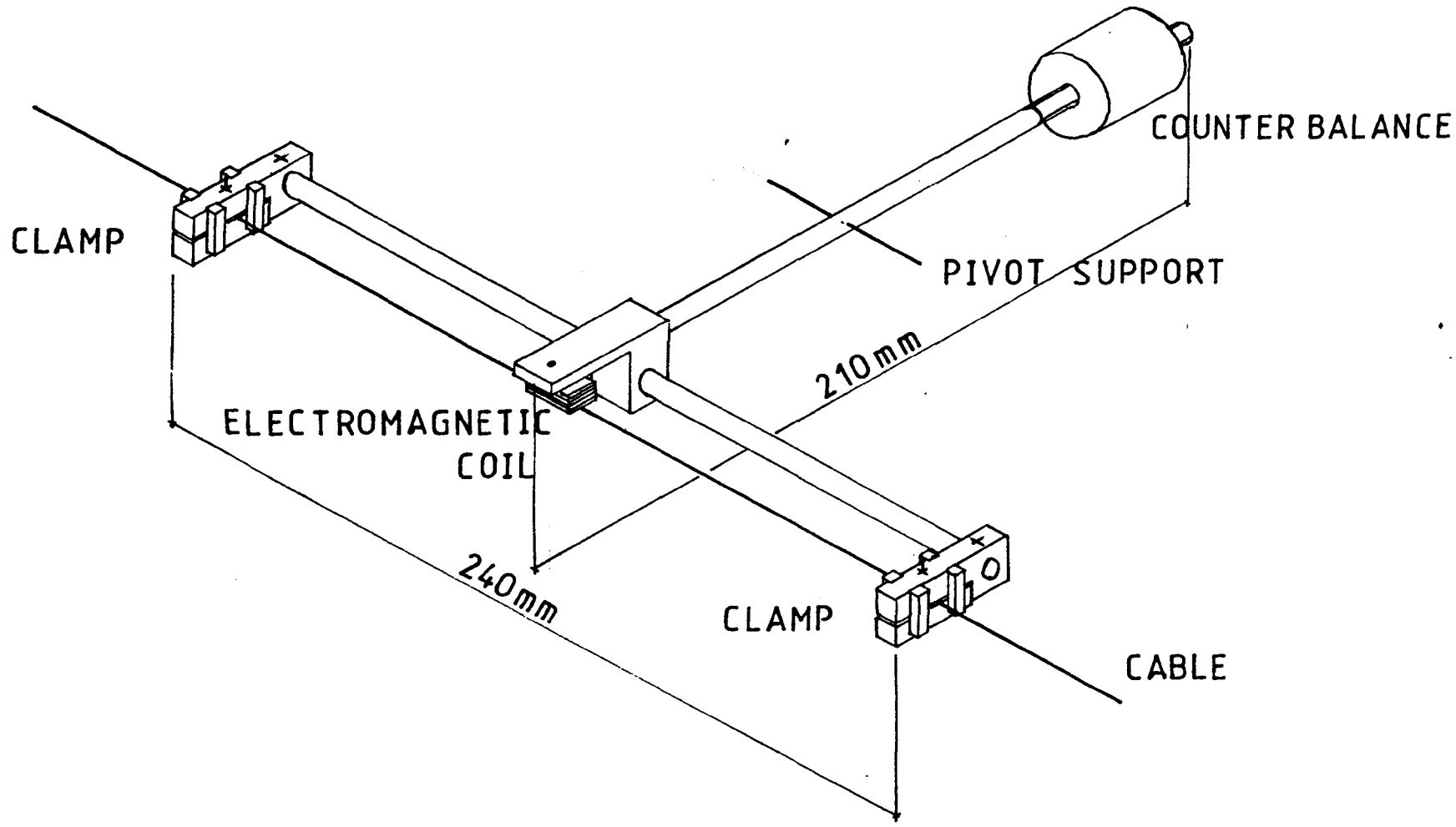

full in Appendix (3.1), since it leads to an iterative solution of transcendental equations without prior approximations.

Calculations based on each of the following three sets of assumptions were carried out and compared with experimental results.

i) No wire stiffness

$$f = \frac{1}{2L}\sqrt{\frac{T}{m}} \tag{3.1}$$

ii) Wire stiffness, pinned ends

$$f = \frac{1}{2L^2}\sqrt{\frac{EI\pi^2}{m} + \frac{TL^2}{m}} \tag{3.2}$$

iii) Wire stiffness, encastré ends

$$f = \lambda^2 \tan \lambda\frac{L}{2}\sqrt{\frac{EI}{m}}\ \frac{1}{2\pi} \tag{3.3}$$

where $$\lambda \tan \lambda\frac{L}{2} + (\lambda^2 + \frac{T}{EI})^{\frac{1}{2}} = 0 \tag{3.4}$$

The experimental results were obtained by measurement of the vibration of a wire in which the tension was known by loading with dead weights (Fig. 3.4).

Section properties of the single stranded wire were found by direct tensile testing and measurement of the wire diameter. (Fig. 3.5) shows a graph of frequency against tension for a single stranded wire.

3.7 Tension Measurement For Stranded Wire

Stranded wire presents the problem of how to establish its section properties. If complete shear transfer between the individual strands of the cable is assumed then a theoretical value for the flexural stiffness EI can be found, for the 18 SWG stranded wire being

FIG 3.4

VIBRATING WIRE CALIBRATION APPARATUS

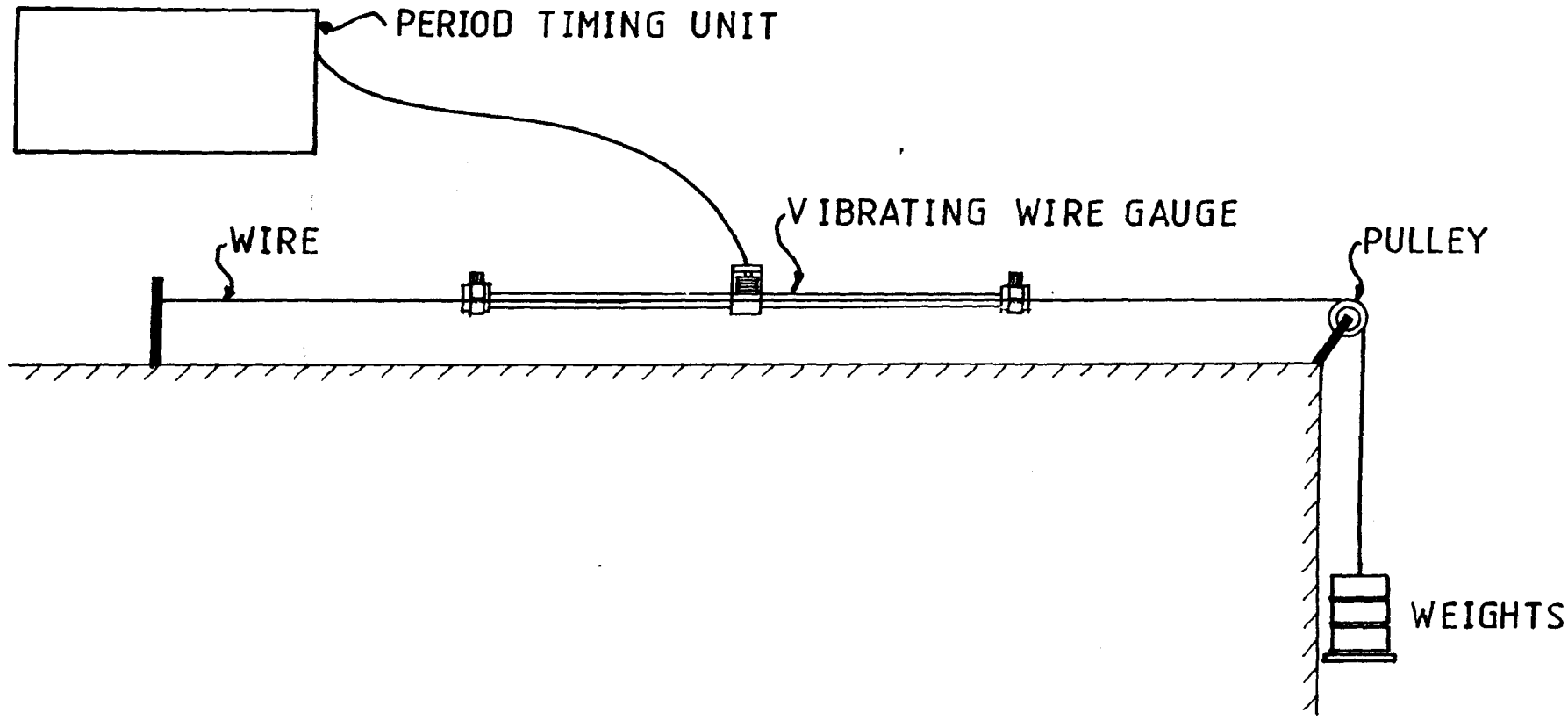

FIG 3.5

CALIBRATION CURVE FOR 30 S.W.G. STEEL WIRE

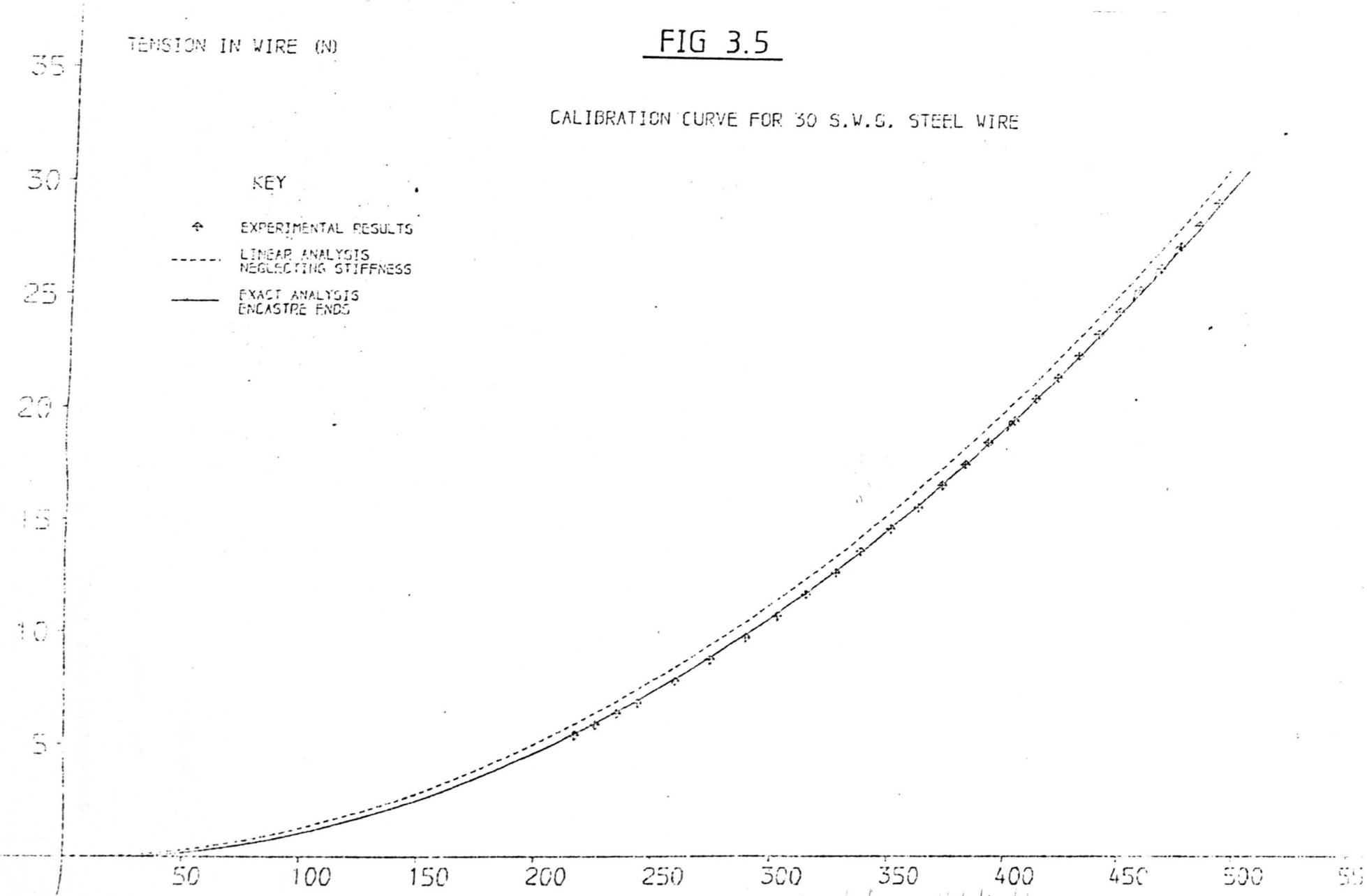

tested this value was 11.254×10^{-3} Nm^2. Using this value the theoretical curves can now be drawn for the relation between tension and frequency (Fig. 3.6). From Figure 3.6 it is seen that the experimental values of frequency obtained in a calibration test lie between the theoretical curves for pinned and encastré ends. To construct a curve which would fit the experimental calibration results the EI values for each of the load increments were calculated from the known tension and measured frequency. The value of the flexural stiffness EI remains constant over a range of tensions 50 N → 200 N (Fig. 3.7). The average stiffness over this range 3.529×10^{-3} Nm^2 was used to obtain a new relation between tension and frequency. The percentage error between this new theoretical frequency and the calibration results is in the order of 0.1%.

3.8 Measurement of Joint Deflections

For the measurement of joint deflections in cable structures the published methods were found to be either too complex for the needs of this work or better suited to smaller scale models. Therefore methods of deflection measurement appropriate to the models investigated were developed.

Photographic methods previously used to measure deflections in cable structure models have involved the use of photogrammetry (3.5). For two dimensional structures a simpler method can be used assuming that the deflections are planar.

The method can best be described by the use of a diagram (Fig. 3.8). At each node point where deflection measurements are required a target is arranged to give a precise image on a photograph.

FIG 3.6

CALIBRATION CURVES FOR STRANDED WIRE

i) ASSUMING COMPLETE SHEAR TRANSFER BETWEEN STRANDS
$EI = 11.254\ Nm^2$

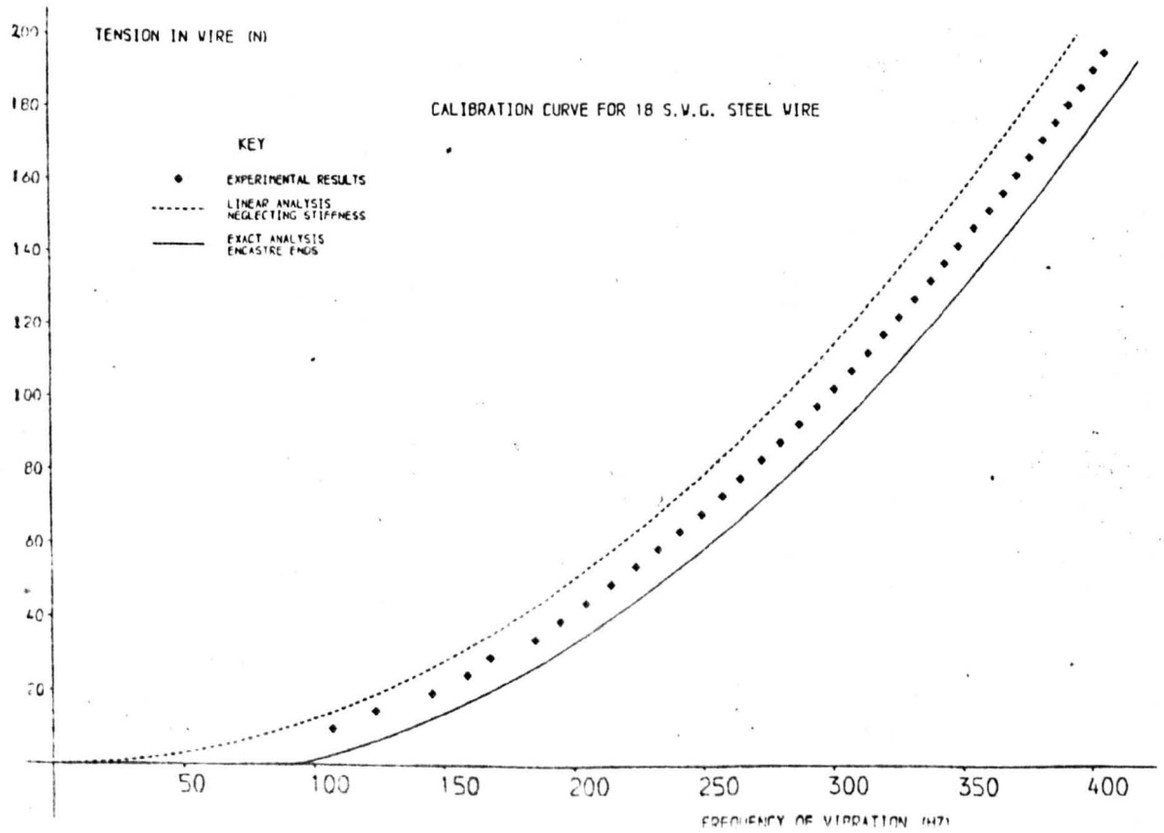

ii) USING CALCULATED STIFFNESS $EI = 3.529\ Nm^2$

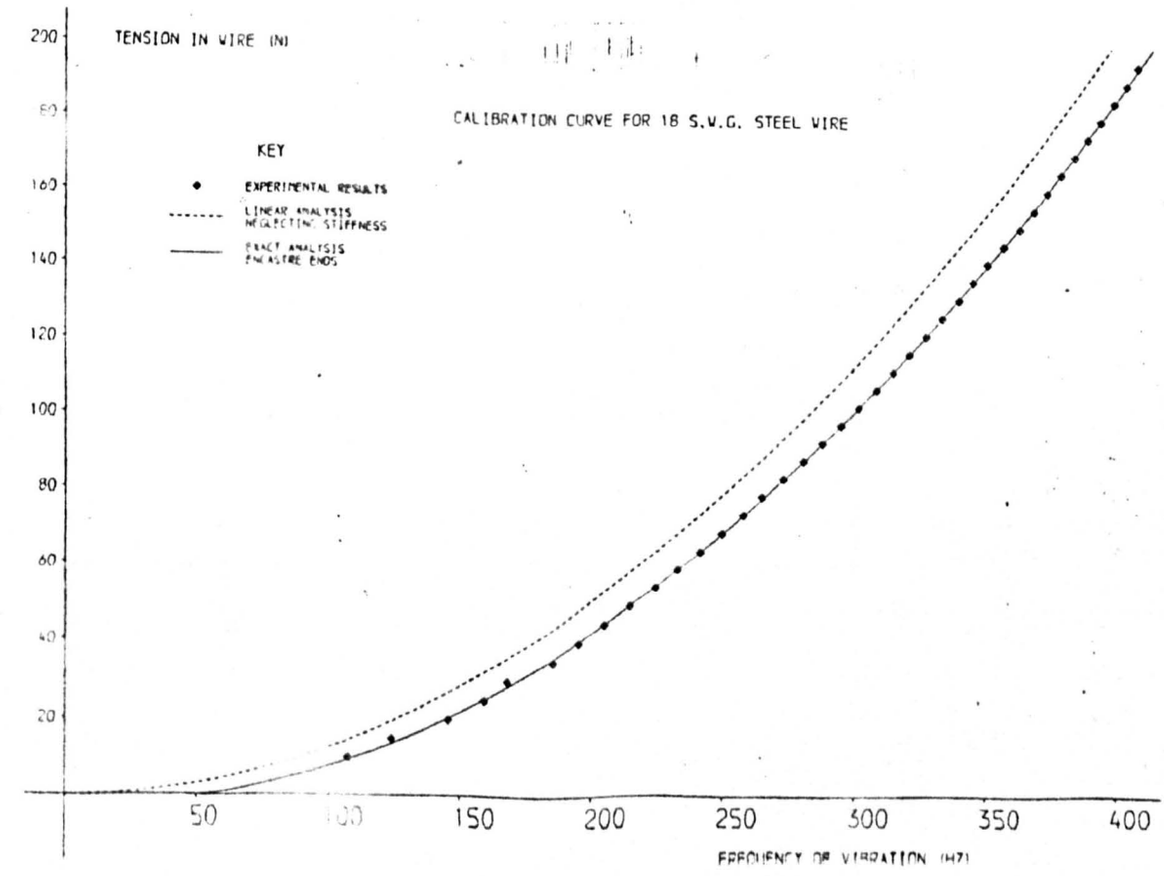

FIG 3.7

THE EFFECT OF TENSION UPON FLEXURAL STIFFNESS (EI) OF STRANDED CABLE

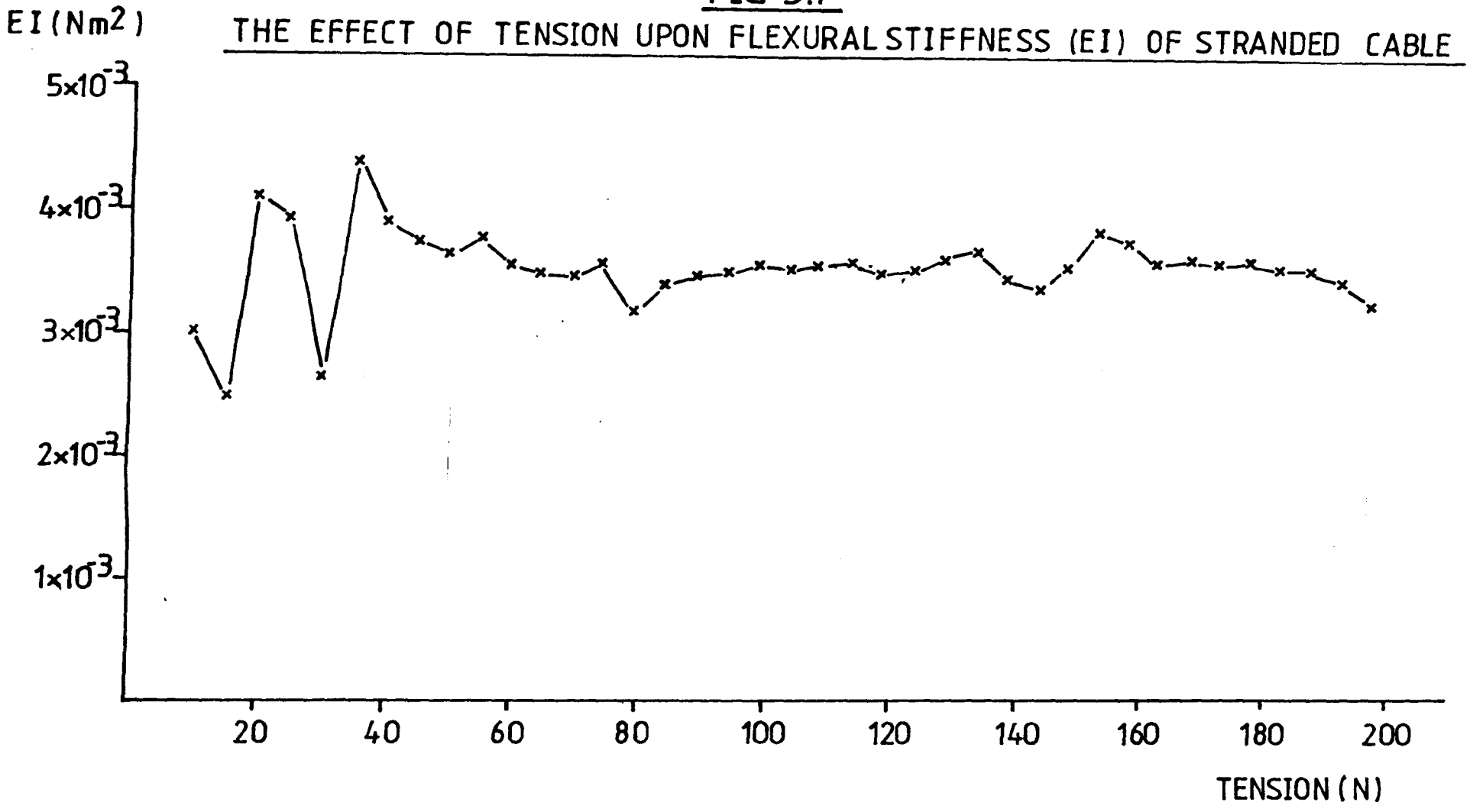

FIG 3.8

PHOTOGRAPHIC METHOD OF DEFLECTION MEASUREMENT

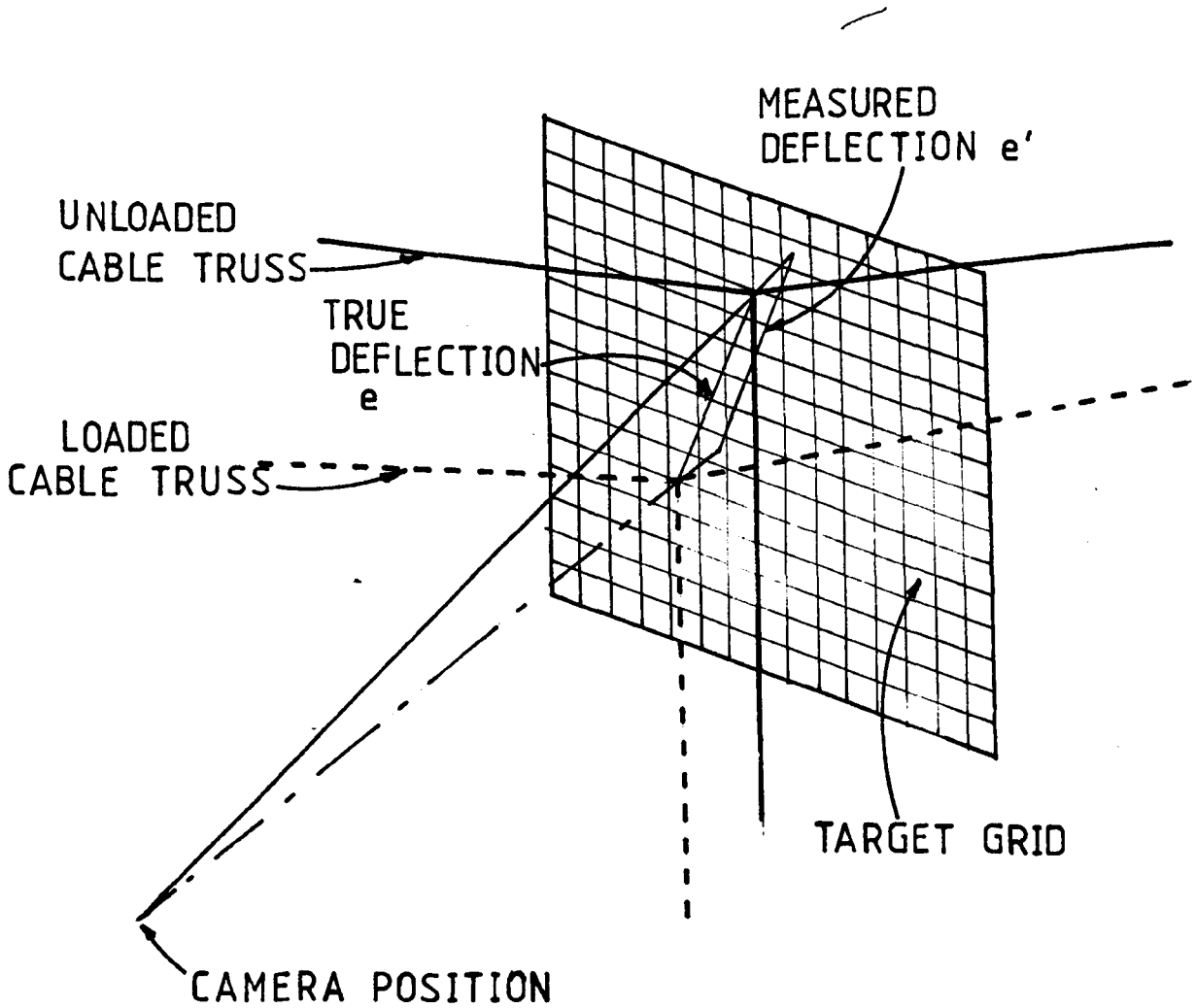

Behind the joint a grid of lines consisting of accurately printed graph paper is placed to cover the envelope of joint deflections. The grid is rigidly supported independently of the structure. Photographs are then taken of the targets with the grids behind for the loaded and unloaded case. The relative coordinates of the target as it appears on the grid can then be read from the negatives of the photograph using the cross hair of a travelling microscope. Because of the effect of parallax the relative coordinates as they appear on the negative are not the true values. This is not considered a disadvantage though since the error can be corrected for (Equation 3.5). The gap between the nodes and the plane of the grids provides room to work around the model.

This method provides a very economical way of measuring deflections with an accuracy comparable to more expensive methods. It is much less sensitive to any movement of the mounting device than microscopic methods and also has the advantage that the photographic negatives provide a permanent record of the measured deflections with no need to correct for camera imperfections.

i) Parallax error

Referring to (Fig. 3.9i) where

d = perpendicular distance of camera from target

e = true deflection of target

$\acute{e}$ = apparent deflection of target

s = distance between target and grid

By considering similar triangles it is seen by inspection that

$$\frac{d}{d+s} = \frac{e}{\acute{e}} \quad , \quad \therefore \quad e = \frac{d}{d+s}\acute{e} \qquad (3.5)$$

FIG 3.9

DEFLECTION MEASUREMENT BY PHOTOGRAPHIC METHODS

(i) PARALLAX ERROR

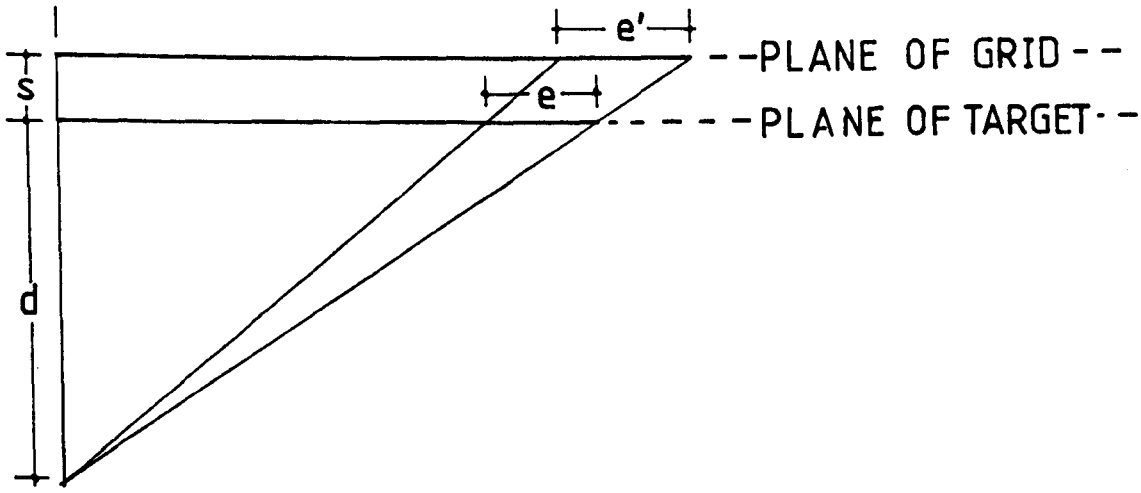

(ii) LATERAL MOVEMENT OF CAMERA

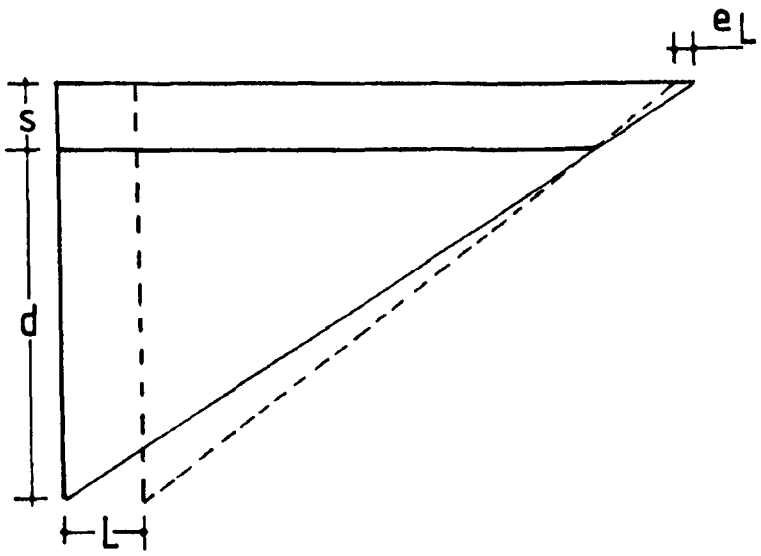

(iii) MOVEMENT OF CAMERA TOWARDS TARGET

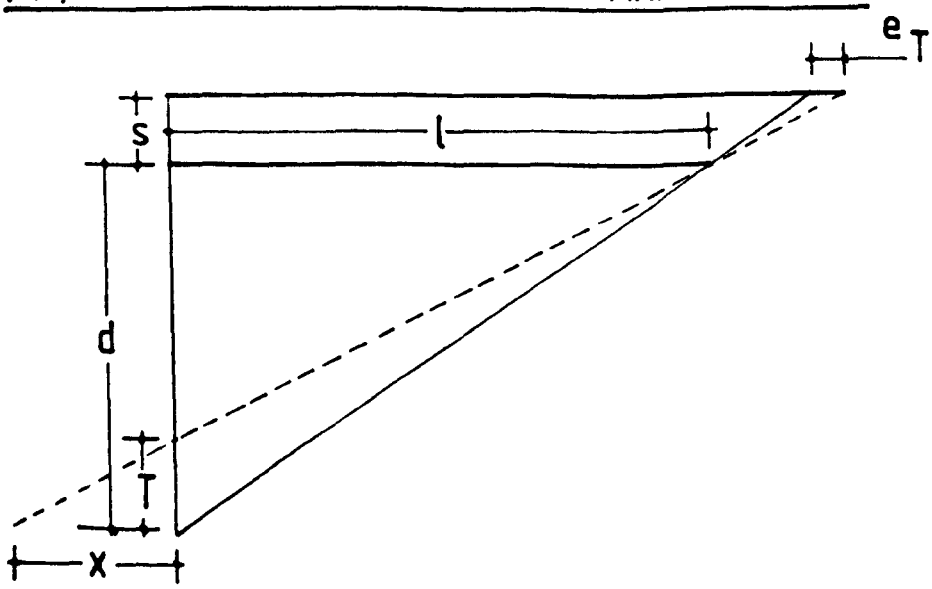

A correction factor $\frac{d}{d+s}$ needs to be applied to the measured deflection $\acute{e}$ to obtain the true deflection e. Typical values are

$$d = 2000 \text{ mm} \qquad s = 40 \text{ mm}$$

$$\therefore \quad e = \frac{2000}{2040}\acute{e} = 0.98\,\acute{e}$$ which represents a 2% error if no correction is applied.

The working space available in the laboratory did not allow a permanent mounting for the camera. Very slight movements of the camera between successive photographs of the deflections may have occurred. The following sets of error analysis show that any error thus induced is not significant.

ii) Error due to lateral movement of camera

If there is a lateral movement of the camera (Fig. 3.9ii) then the position of the target on the grid is affected. Referring to (Fig. 3.9ii) again by similar triangles we have

$$\frac{\ddot{e}L}{s} = \frac{L}{d} \qquad \therefore \quad \ddot{e}L = \frac{Ls}{d} \tag{3.6}$$

For a lateral movement of 5 mm and the values of s and d as before we have

$e_L = \frac{5 \times 40}{2000} = 0.1$ mm which represents a 1% error for a 10 mm joint deflection. In practise any camera movement will be much less than 5 mm.

iii) Error due to movement of camera towards target

The position of the target on the grid is also affected by movement of the camera towards the target. Referring to (Fig. 3.9iii) and introducing ℓ, the offset distance of the target from the camera

an expression for e_T can be obtained. The movement towards the camera can be converted into an equivalent lateral movement

$$x = \frac{\ell T}{d - T} \tag{3.7}$$

Also $\frac{e_T}{s} = \frac{x}{d}$

$$\therefore \quad e_T = \frac{s.x}{d} = \frac{s.\ell.T}{(d - T)d} \tag{3.8}$$

3.9 Tension Measurement at Cable Supports

To form the initial shape of a tension structure it is essential to know accurately the tension at all of the cable supports where a cable end is connected to the boundary member. In the case of the two dimensional truss experiment discussed in Chapter 4 it was possible to use a simple pulley arrangement (Fig. 3.10) to pretension the cable ends. For the three dimensional cable net experiment, discussed in Chapter 5, having twenty support nodes this method would not be practicable.

The vibrating wire method of tension measurement described previously is best suited, from a practical point of view to measuring the tension in a single cable for a number of load cases. A permanent tension measuring device was therefore developed for use on the three dimensional net model.

The primary requirement of the device is to give a precise and accurate ($\pm$ 0.5 N) measure of the tension at the cable support point without affecting the response of the structure. An ability to monitor the tensions at all support nodes continuously during the initial pretensioning of the cable structure (which can be likened to

FIG 3.10

METHOD OF PRETENSIONING FOR CABLE TRUSS MODEL

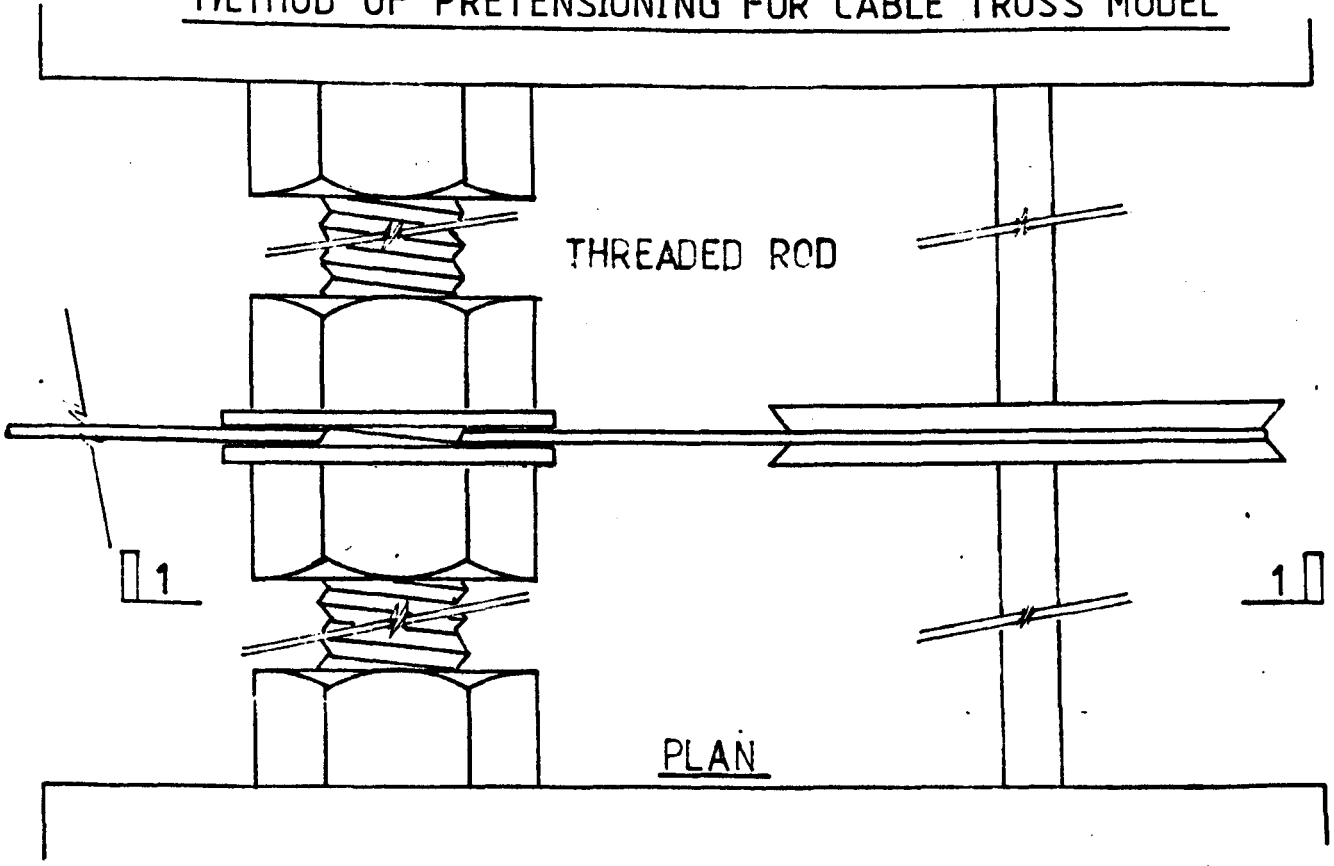

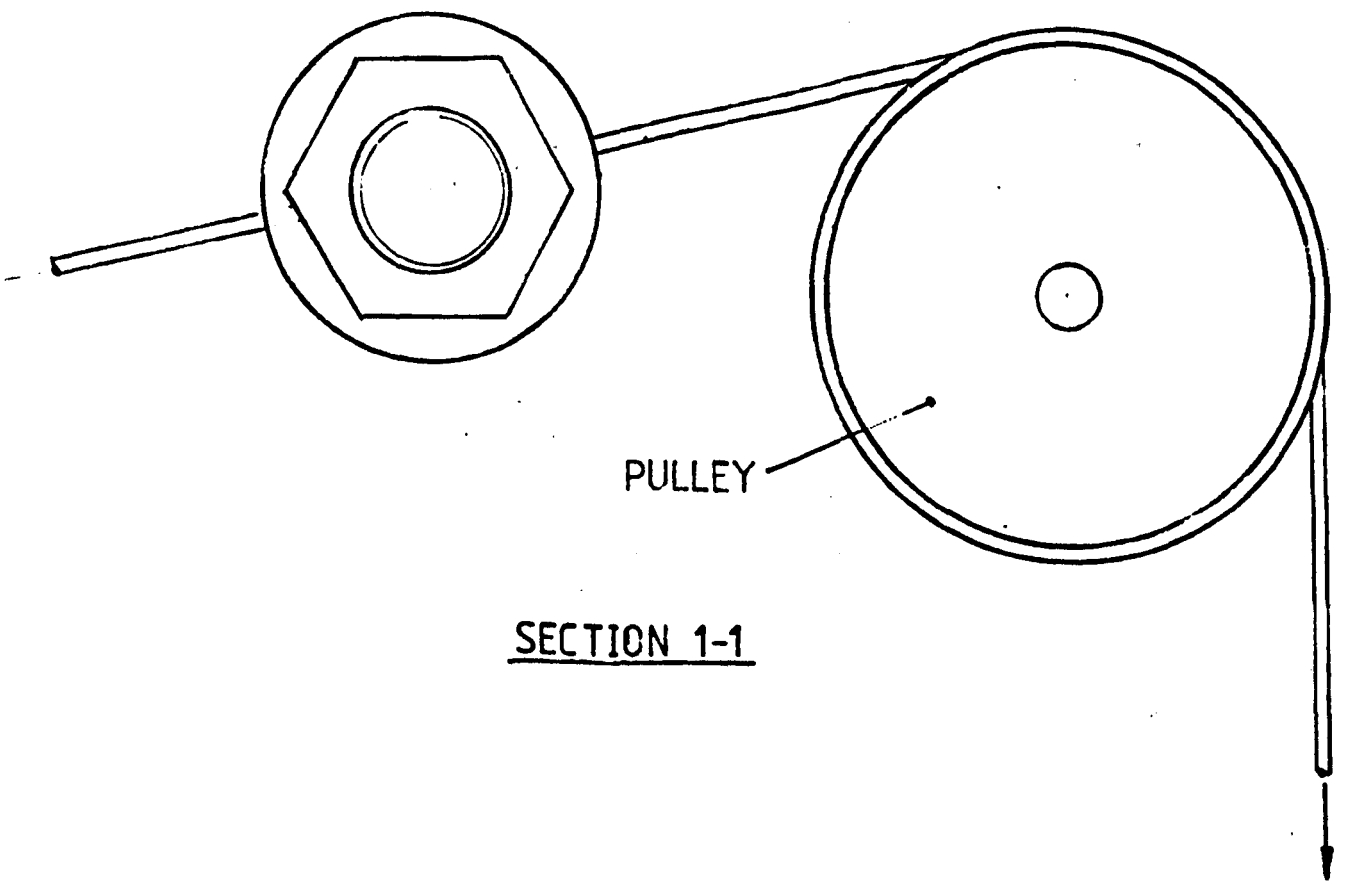

SECTION 1-1

PRETENSION FORCE

a fine tuning process) is essential. These requirements could be met with a series of electrical resistance strain gauges connected to a central 100 channel Solatron Logger which is sensitive to one microstrain resolution.

A direct strain measure was used to determine the tension in the cables as opposed to an indirect measure, such as bending stress in a ring gauge, which would cause a greater extension along the length of the cable member. The use of a link inserted along the length of the cable was discounted because of the affect on the stiffness of the cable and the self weight of any link. The position of the tension measuring device is therefore limited to the region of the boundary support.

A thin walled steel compression cylinder fitted with electrical resistance strain gauges (type FLA-6-11) was chosen as the strain measuring device and also incorporated into the tensioning and anchorage facility at the end of each boundary cable (Fig. 3.11). By having the cylinder acting in compression outside the boundary as shown, the tension in the cable is not affected by the self weight of the cylinder and anchorage assembly. The self weight is transferred to the much stiffer boundary member.

The form of the compression cylinder and associated electrical resistance strain gauges is governed by a number of contradictory factors. The ratio between cylinder diameter and wall thickness has to be sufficient to provide strains of the order (10^{-3}) in the gauges but thick enough to prevent buckling of the cylinder walls (3.6).

FIG 3.11

THIN WALLED STEEL COMPRESSION CYLINDER

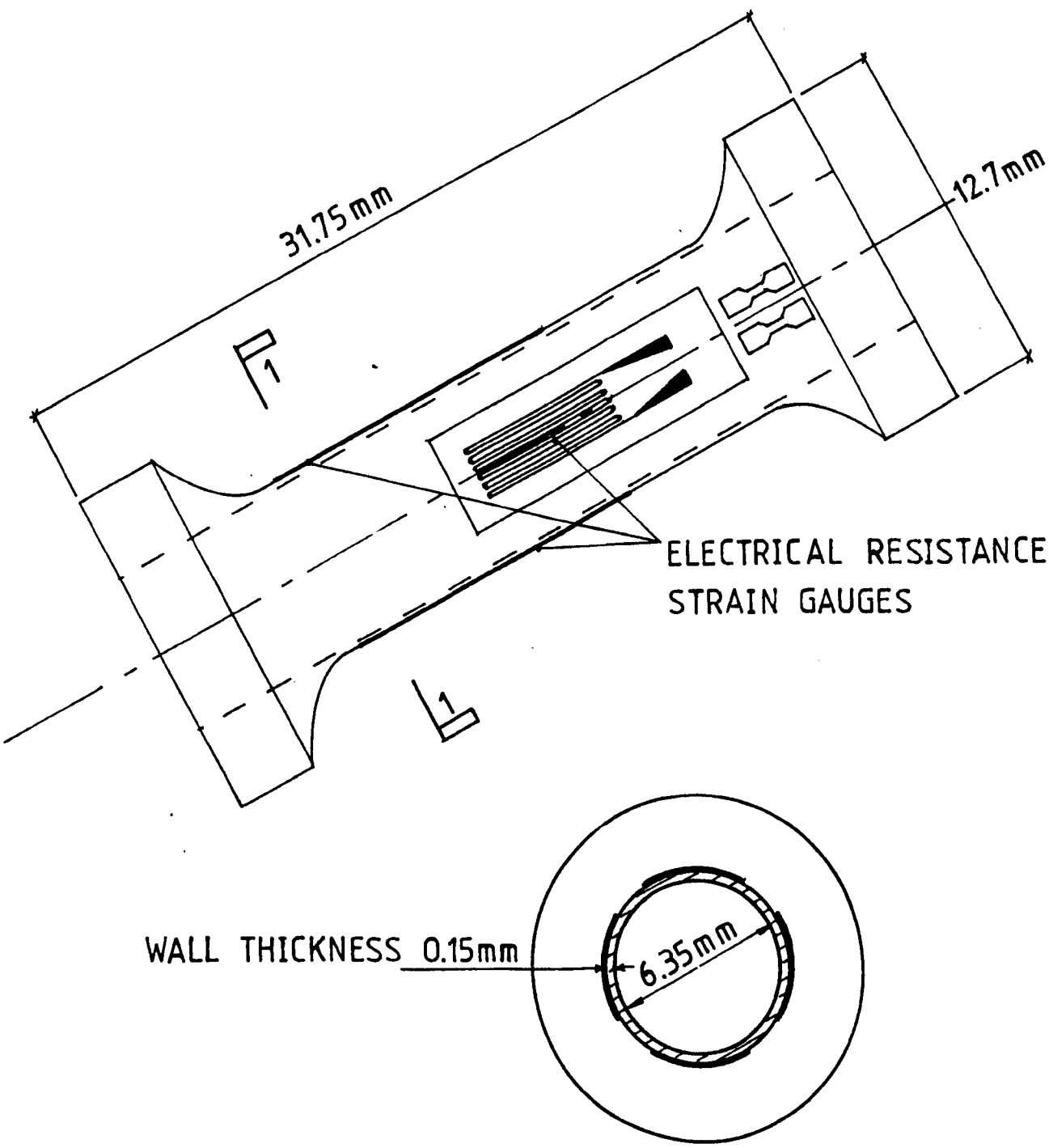

SECTION 1-1

To increase the stability of the cylinder and provide a good end bearing they were machined from a much thicker section with a reduced waist section in the middle to which the strain gauges were mounted using P2 type adhesive.

A circuit diagram for the electrical resistance strain gauges and the dummy gauges within the logger is shown in (Fig. 3.12). The arrangement of the gauges on the cylinder provides for full bending compensation for any non-axial loading of the cylinder. The foil type electrical resistance gauges are matched to the thermal properties of the steel on which they are mounted so that no thermal strains are measured in the range 18-36^{o}C. The gauges form the active arm in a single arm active wheatstone bridge circuit within the logger. Any change in resistance of the connecting wires is compensated for by the use of the three wire connection as shown in (Fig. 3.13).

After fabrication each of the gauged cylinders was calibrated individually, a typical calibration curve is given in Fig. 3.14. The readings from the logger in mV are a direct equivalent in $\mu\varepsilon$ of the strain in the cylinder walls. Since an accurate measure of the x sectional area of the cylinders was not available due to construction tolerances in the wall thickness the direct reading of strain could not be transferred to an accurate measure of the compression force in the cylinder. However regression analysis of the calibration results gave a linear relation between tension and the logger reading. The average maximum deviation from the linear interpolation was less than 1%.

FIG 3.12

CIRCUIT DIAGRAM FOR ELECTRICAL RESISTANCE STRAIN GAUGES

SECTION OF GAUGED CYLINDER

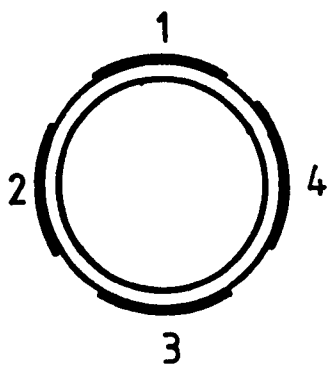

FORMING ACTIVE ARM OF $^1/_4$ BRIDGE CIRCUIT

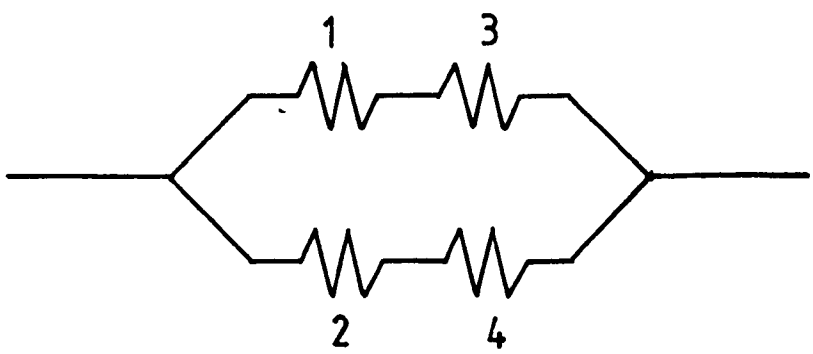

FIG 3.13

THREE WIRE CONNECTION

WHEATSTONE BRIDGE CIRCUIT

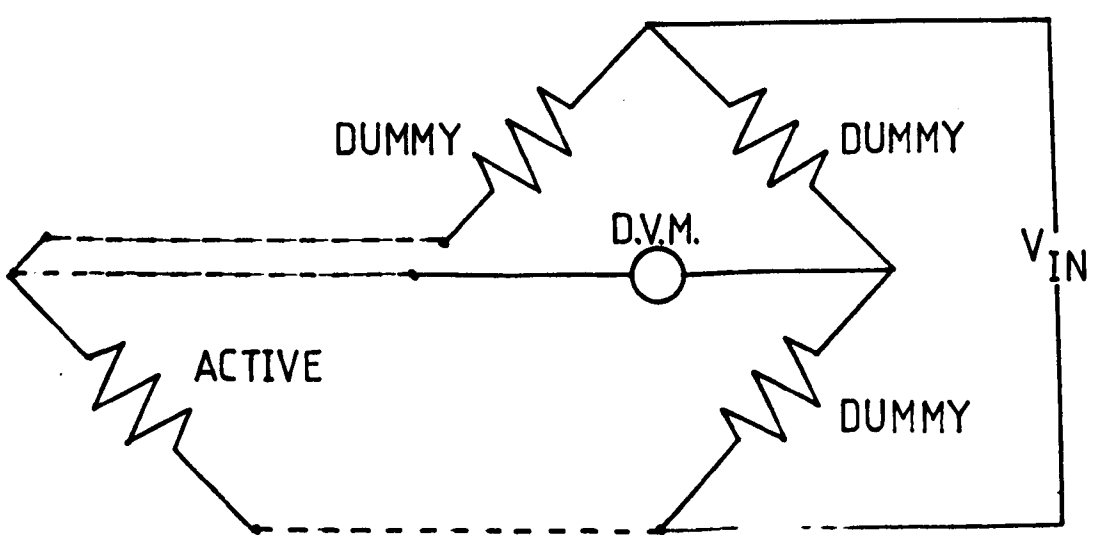

FIG 3.14

TYPICAL CALIBRATION RESULTS FOR GAUGED CYLINDER

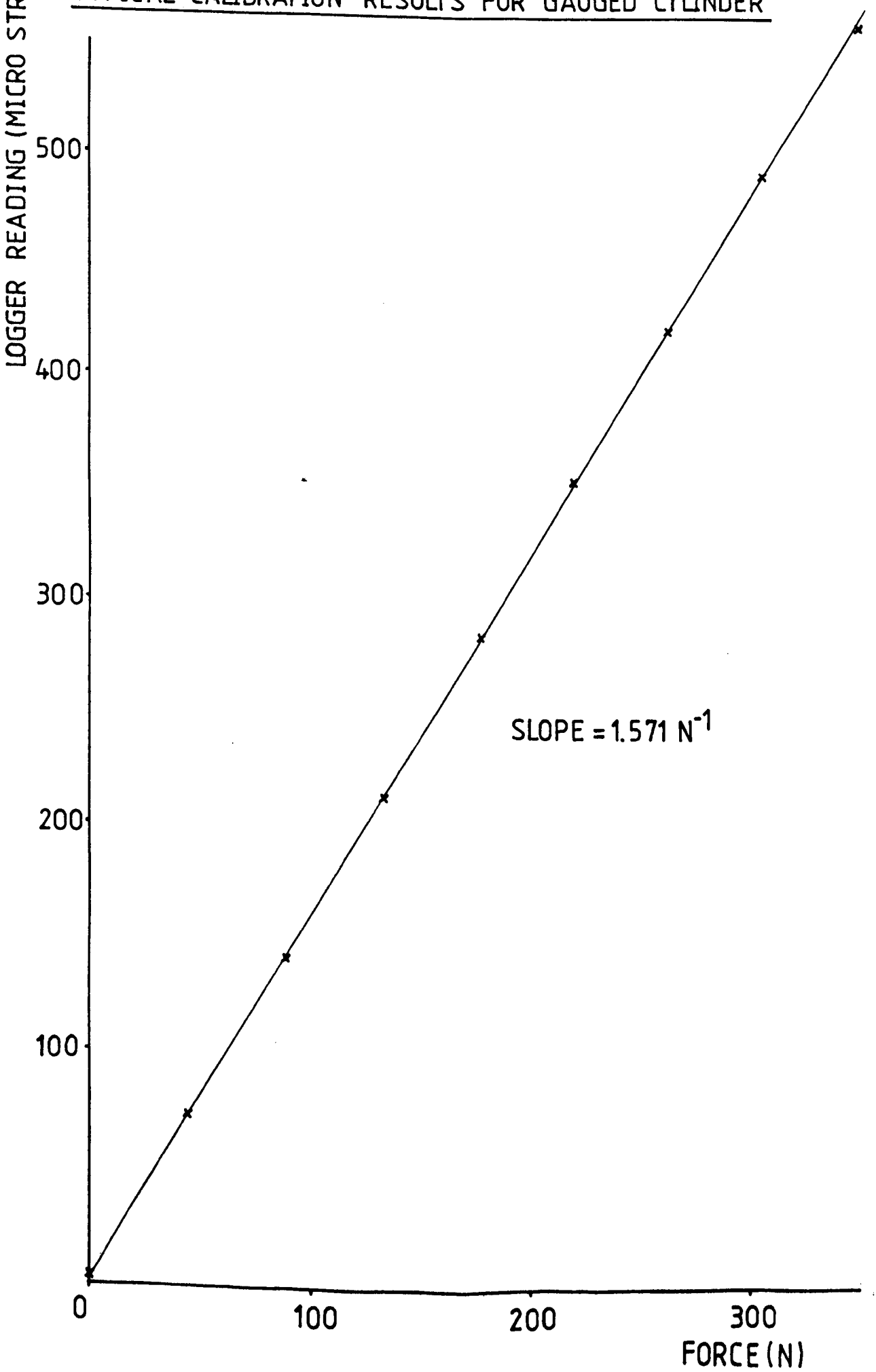

CHAPTER 4

A TWO-DIMENSIONAL CABLE TRUSS EXPERIMENT

4.0 Introduction

This chapter describes experimentation upon a model two-dimensional pretensioned cable truss. The results are subsequently compared with theoretical predictions. A specification for the design of the truss is presented together with the method of construction used.

Previous work in this field has made use of model analysis, (4.1-4.4). Published work has confined itself to a brief description of apparatus followed by an account of the procedure and results obtained. Here a full account of the design and construction of the model is given as well as the experimental procedure, results and discussion.

4.1 Design of a Two-Dimensional Cable Truss

The design of a two-dimensional cable truss experiment, its general requirements and some practical design details are discussed.

The model is required primarily as a source of accurate experimental data to compare with theoretical results. Joint spacings must be large enough to allow the use of the vibrating wire method of tension measurement of member forces. Joint deflections, when the truss is loaded, must be of sufficient magnitude, of the order of 10 mm, such that the precision of the photographic method of deflection measurement ($\pm$ 0.25 mm) does not cause large errors. The model also needs to have several degrees of freedom so that the theoretical analysis

with which the results are being compared is representative of full sized structures and provides a 'fair test' for the theoretical analysis.

The choice of wire diameters is governed by three factors. Most importantly the range of wire diameters must be within the range of the vibrating wire method of tension measurement. For an economic structure the stress in all wires is of a similar order, the area of the wire is therefore chosen in proportion to the force it will carry. Thirdly a maximum working stress of one half of the yield stress of the wire was used in the model so that member extensions remained well within the elastic limit of the material.

Referring to the above specification a prestressed cable truss was constructed consisting of two prestressed cables fixed at each end joined by ten vertical hangers giving 40 degrees of freedom for the structure. A parabolic shape was chosen for the locus of the joints along the prestress cables, with the hangers spaced equally in a horizontal direction thus ensuring an equal force in each of the hangers and ease of computation for the initial unloaded state.

A sag to span ratio of 1 : 16 gives the ratio of hanger force to horizontal force in the pretension wire of 1 : 22. Solid steel wire of 30 SWG (0.3175 mm) diameter was used for the hangers and 18 SWG (1.21 mm) for the pretension cables. This gives a relative area for the wires of 1 : 15 ensuring that both hanger and pretension cables are stressed to a similar degree.

The joint arrangement between hanger and prestress wire (Fig. 4.1) has been designed in two parts for accuracy of location. Each

FIG 4.1

JOINT BETWEEN HANGER AND PRESTRESS WIRES

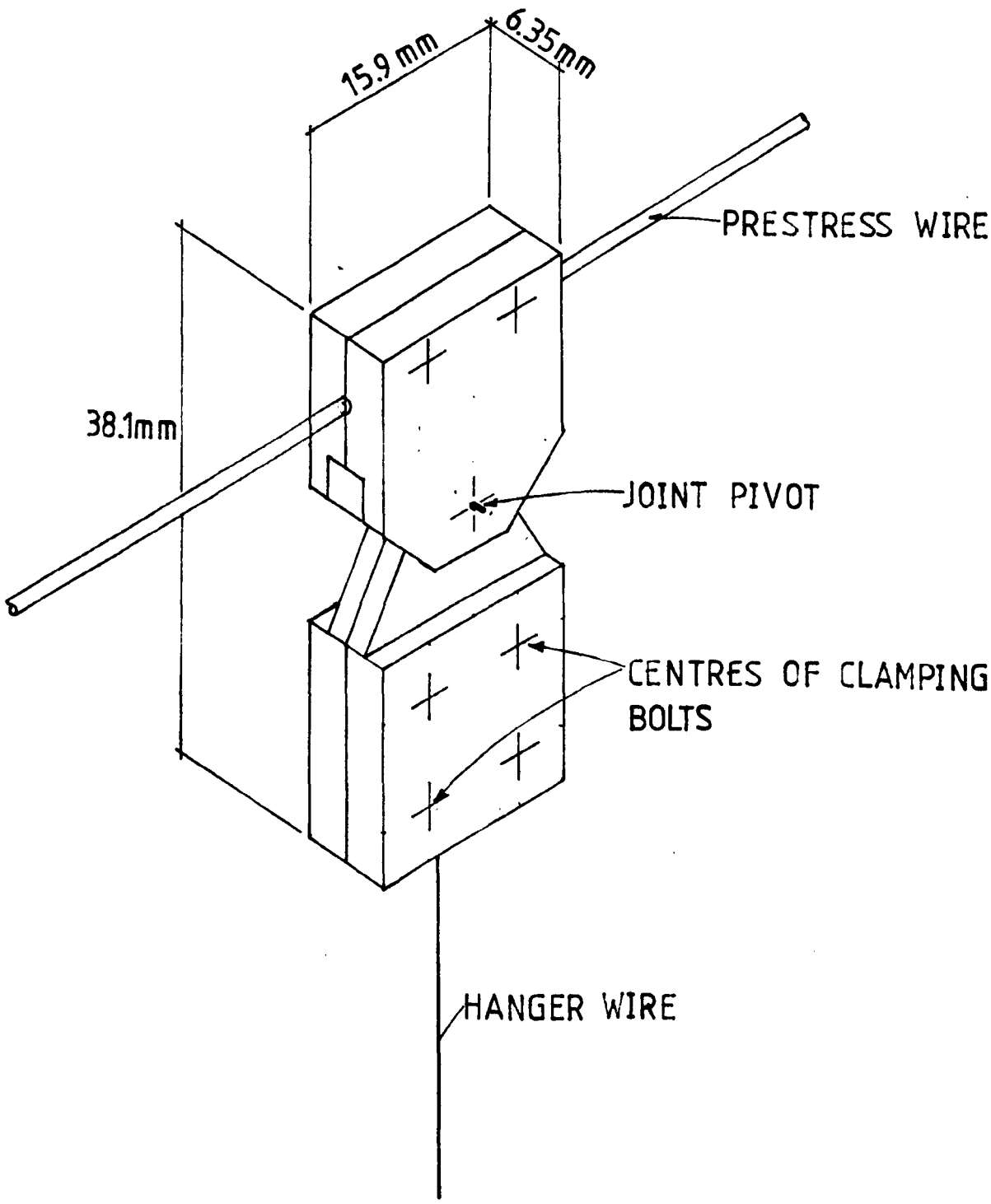

section can be individually fitted to the respective hanger or pretension wire and then joined for final construction. Joints are fitted with targets for the photographic method of deflection measurement and the lower joints with hooks for weight hanger support.

In determining the forces required at the ends of the pretension cables account was taken of the self weight of the cable truss. It is assummed that the self weight acts as the nodes. This is not unreasonable since the majority of the self weight is caused by the joints. Figure 4.2 shows the forces acting on the pretension cables. To maintain the symmetry of the model the horizontal component of tension in the top cable is increased from 22T to 22(T + w) and in the bottom cable reduced from 22T to 22(T - w) where T is the tension force in the hanger and w the self weight of the truss acting at the node.

Referring to (Fig. 4.3) the following table gives the member lengths and forces in the initial equilibrium state.

4.2 Construction of the Model Cable Truss

The wires used in the construction of the model arrived coiled, to remove the effect of this 'pre-set' they were loaded to 50% of their ultimate stress for 48 hours. It is assumed that some form of slow yield took place so that the wires became straight, the exact mechanism of this behaviour is not known. Curved wires would have introduced a bending action along the member which was not allowed for in the theory developed earlier.

Particular care was taken in the formation of the member lengths since it is these which determine how closely the initial unloaded state of the model is to that designed.

FIG 4·2

FORCES ACTING ON PRETENSION CABLES

W = SELF WEIGHT ACTING AT JOINT

T = HANGER TENSION

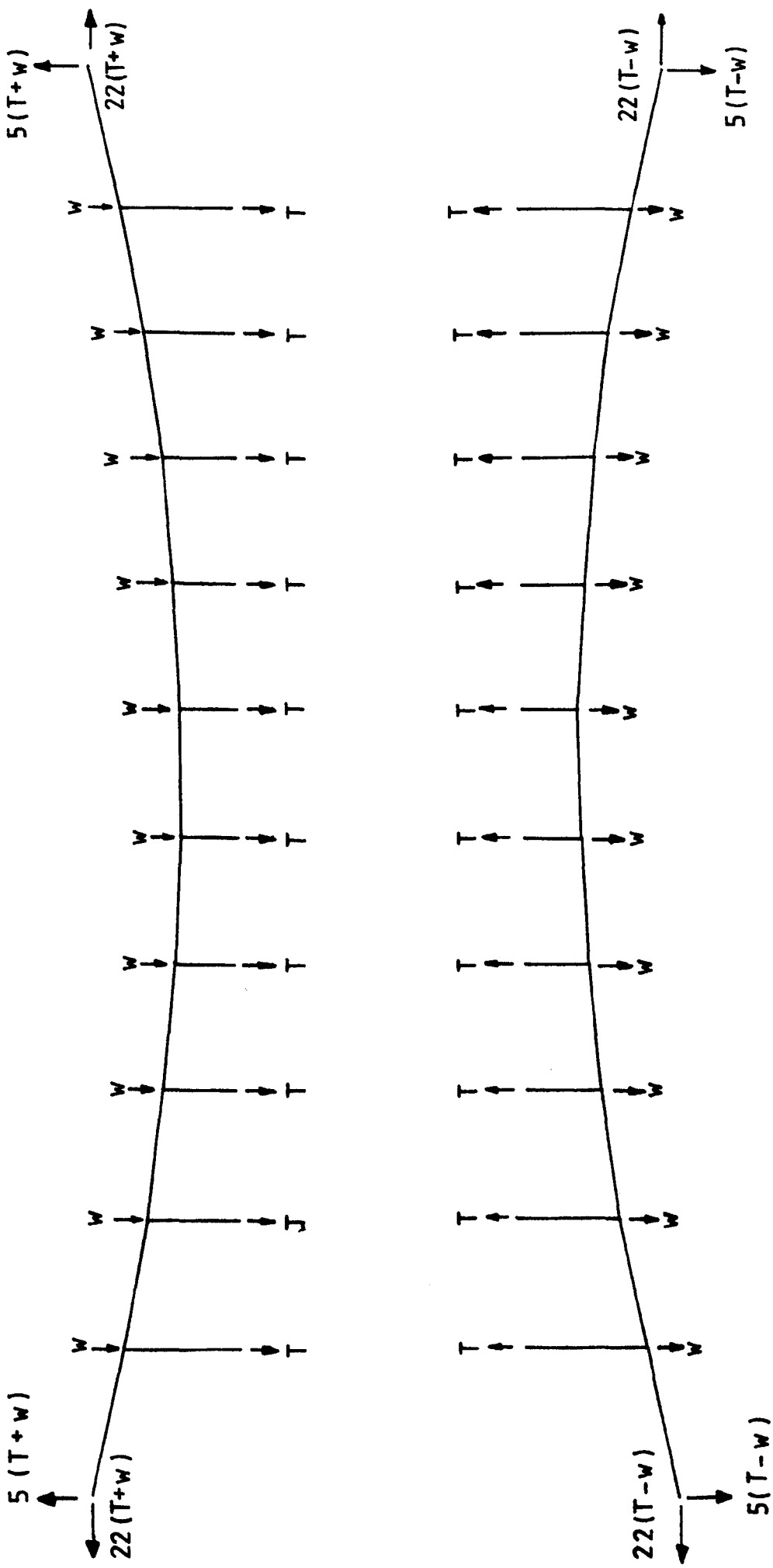

FIG 4.3

CABLE TRUSS MEMBER AND JOINT DATA

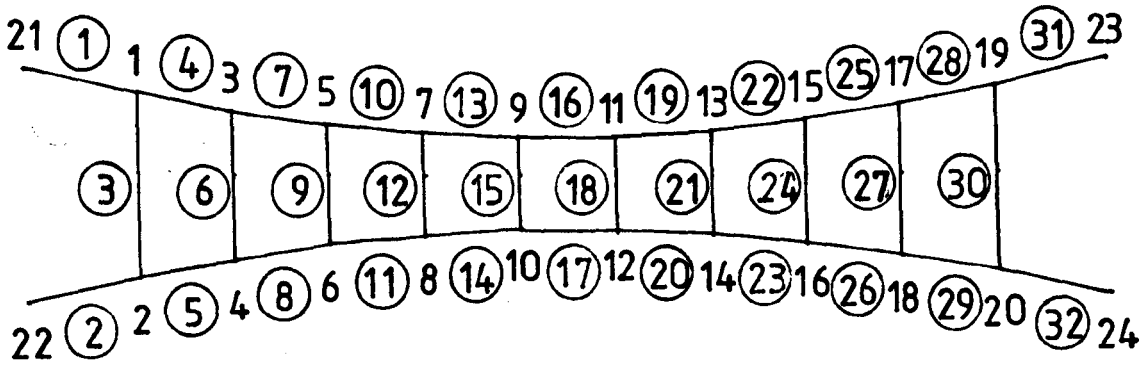

JOINT NUMBER	X COORDINATE (m)	Y COORDINATE (m)	MEMBER NUMBER	MEMBER FORCE (N)
1	0.470	0.1068	1	217.18
2	0.470	0.8584	2	225.32
3	0.870	0.1795	3	9.81
4	0.870	0.7857	4	215.25
5	1.270	0.2341	5	223.32
6	1.270	0.7311	6	9.81
7	1.670	0.2704	7	213.74
8	1.670	0.6948	8	221.75
9	2.070	0.2886	9	9.81
10	2.070	0.6766	10	212.65
11	2.470	0.2886	11	220.62
12	2.470	0.6766	12	9.81
13	2.870	0.2704	13	211.99
14	2.870	0.6948	14	219.94
15	3.270	0.2341	15	9.81
16	3.270	0.7311	16	211.78
17	3.670	0.1795	17	219.72
18	3.670	0.7857	18	9.81
19	4.070	0.1068	19	211.99
20	4.070	0.8584	20	219.94
21	0.000	0.000	21	9.81
22	0.000	0.9652	22	212.65
23	4.540	0.000	23	220.62
24	4.540	0.9652	24	9.81
			25	213.74
			26	221.75
			27	9.81
			28	215.25
			29	223.32
			30	9.81
			31	217.18
			32	225.32

To attach the joint blocks as accurately as possible the following method was applied. A length of the 30 SWG hanger wire was stressed to the initial prestress tension it was due to receive in the completed structure (9.81 N). The required positions of the hanger blocks were then marked on the wire, the wire cut to length and the blocks attached. Accuracy in the marking of the wire was achieved by using self adhesive labels which were lightly secured to a metre rule at the required distance apart and then transferred directly onto the wire. A similar procedure was adopted to position the joint blocks and cable ends, on the pretension wires.

The pretension wires were then strung between their end supports and the hangers attached between them. A prestress force of 225 N was applied to the end of the top prestress wire and 217 N to the end of the bottom one by means of dead weights applied through a pulley arrangement at one end of each wire. (Fig. 4.4) The maximum misclosure between the marked position of the anchorage point and the actual one was 6 mm over a span of 4770 mm. This misclosure was split equally between all four support points and the hangers checked for plumb. Once the initial prestress configuration had been obtained the free ends of the pretension wires were clamped in position.

A check on the hanger tensions was carried out using the vibrating wire method of tension measurement. The average hanger tension was found to be 9.58 N within 3% of the design value of 9.81 N.

4.3 Experimental Procedure

Tests were carried out to determine the behaviour of the model under gravity loads. Two load cases were applied,one symmetrically with all of the lower nodes loaded (load case 1),and one unsymmetric-

FIG 4.4

SUPPORT DETAIL OF CABLE TRUSS MODEL

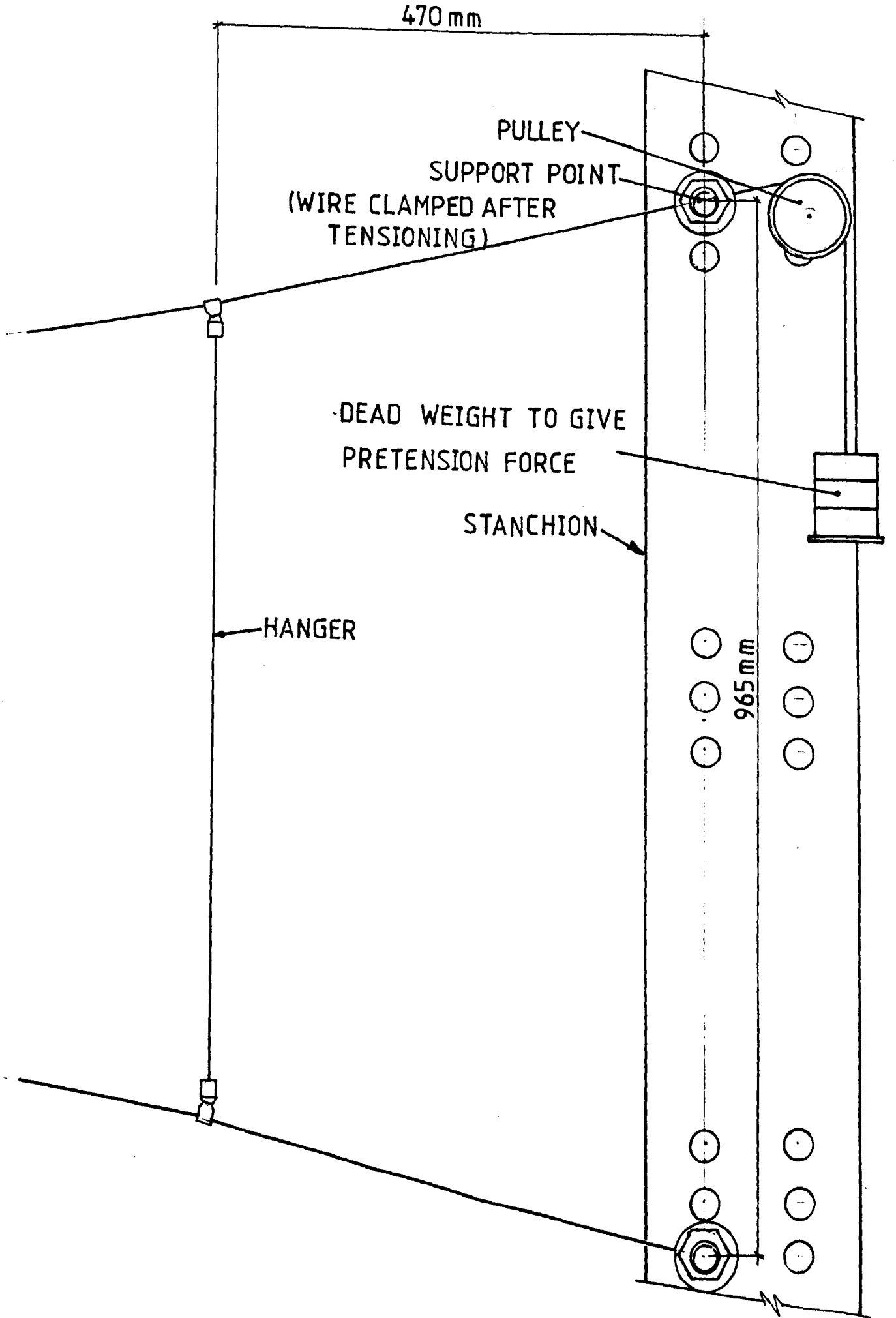

ally with half of the nodes loaded (load case 2). Weights were applied on hangers incrementally up to 2.0 kg. In load case 1, one of the lower main cable members became redundant (i.e. the force in it dropped to zero). In a practical structure this could indicate a failure state since lateral stiffness would be zero at least at one point.

For each of the increments in load the change in the hanger tension was measured using the vibrating wire gauge (Fig. 4.5). The procedure adopted was to set up the vibrating wire gauge so that the wire clamps were in line with the member in which the tension was being measured, the counterbalance on the gauge ensured that no weight was transferred to the cable member. The cable is then clamped and the natural frequency of vibration of the wire measured, the cable is unclamped and reclamped twice more to check that the frequency readings are consistent. Readings were taken for both the loading and unloading cycle. It was found to be more convenient to carry out the full loading sequence while the tension in one member was measured rather than move the gauge from member to member for a given load.

Deflection measurements were carried out for the same two cases, using the photographic method of deflection measurement as described in Chapter 3.

Throughout the experimental programme care was taken to minimise the effect of temperature changes upon the results. The apparatus was situated in an area of the laboratory which received a minimum of direct sunlight. No experimentation was carried out in direct sunlight or when the apparatus was subject to draughts due to the loading bay being open. Also, a note of the temperature at the initial prestressing, 21.1^{o}C, was

FIG 4.5

CABLE TENSION MEASUREMENT USING THE VIBRATING WIRE GAUGE

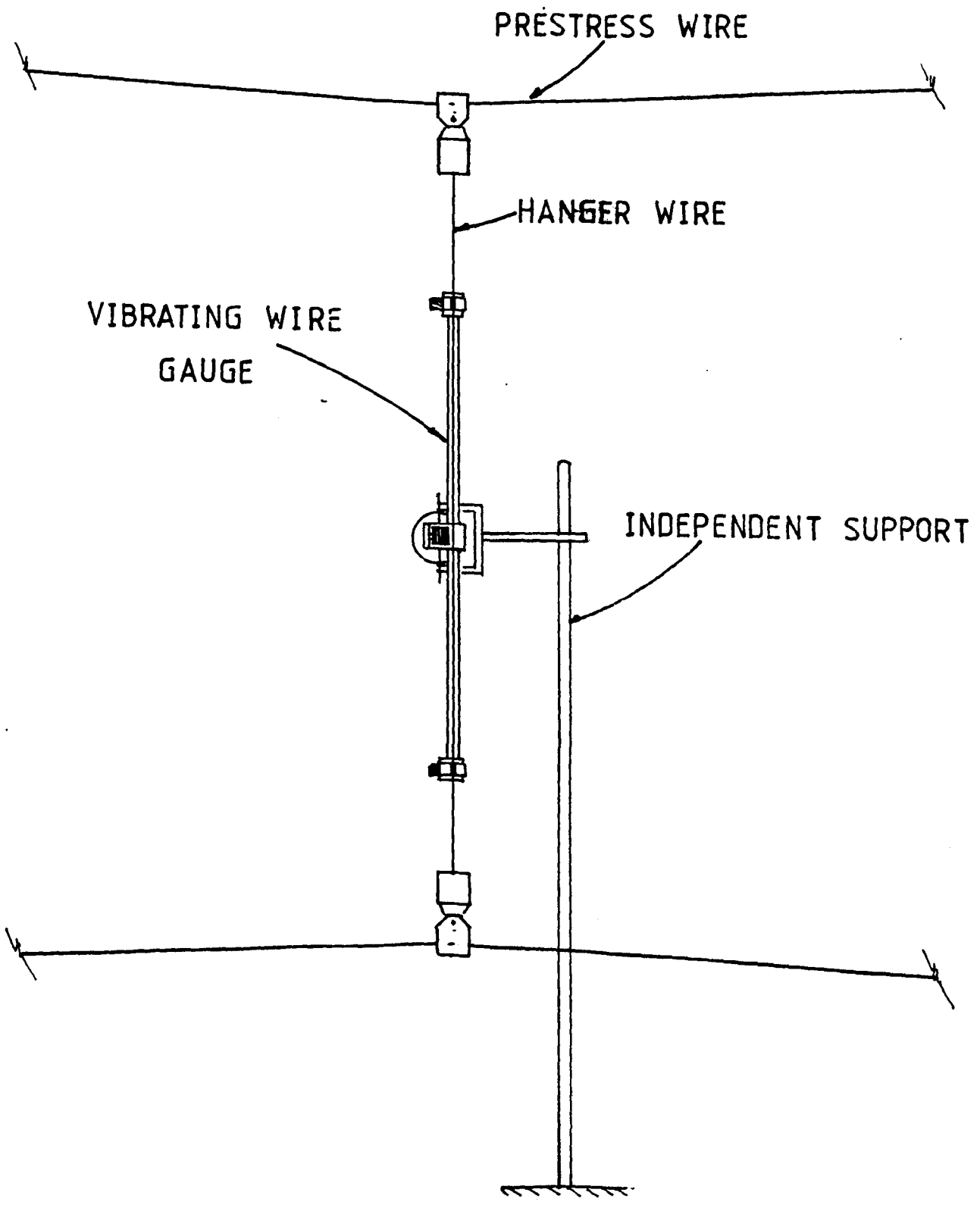

made and no subsequent work was carried out at $\pm 2^{o}C$ from this value.

4.4 Material Properties of Wires

In order that the experimental results can be compared accurately with the theory developed earlier the physical properties of the wires used in the experiment are required.

Both the 18 and 30 SWG wires were tested using an Instron machine giving graphical output. Typical stress/strain curves for the wires are shown in Figs. 4.6, 4.7. The range of experimental stresses is within the elastic range of the material, this is important as no account is taken in the theory of a non-linear stress/strain relation. A series of curves were plotted using the testing machine to give a representative sample of the wire stiffness. Figs. 4.8 and 4.9 show histogrammes of the value of Young's modulus E obtained from the tests. The mean values of E for the 30 SWG and 18 SWG wires respectively are 193.3 KN/mm^2 and 202.5 KN/mm^2.

4.5 Results

i) Deflection results

A full tabulated set of results comparing the theoretical and experimental deflection results appears in Appendix 4.1.

Figures 4.10 to 4.13 present a summary of the cable truss behaviour. Diagrams are presented for symmetrical and non-symmetrical loadings. For the symmetrical case half of the truss was measured with four additional sets on the other half to check the symmetry of the results. All of these agreed to within 0.5 mm confirming that a high degree of symmetry had been retained.

FIG 4.6

TYPICAL STRESS/STRAIN GRAPH FOR 30 S.W.G. SINGLE STRAND STEEL WIRE

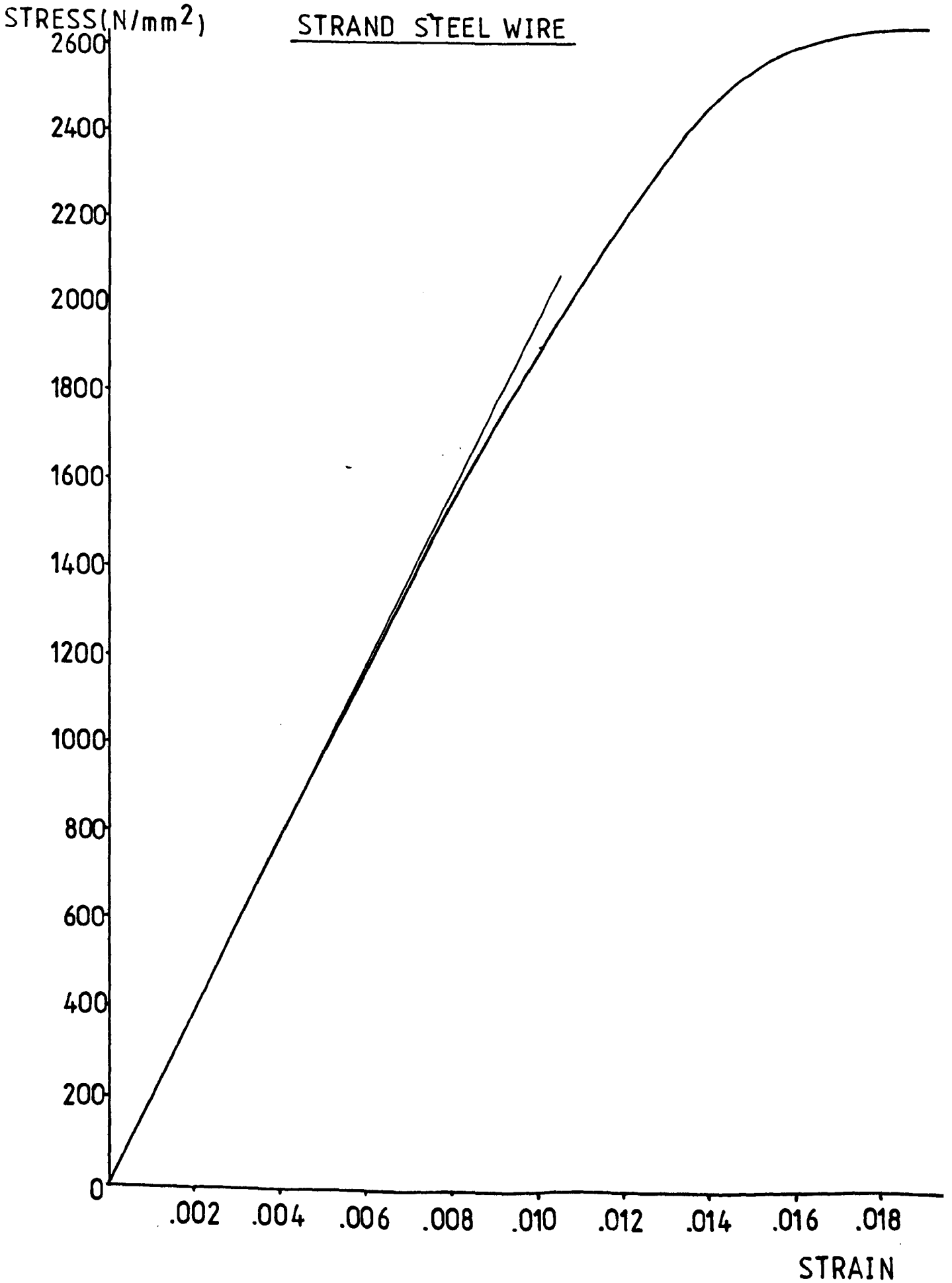

FIG 4.7

TYPICAL STRESS/STRAIN GRAPH FOR 18 S.W.G. SINGLE STRAND STEEL WIRE

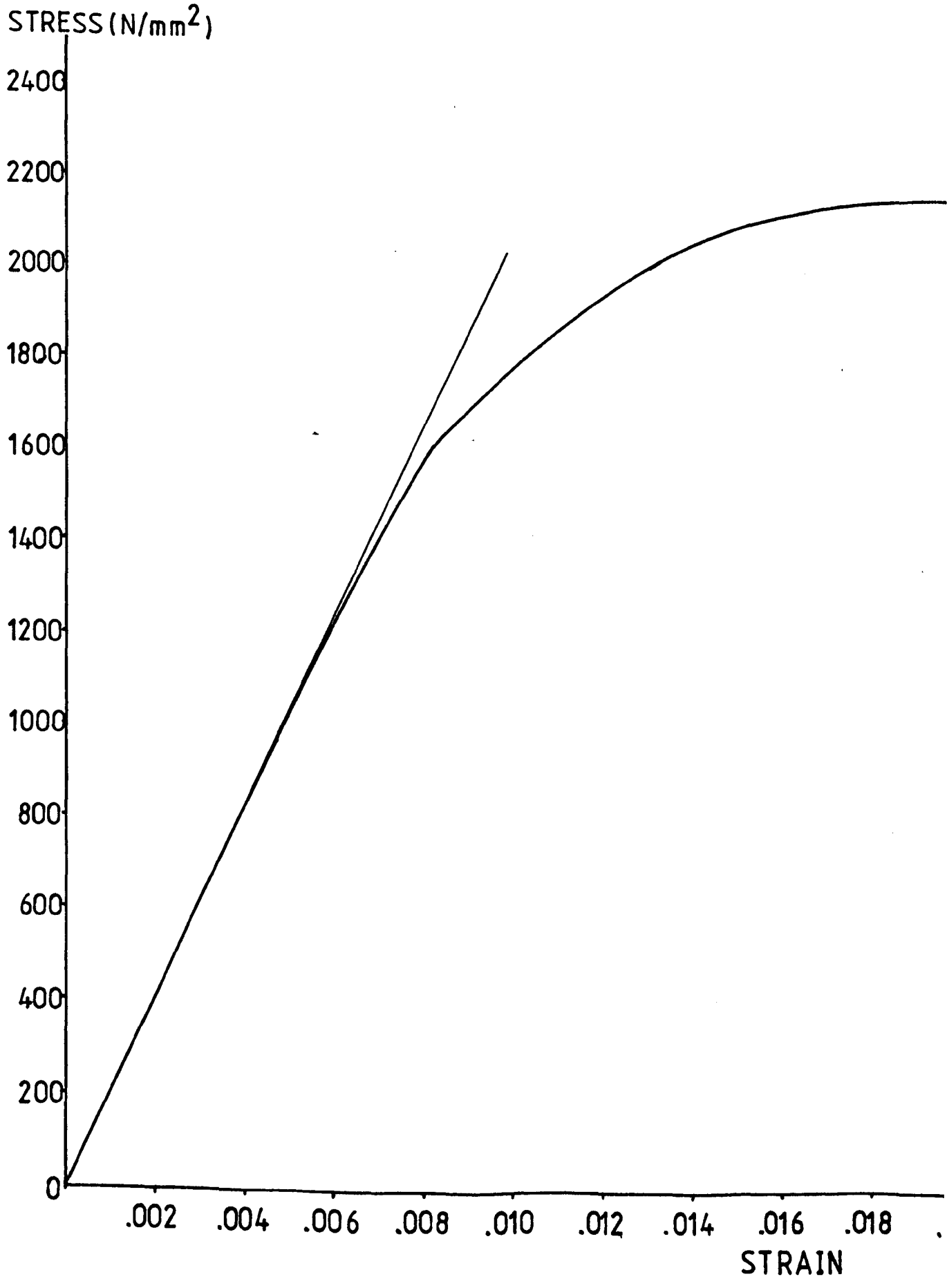

FIG (4·8)

HISTOGRAMME OF YOUNG'S MODULUS FOR 30 S.W.G. SINGLE STRAND STEEL WIRE

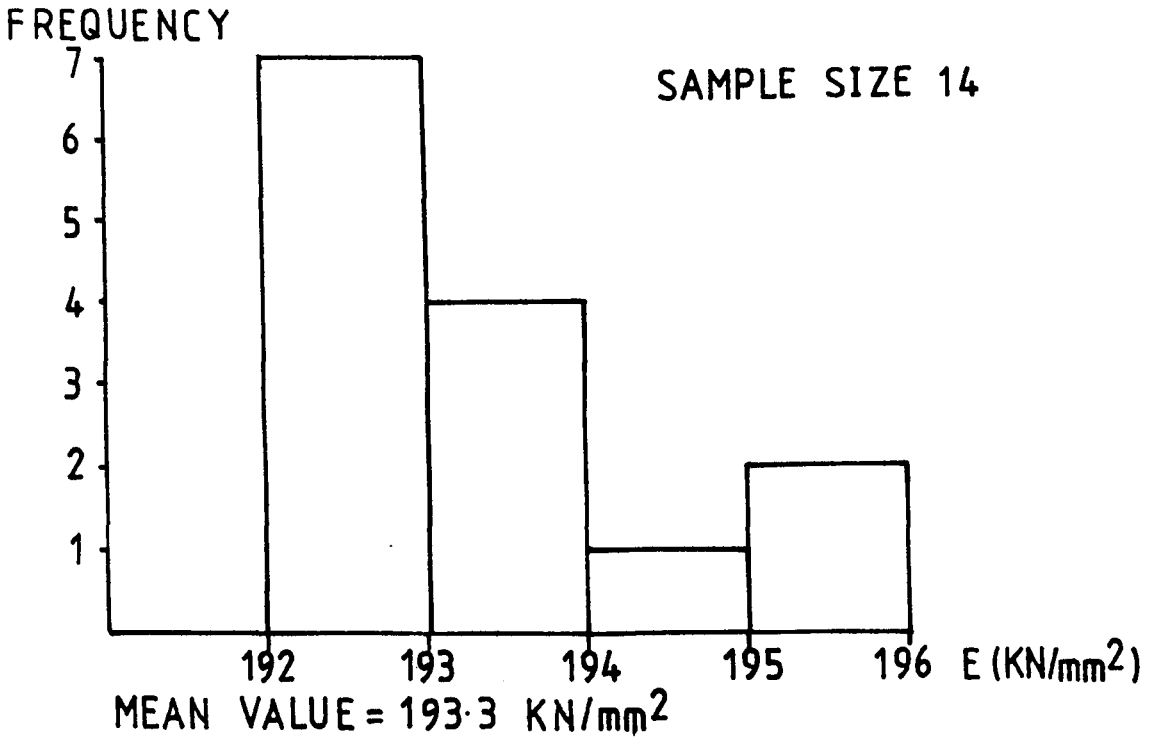

MEAN VALUE = 193·3 KN/mm^2

FIG (4·9)

HISTOGRAMME OF YOUNG'S MODULUS FOR 18 S.W.G. SINGLE STRAND STEEL WIRE

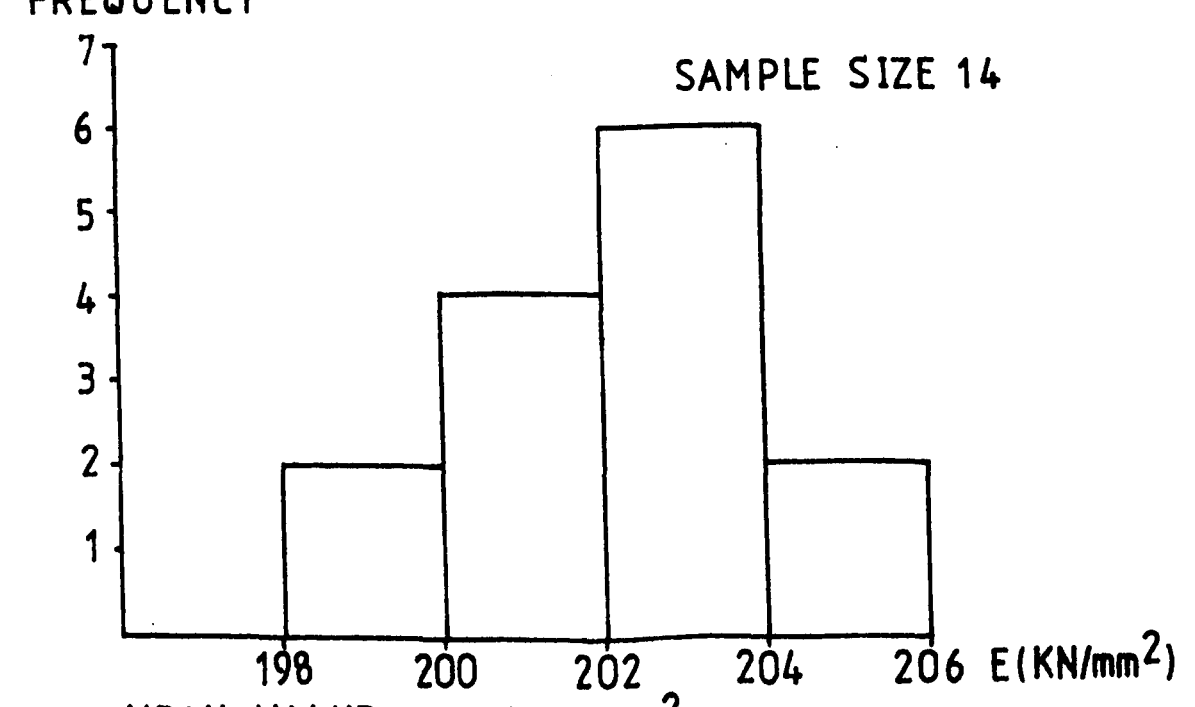

MEAN VALUE = 202·5 KN/mm^2

FIG 4·10

GRAPH OF TRUSS JOINT DEFLECTIONS FOR SYMMETRICAL LOADING

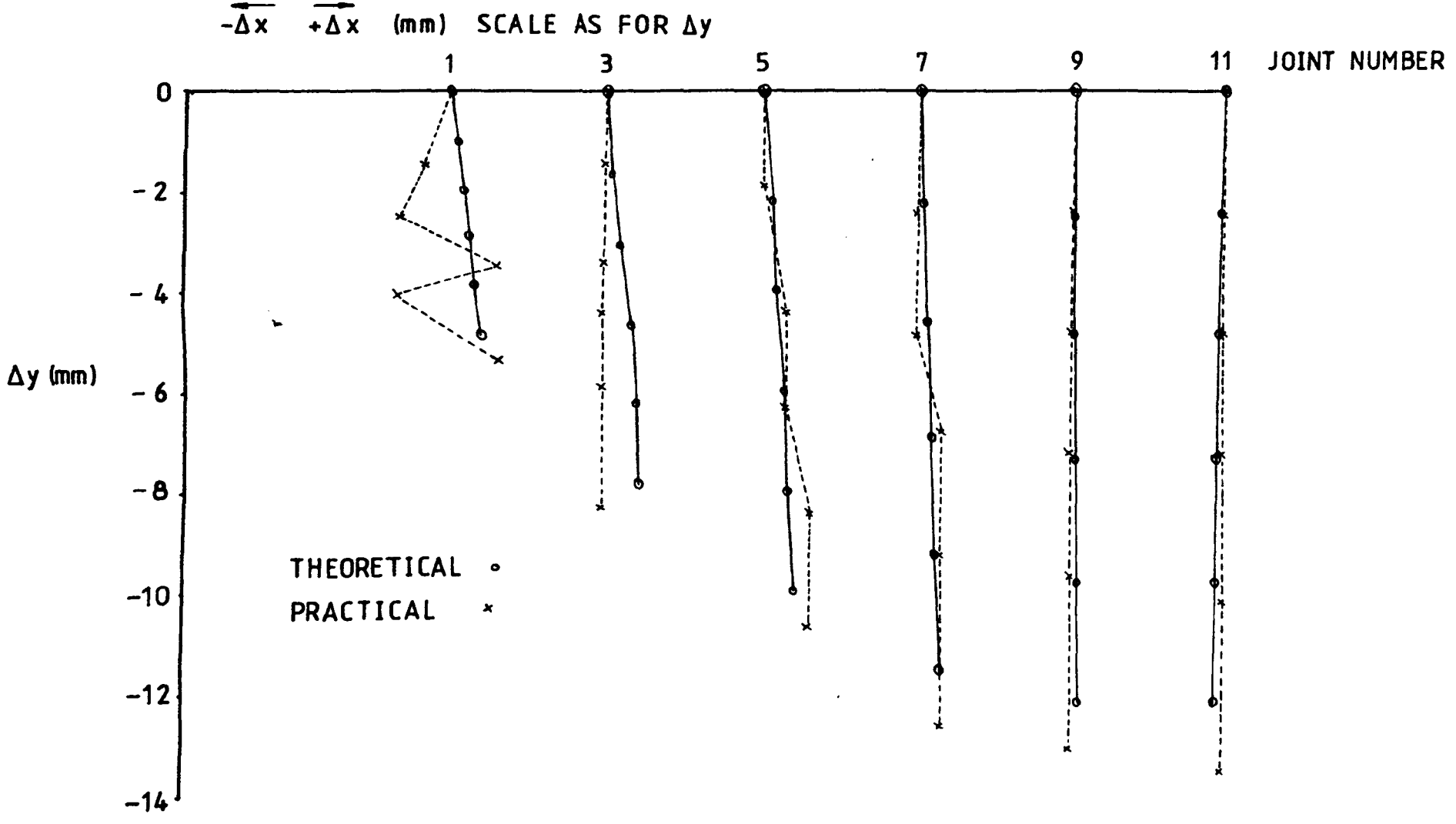

FIG 4·11

GRAPH OF TRUSS JOINT DEFLECTIONS FOR SYMMETRICAL LOADING

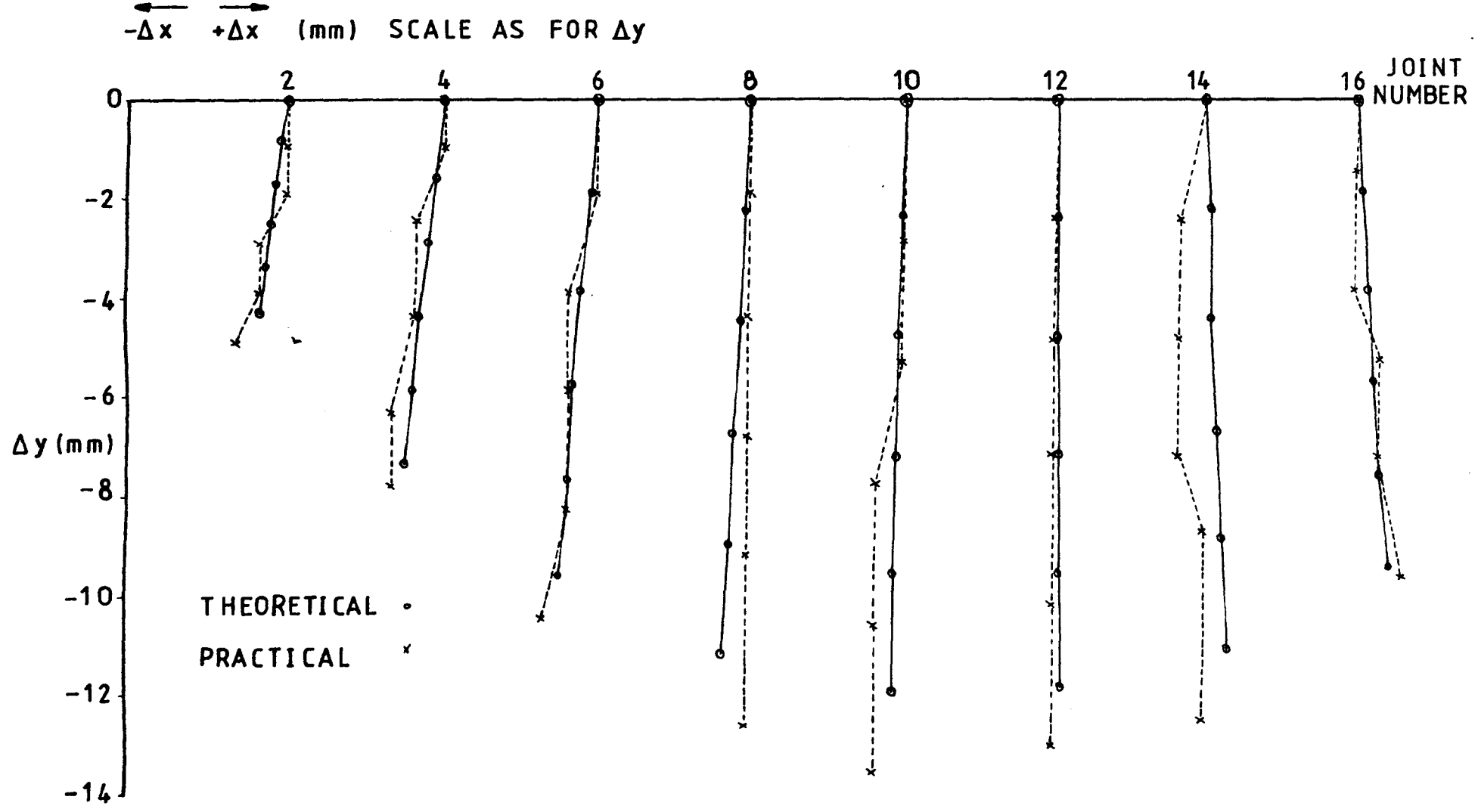

FIG 4.12

TRUSS JOINT DEFLECTIONS FOR NON SYMMETRICAL LOADING

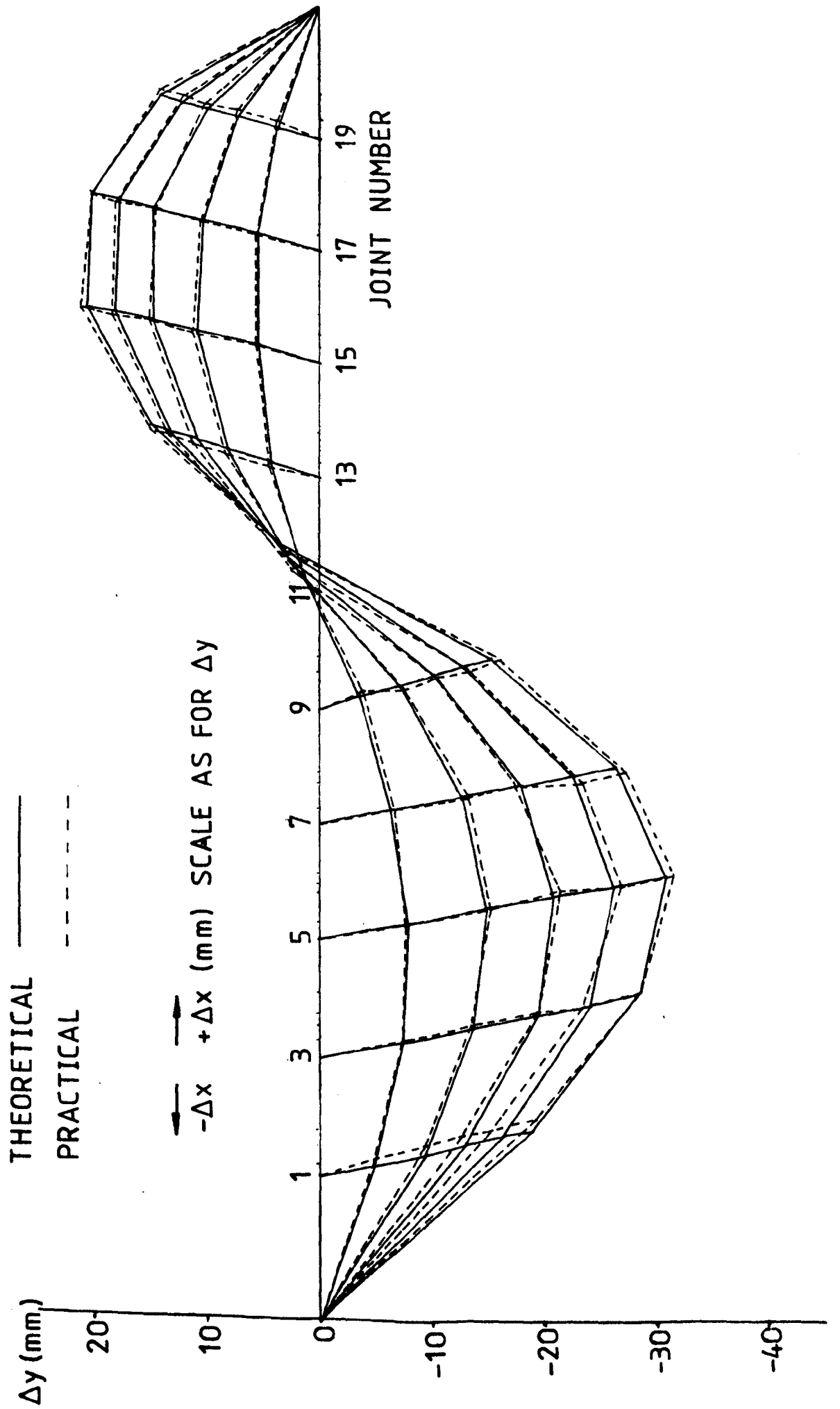

FIG 4.13

TRUSS JOINT DEFLECTIONS FOR NON SYMMETRICAL LOADING

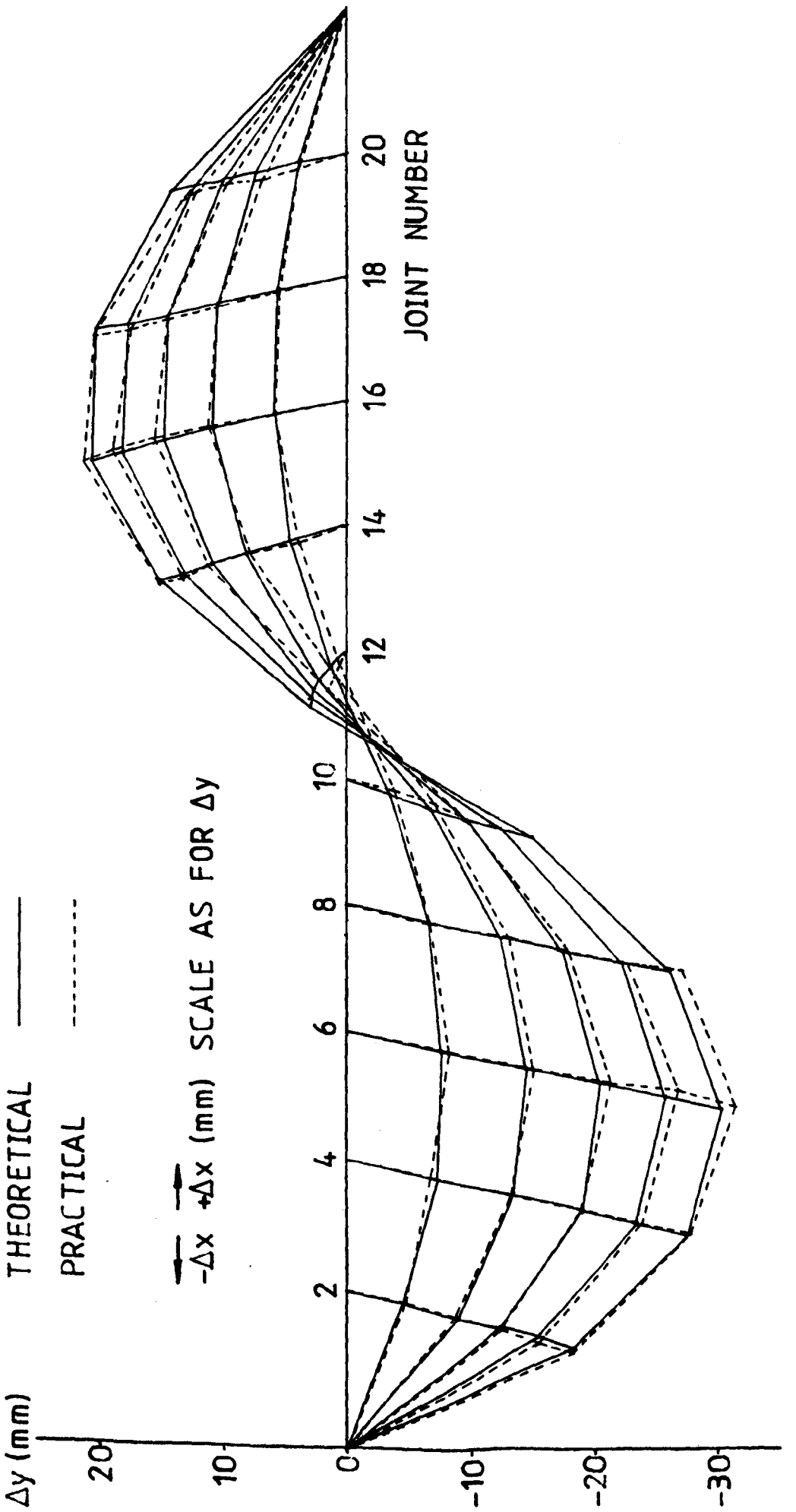

By comparing results for both load cases the effect of the loading upon the nature of the response is apparent. The symmetrical loading gave a near linear load deflection relation with typical horizontal displacements 10% of the vertical displacements. The response to non-symmetrical loading is quite different, there is a noted stiffening of the structure as loads are applied. At node 6 the measured vertical displacement for the first weight increment 0 - 400 gm was 8.3 mm comparing with 4.4 mm for the increment from 1600 - 2000 gm. Significant horizontal displacements were also observed and for nodes 11 and 12 were greater than the vertical components.

The maximum vertical deflections for both load cases with the same nodal load (i.e. half as much total load for the non-symmetrical case) were compared, 31.9 mm for the non-symmetrical against 13.7 mm for the symmetrical case. This greater magnitude for the non-symmetrical load gives a greater accuracy of deflection measurement in percentage terms. At the maximum loading of 2000 gm per loaded node the displacements have been predicted to within an average of 2%. For this magnitude of deflection the photographic method was believed to be accurate to within 1.5%. The experimental deflections are consistently slightly greater than the theoretical ones, this may be due to the understress by 3% of the model in its unloaded state. The photographic method of measurement has shown to be an economic and accurate method of deflection measurement.

ii) Tension Results

The measurement of tension changes in the cable members has been concentrated upon the hanger forces, since these are most sensitive to change due to gravity loading. Again, full tabulated results

are given in Appendix 4.2. Typical results for load case 1 are shown in Figs. 4.14 to 4.16 and for load case 2 in Figs. 4.17 to 4.19. Use has been made of the 1906 computer and standard subroutines to produce the graphical output for the above figures.

Where the initial pretension force has been within 1% of its design value all subsequent measures of the cable tension have been predicted to within 2% over the full loading range (0 - 2000 gm per joint) for both load cases. Refer to Figs. 4.14, 4.16, 4.17 and 4.19. The average error between experimental and theoretical results for these tension measurements was less than 1%.

Where there has been an initial misclosure between the initial cable tension and its design value this error is consistently maintained through the loading range. Referring to Fig. 4.18 the initial tension is 6.9% below the design value, all subsequent measured tension values over the full loading range are between 5.6% and 6.9% below the theoretical values.

As was noted in the deflection results the uniform loading case produced a near linear response in the cable forces. Over the full load range the change in slope of the cable force/nodal load graph was around 15%, this contrasts with a change of 150% for the non-symmetrical load case. This illustrates the need for a fully developed non-linear algorithm to produce accurate results for design purposes.

The vibrating wire method of tension measurement has shown to be an accurate method which can be operated as a fully demountable gauge. The behaviour of the pretensioned cable truss has been accurately mirrored by the theoretical anlaysis. Absolute agreement between results

FIG 4.14

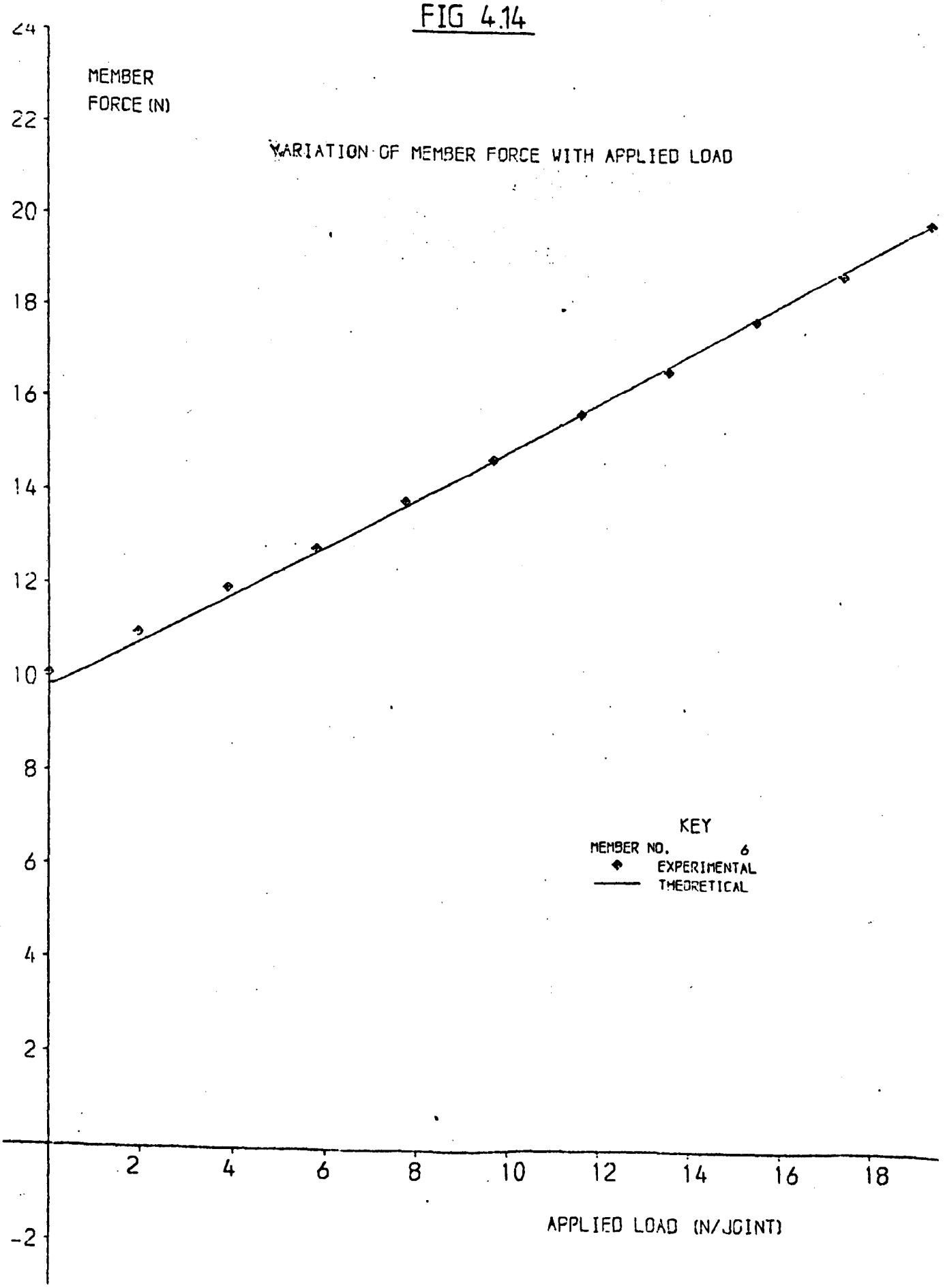
MEMBER
FORCE (N)
VARIATION OF MEMBER FORCE WITH APPLIED LOAD
24
22
20
18
16
14
12
10
8
6
4
2
-2
2
4
6
8
10
12
14
16
18
APPLIED LOAD (N/JOINT)
KEY
MEMBER NO. 6
EXPERIMENTAL
THEORETICAL

FIG 4.15

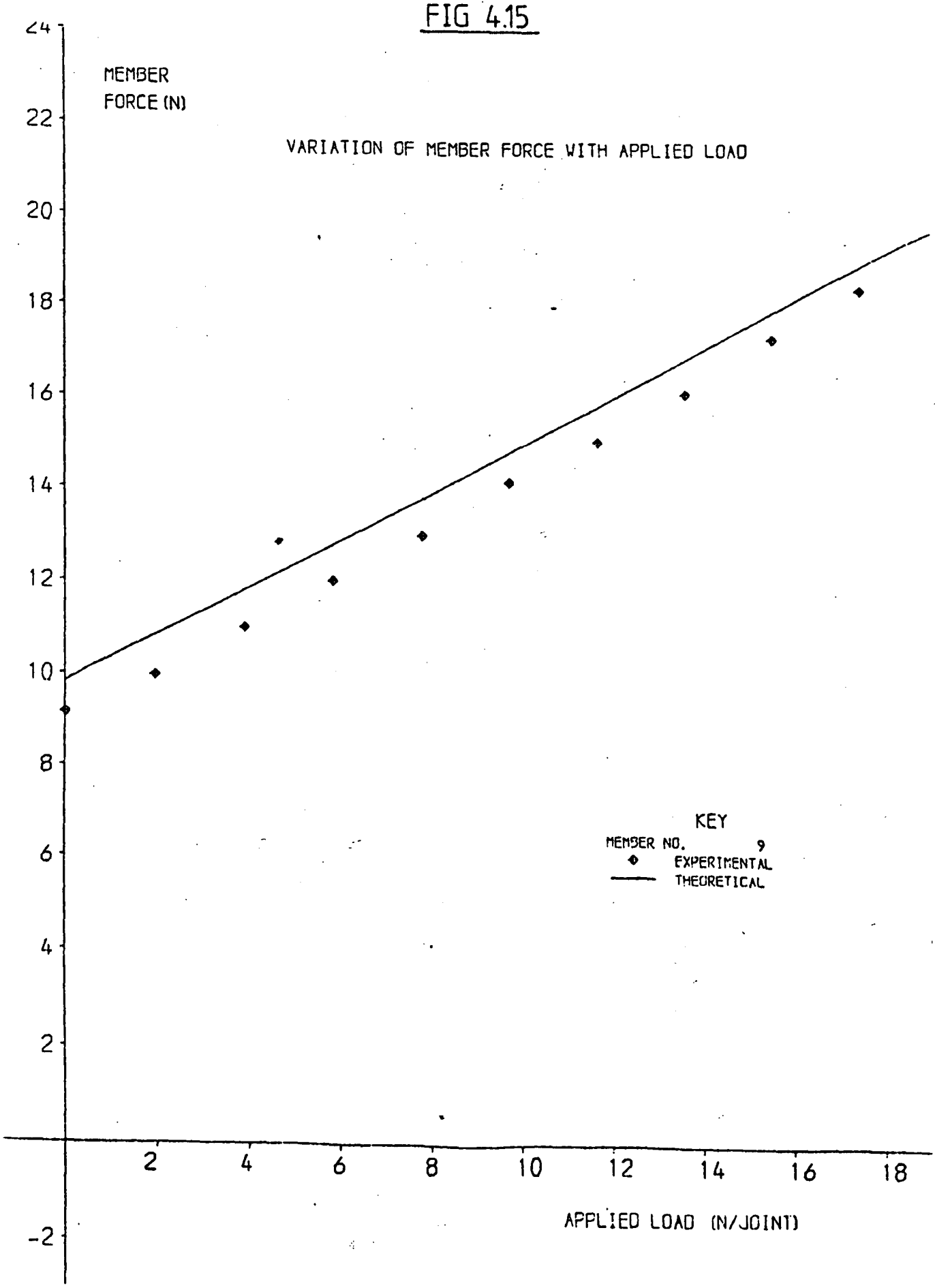
MEMBER
FORCE (N)
VARIATION OF MEMBER FORCE WITH APPLIED LOAD
24
22
20
18
16
14
12
10
8
6
4
2
-2
2
4
6
8
10
12
14
16
18
APPLIED LOAD (N/JOINT)
KEY
MEMBER NO. 9
EXPERIMENTAL
THEORETICAL

FIG 4.16

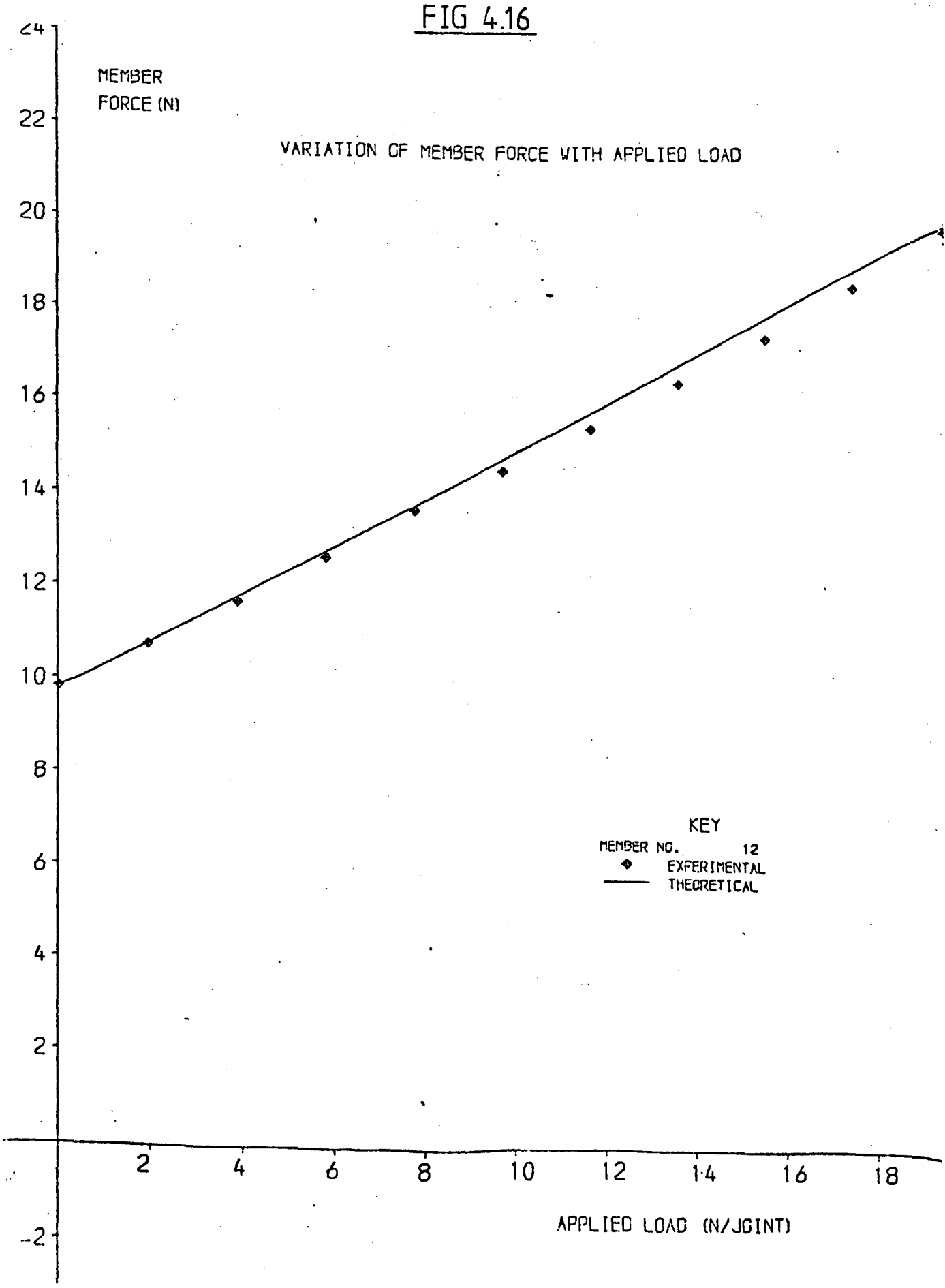
MEMBER
FORCE (N)
VARIATION OF MEMBER FORCE WITH APPLIED LOAD
24
22
20
18
16
14
12
10
8
6
4
2
-2
2
4
6
8
10
12
14
16
18
APPLIED LOAD (N/JOINT)
KEY
MEMBER NO. 12
EXPERIMENTAL
THEORETICAL

FIG 4.17

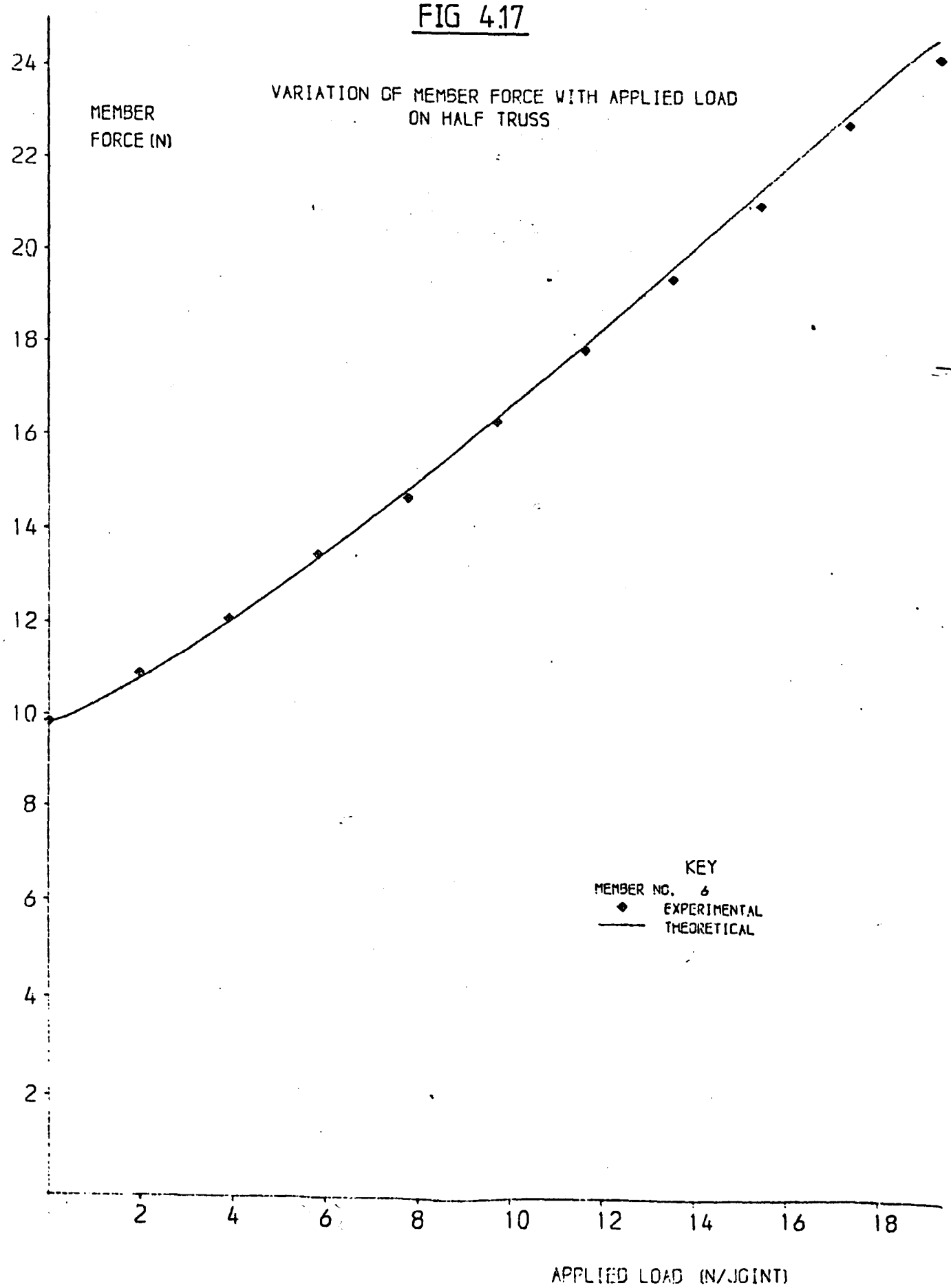
VARIATION OF MEMBER FORCE WITH APPLIED LOAD ON HALF TRUSS
MEMBER FORCE (N)
24
22
20
18
16
14
12
10
8
6
4
2
2
4
6
8
10
12
14
16
18
APPLIED LOAD (N/JOINT)
KEY
MEMBER NO. 6
EXPERIMENTAL
THEORETICAL

FIG 4.18

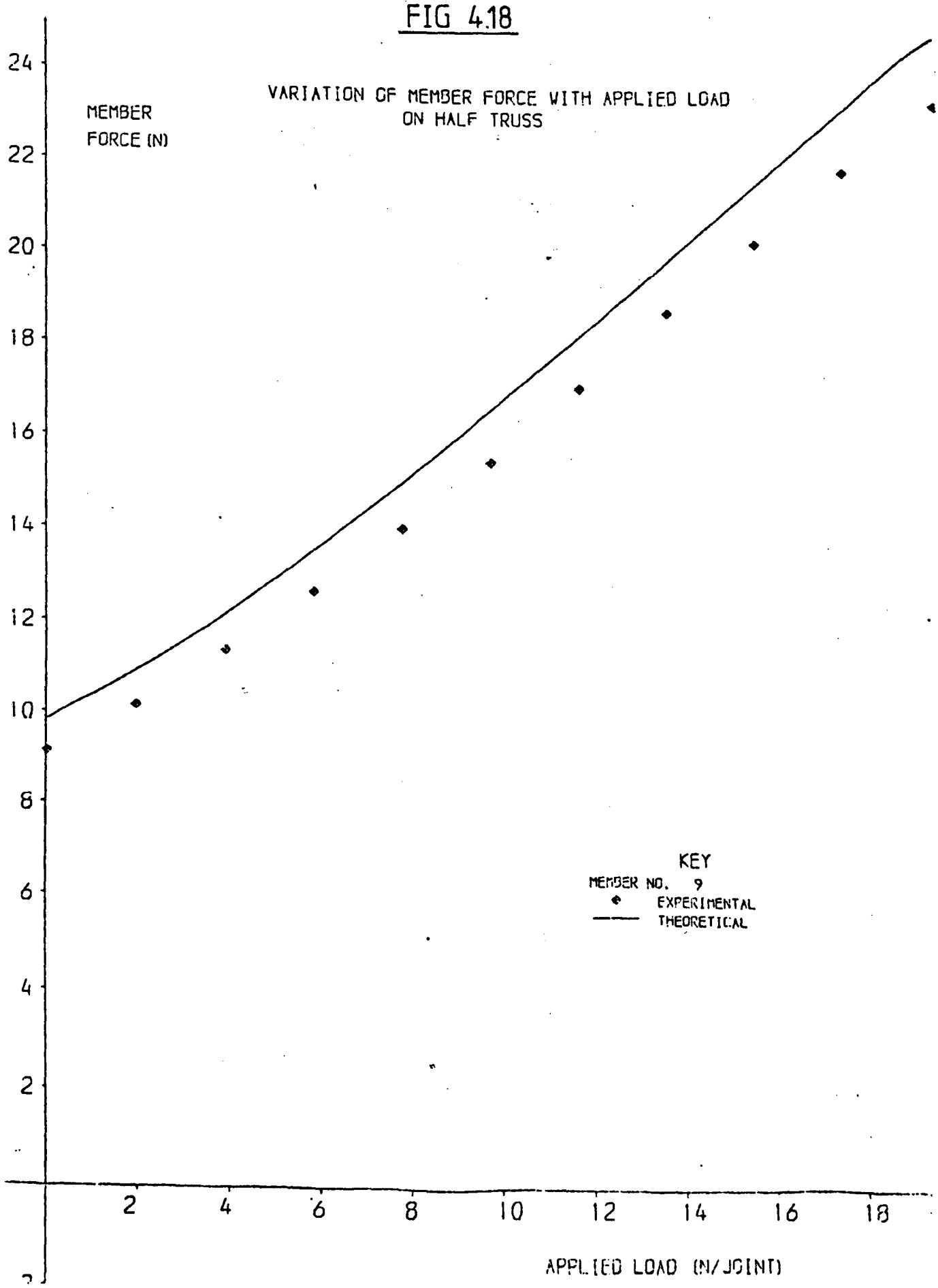
VARIATION OF MEMBER FORCE WITH APPLIED LOAD ON HALF TRUSS
MEMBER FORCE (N)
24
22
20
18
16
14
12
10
8
6
4
2
2
4
6
8
10
12
14
16
18
APPLIED LOAD (N/JOINT)
KEY
MEMBER NO. 9
EXPERIMENTAL
THEORETICAL

FIG 4.19

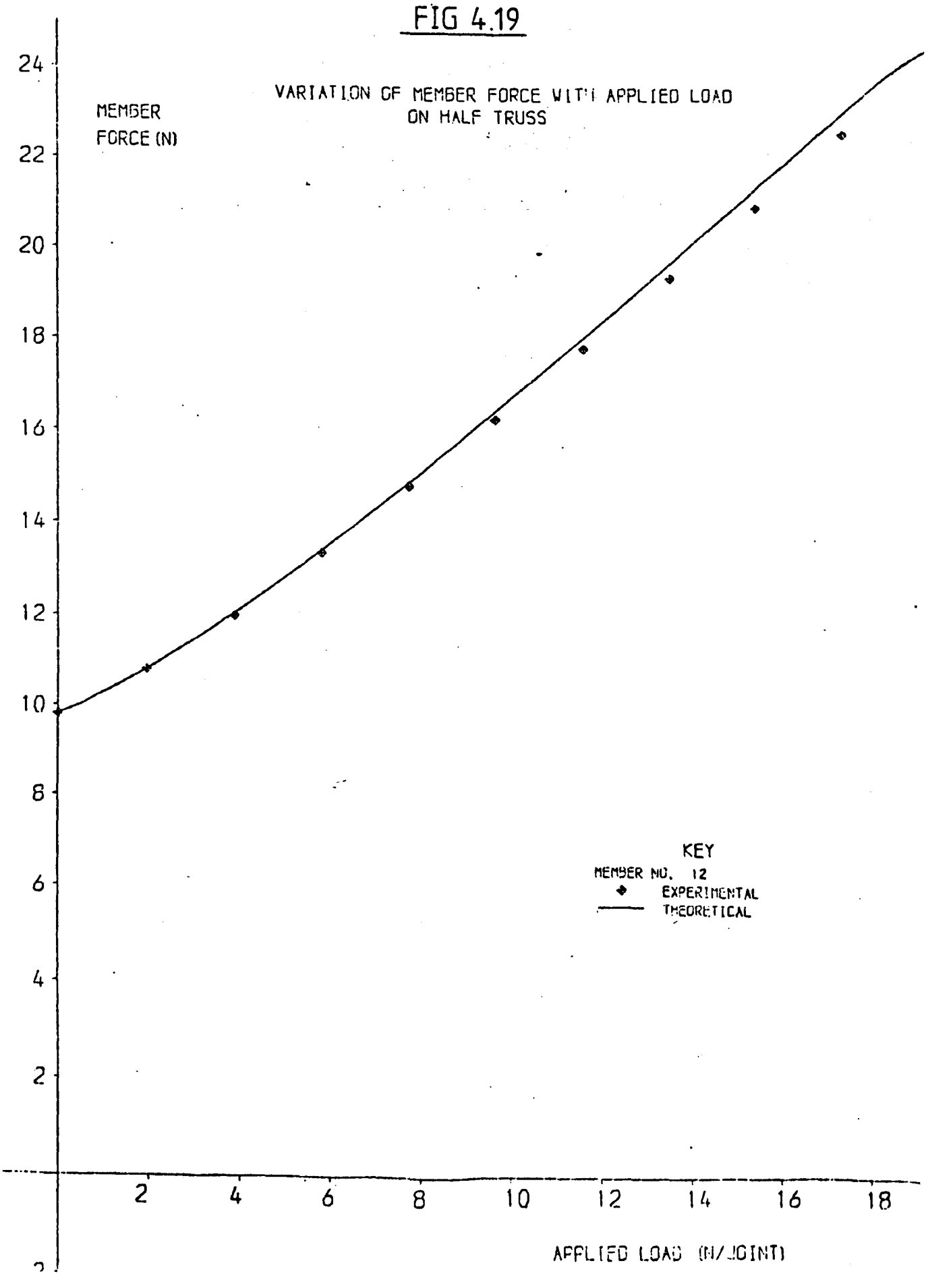
VARIATION OF MEMBER FORCE WITH APPLIED LOAD
ON HALF TRUSS
MEMBER
FORCE (N)
24
22
20
18
16
14
12
10
8
6
4
2
2
4
6
8
10
12
14
16
18
APPLIED LOAD (N/JOINT)
KEY
MEMBER NO. 12
EXPERIMENTAL
THEORETICAL

has been shown to be particularly sensitive to the initial prestress forces where any misclosure is consistently maintained through the load range.

CHAPTER 5

A THREE-DIMENSIONAL CABLE NET EXPERIMENT

5.0 Introduction

Contained in this chapter is a description of the design and construction of a three-dimensional pretensioned cable net. An account of the experimental procedure is followed by a comparison of theoretical and experimental results.

5.1 Design of a Three-Dimensional Cable Net

The cable net experiment was designed to meet the primary requirement to provide non-linear deformation data for comparison with theoretical results. It was thought to be of value to incorporate flexible boundary cable supports into the design of the model to increase the generality of the results. As was the case for the two-dimensional model the stiffness of the structural assembly depends on pretensioning.

Previous experimenters with three-dimensional nets (5.1 - 5.4) have mostly confined themselves to fixed boundaries or relatively stiff straight boundary members. For practical structures it is more economic to have curved boundary members whose predominant forces are compressive with minimum bending; in this way the slenderness of the boundary member can be increased. Comparison with a more general theoretical treatment of the boundary requires the boundary members of the model to exhibit significant deflection while remaining stable under the application of loads to the main cables.

The study of minimum surfaces (i.e. the shape taken by a uniform elastic membrane between a closed curve) and the initial form finding of cable structures has not been investigated beyond the requirements of this model. Møllmann(5.5) has shown that for a prestressed net with uniform stresses in orthogonal directions the boundary curve is in the shape of an arc of an ellipse following the line of thrust corresponding to the projected cable forces, provided the ratio of the major to minor axis $\frac{a}{b} = \sqrt{\frac{Hx}{Hy}}$ (5.1)

The derivation of equation (5.1) is given in Appendix 5.1. The use of constant horizontal components of cable tensions Hx, Hy and orthogonal cables leads to a simple method for the initial shape determination (Section 2.10).

The shape of the model boundary was formed from two semi ellipses inclined at 22.6^{o}. A grid size of 30 cm x 30 cm was chosen for the cables in plan, thus allowing clearance for the vibrating wire tensometer. Four hanging cables prestressed against six hogging cables gave an overall size for the model of 2.1 m x 1.5 m with twenty four internal nodes and twenty support nodes. From equation (5.1) the ratio of horizontal forces $\frac{Hx}{Hy} = 1.96$.

The size of model maintained the balance between the overall number of degrees of freedom and the cost of construction. Fig. 5.1 shows a line diagram of the net model with plan view and elevations.

5.2 Calculation of Initial Prestress Forces

The initial prestress forces and member lengths are required both for construction and for data in the theoretical analysis.

FIG 5.1

LINE DIAGRAM OF CABLE NET MODEL

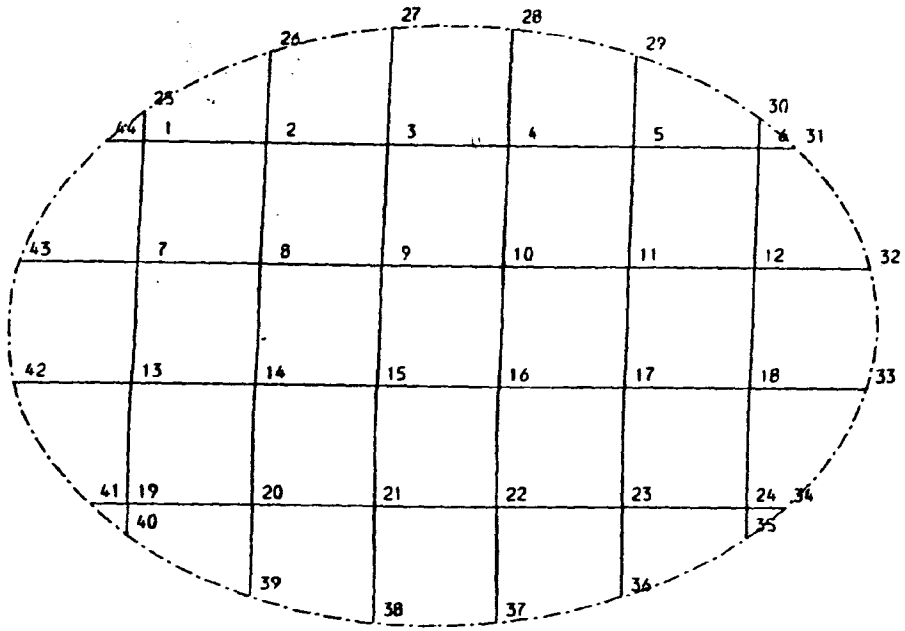

PLAN

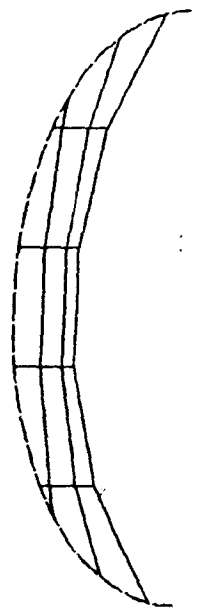

SIDE VIEW

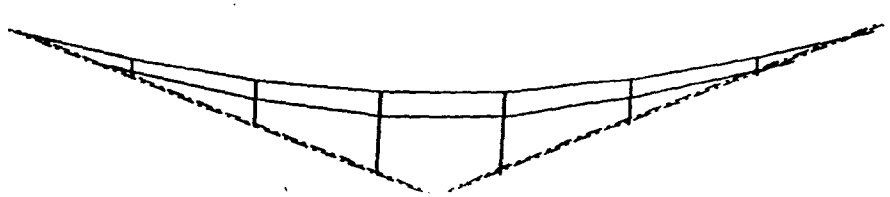

The method of form finding used for fixed boundary orthogonal prestressed nets has been described in section 2.10 and the basis of analysis of the boundary ring beam in section 2.11. Earlier work has not shown how to deal with the combined problem. The following iterative method is proposed. Starting with the boundary nodes fixed in position corresponding to the unloaded boundary member, the internal cable force and node positions are calculated. The boundary is then allowed to deflect under the action of the cable forces to give new boundary node positions. The internal cable forces and node positions are then recalculated and any change in the cable forces applied to the boundary. Boundary node positions and cable forces were found to stabilise after a maximum of five cycles of iteration as shown by Fig. 5.2. A single stage initial form finding analysis was not considered in view of the very economical and satisfactory convergence obtained. It is thought that this method may have general value.

To provide a visual check on the initial data computer programs were written to give a plan view and side elevations of the cable net shape together with a three dimensional view from different angles. These computer prints appear in Fig. 5.3.

5.3 Design and Construction of Cable Net Components

Detailed design of the components of the cable net model are now discussed. The success of model analysis depends on achieving accurate simulation of design details which can be simulated theoretically.

(i) Cable joints

The cable joints were required to provide a fixed node point where two orthogonal pretensioned wires crossed. During pre-

FIG 5.2

CONVERGENCE OF ITERATIVE FORM FINDING METHOD

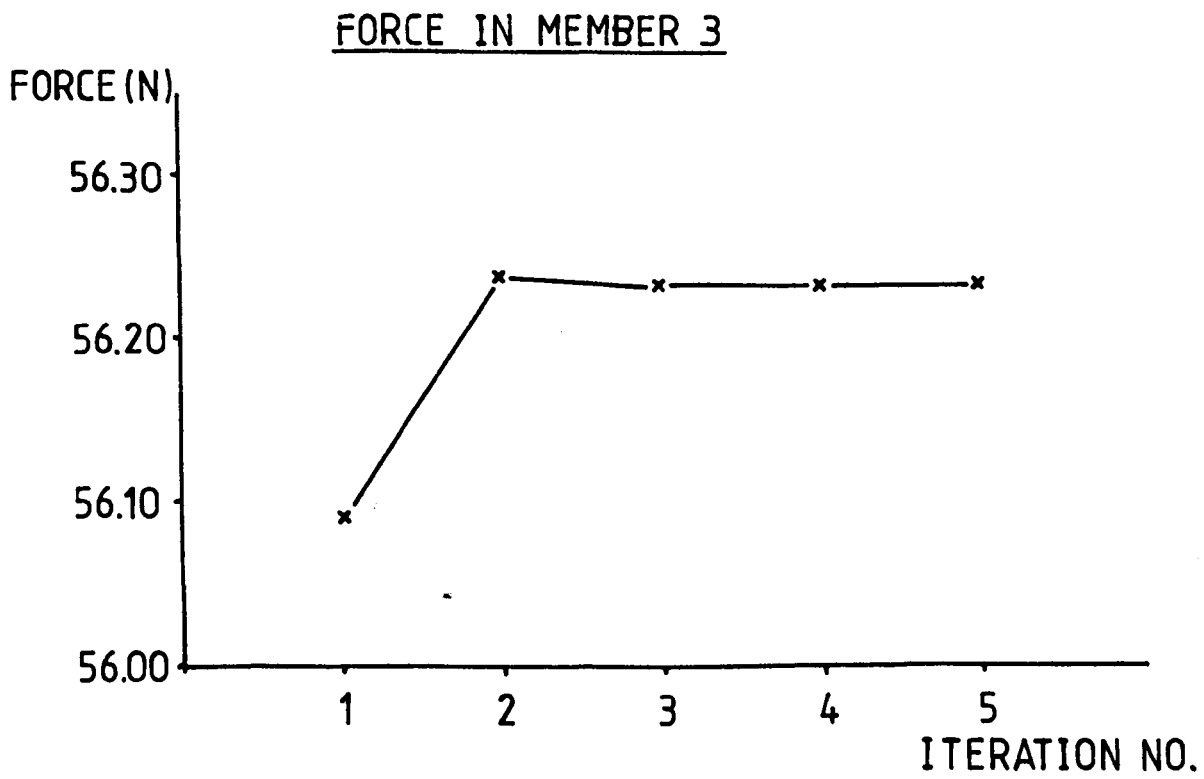

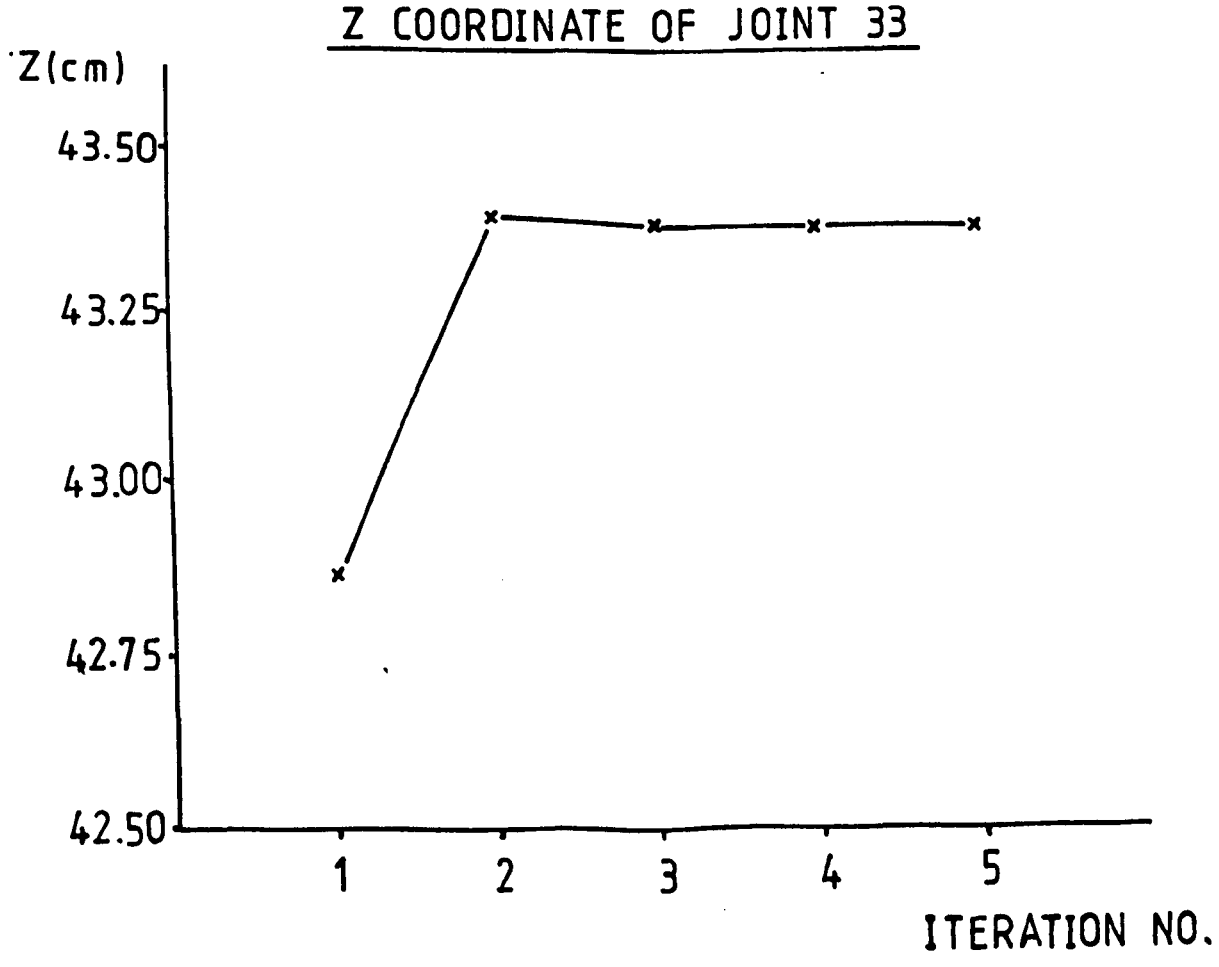

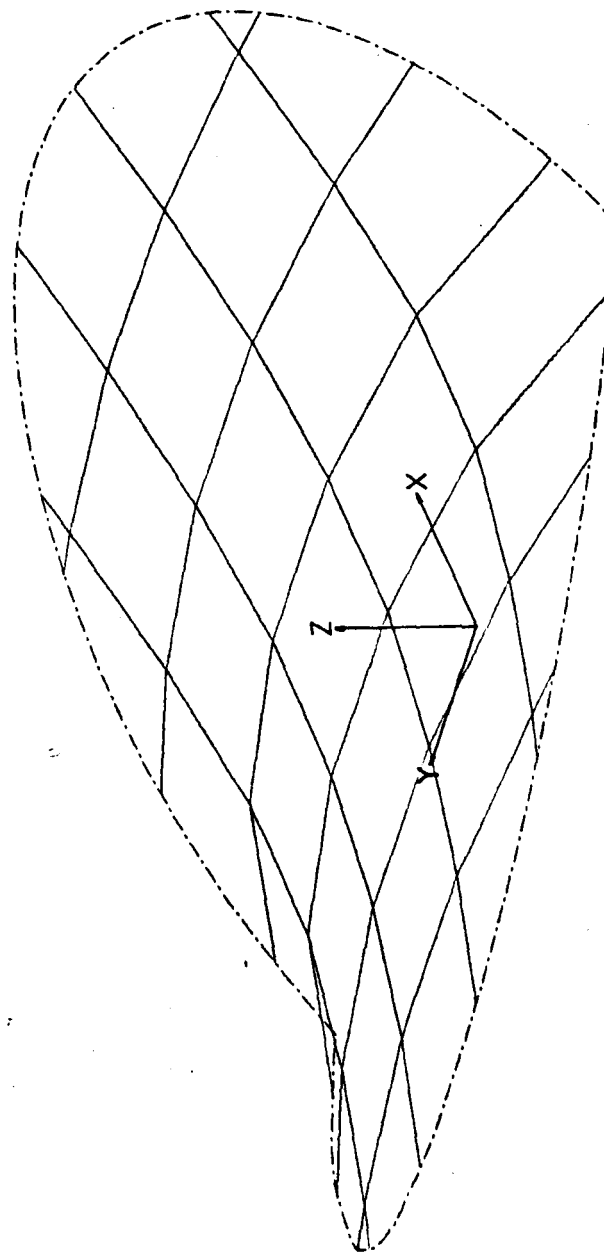

FIG 5.3
ISOMETRIC VIEW OF CABLE NET

tensioning relative movement of the wires at the node points is required to allow the net to take up its initial prestressed shape. Fig. 5.4 shows the joint arrangement. The keeper plate ensures that only a compressive clamping force is exerted between the cables.

(ii) Boundary ring beams

The boundary ring beams consisted of two mild steel bars bent to the required shape. To ensure accuracy ($\pm$ 1 mm in position) an alloy template was fabricated to a quarter ellipse shape and lines scribed to indicate where the cables meet the boundary (Fig. 5.5). The half ellipses were rolled from 3/16" x 1½" mild steel bar to the template profile by Reliance Sheet Metal and Engineering Works of Nottingham.

A specified orientation as well as position was required for the cable holes in the ring beam. This direction was of a generally varying obliquity to the surface of the ring beam at the cable joint. The misdirection caused by the flexibility of the workpiece and drill bit precluded the straight drilling of each hole. Guide blocks (Fig. 5.6), which located onto the ring beam were therefore prepared tc give angular and positional accuracy for the 6.35 mm holes through the beam.

(iii) Cable Anchorages

The requirements for the cable anchorage device are that it:-

1. holds the ends of the cables securely in position,
2. provides tension adjustment in the cable,
3. measures the cable tension,
4. transfers the cable force to the ring beam through its neutral axis.

FIG 5.4
TYPICAL CABLE JOINT

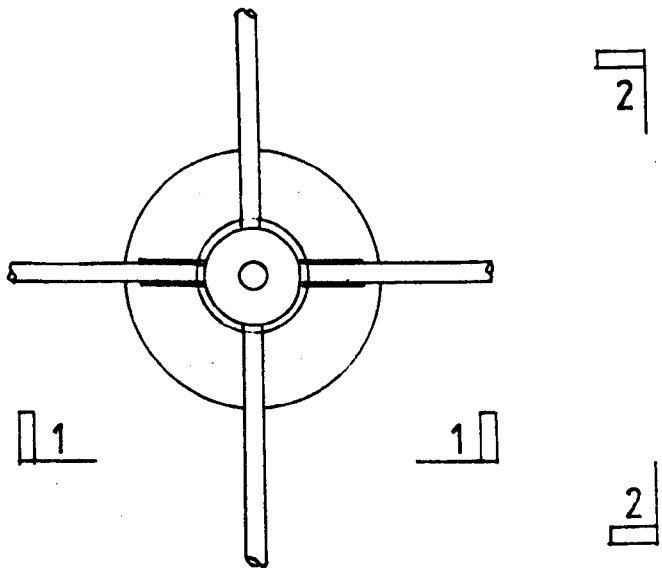

PLAN

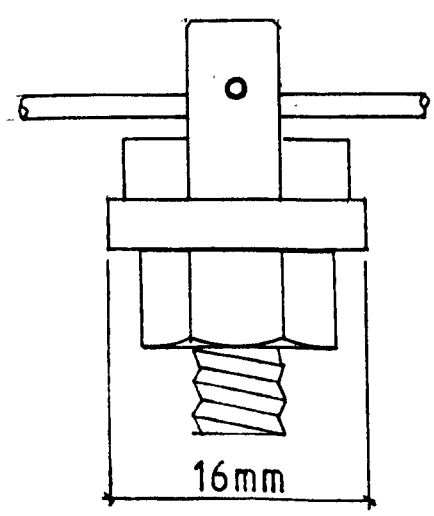

SECTION 1-1

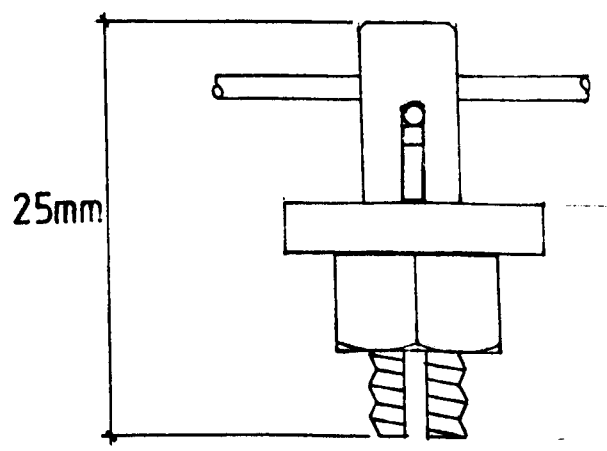

SECTION 2-2

FIG 5.5

TEMPLATE FOR BOUNDARY BEAM

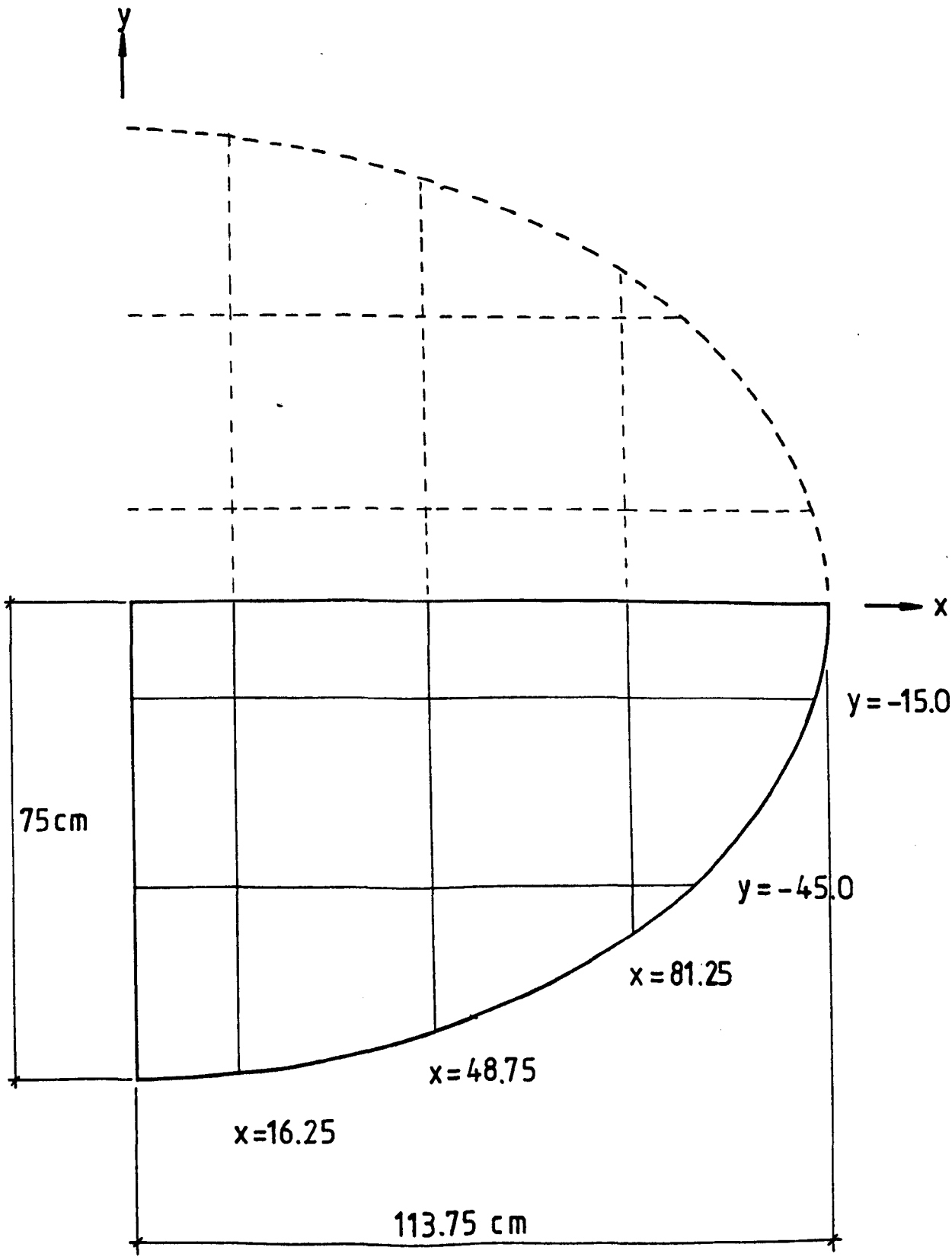

FIG 5.6

GUIDE BLOCK

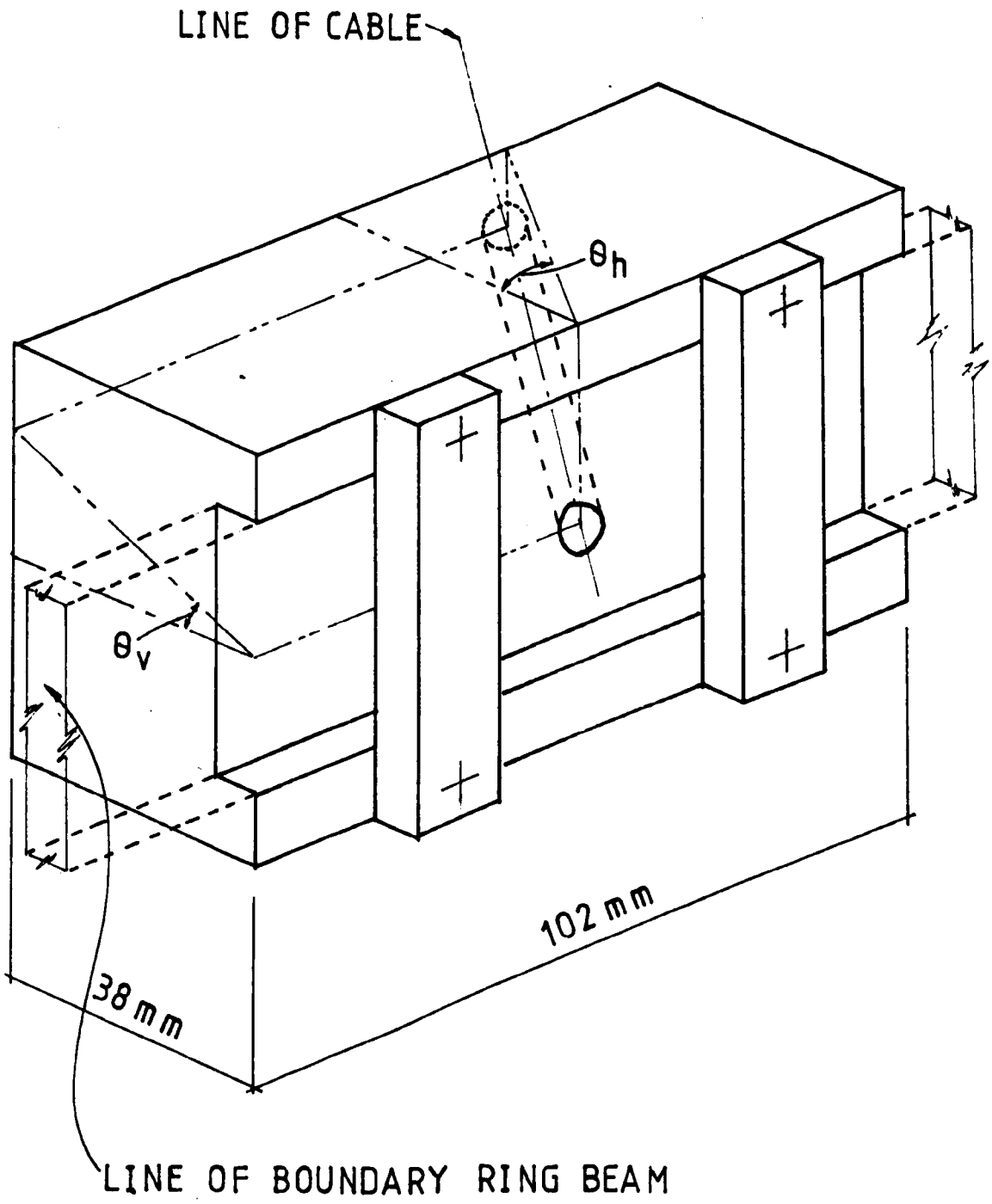

The design of the compression cylinder to measure tensions has been described in Chapter 3. A ball and socket arrangement centred the anchorage upon the locating hole in the beam. The base of the socket was milled to suit the angle between the plane of the cable and the surface of the boundary beam. An exploded diagram of the anchorage assembly is shown in Fig. 5.7. The cable end is held by the anchorage bolt which together with the adjusting nut provides tension variation in the cable.

(iv) Wire Cable

Direct tensile tests were required to determine the stress/strain relation for the stranded wire cable. The Instron testing machine previously used successfully for single stranded wire did not give consistent results. The most likely source of error was slippage of the extensometer gauge as the helical strands contracted during stressing. To overcome this problem two demountable collars were fabricated and fixed to the wire at a preset gauge length. The strain between these points could then be measured using an Amsler extensometer. Consistent results were obtained (Fig. 5.8) provided care was taken not to allow the stranded wire to untwist during the loading sequence.

5.4 Construction of Model

To give a convenient working height for the model and provide a rigid foundation, two large concrete blocks were set on edge 1.2 m apart. 102 mm x 64 mm x 7 mm thick angle sections were bolted to the top surface of the concrete blocks, bolted to the angles in turn were the ring beam anchorage blocks, (Fig. 5.9). To compensate for any lack of location

FIG 5.7
CABLE ANCHORAGE ASSEMBLY

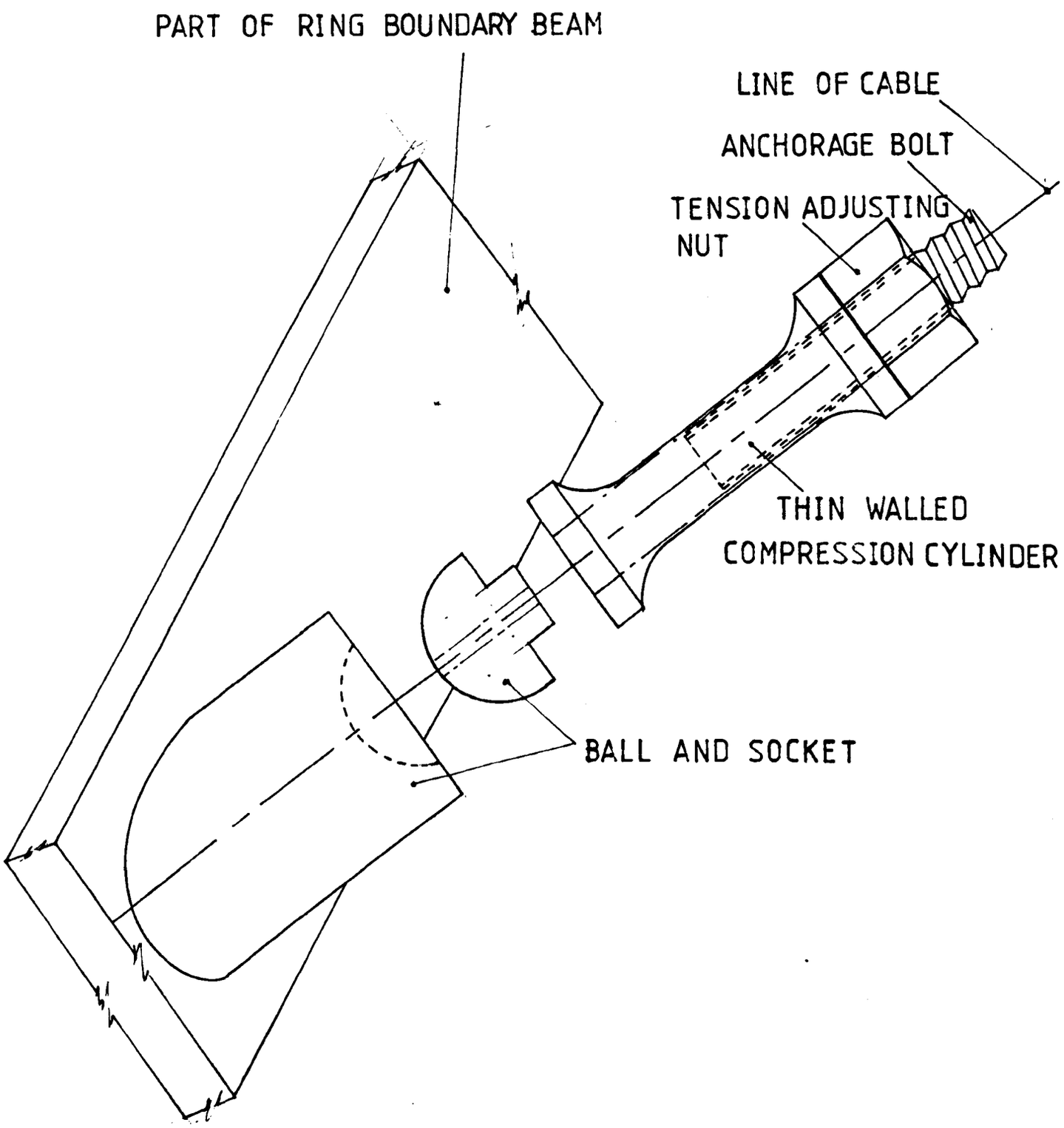

FIG 5.8

STRESS/STRAIN GRAPH FOR MULTISTRAND WIRE

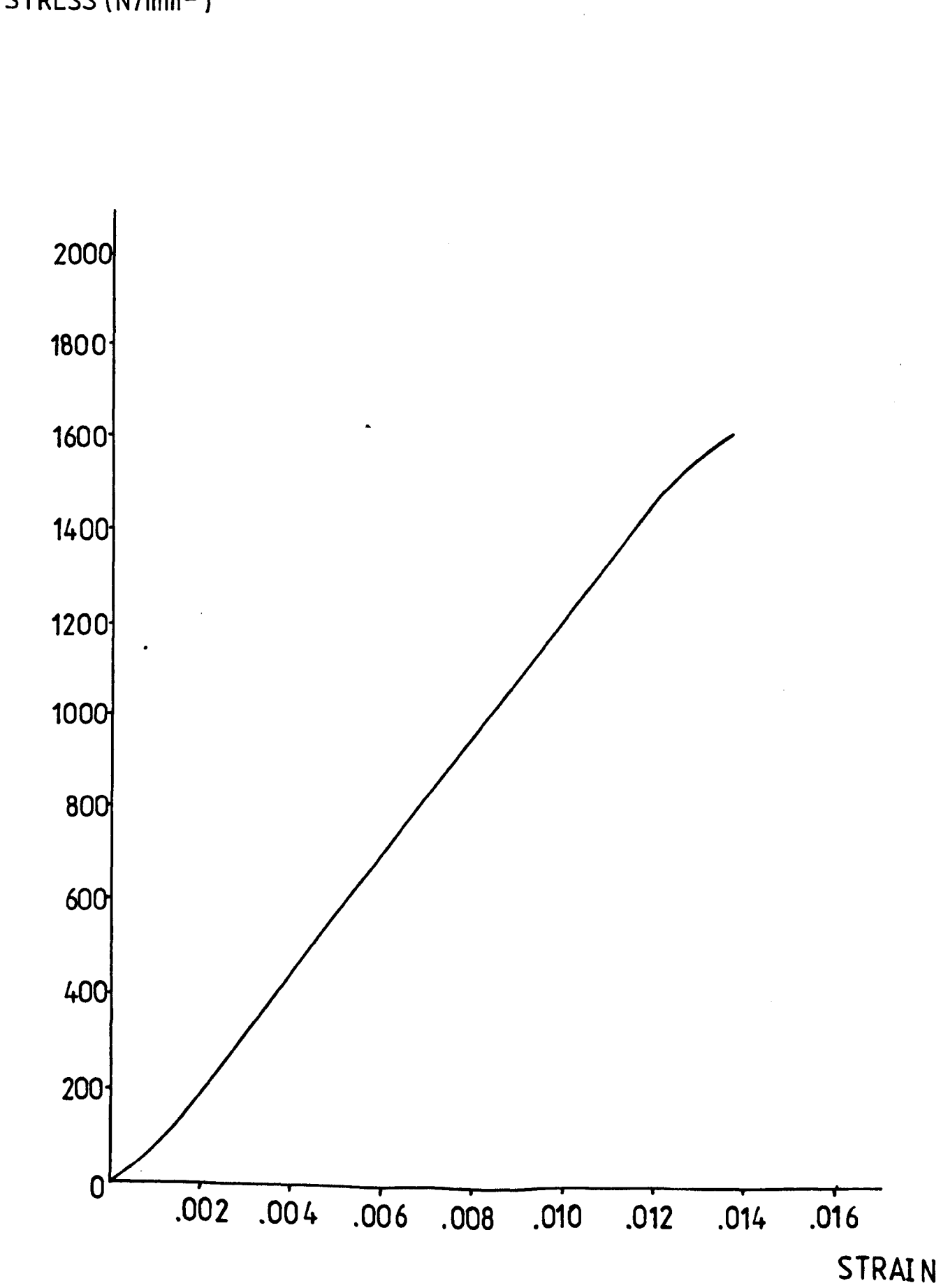

FIG 5.9

BOUNDARY BEAM ANCHORAGE BLOCK

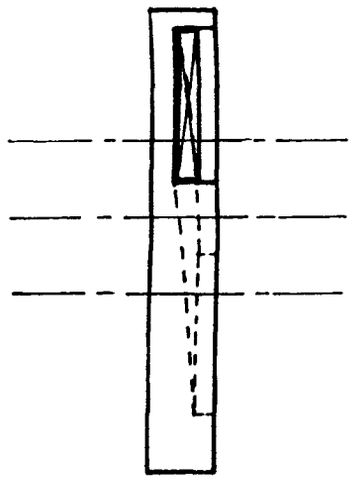

SECTION 1 1

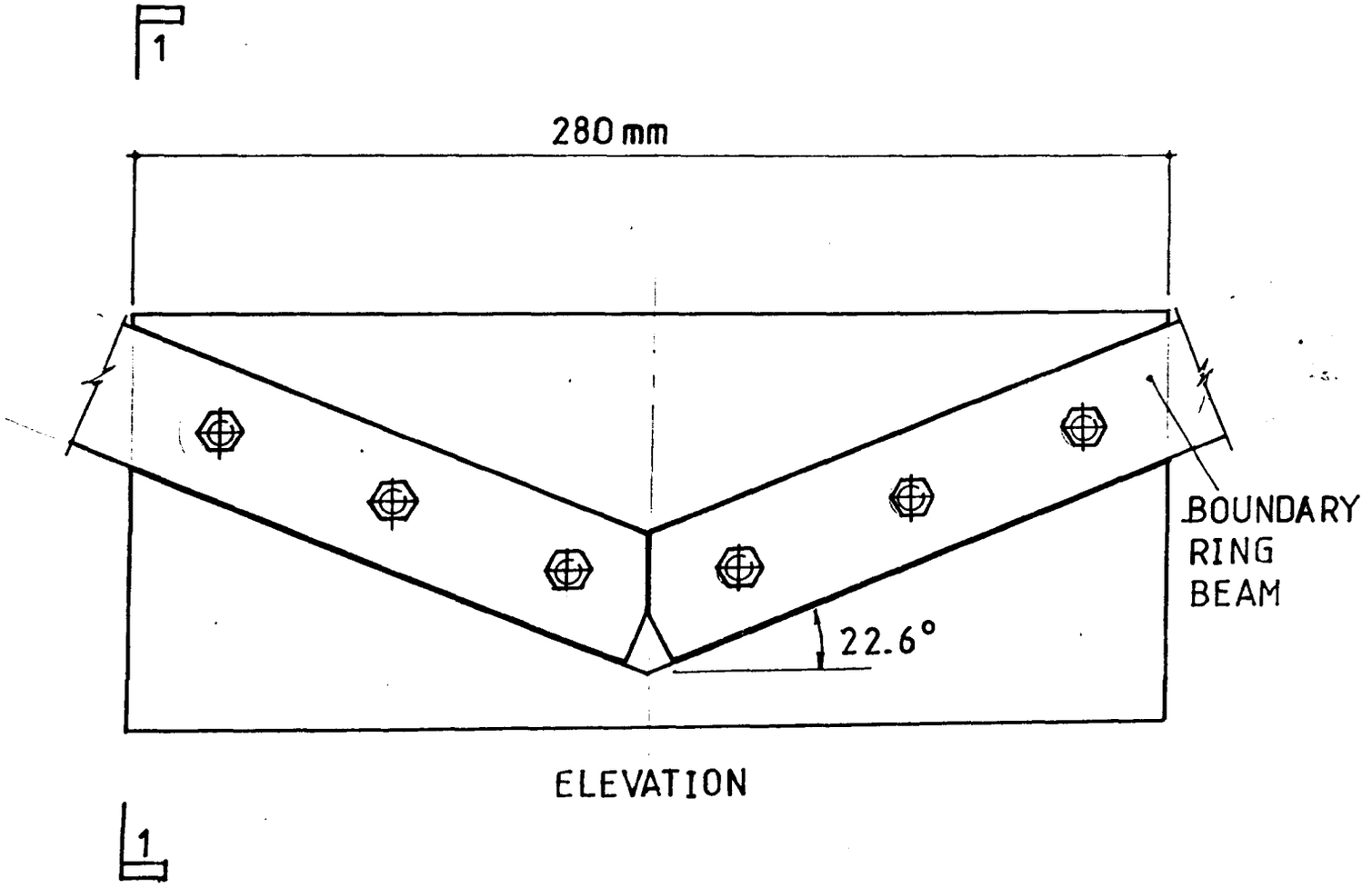

ELEVATION

in the concrete blocks adjustment was available in the line and level of the angle sections. The anchorage blocks were set up to run parallel and level and the ring beams then bolted to them ready for the next stage of threading the cables.

As was the case for the single strand wire used in the two-dimensional experiment the multistrand wire arrived coiled. Again the initial curvature is largely removed by hanging lengths of wire under dead weight at 50% of the ultimate tensile stress with the ends restrained from untwisting. Creep deformation probably associated with restabilisation of the helical strands had effectively ceased after four days. Figure 5.10 shows a graph of extension against time for three of the wires.

Wires were then cut overlength to form the ten main cable members of the net. Anchorage bolts were braised onto one end of each cable. The cable was threaded through the locating ball and socket, ring beam and cable joints then back through the opposite beam and socket. The anchorage bolt was then braised to the far end of the cable.

The availability of a 100 channel logger and the low cost for cylinder gauges encouraged the measurement of anchor forces at every cable end. This was important at the initial pretensioning stage of construction.

Table 5.1 gives the required tension in each of the prestressed wires in terms of the logger reading for each gauge. The tension adjusting nuts were attached to the anchorage bolts and tightened to give the required readings. The tensioning process can be likened to a tuning of the wires, a systematic approach was taken adjusting the

FIG 5.10

CREEP OF THREE STRANDED WIRES

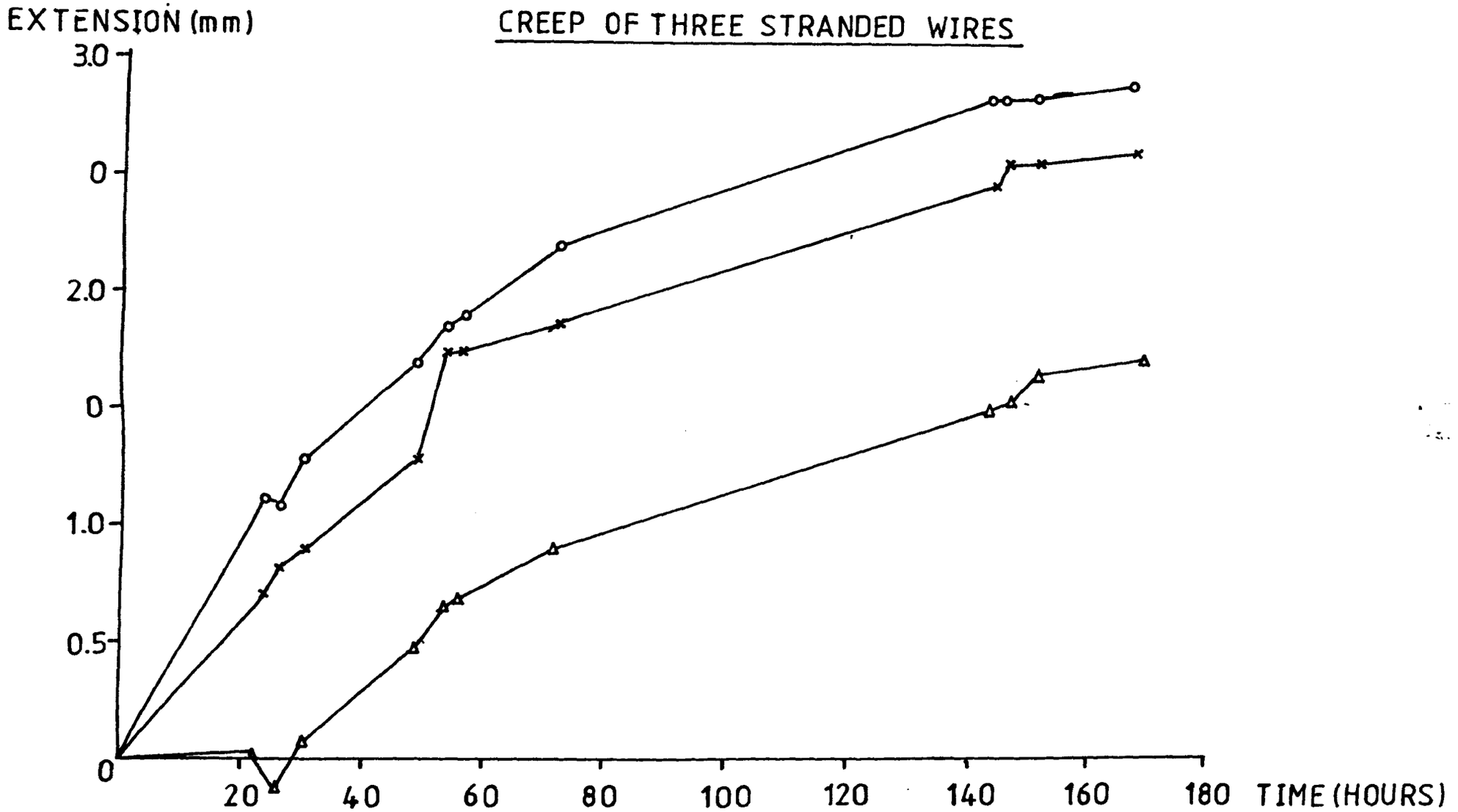

TABLE 5.1

INITIAL PRESTRESS REQUIREMENTS FOR CABLE NET EXPERIMENT

JOINT NUMBER	MEMBER NUMBER	GAUGE CALIBRATION FACTOR N^{-1}	INITIAL PRESTRESS FORCE (N)	REQUIRED LOGGER READING (MICRO-STRAIN)
25	1	-1.397	50.89	-71
26	2	-1.649	52.39	-86
27	3	-1.383	56.23	-78
28	4	-1.309	56.23	-74
29	5	-1.408	52.39	-74
30	6	-1.571	50.88	-80
31	13	-1.288	101.48	-131
32	26	-1.423	101.02	-144
33	39	-1.547	101.02	-156
34	52	-1.363	101.48	-138
35	58	-1.442	50.89	-73
36	57	-1.419	52.39	-74
37	56	-1.549	56.23	-87
38	55	-1.581	56.23	-89
39	54	-1.447	52.39	-76
40	53	-1.525	50.89	-78
41	46	-1.418	101.48	-144
42	33	-1.298	101.02	-131
43	20	-1.415	101.02	-143
44	9	-1.595	101.48	-162

sagging and hogging cables in turn. The hogging cables were tensioned to within 2% of the required tension and the sagging cables to within 5%, this gave an average misclosure of -1.5 N, $\pm$ 2.5 N. The deflection at the crown of each ring beam is compared with the analysis later.

5.5 Test Procedure

To give a rigorous test to the theory four separate load cases were applied to the net (Fig. 5.11).

i) Load case 1 - all of the nodes are loaded

ii) Load case 2 - half of the nodes loaded

iii) Load case 3 - opposite quadrants loaded

iv) Load case 4 - one quadrant loaded

The load cases were designed to investigate the behaviour of the model under both symmetrical and non-symmetrical loading. Loads were applied at the cable joints in 500 gm increments, using weight hangers suspended from 'S' hooks.

Full advantage was taken of the scanning facility on the logger which enabled large numbers of readings to be taken and recorded on punched tape.

For each load case above the loads were removed after each increment so that a check on the no load condition of the model could be made. Three scans of the logger were taken for any given tension reading then any spurious values caused by misreading or mis-punching of the paper data tape could be detected.

Deflection measurements of the ring beam were made using independently mounted dial gauges ($\pm$ 0.005 mm). These are acceptable because of the much greater stiffness of the ring beam compared with

FIG 5.11

LOAD CASES USED IN CABLE NET EXPERIMENT

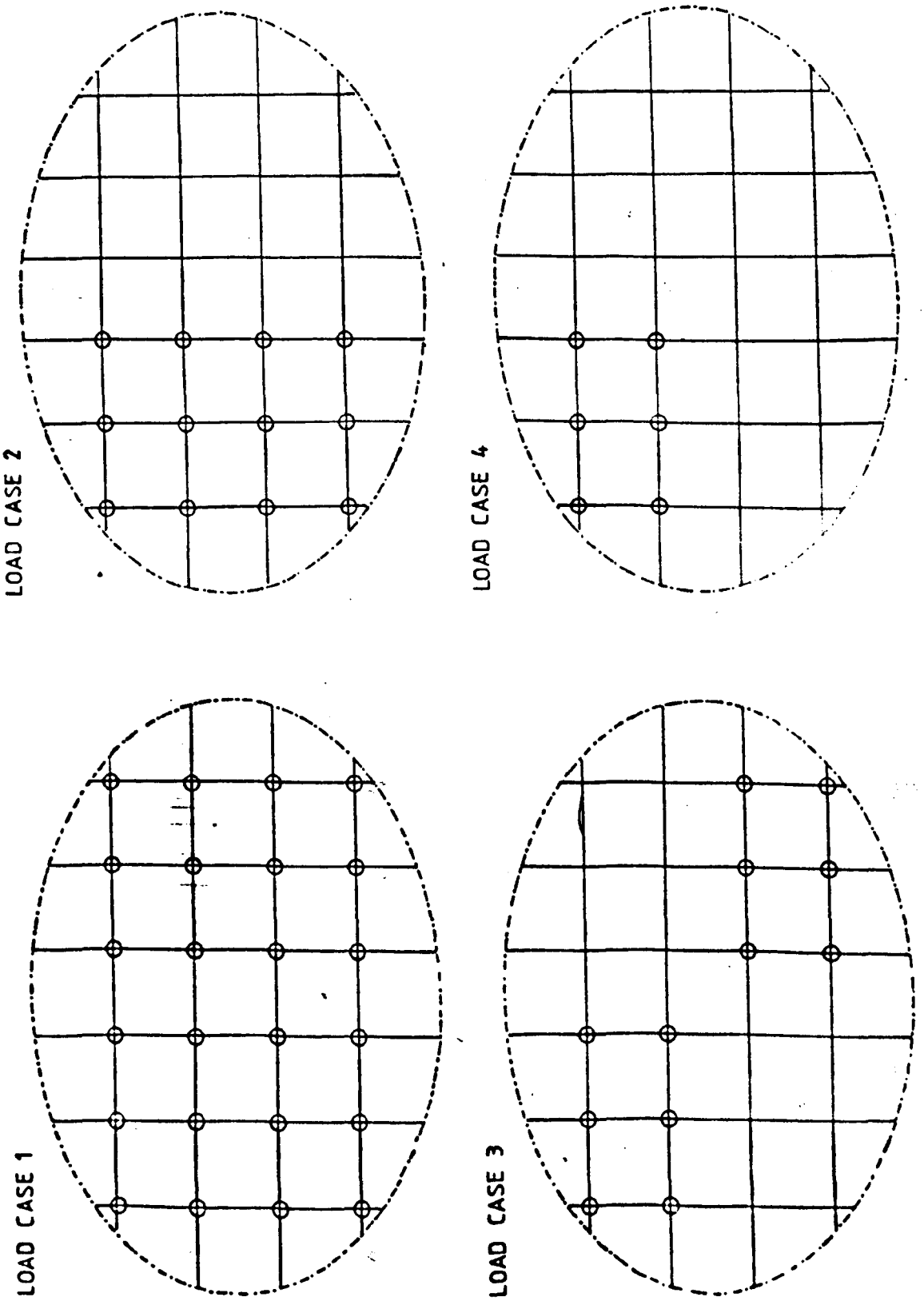

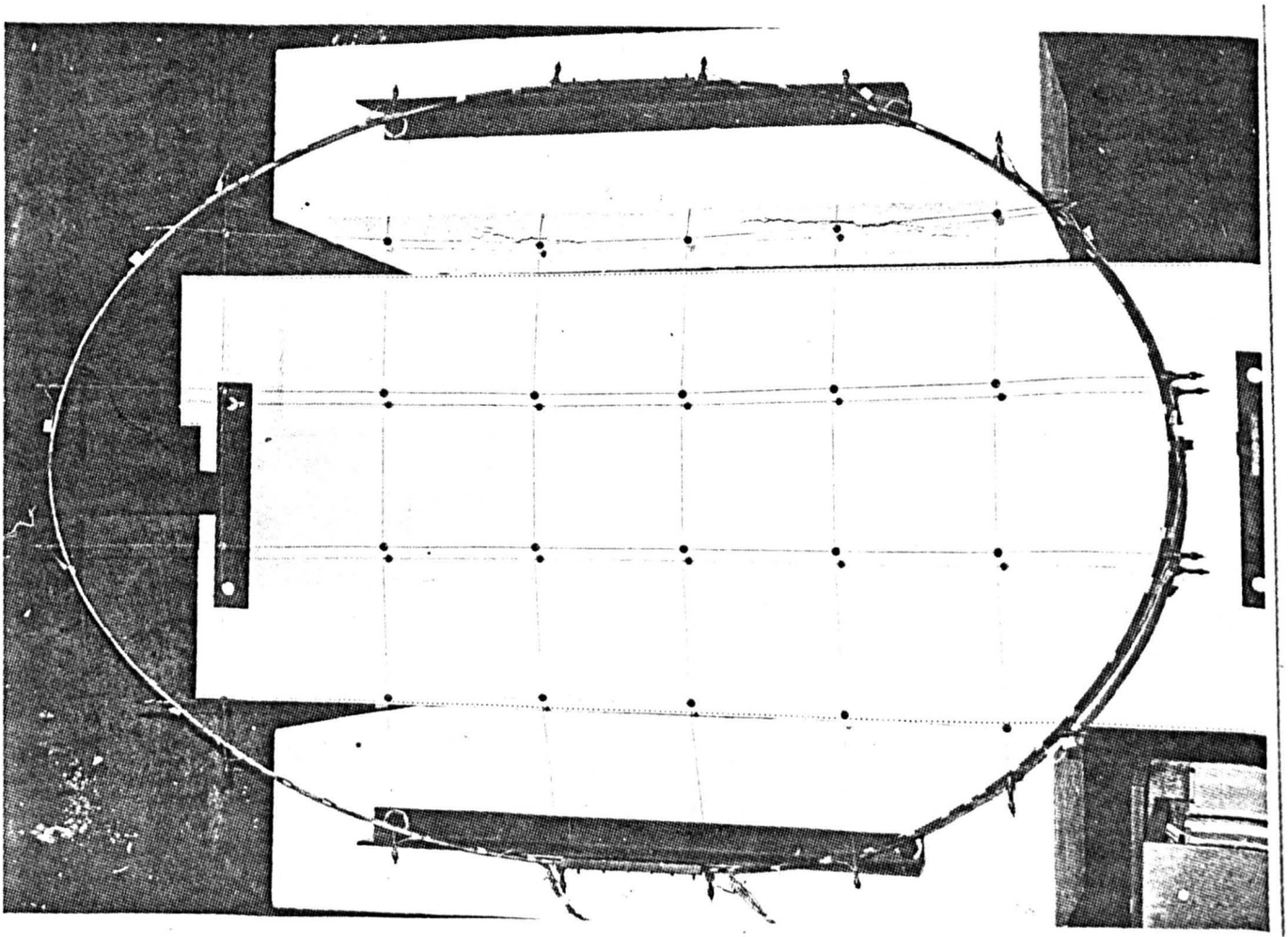

PLATE 1 : Plan view of cable net model

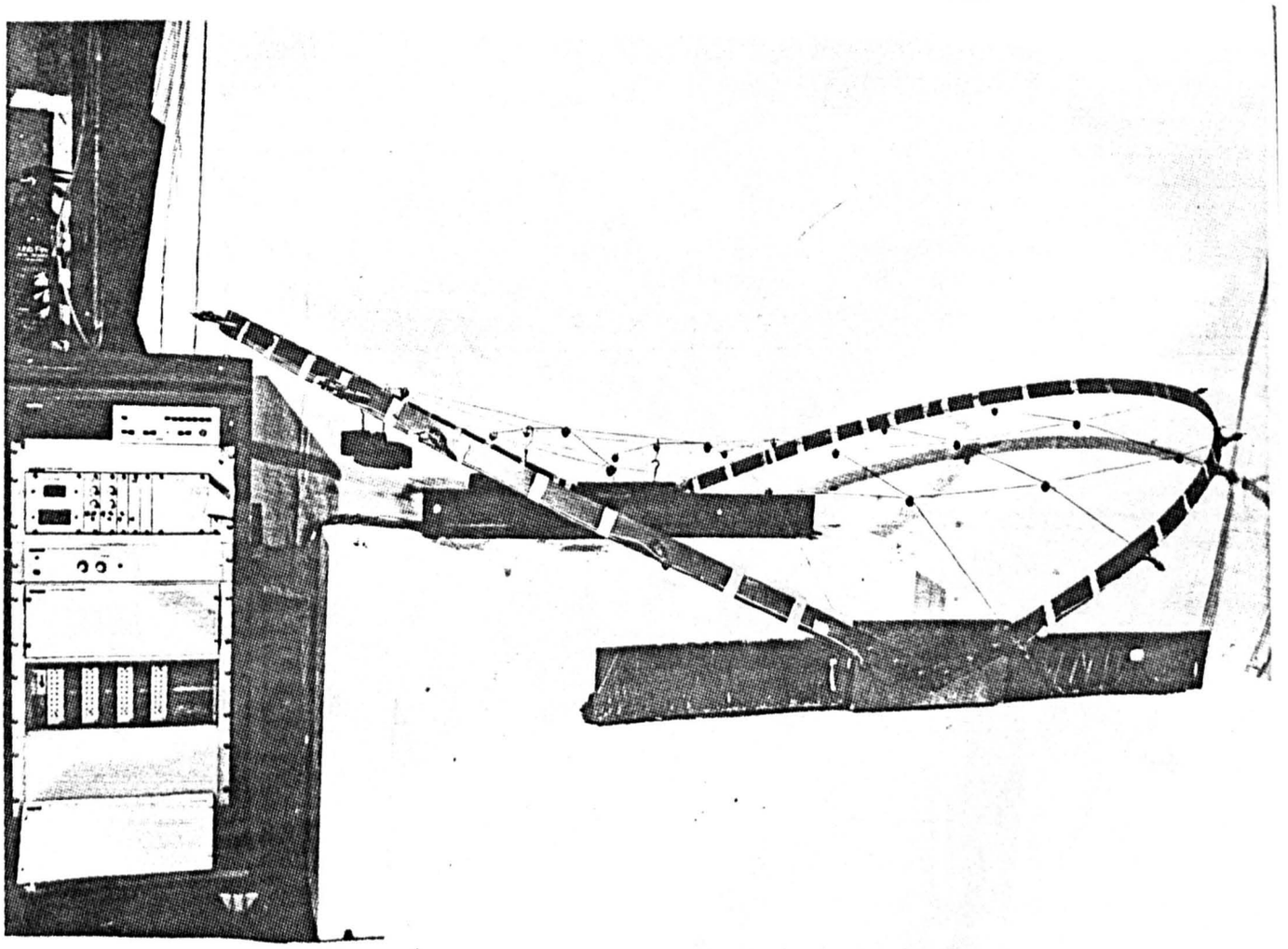

PLATE 2 : Elevation of cable net and logger

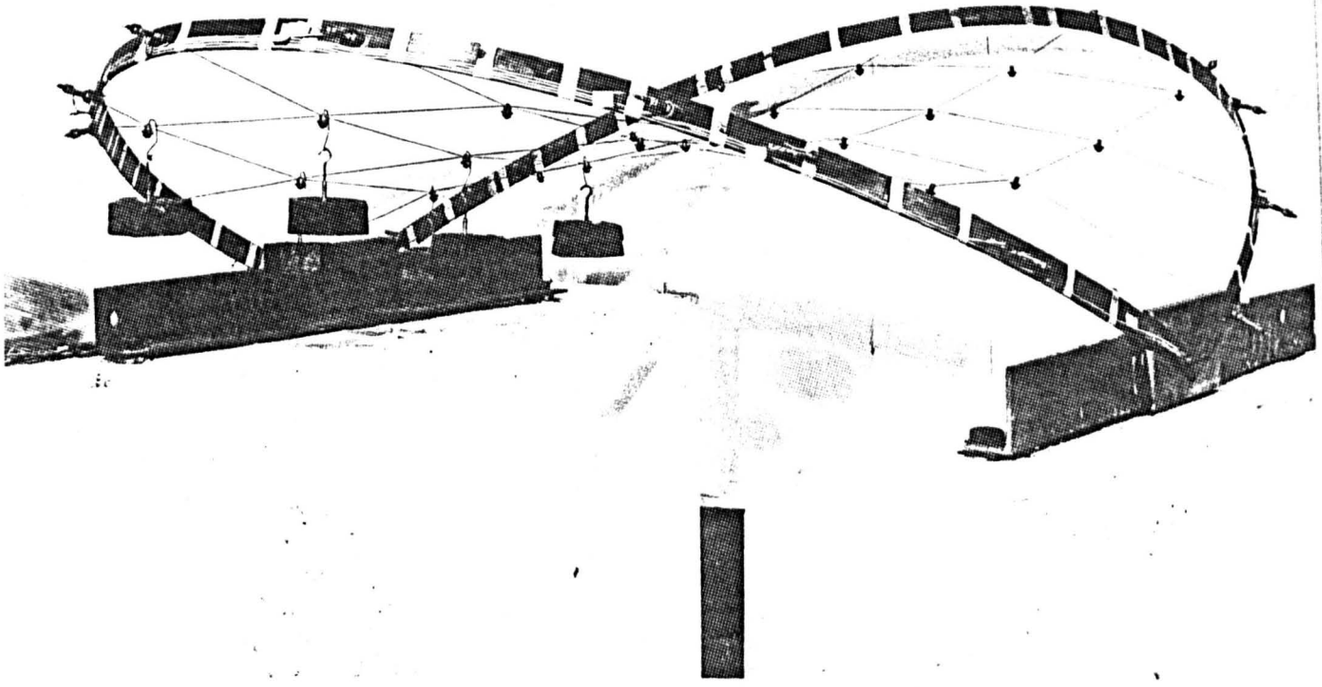

PLATE 3 : Elevation of cable net model

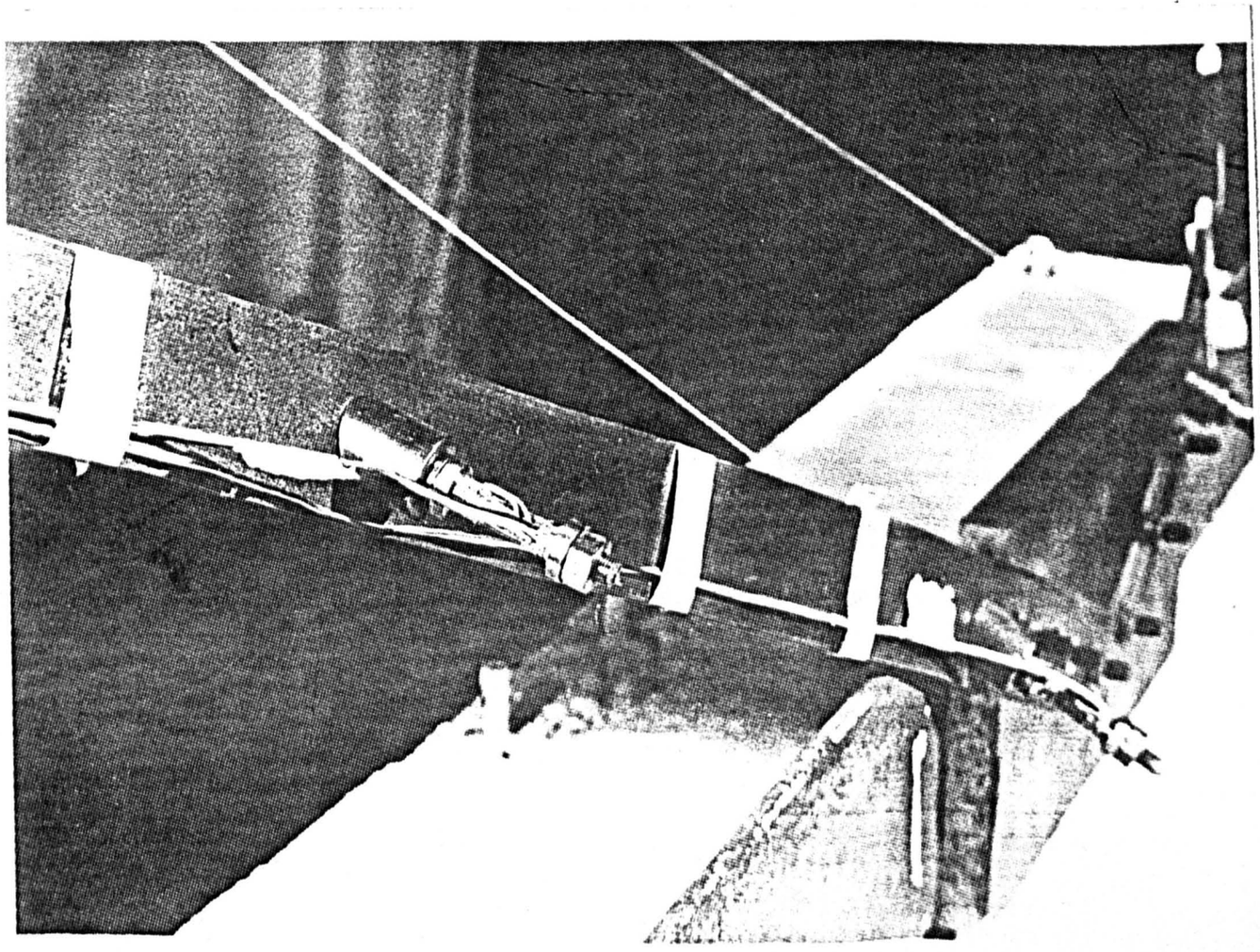

PLATE 4 : Detail of ring beam

the cable net. Gauges were mounted at the crown of each semi-ellipse to measure in-plane and out of plane deflection of the ring beam and also at the beam supports to check for any lack of fixity. Although the transducer gauges were adequately matched for thermal expansion and temperature change, variations were observed due to draughts and temperature changes, probably from the compensating logger circuits, and in consequence the experimentation was carried out in the early evening when steady state conditions prevailed.

5.6 Preliminary Results

Table 5.2 lists the results and section properties that are required as input data in the theoretical analysis for comparison with the experimental results. The initial member tensions and joint coordinates were obtained from the form finding analysis. Section properties of the ring beams were found by direct micrometer measurement of the section. The direct and torsional stiffness values were taken as the standard reference data for mild steel since considerable experimentation and additional expense would be involved for little or no greater precision in the values.

The nature of the stranded cable necessitated that the elastic stiffness be found by direct tensile testing (Section 5.3).

The ring beam is assumed to be perfectly encastré at the junction with the anchorage block. Experimental results P_1, P_2 (Fig. 5.12) for the deflection of the crown of the beam during pretensioning differ markedly from that predicted by theory T_o. Analysis shows that the deflection is very sensitive to the position of the point of fixity. T_1, T_2 show the predicted deflections when the beam ends are extended by 70 mm and 140 mm respectively into the anchorage block to be perfectly

TABLE 5.2

INITIAL INPUT DATA FOR THEORETICAL ANALYSIS OF 3D CABLE NET

NET DATA					
JOINT NUMBER	COORDINATES (cm) X	Y	Z	MEMBER NUMBER	TENSION (N)
1	-74.9064	45.0342	32.9043	1	50.888
2	-44.9896	45.0342	25.9393	2	52.394
3	-15.0000	45.0342	21.2763	3	56.233
4	15.0000	45.0342	21.2763	4	56.233
5	44.9896	45.0342	25.9393	5	52.394
6	74.9064	45.0342	32.9043	6	50.888
7	-74.9064	15.0010	36.4626	7	101.483
8	-44.9896	15.0010	30.7923	8	100.621
9	-15.0000	15.0010	27.5805	9	99.178
10	15.0000	15.0010	27.5805	10	98.000
11	44.9896	15.0010	30.7923	11	99.178
12	74.9064	15.0010	36.4626	12	100.621
13	-74.9064	-15.0010	36.4626	13	101.483
14	-44.9896	-15.0010	30.7923	14	50.350
15	-15.0000	-15.0010	27.5805	15	50.649
16	15.0000	-15.0010	27.5805	16	51.090
17	44.9896	-15.0010	30.7923	17	51.090
18	74.9064	-15.0010	36.4626	18	50.649
19	-74.9064	-45.0342	32.9043	19	50.350
20	-44.9896	-45.0342	25.9393	20	101.016
21	-15.0000	-45.0342	21.2763	21	99.745
22	15.0000	-45.0342	21.2763	22	98.560
23	44.9896	-45.0342	25.9393	23	98.000
24	74.9064	-45.0342	32.9043	24	98.560
25	-74.9064	52.5407	31.4830	25	99.745
26	-44.9896	67.8193	18.8041	26	101.016
27	-15.0000	74.2309	6.2500	27	50.000
28	15.0000	74.2309	6.2500	28	50.000

NET DATA

JOINT NUMBER	COORDINATES (cm) X	Y	Z	MEMBER NUMBER	TENSION (N)
29	44.9896	67.8193	18.8041	29	50.000
30	74.9064	52.5407	31.4830	30	50.000
31	83.8589	45.0342	35.3122	31	50.000
32	102.5859	15.0010	43.3821	32	50.000
33	102.5859	-15.0010	43.3821	33	101.016
34	83.8589	-45.0342	35.3122	34	99.745
35	74.9064	-52.5407	31.4830	35	98.560
36	44.9896	-67.8193	18.8041	36	98.000
37	15.0000	-74.2309	6.2500	37	98.560
38	-15.0000	-74.2309	6.2500	38	99.745
39	-44.9896	-67.8193	18.8041	39	101.016
40	-74.9064	-52.5407	31.4830	40	50.350
41	-83.8589	-45.0342	35.3122	41	50.649
42	-102.5859	-15.0010	43.3821	42	51.090
43	-102.5859	15.0010	43.3821	43	51.090
44	-83.8589	45.0342	35.3122	44	50.649
				45	50.350
				46	101.483
				47	100.621
				48	99.178
				49	98.000
				50	99.178
				51	100.621
				52	101.483
				53	50.888
				54	52.394
				55	56.233
				56	56.233
				57	52.394
				58	50.888

BOUNDARY BEAM SECTION PROPERTIES

$GJ = 1074 N cm^2$, $E = 21000\ N/cm^2$

$I_{yy} = 2.195\ cm^4$ $I_{zz} = 0.0343\ cm^4$

$A = 1.815\ cm^2$

CABLE STIFFNESS $EA = 78\ kN$

FIG 5.12

DEFLECTION AT CROWN OF RING BEAMS DURING PRETENSIONING

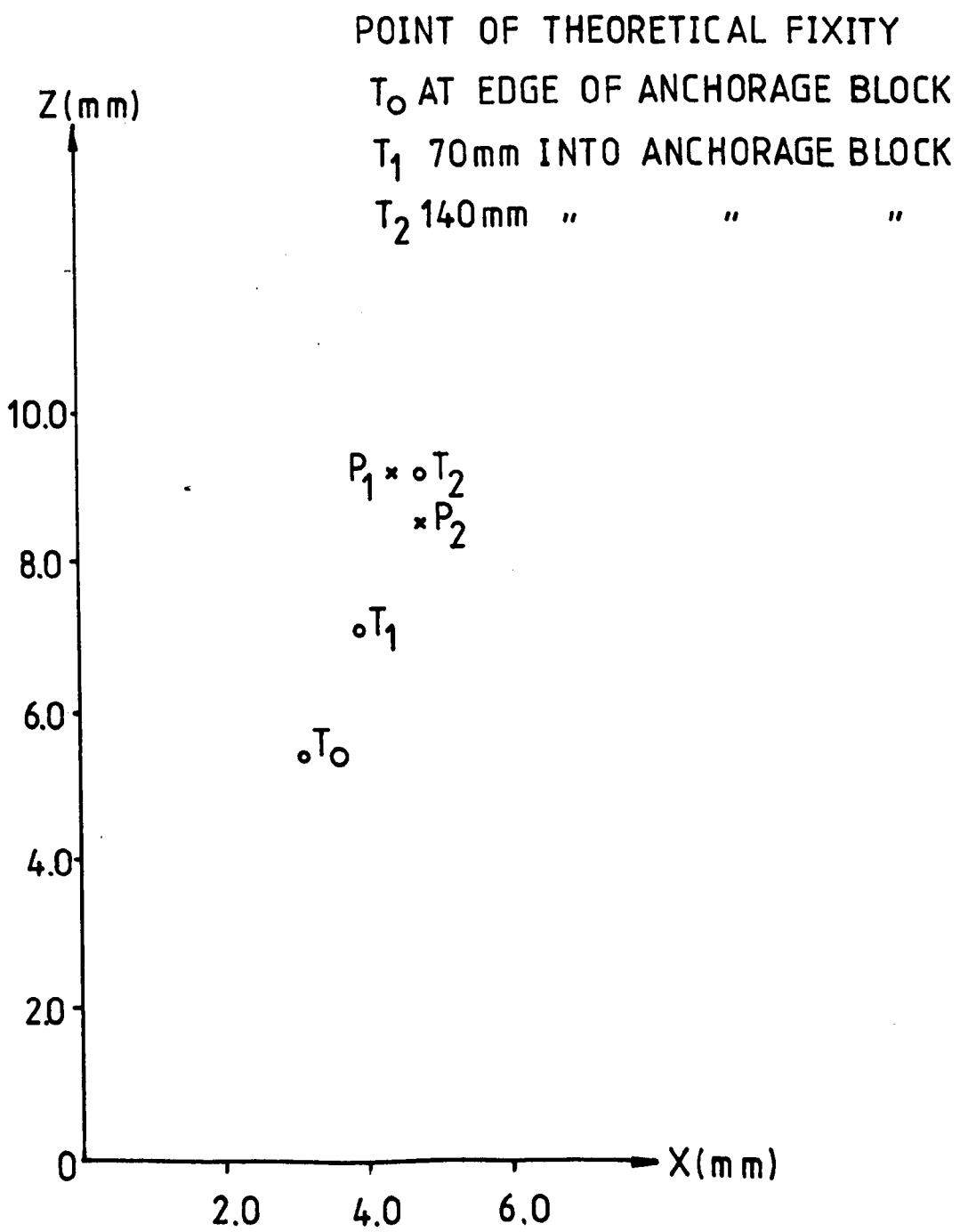

encastre there.

Expense and time ruled out modifications to a more rigid mounting but the pretensioned cable system was expected to be less sensitive to questions of pretension. This illustrates the need in practical structures to allow for some lack of fixity where structure meets foundations.

For economy in computing, test programs were devised to obtain an optimum relaxation factor (RF) in the iteration between cable net forces and the ring beam described in Chapter 2. The effect is shown in Fig. 5.13 where the convergence rate is improved with increase in factor up to 0.15, above that value a convergent iteration could not be achieved. Without further tests this optimum factor was used in all subsequent load patterns.

5.7 Results of Cable Net Experiment

A comparison of the theoretical and practical results relating to the cable net experiment is now presented.

Theoretical results have been formulated using the non-linear deformation theory developed in Chapter 2. For each of the four load cases an output giving member forces and joint deflections for load increments of 0.25 kg per loaded joint was obtained. Allowance was made in the computer analysis for the possibility of a cable member becoming slack (i.e. compressive forces were not allowed). Instability in the iterative minimum energy solution occurred when adjacent cable members became slack. This lack of convergence limited the range over which results could be obtained for load cases 1 and 2.

FIG 5.13

THE EFFECT OF RELAXATION FACTOR (RF) UPON THE CONVERGENCE RATE OF THE COMBINED NET / FLEXIBLE BOUNDARY PROBLEM

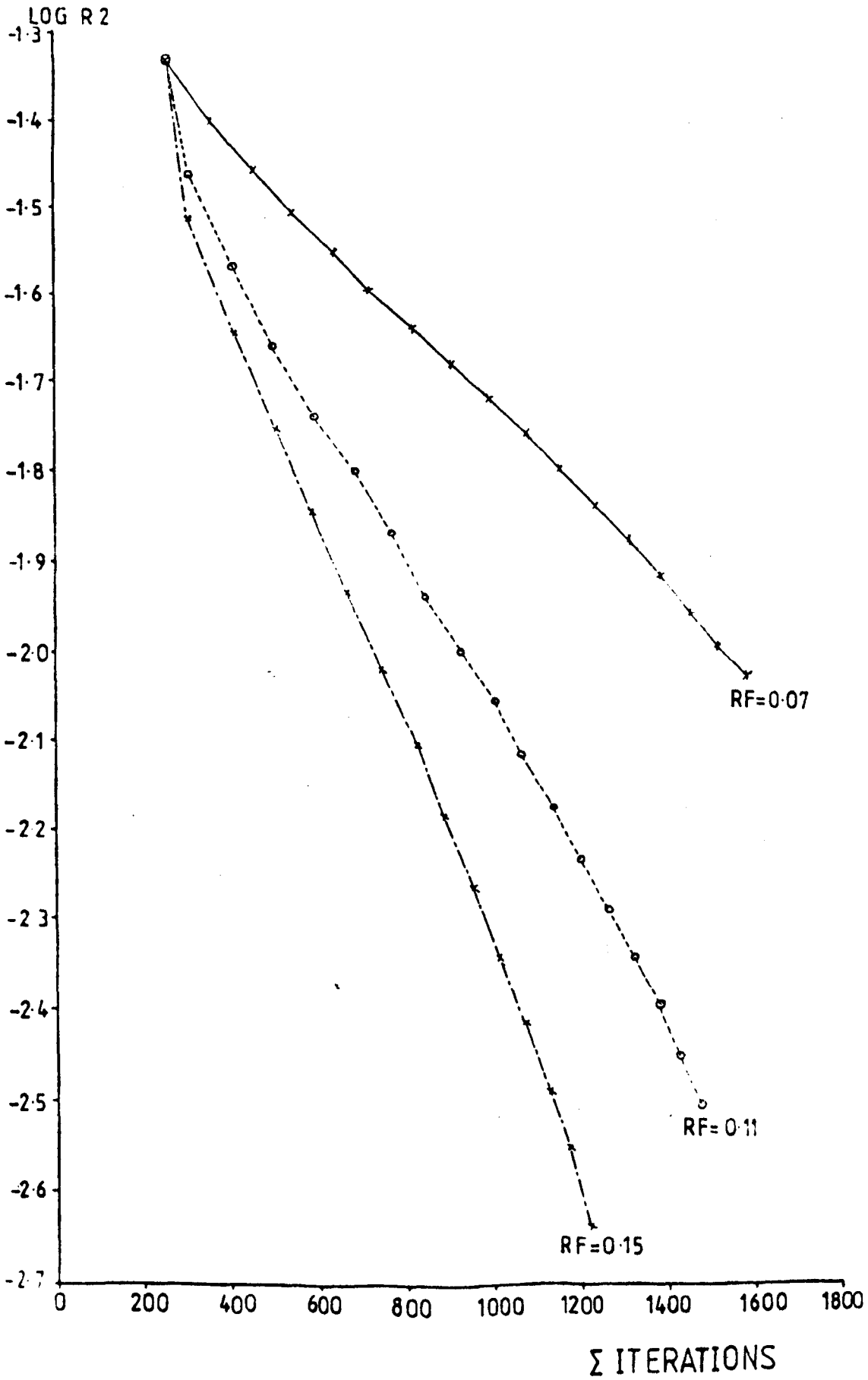

Fig. 5.14 shows a plot of cable forces for member numbers 3, 16 and 29 which form half of the central hogging cable (this cable slackens first under gravity loading) against load per joint for all four load cases. The non-convergence for load cases 1 and 2 at a load of 1.3 kg per loaded joint is caused by each of the cable members (3.16 and 29) becoming slack leading to a general instability across the model, whereas for load case 3 only member number 3 becomes slack so that any instability is localised and the analysis continues to be stable for increased loads.

The slackening of cable members was reflected in the experimental analysis, again referring to Fig. 5.14, for each load case the load which first caused slackening of member 3 is given. The weights available for load case 1 imposed a large load increment of 1 kg/joint and the observed slackening load is therefore too high at 2 kg instead of 1.25 kg. The experimental structure gave a load deflection curve beyond the point at which theory broke down, however steady states were not achieved quickly at this load. This led to a decision not to search for an extension to the iterative theory. For practical cable structures, slackening would be undesirable in a clad net.

(i) Cable forces

The bulk of the practical results concern the changes in cable forces at the boundary support points which were recorded directly onto punched data tape.

The raw data from the gauge cylinders was checked for consistency over the three scans and, using the individual calibration factors, converted to values of change in tension for the given loadings. For visual presentation and checking of results a computer program then gave an output of the changes in the cable tensions superimposed on a

FIG 5.14

CABLE MEMBER FORCE AGAINST JOINT LOAD

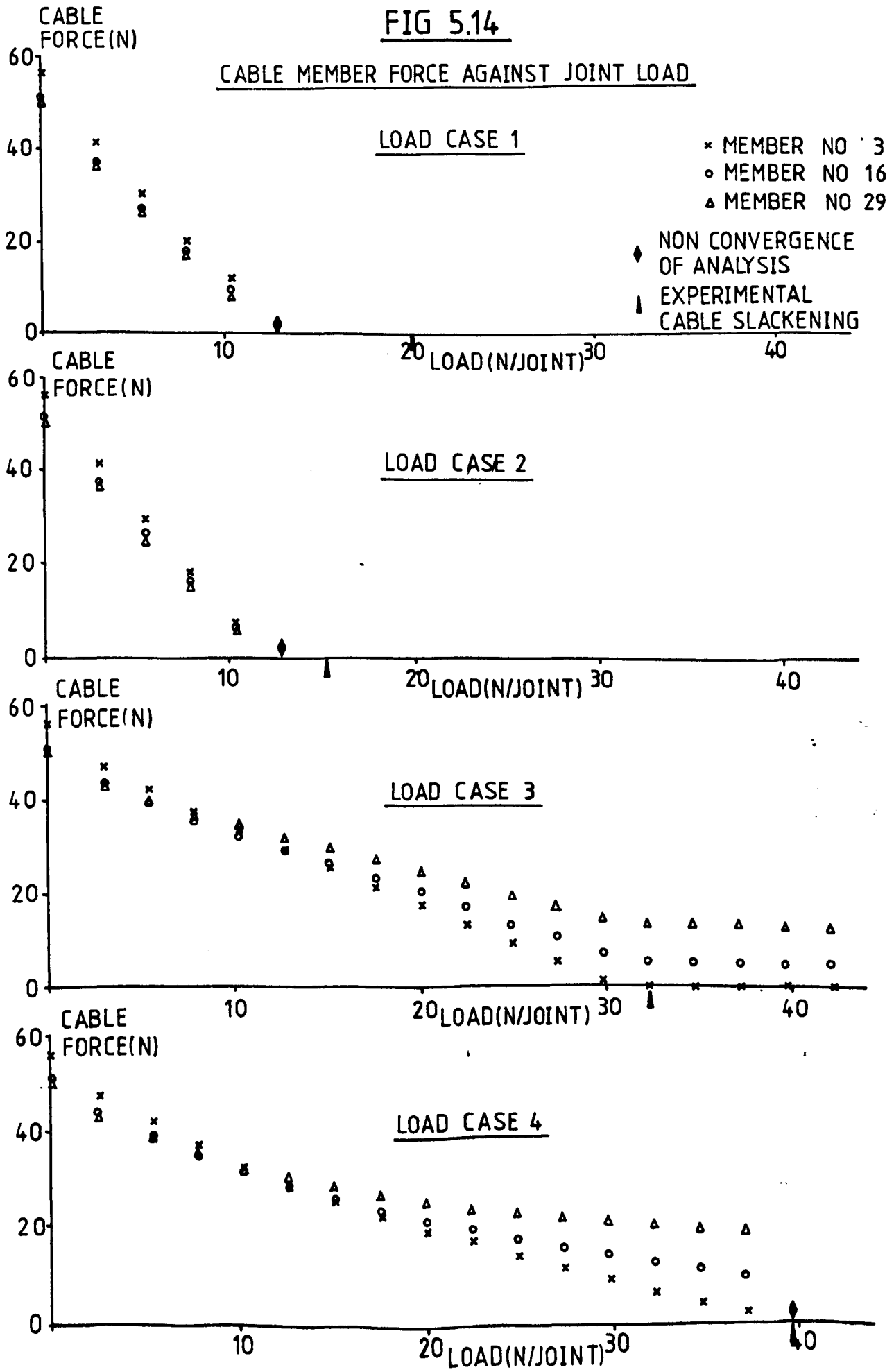

plan view of the cable net. Figs. 5.15 to 5.18 give typical examples of this for each of the four load cases with a load of 10.30 N per joint.

Tables in Appendix 5.2 give a full record of all the experimental tension measurement results for the four load cases. Figs. 5.19 and 5.20 present a summary comparing practical and theoretical results for load case 1 and 2 showing the change in member force with load. Because of the symmetrical nature of the loading for load case 1 the cable tensions in one quadrant are repeated in the other three. The plotted values are the average of four (standard deviation $\pm$ 1.05 N).

Because of the limited range over which the theoretical results could be obtained little detailed conclusion can be drawn from these results. The relative order of the change in member forces has been predicted by the theory. For load case 1, with a 10.30 N per joint, results vary between 9.2 N and 22.7 N above the theoretical ones. The discrepancy between the sets of results increases the further the boundary node is from the ring beam support. Prediction of deflection, presented later, is not so bad but no reason has been found for the poor correspondence of forces which are so markedly at variance with those for load cases 2, 3 and 4.

For load cases 3 and 4 a full set of experimental and theoretical results are avaiable for a more detailed comparison. Figs. 5.21 to 5.25 show graphs of change in member force with applied load. The computer graph plotting facilities have been used to produce these figures. Lines representing the theoretical results are formed by a smooth curve fitting subroutine which joins the series of theoretical points. In these figures a second theoretical line, shown dotted, has

FIG 5.15

MEASURED CHANGE IN CABLE TENSION FOR LOAD CASE 1 AT 10.30 N/JOINT

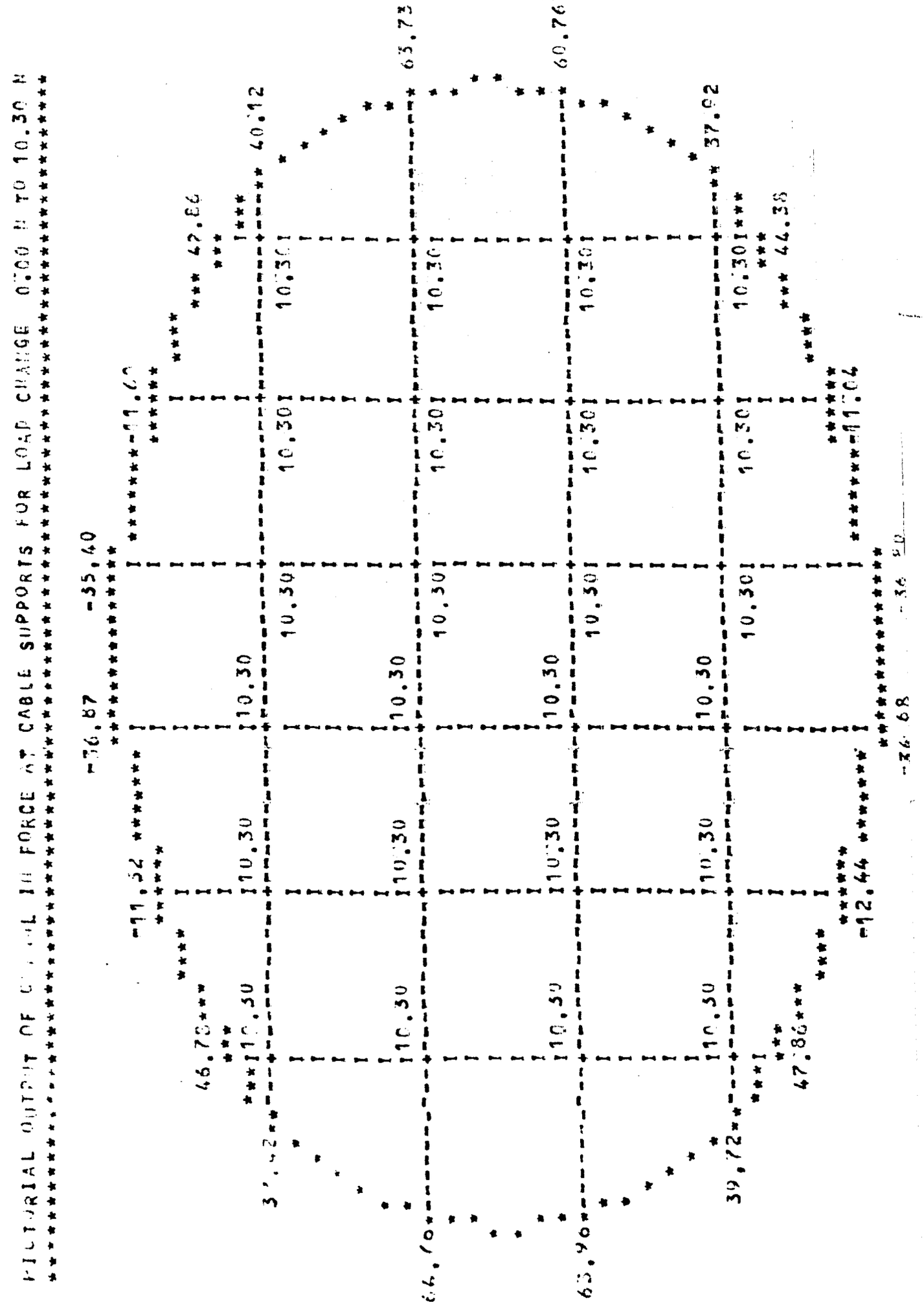

FIG 5.16

MEASURED CHANGE IN CABLE TENSION FOR LOAD CASE 2 AT 10.30 N/JOINT

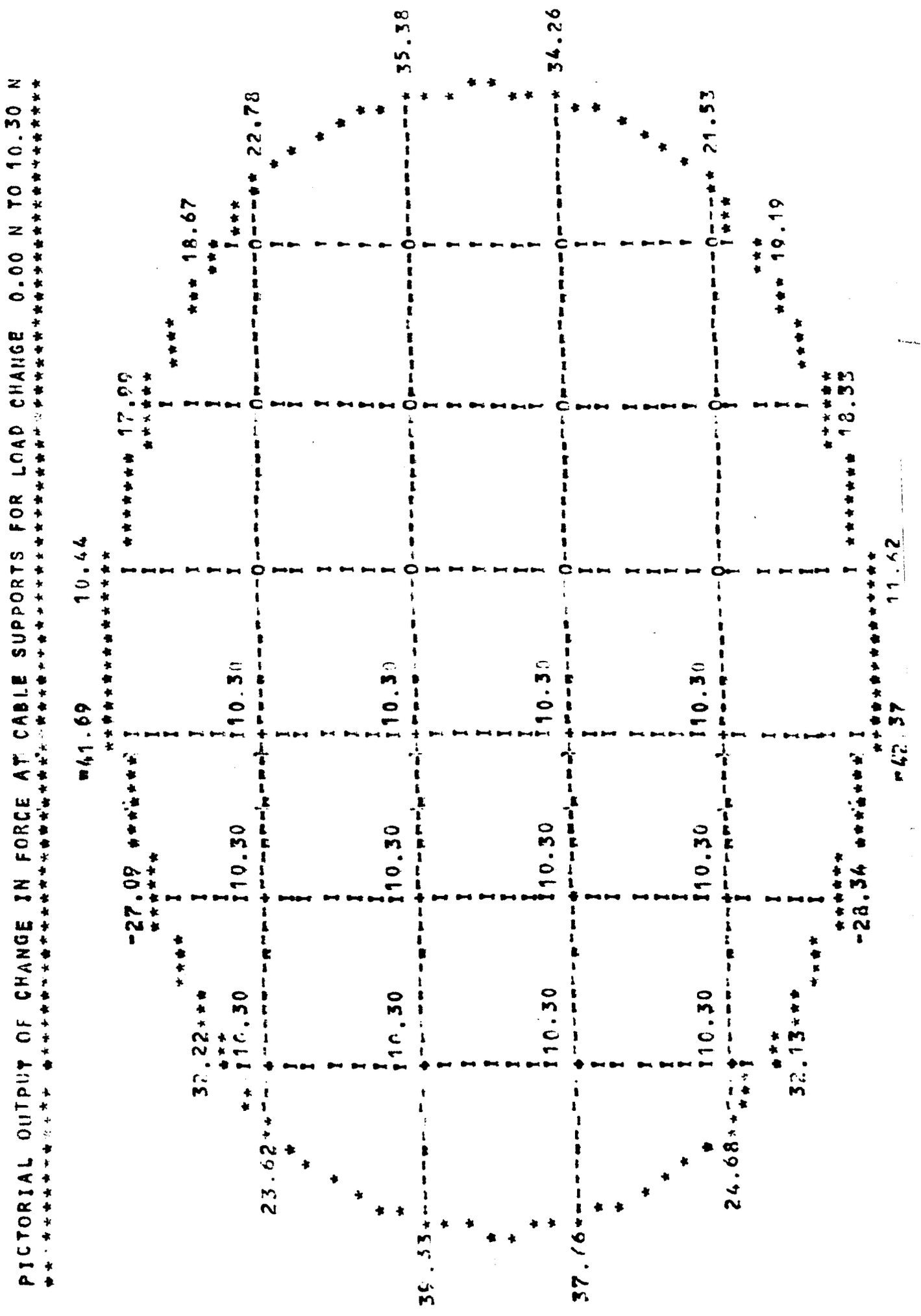

FIG 5.17

MEASURED CHANGE IN CABLE TENSION FOR LOAD CASE 3

AT 10.30 N/JOINT

FIG 5.18

MEASURED CHANGE IN CABLE TENSION FOR LOAD CASE 4

AT 10.30 N/JOINT

FIG 5.19

GRAPH SUMMARISING CHANGE IN MEMBER FORCE WITH LOAD FOR LOAD CASE 1

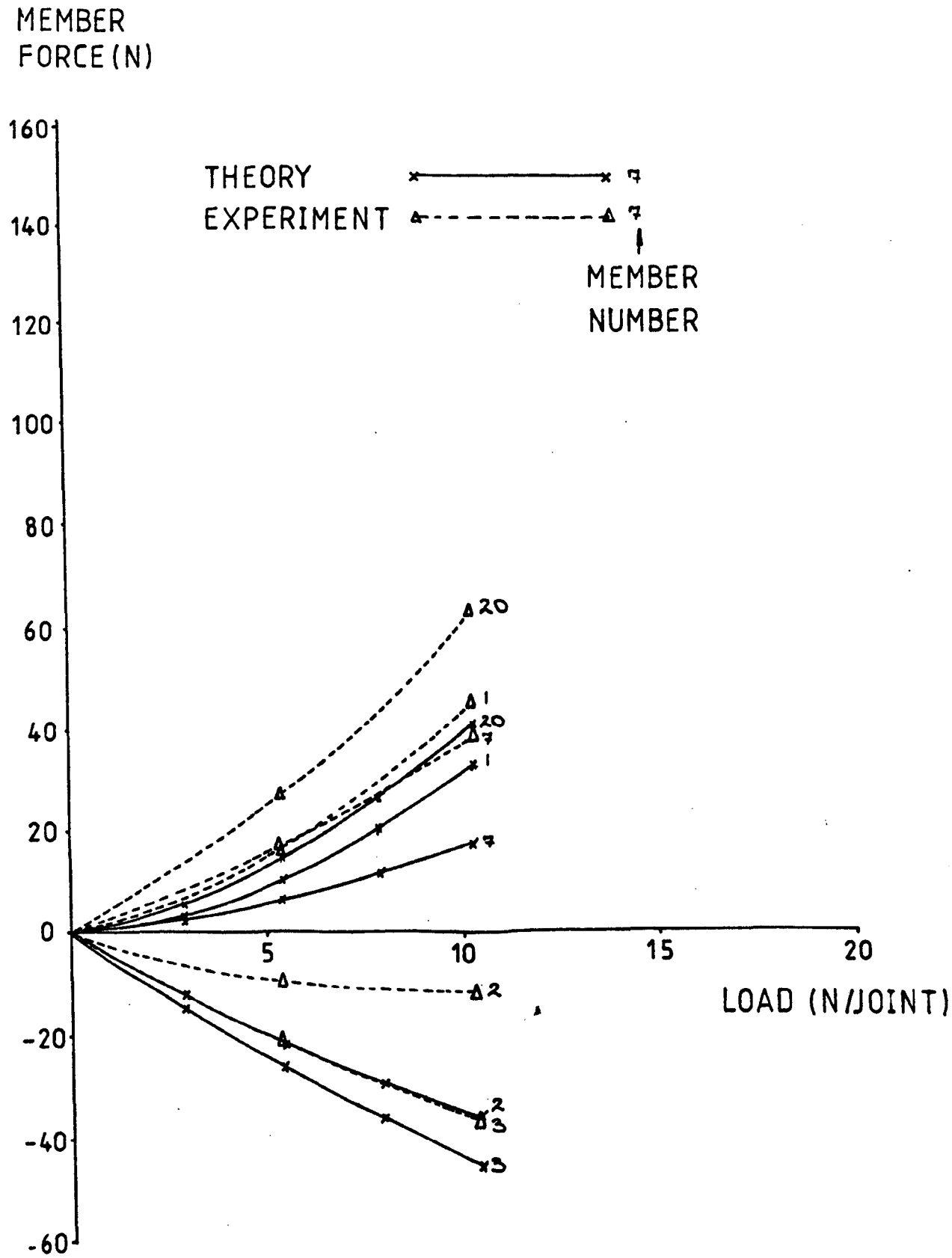

FIG 5.20

GRAPH SUMMARISING CHANGE IN MEMBER FORCE WITH LOAD FOR LOAD CASE 2

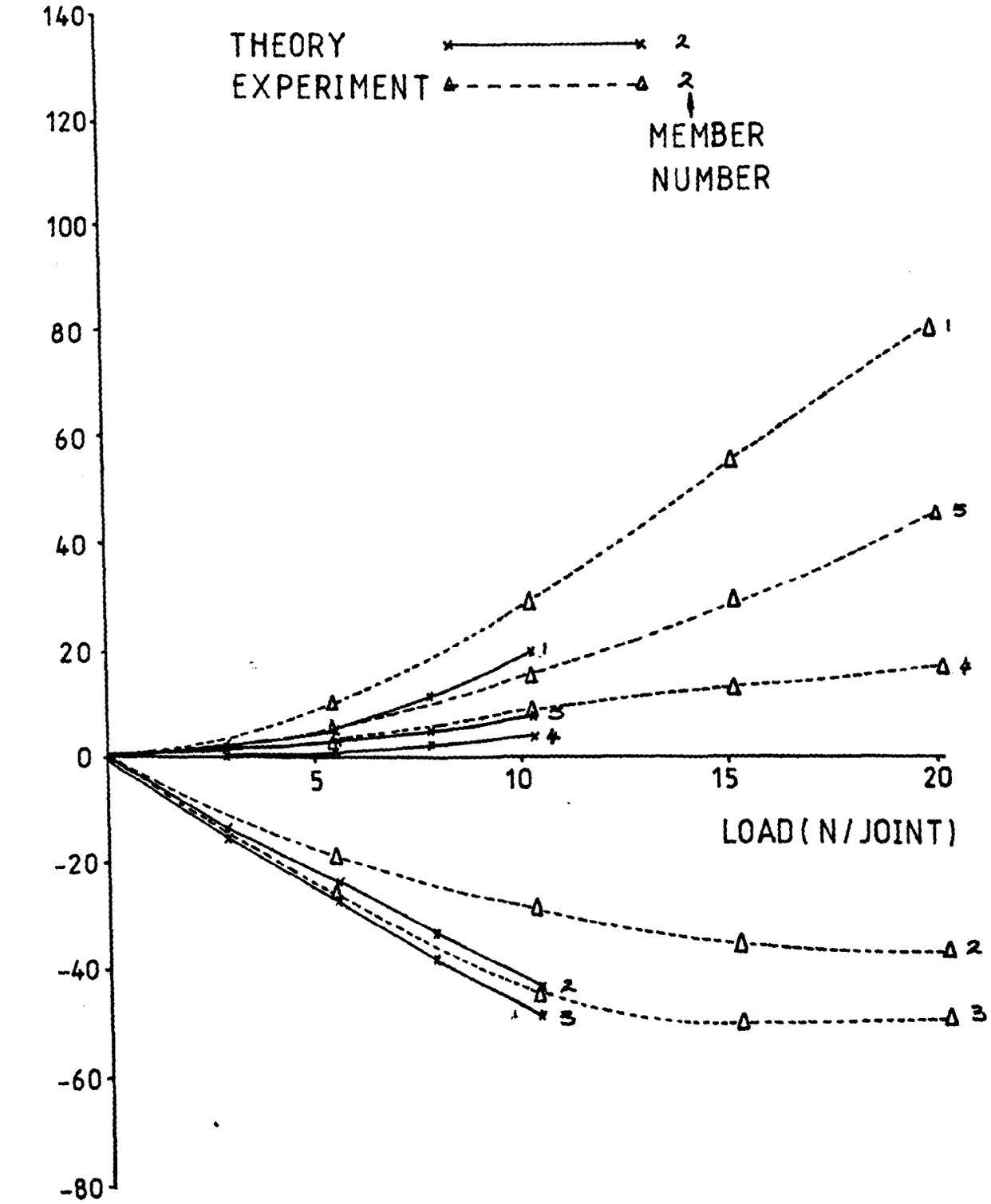

FIG 5.21

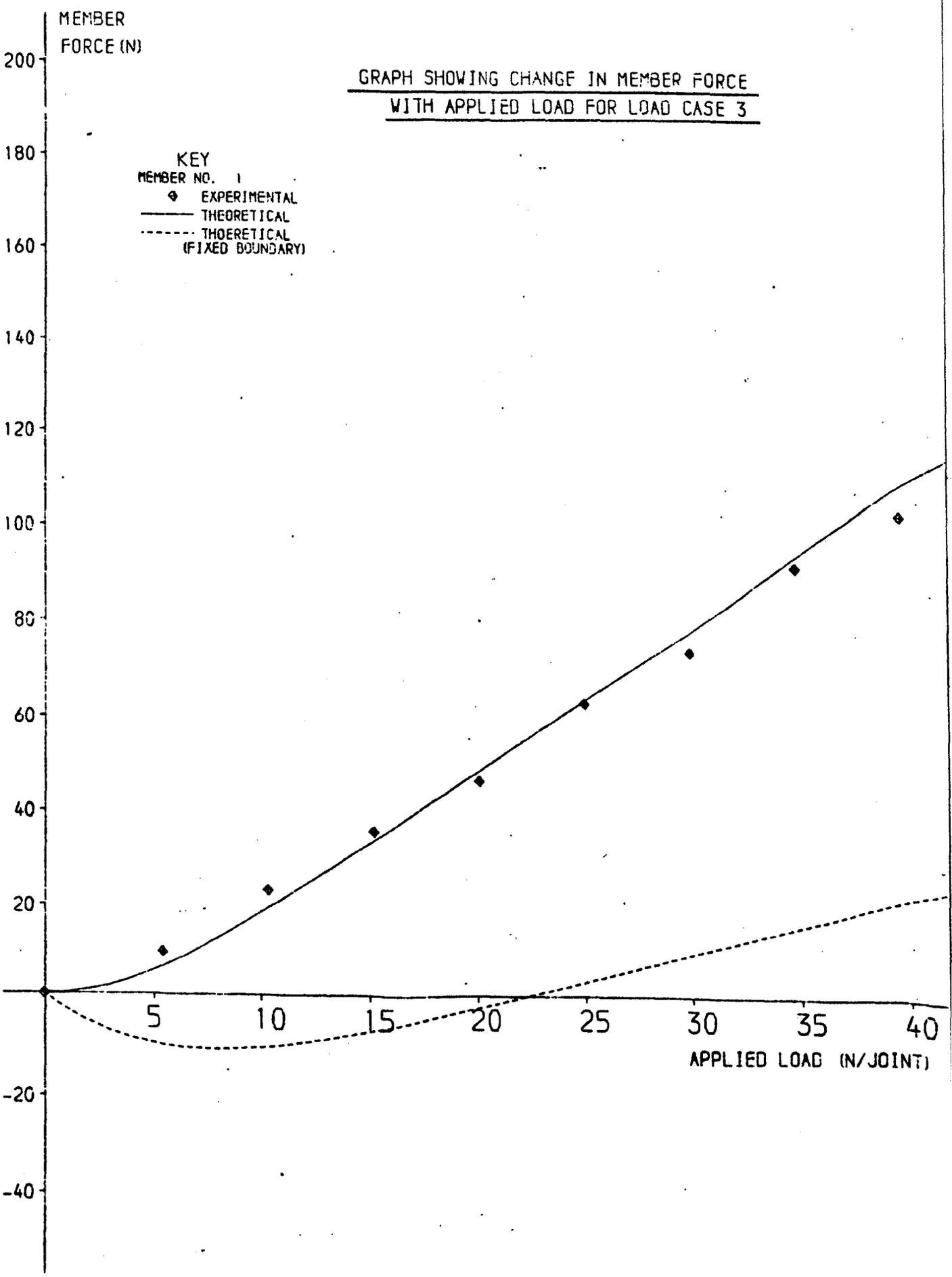

GRAPH SHOWING CHANGE IN MEMBER FORCE WITH APPLIED LOAD FOR LOAD CASE 3

FIG 5.22

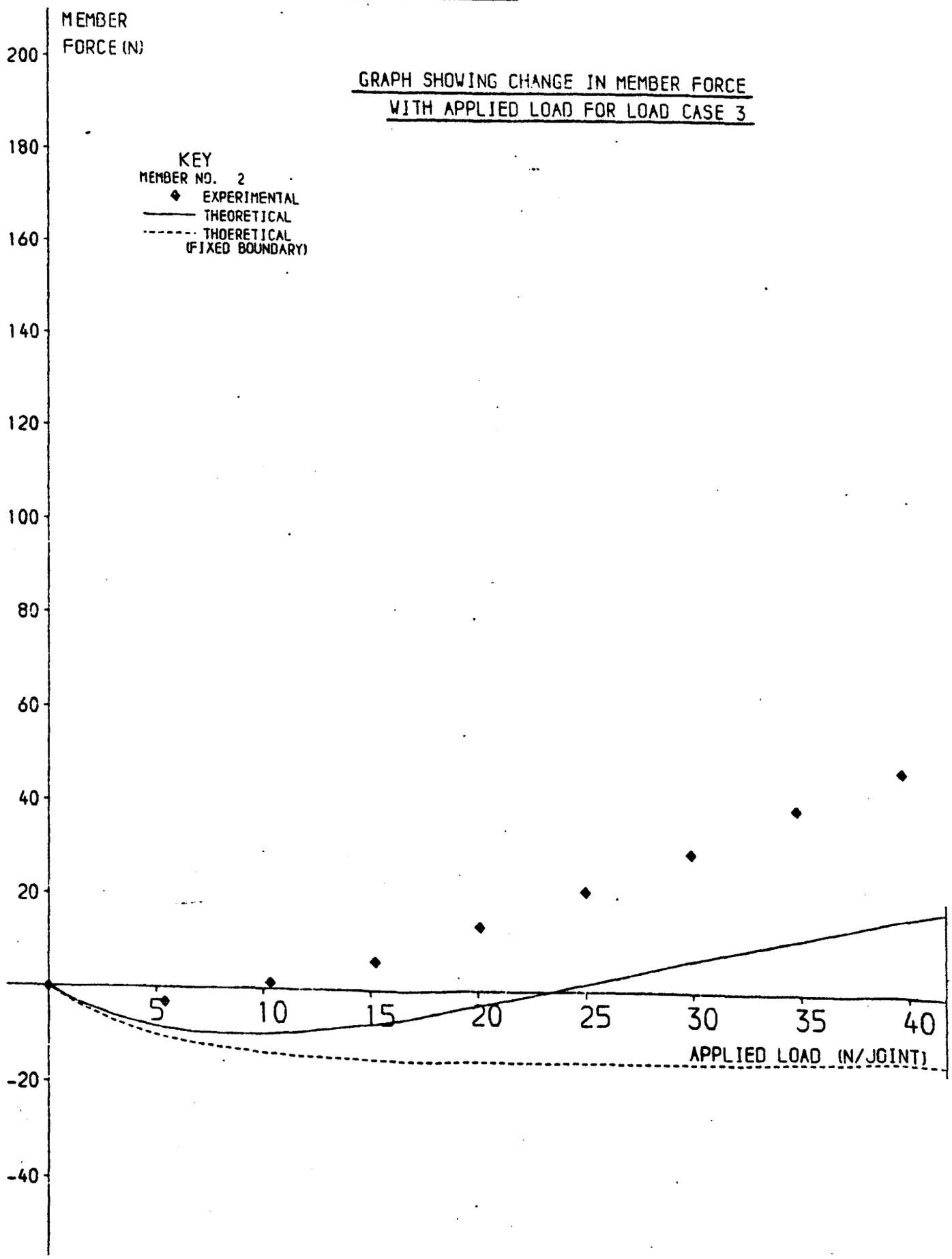

GRAPH SHOWING CHANGE IN MEMBER FORCE WITH APPLIED LOAD FOR LOAD CASE 3

FIG 5.23

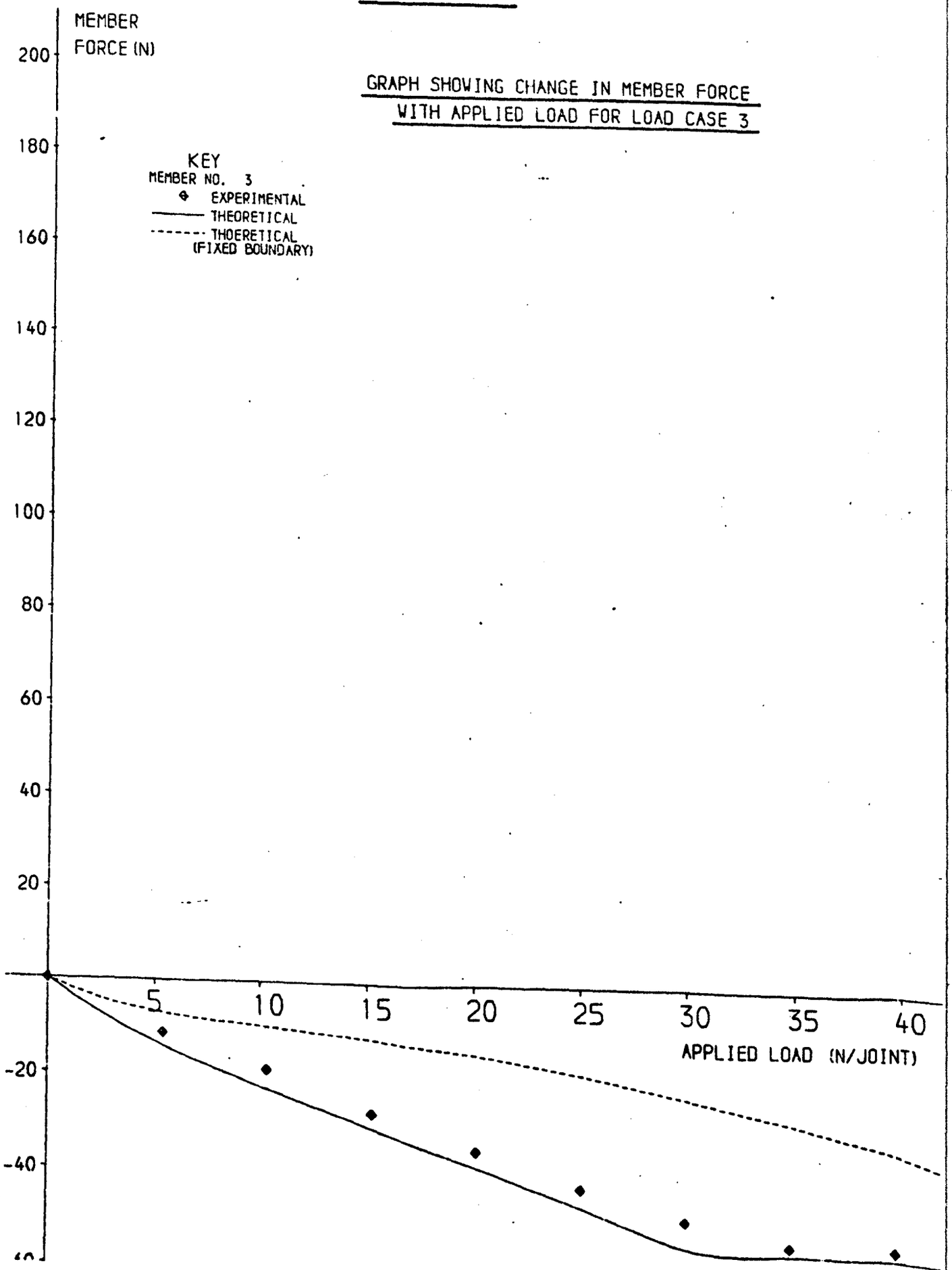

GRAPH SHOWING CHANGE IN MEMBER FORCE WITH APPLIED LOAD FOR LOAD CASE 3

FIG 5.24

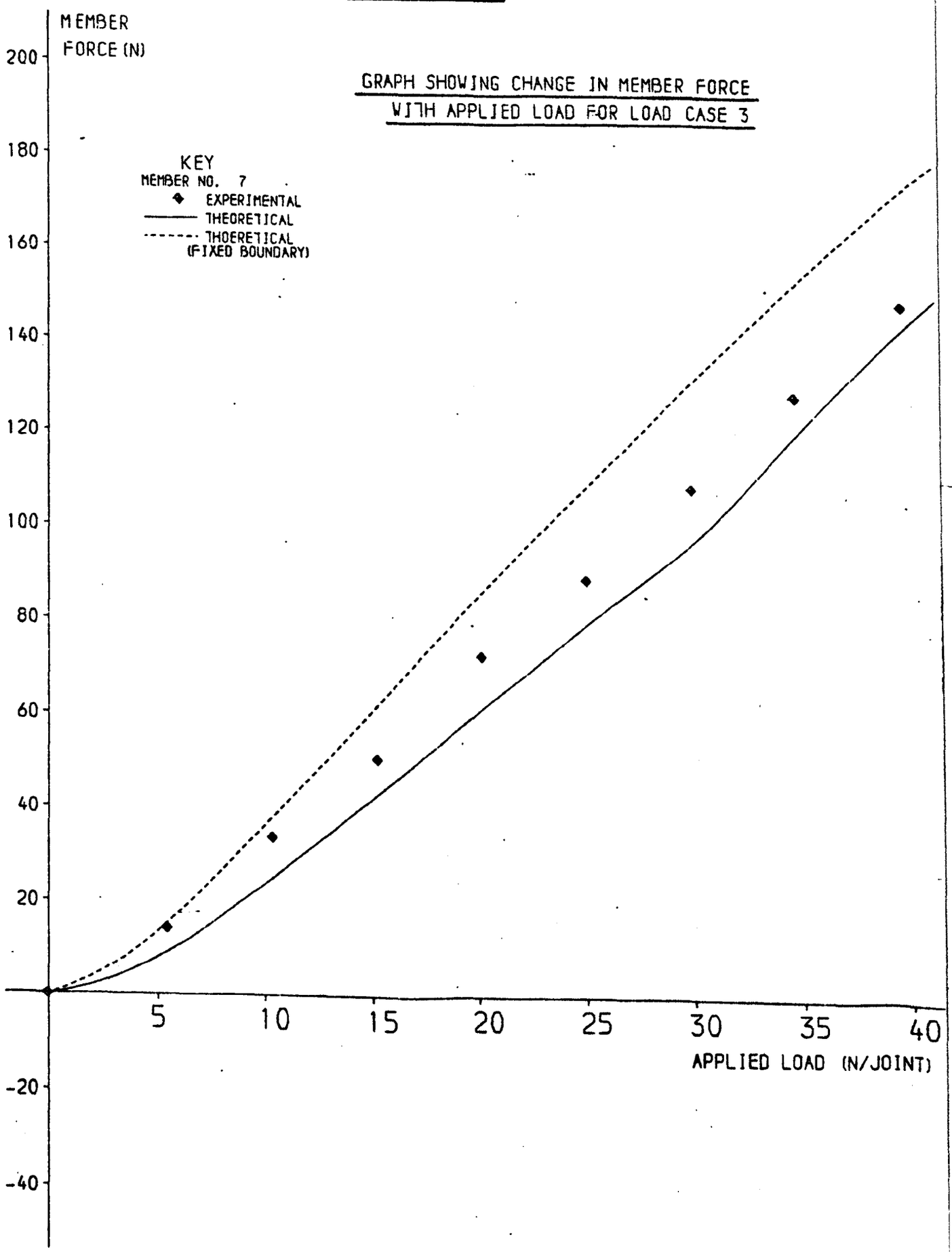

GRAPH SHOWING CHANGE IN MEMBER FORCE WITH APPLIED LOAD FOR LOAD CASE 3

FIG 5.25

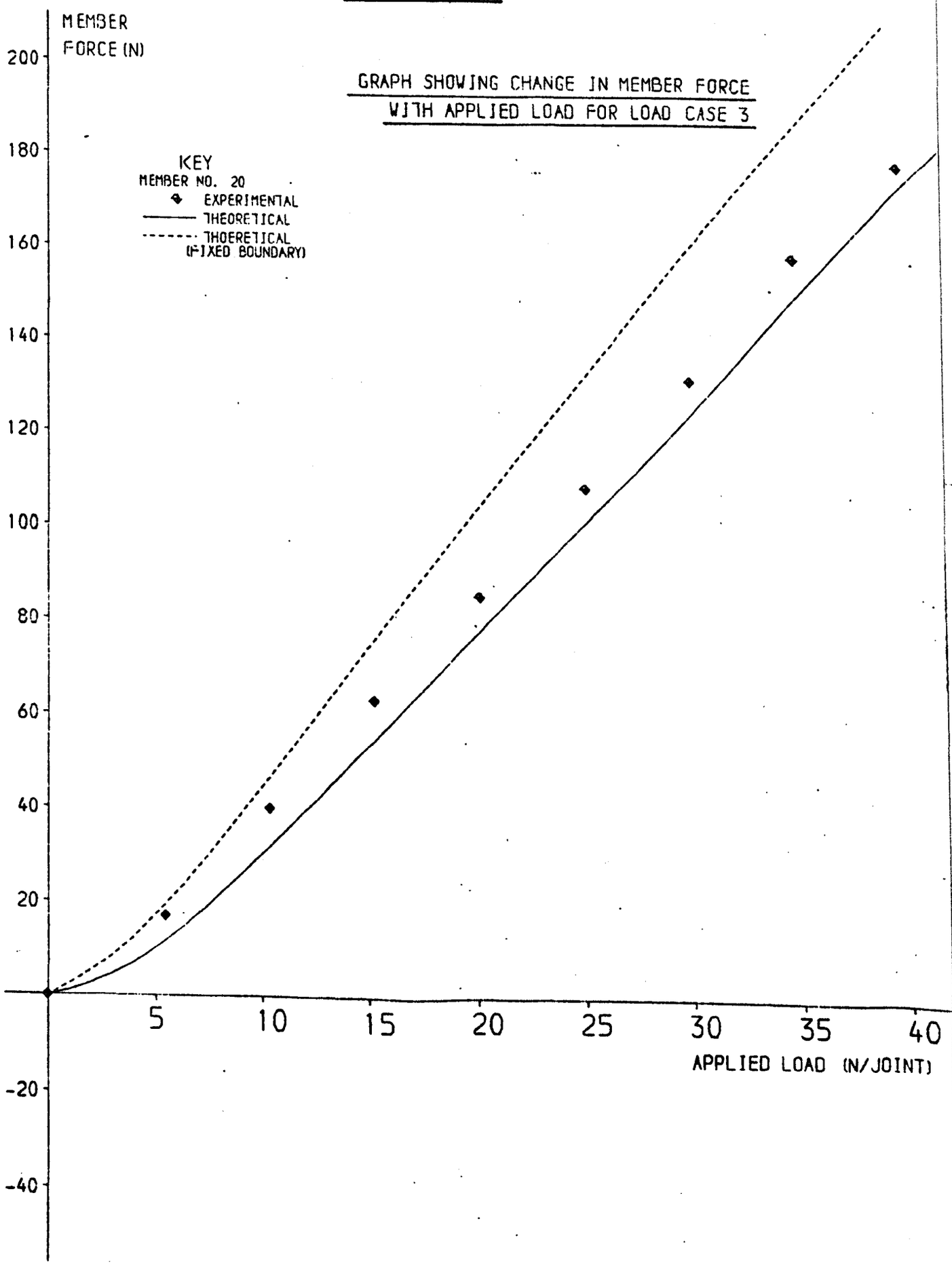
MEMBER
FORCE (N)
200
180
160
140
120
100
80
60
40
20
-20
-40
GRAPH SHOWING CHANGE IN MEMBER FORCE
WITH APPLIED LOAD FOR LOAD CASE 3
KEY
MEMBER NO. 20
EXPERIMENTAL
THEORETICAL
THOERETICAL
(FIXED BOUNDARY)
5
10
15
20
25
30
35
40
APPLIED LOAD (N/JOINT)

been drawn showing the effects of assuming a fixed boundary upon the analysis.

Of particular note is Fig. 5.23 where the slackening of member number 3 has been accurately predicted by the theory. The effect of the slackening upon the general stiffness of the structure is reflected in the other figures by a change in slope of the graph at an applied load of 30 N/joint. This is most noticeable in Fig. 5.24 for member number 7.

Fig. 5.22 for member number 2 shows the high degree of non linear behaviour displayed by the model. Under the application of small loads the cable force decreases but then increases again for larger joint loads.

(ii) Boundary deflections

The experimental boundary deflection measurements made at the crown of the two ring beams gave components of deflection within the plane of the beam and perpendicular to it. Theoretical deflections from the computer analysis in terms of global coordinates have been transformed to match the experimental results.

Fig. 5.26 shows the very good agreement achieved between theoretical and practical results for load case 3. For load cases 2 and 4 (Figs. 5.27, 5.28) the agreement is not so good both of these load cases apply a non-symmetrical loading to the ring beam supports. The errors in the out of plane deflections are consistent with a rotation at the boundary supports, or a movement of the effective point of encastrément of the ring beam. This shows that the fixity of the model foundations were not adequate.

FIG 5.26

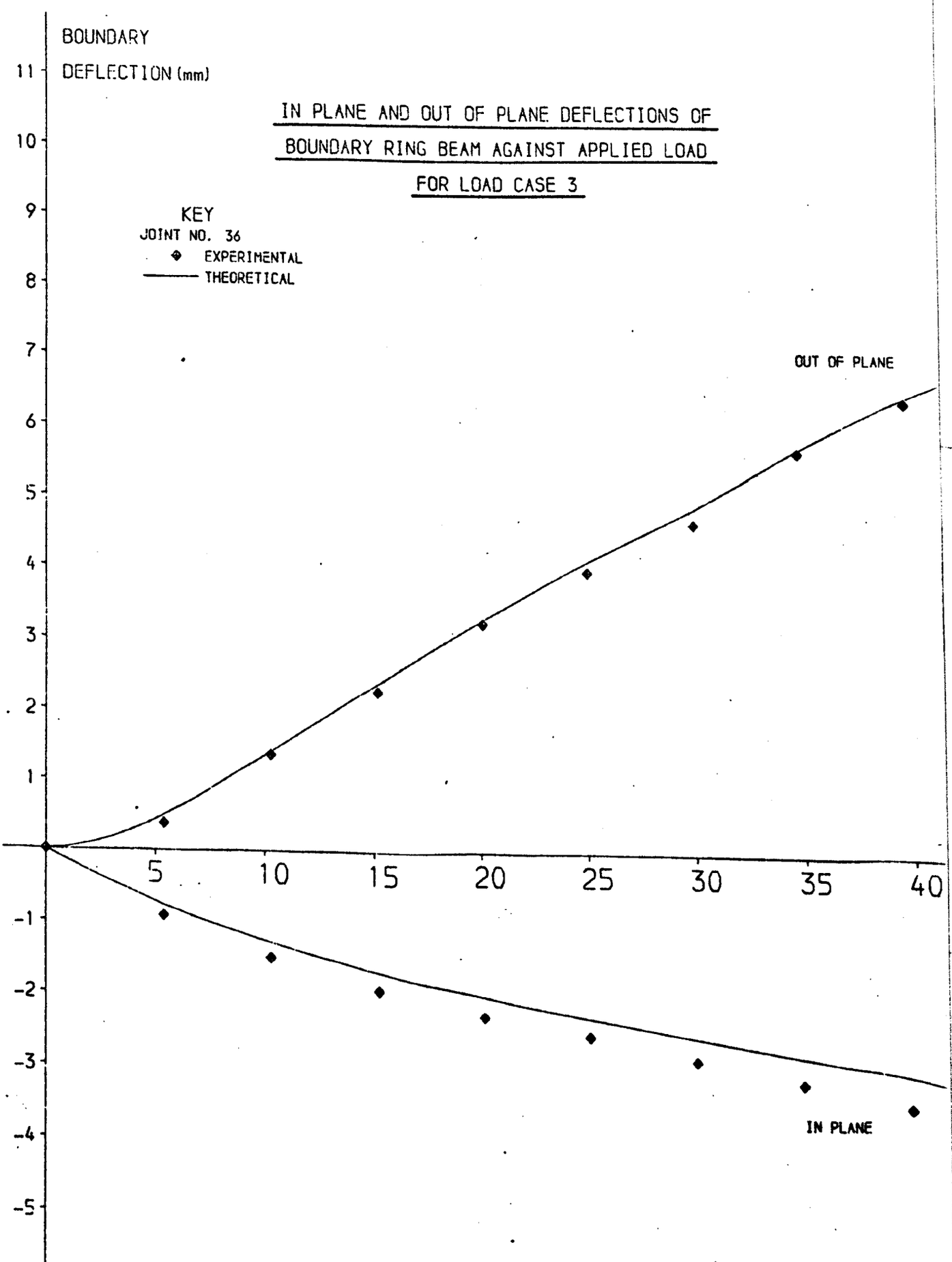
BOUNDARY
DEFLECTION (mm)
IN PLANE AND OUT OF PLANE DEFLECTIONS OF
BOUNDARY RING BEAM AGAINST APPLIED LOAD
FOR LOAD CASE 3
KEY
JOINT NO. 36
EXPERIMENTAL
THEORETICAL
OUT OF PLANE
IN PLANE
11
10
9
8
7
6
5
4
3
2
1
-1
-2
-3
-4
-5
5
10
15
20
25
30
35
40

FIG 5.27

IN PLANE AND OUT OF PLANE DEFLECTIONS OF BOUNDARY RING BEAM AGAINST APPLIED LOAD FOR LOAD CASE 2

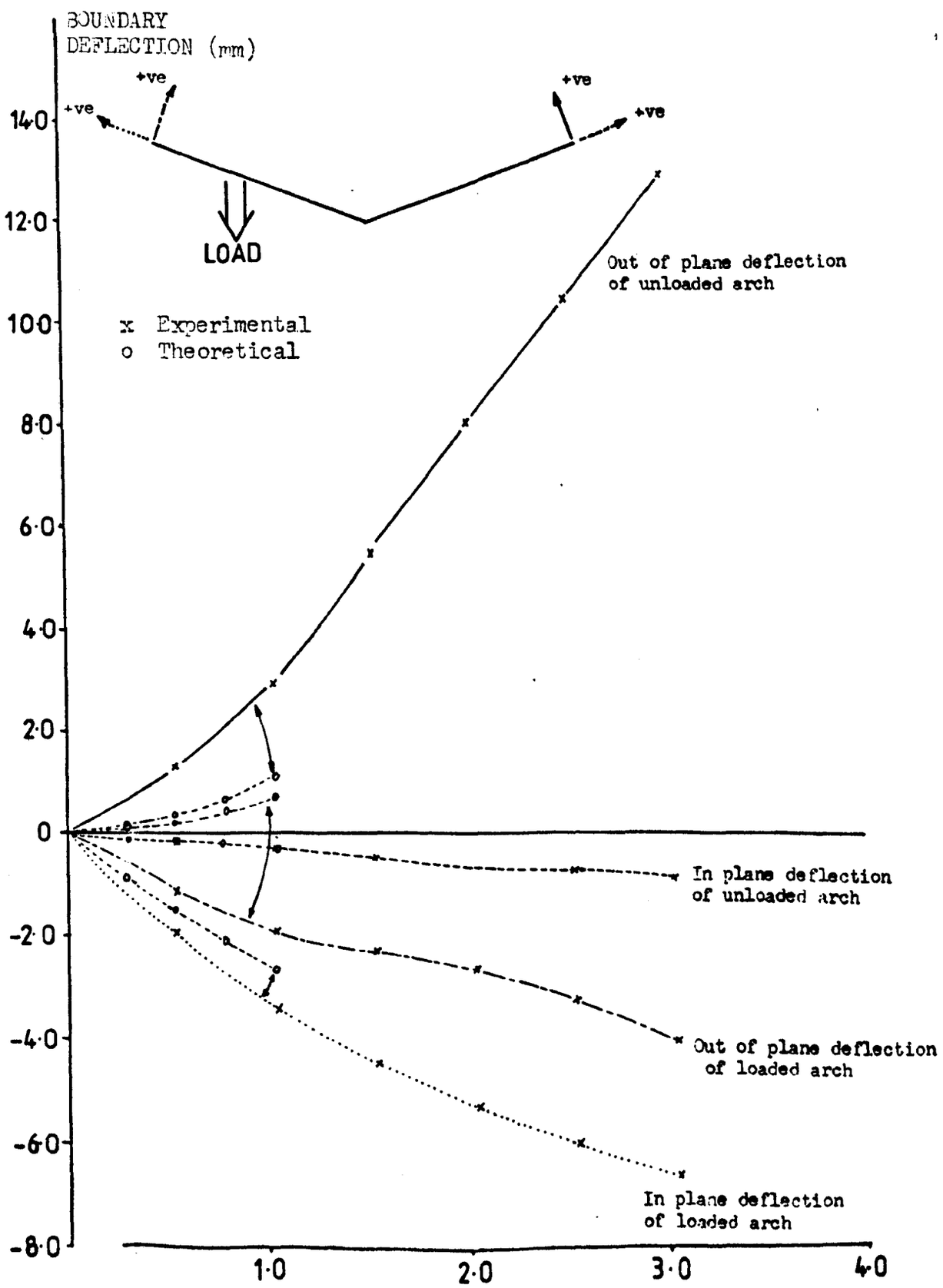

FIG 5.28

IN PLANE AND OUT OF PLANE DEFLECTIONS OF BOUNDARY RING BEAM AGAINST APPLIED LOAD FOR LOAD CASE 4

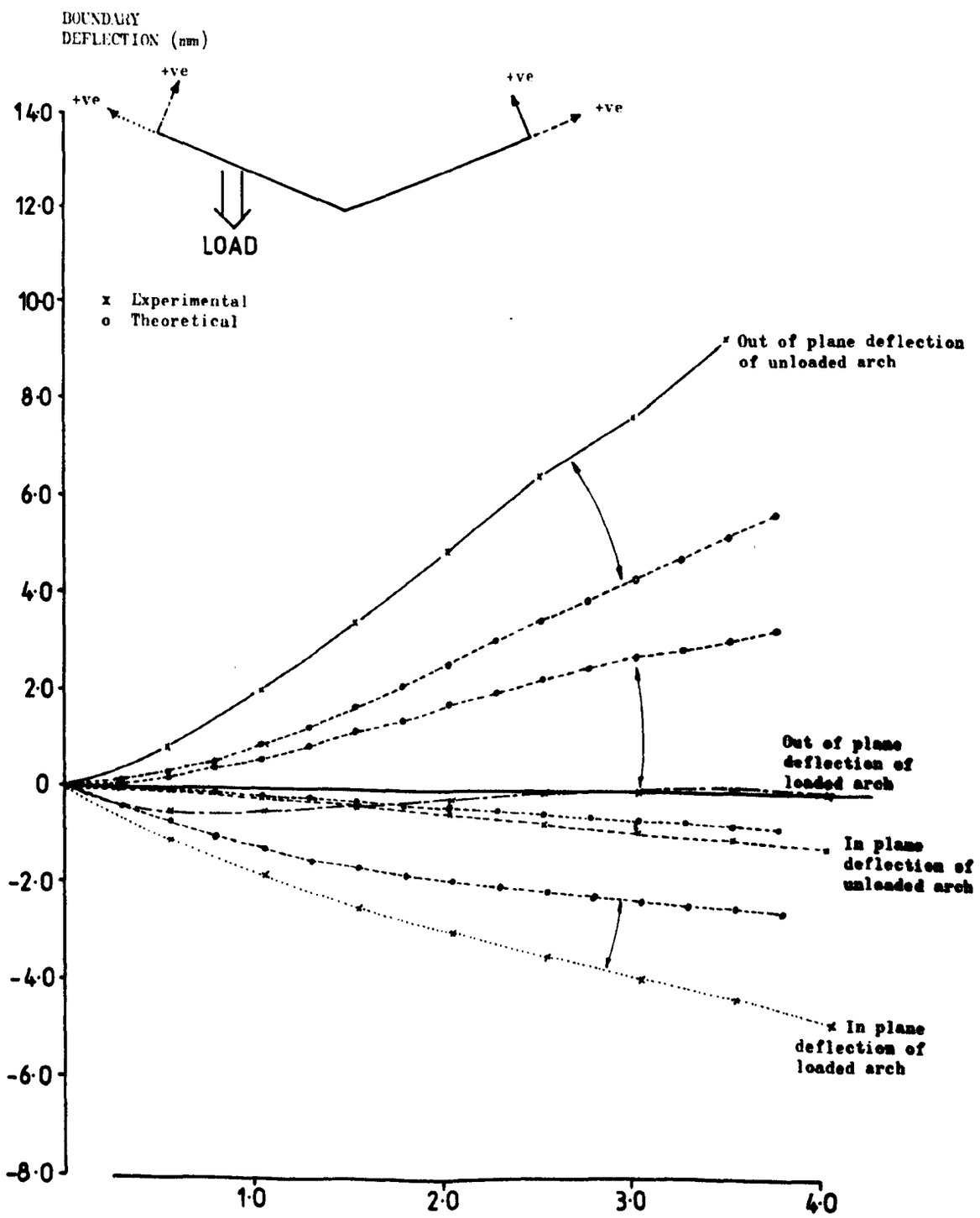

It was not possible to measure the internal deflections and cable tensions in internal segments due to lack of time. Theoretical deflections are available from the anlaysis. Fig. 5.29 shows a plan view of the net with points of equal displacement in the z direction along the cable elements joined to form linearly interpolated "deflection contours".

FIG 5.29

DEFLECTION CONTOURS AT 5mm INTERVALS FOR LOAD CASE 3

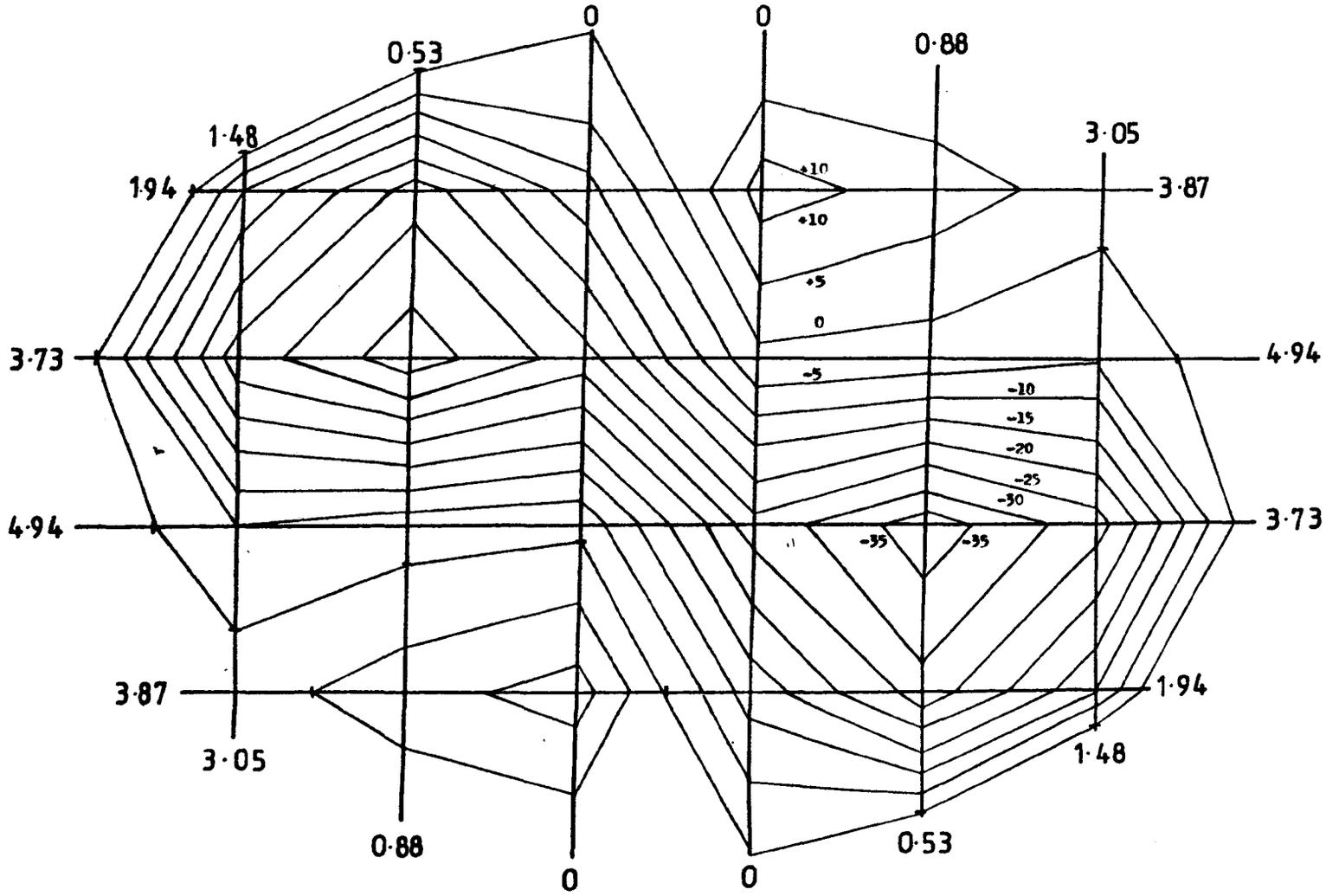

CHAPTER 6

CONCLUSIONS

6.0 Introduction

A general rigorous theoretical analysis of geometrically non-linear two and three dimensional pretensioned cable structures has been presented. The theory has been compared with the measured behaviour of two model structures and with some reservations is thought to be substantially confirmed.

The experiments were designed to provide a comprehensive test of the theory having to discriminate between two different non-linear contributions.

6.1 Theoretical Analysis

Equilibrium equations for cable member and joints have been formulated. It has been shown that previous analyses are internally inconsistent in the approximations neglecting higher order terms of the relative displacement vector $\delta\underset{\sim}{u}_{ij}$.

Gradient methods have been used for the solution of the equilibrium equations and in common with Buchholdt (6.1) the conjugate gradients method of minimisation has been found to be the most ecomonic. Two important differences from the general conjugate gradients algorithm have been introduced. Scaling of the total potential energy "surface" and a new process for obtaining the initial solution have been shown to have considerable computational advantage. With these modifications it appears that the equilibrium (minimum energy) config-

uration can be obtained with rapidly convergent processes in the wide range of problems tested and the numerical difficulties reported elsewhere appear to be totally overcome.

For some structures and some load cases the additional terms that follow from the rigorous treatment adopted here have as great an effect upon the degree of non-linearity as the earlier incorrect treatment has on the departure from the linearity. The rigorous analysis does not lead to computational problems and in all of the iterative regimes followed convergence was very similar to that for the incomplete terms used by Buchholdt. (Appendix 6.1)

In extending the analysis to space structures with flexible boundaries iterative methods were chosen to portray the interaction between cable net and non-rigid elastic boundary structure. Møllmann (6.2), in the only reported anlaysis of fully flexible boundaries, encountered non-convergence for significant lack of rigidity in the boundary. Simple use of under relaxation has been shown to give useful results. An optimum relaxation factor was obtained for one load configuration, larger factors lead to non-convergence. This relaxation factor was used successfully for other load configurations but may not necessarily still be the optimum. Convergence was lost when a significant part of the structure became slack.

6.2 Prestressed Cable Models

There are two innovations in the measurement techniques used in the model cable truss experiments. The use and accuracy of a simple photographic method of deflection measurement is carefully justified. In the unsymmetrically loaded truss the theoretical and measured deflections which agree to within 2% are believed to be

experimentally accurate to 1.5%.

The vibrating wire tension measuring system has been developed from previously described use and the objections of earlier workers have been overcome. The calibration tests established an accuracy of 0.1%. Of those cable lengths which exhibited significant change in force under load the difference between theoretical and practical results was as low as 1%. Where the agreement is poorer this is almost entirely associated with the difficulty of getting an exact initial shape.

It has been shown from the two load cases applied that the degree of geometrical non-linearity in the response is strongly governed by the nature of the loading. For a uniform loading the change in the hanger forces with load is almost linear whereas for a non-symmetrical loading it is considerably non-linear. The difference in response is illustrated by the respective changes in slope in the graph of hanger force against applied load, 15 %for the uniform loading, 150% for the non-uniform.

Earlier experiments on three-dimensional net structures have retained fixed boundary points which was thought to be unrepresentative of the structural options available. A comparison between theory and experiment for a cable net with totally flexible curved boundary elements has not been published before. The agreement between results depended upon the type of loading. Variations in the results appeared likely to reflect a lack of precision with which the flexible boundary was anchored. On reflection a completely three-dimensional fixity is perhaps very difficult to achieve at modest cost in experimental work.

The practical response of the net to gravity loading has been accurately predicted by the theory for the asymmetrical load case. Cable tensions agree to within 5% boundary deflections to within 3%. This loading produces the highest degree of non-linear behaviour. For the uniform loading in contrast with the other results the predicted response has not been achieved to any degree of accuracy. It is thought that a lack of fixity at the ring beam springings may be the cause of this discrepancy. With more time available a systematic search for the source of the error would have been undertaken. By measuring internal cable forces, equilibrium at node positions could be checked. The point of fixity for the boundary ring beams could be altered in the theoretical analysis and a revised anchorage block design could have been developed to provide greater fixity at the beam springings.

Summary

It is felt that the main aims of the work have been achieved. A general algorithm for the analysis of geometrically non-linear cable structures has been presented and shown to be effective for different types of pretensioned cable structure. Precise and accurate measurement techniques have been developed and applied to two and three dimensional model structures. The non-linear response of these structures to non-symmetrical loading has been accurately predicted.

There are a number of areas where it is felt that further work would be of value, these are now briefly discussed.

6.3 Suggestions for Further Work

In the analysis of space structures there are a number of areas for further study. A systematic algorithm for the accommodation of flexible boundaries in an optimum way would be useful, but exploring

the numerical characteristics of a representative range of problems could be computationally expensive. Also it has been noted that experimental cable equilibrium positions with many slack members have been obtained for loadings well beyond the breakdown of the best minimum search techniques. This is not seen as a practical limitation since the models at such loadings exhibited considerable vibration effects with low damping, but further work might increase the understanding of the nature of the minimum energy surface.

Experimentally the difficulty of fixity and in particular its effect upon the establishment of a good "initial form" for the models would merit further consideration. An economic and accurate method of three-dimensional displacement measurement is required for full verification of the non-linear theory. Lack of time prevented the formation of some trigonometrical methods using precision surveying equipment which can be expected to give adequate accuracy.

The general non-linear theory of large displacements could profitably be extended to contain general loads along cable members including the effect of self weight between node points. Material non-linearity could also be incorporated without difficulty. In the investigation of reasonably sized models with significant pretensioning the effect of cable self weight is unlikely to be measurable.

REFERENCES

1.1 Steinman, D. B. 'Famous Bridges of the World', Dover Publications, New York, 1953.

1.2 Jowerth, D. "Forspand hangkonstrukion met mot varandra spanda linor", Byggmastaren, 1959. nr 10 pp 223-236.

1.3 Tsuboi, Y and Kawaguchi, M "The Analysis and Design of a Suspension Roof Stucture", International Conference on Space Structures, University of Surrey, 1966.

1.4 Tietz, S. "Masted Structures", Building 20 Nov. 1981, pp 32-34.

1.5 Otto, F. 'Tensile Structures' Vol 2 Cable Structures, The M.I.T. Press 1969.

1.6 Siev, A. "A General Analysis of Prestressed Nets", I.A.B.S.E. Vol. 23, 1963.

1.7 Møllmann, H. and Mortensen "The Analysis of Prestressed Suspended Roofs", International Conference on Space Structures, University of Surrey, 1966.

1.8 Møllmann, H. 'Analysis of Hanging Roofs by Means of the Displacement method', Polyteknisk Forlag, Lyngby, 1974.

1.9 Barnes, M. R. "Dynamic Relaxation Analysis of Tension Networks", International Conference on Tension Roof Structures, P. C. L. London, 1974.

1.10 Day, A. S. "An Introduction to Dynamic Relaxation", The Engineer, 1965, pp 218-221,

1.11 Otter, J. R. H. "Dynamic Relaxation", I.C.E. Proceedings, Vol 35, Dec. 1966, pp 633-656.

1.12 Reid, J.K. "On the Method of Conjugate Gradients for the Solution of Large Sparse Systems of Linear Equations". (Oxford Conf.). Ed. J.K. Reid, Acedemic Press, London 1971 pp 231-254.

1.13 Buchholdt, H. A. "A Non-Linear Deformation Theory Applied to Two-Dimensional Pre-Tensioned Cable Assemblies", Proc. I.C.E. Vol 42, Jan 1969, pp 129-41.

1.14 Fletcher, R. and Reeves, C. M. "Function Minimisation by Conjugate Gradients", Computer Journal 1964, 7, No. 2 pp 149-153.

1.15 Nooshin, H. and Butterworth, J. W. "Experimental Study of A Prestressed Cable Roof", International Conference on Tension Roof Structures, P.C.L. London, 1974.

1.16 Gallo-Curcio, A and Piccarreta, F. "Experimental Tests on a Hanging Roof Model of the New Palasport in Milan", International Conference on Tension Roof Structures, P.C.L. London 1974.

1.17 Krishna, P. "Experiments on the Wire Model of a Suspended Cable Structure", Journal of the Inst. of Engineers (India), Vol.68, Part CI3, Jan. 1968.

1.18 Poskitt, T. J. "Numerical Solution of Non-Linear Structures", Journal of the Structural Division, Proc. of A.S.C.E., Aug. 1967, pp 69-94.

1.19 Buchholdt, H. A. and McMillan, B. R. "A Non-Linear Vector Method For the Analysis of Vertically and Laterally Loaded Cables and Cable Assemblies", Proc. I.C.E., 1973, pp 211-227.

1.20 Buchholdt, H. A. "Pretensioned Cable Girders", Proc. I.C.E. Vol 45, Mar. 1970, pp 453-469.

1.21 Foster, E. P. and Beaufait, F. W. "Theoretical and Experimental Analysis of Cable Net Roof Systems with Precast Panels", International Conference on Tension Roof Structures, P.C.L. London, 1974.

1.22 Buchholdt, H. A., Das, N. K. and Al-Hilli, A. J. "A Gradient Method for the Analysis of Cable Structures with Flexible Boundaries", International Conference on Tension Roof Structures, P.C.L. London, 1974.

1.23 Siev, A. "Prestressed Suspended Roofs Bounded by Main Cables", International Association for Bridge and Structural Engineering, Vol. 27, 1967, pp 171-186.

1.24 Krishna, P. and Agarwal, T. P. "Study of Suspended Roof Model", Journal of the Structural Division Proc. A.S.C.E. June 1971.

2.1 Buchholdt, H. A. "A Non-Linear Deformation Theory Applied to Two-Dimensional Pre-tensionsed Cable Assemblies", Proc. I.C.E., Vol. 42, Jan. 1969, pp 129-141.

2.2 Vilnay, O. "Structures Made of Infinite Regular Tensegric Nets", Bulletin Int. Assoc. for Shell and Spatial Structures, Vol. 18 : 63, April 1977, pp 51-57.

2.3 Booth, A. D. "An Application of the Method of Steepest Descent to the Solution of Non-Linear Simul-

taneous Equations", Quarterly Journal of Mechanics and Applies Mathematics, Vol. 2, 1949, pp 460-468.

2.4 Hestenes, M. R. and Stiefel, E. "Method of Conjugate Gradients for Solving Linear Systems", Journal of Research of the National Bureau of Standards, B, Vol. 49, 1952, pp 409-436.

2.5 Fletcher, R. and Reeves, C. M. "Function Minimisation by Conjugate Gradients", Computer Journal 1964, 7, No. 2, pp 149-153.

2.6 Argyris, J. H. Angelopoulos, T. and Bichat, B. "A General Method for the Shape Finding of Light Weight Tension Structures", International Conference on Tension Roof Structures. P.C.L. London April, 1974.

2.7 Livesley, R. K. "Matrix Methods of Structural Analysis", Pergamon Press Ltd., 1964.

2.8 Poskitt, T. J. Discussion of paper 7153, "A Non-Linear Deformation Theory Applied to Two-Dimensional Pretensioned Cable Assemblies", by H. A. Buchholdt. Proc. I.C.E. Vol. 43, May, 1969, pp 665-674.

2.9 Buchholdt, H. A. and McMillan, B. R. "Iterative Methods for the Solution of Pre-Tensioned Cable Structures and Pin-jointed Assemblies Having Significant Geometrical Displacements", Proc. 1971 IASS Pacific Symposium, Part II on Tension Structures and Space Frames, Tokyo and Kyoto, pp 306-316.

3.1 Krishna, P. "Experiments on the Wire Model of a Suspended Cable Structure", Journal of the Inst. of Eng. (India) Vol. 68, Part CI3, Jan. 1968.

3.2 Nooshin, H. and Butterworth, J. W. "Experimental Study of a Pre-Stressed Cable Roof", International Conference on Tension Roof Structures, P.C.L., London April 1974.

3.3 Parrot, L. J. "The Construction and Stability of a Surface Mounted Vibrating Wire Strain Gauge", 'Strain', Oct. 1973, pp146-148.

3.4 Mainstone, R. J. "Vibrating Wire Strain Gauge for Use in Long Term Tests on Structures", Engineering Vol. 176, July 1953, pp 153-156.

3.5 Atkinson, K. B. "The Measurement of Models With Particular Reference to a Suspended Roof Structure", Photogrammetric Record 1972, 7(39) pp 334-337.

3.6 Donnell, L. H. 'Beams, Plates and Shells', McGraw-Hill, 1976.

4.1 Krishna, P. "Experiments on the Wire Model of a Suspended Cable Structure", Journal of the Inst. of Engineers (India), Vo. 68, Part CI3 Jan. 1968.

4.2 Poskitt, T. J. "Numerical Solution of Non-Linear Structures", Journal of the Structural Division, Proc. of A.S.C.E., Aug. 1967, pp 69-94.

4.3 Buchholdt, H. A. and McMillan, B. R. "A Non-Linear Vector Method for the Analysis of Vertically and Laterally Loaded Cables and Cable Assemblies", Proc. I.C.E., 1973, pp 211-227.

4.4 Buchholdt, H. A., "Pretensioned Cable Girders", Proc. I.C.E., Vol. 45, Mar. 1970, pp 453-469.

5.1 Foster, E. P. and Beaufait, F. W. "Theoretical and Experimental Analysis of Cable Net Roof Systems with Precast Panels", International Conference on Tension Roof Structures, P.C.L., London, 1974.

5.2 Barnes, M. R. "Dynamic Relaxation Analysis of Tension Networks", International Conference on Tension Roof Structures, P.C.L. London, 1974.

5.3 Siev, A. "Prestressed Suspended Roofs Bounded by Main Cables", International Association for Bridge and Structural Engineering, Vol. 27, 1967, pp 171-186.

5.4 Krishna, P. and Agarwal, T. P. "Study of Suspended Roof Model", Journal of the Structural Division Proc. A.S.C.E. June 1971.

5.5 Møllmann, H. 'Analysis of Hanging Roofs by Means of the Displacement Method' Polyteknisk Forlag, Lyngby 1974.

6.1 Buchholdt, H. A., Das, N. K. and Al-Hilli, A. H. "A Gradient Method for the Analysis of Cable Structures with Flexible Boundaries", International Conference on Tension Rock Structures, P.C.L., London, 1974.

6.2 Møllmann, H. 'Analysis of Hanging Roofs by Means of the Displacement Method', Polyteknisk Forlag, Lyngby 1974.

APPENDIX 2.1

Stiffness Matrix for a Flexural Beam Element

Consider the equilibrium of a rigid straight member of uniform cross-section. It is assumed that the member obeys Hooke's Law and that linear theory applies. The beam element (Fig. A2.1) can be acted upon by a series of loadings.

$\underset{\sim}{P} = [P_x, P_y, P_z, M_x, M_y, M_z]^T$ which cause corresponding displacements $\underset{\sim}{d}$ $[d_x, d_y, d_z, \theta_x, \theta_y, \theta_z]^T$

For a beam element with end 1 and 2 the displacement equations may be written in the generally accepted form.

$$\underset{\sim}{P}_1 = k_{11}\,\underset{\sim}{d}_1 + k_{12}\,\underset{\sim}{d}_2$$

$$\underset{\sim}{P}_2 = k_{21}\,\underset{\sim}{d}_1 + k_{22}\,\underset{\sim}{d}_2$$

where $k_{11} =$

$$\begin{bmatrix} \frac{EA}{L} & 0 & 0 & 0 & 0 & 0 \\ 0 & \frac{12EI_z}{L^3} & 0 & 0 & 0 & \frac{6EI_z}{L^2} \\ 0 & 0 & \frac{12EI_y}{L^3} & 0 & \frac{-6EI_y}{L^2} & 0 \\ 0 & 0 & 0 & \frac{GJ}{L} & 0 & 0 \\ 0 & 0 & \frac{-6EI_y}{L^2} & 0 & \frac{4EI_y}{L} & 0 \\ 0 & \frac{6EI_z}{L^2} & 0 & 0 & 0 & \frac{4EI_z}{L} \end{bmatrix}$$

FIG A2.1

BEAM ELEMENT

LOAD COMPONENTS

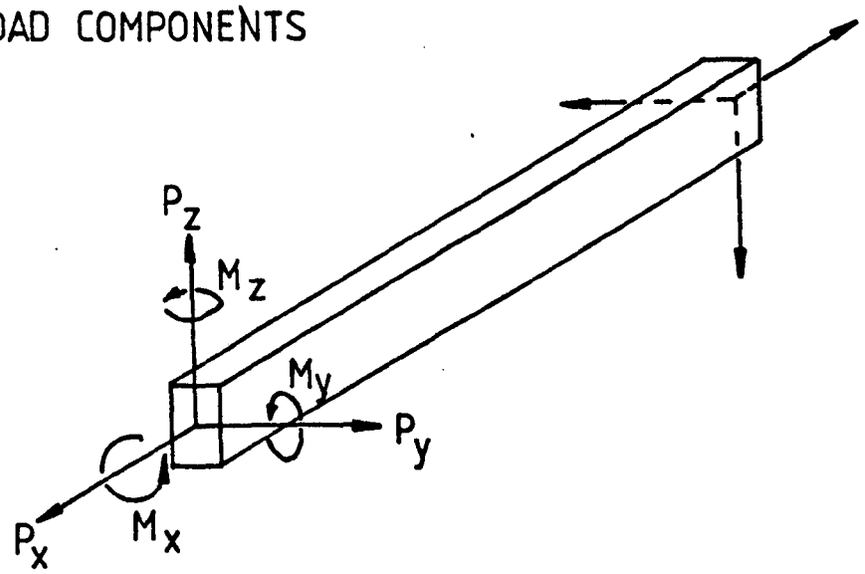

DISPLACEMENT COMPONENTS

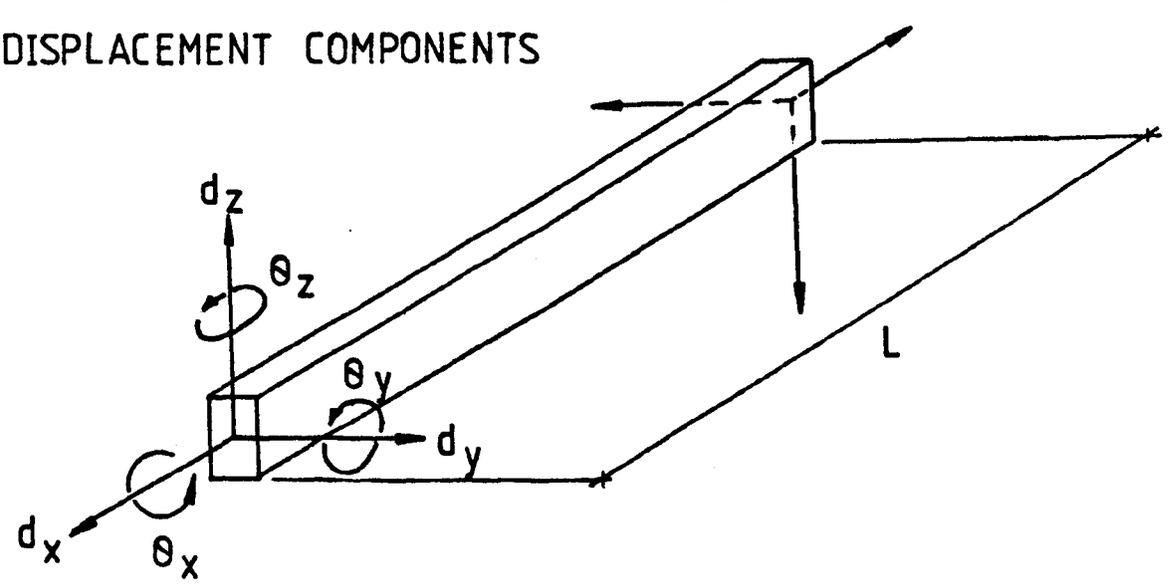

SECTION PROPERTIES

A CROSS SECTIONAL AREA
E YOUNG'S MODULUS
I SECOND MOMENT OF AREA
J POLAR SECOND MOMENT OF AREA
G SHEAR MODULUS

$$k_{12} = k_{21}^{T} \begin{bmatrix} -\frac{EA}{L} & 0 & 0 & 0 & 0 & 0 \\ 0 & \frac{-12EI_z}{L^3} & 0 & 0 & 0 & \frac{6EI_z}{L^2} \\ 0 & 0 & \frac{-12EI_y}{L^3} & 0 & \frac{-6EI_y}{L^2} & 0 \\ 0 & 0 & 0 & \frac{-GJ}{L} & 0 & 0 \\ 0 & 0 & \frac{6EI_y}{L^2} & 0 & \frac{2EI_y}{L} & 0 \\ 0 & \frac{-6EI_z}{L^2} & 0 & 0 & 0 & \frac{2EI}{L} \end{bmatrix}$$

$k_{22} = k_{11}$ with off diagonal signs reversed.

APPENDIX 3.1

Natural Frequency of a Taut Stiff String with Encastre Ends

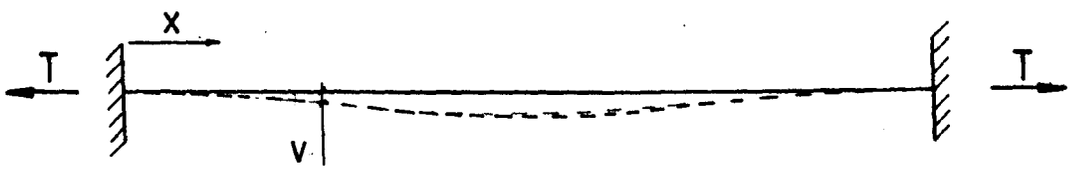

Consider an element of the displaced string dx

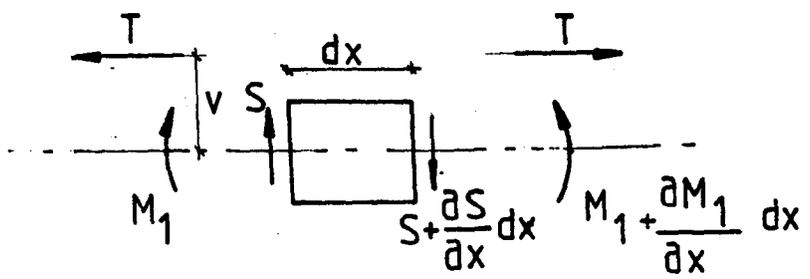

Displacement v(x) transverse

Shear force $S = \frac{\partial M_1}{\partial x}$ (1)

Moment curvature relation $M_T = M_1 - T.v = -EI \frac{\partial^2 v}{\partial x^2}$ (2)

Transverse force on an element $\frac{\partial S}{\partial x} = \rho A \frac{\partial^2 v}{\partial t^2}$ (3)

Where EI is wire stiffness, ρ wire density A is cross section area.

Differentiating equation (1) with respect to x and substituting into (2) and (3) gives

$$\frac{\partial S}{\partial x} = \frac{\partial^2 M_1}{\partial x^2} = -EI \frac{\partial^4 v}{\partial x^4} + T \frac{\partial^2 v}{\partial x^2} = \rho A \frac{\partial^2 v}{\partial t^2} \quad (4)$$

$$\therefore \quad \rho A \frac{\partial^2 v}{\partial t^2} + EI \frac{\partial^4 v}{\partial x^4} - T \frac{\partial^2 v}{\partial x^2} = 0 \quad (5)$$

Note at any section there are two contributions to bending moment.

1. $M_1(x)$ due to the distributed transverse inertial force of

$$\rho A \frac{\partial^2 v}{\partial t^2} \text{ per unit length}$$

2. $M_2(x) = -Tv$ due to the wire tension.

For general end conditions the solution of equation (5) is of the form

$$v = B\, e^{rx} \sin(wt + \alpha)$$

Which gives $$\rho\frac{Aw^2}{EI} + r^4 - \frac{Tr^2}{EI} = 0 \qquad (6)$$

Solving the quadratic in r^2 gives

$$r^2 = \frac{T}{2EI} \pm \left[\left(\frac{T}{2EI}\right)^2 + \rho\frac{Aw^2}{EI}\right]^{\frac{1}{2}}$$

Thus

$$v = [B_1 \sinh r_1 x + B_2 \cosh r_1 x + B_3 \sin\lambda x + B_4 \cos\lambda x] \sin(wt + \alpha) \qquad (7)$$

Where

$$r_1 = \left[\left\{\left(\frac{T}{2EI}\right)^2 + \rho\frac{Aw^2}{EI}\right\}^{\frac{1}{2}} + \frac{T}{2EI}\right]^{\frac{1}{2}} \qquad (8a)$$

$$\lambda = \left[\left\{\left(\frac{T}{2EI}\right)^2 + \rho\frac{Aw^2}{EI}\right\}^{\frac{1}{2}} - \frac{T}{2EI}\right]^{\frac{1}{2}} \qquad (8b)$$

To solve for the constants B_1, B_2, B_3 and B_4 we make use of the end conditions of the wire.

End conditions into equation (7)

i) $x = 0 \qquad v = 0$

$0 = B_2 + B_4 \qquad \therefore B_4 = -B_2$

ii) $x = 0 \qquad v' = 0$

$$v' = [B_1 r_1 \cosh r_1 x + B_2 r_1 \sinh r_1 x + B_3 \lambda \cos\lambda x - B_4 \lambda \sin\lambda x] \sin(wt + \alpha)$$

$$0 = B_1 r_1 + B_3 \lambda \qquad \therefore B_3 = -B_1 \frac{r_1}{\lambda}$$

iii) $x = \frac{L}{2}$ $v' = 0$

$$0 = B_1 r_1 \cosh r_1 \frac{L}{2} + B_2 r_1 \sinh r_1 \frac{L}{2} - \frac{B_1 r_1 \lambda}{\lambda} \cos\lambda \frac{L}{2} + B_2 \lambda \sin\lambda \frac{L}{2}$$

Multiplying above by r_1^2 gives

$$0 = B_1 (r_1^3 \cosh r_1 \frac{L}{2} - r_1^3 \cos\lambda \frac{L}{2}) + B_2 (r_1^3 \sinh r_1 \frac{L}{2} + \lambda r_1^2 \sin\lambda \frac{L}{2}) \qquad (9)$$

iv) $x = \frac{L}{2}$ $v''' = 0$

$$v''' = B_1 r_1^3 \cosh r_1 x + B_2 r_1^3 \sinh r_1 x - B_3 \lambda^3 \cos\lambda x + B_4 \lambda^3 \sin\lambda x$$

$$0 = B_1 r_1^3 \cosh r_1 \frac{L}{2} + B_2 r_1^3 \sinh r_1 \frac{L}{2} + B_1 r_1 \lambda^2 \cos\lambda \frac{L}{2} - B_2 \lambda^3 \sin\lambda \frac{L}{2}$$

$$0 = B_1 (r_1^3 \cosh r_1 \frac{L}{2} + r_1 \lambda^2 \cos\lambda \frac{L}{2}) + B_2 (r_1^3 \sinh r_1 \lambda \frac{L}{2} - \lambda^3 \sin\lambda \frac{L}{2}) \qquad (10)$$

Subtracting equation (9) from (10) and dividing by r_1^3 gives

$$B_1 (\frac{\lambda^2}{r_1^2} \cos\lambda \frac{L}{2} + \cos\lambda \frac{L}{2}) - B_2 (\frac{\lambda}{r_1} \sin\lambda \frac{L}{2} + \frac{\lambda^3}{r_1^3} \sin\lambda \frac{L}{2}) = 0$$

$$\therefore \frac{B_1}{B_2} = \frac{(\frac{\lambda}{r_1}) \sin\lambda \frac{L}{2} + (\frac{\lambda}{r_1})^3 \sin\lambda \frac{L}{2}}{(\frac{\lambda}{r_1})^2 \cos\lambda \frac{L}{2} + \cos\lambda \frac{L}{2}} = \frac{\lambda}{r_1} \tan\lambda \frac{L}{2} \qquad (11)$$

Multiplying equation (9) by $(\frac{\lambda}{r_1})^2$ and adding to (10) gives

$$0 = B_1 (\frac{\lambda^2}{r_1^2} \cosh r_1 \frac{L}{2} + \cosh r_1 \frac{L}{2}) + B_2 (\frac{\lambda^2}{r_1^2} \sinh r_1 \frac{L}{2} + \sinh r_1 \frac{L}{2})$$

$$\therefore \frac{B_1}{B_2} = - \frac{(\frac{\lambda}{r_1})^2 \sinh r_1 \frac{L}{2} + \sinh r_1 \frac{L}{2}}{(\frac{\lambda}{r_1})^2 \cosh r_1 \frac{L}{2} + \cosh r_1 \frac{L}{2}} = - \tanh r_1 \frac{L}{2} \qquad (12)$$

Combining equations (11) and (12) gives

$$\frac{B_1}{B_2} = \frac{\lambda}{r_1} \tan\lambda\frac{L}{2} = - \tanh r_1 \frac{L}{2}$$

$$\lambda\tan\lambda\frac{L}{2} + r_1\tanh r_1 \frac{L}{2} = 0 \qquad \text{but } r_1 = \left(\lambda^2 + \frac{T}{EI}\right)^{\frac{1}{2}}$$

$$\lambda\tan\lambda\frac{L}{2} + \left(\lambda^2 + \frac{T}{EI}\right)^{\frac{1}{2}} \tanh\underbrace{\left(\lambda^2 + \frac{T}{EI}\right)^{\frac{1}{2}} \frac{L}{2}}_{\gg 1} = 0$$

$$\simeq 1$$

$$\lambda\tan\lambda\frac{L}{2} + \left(\lambda^2 + \frac{T}{EI}\right)^{\frac{1}{2}} = 0$$

APPENDIX 4.1

Tabulated Deflection Results for 2D Cable Truss Experiment

TABLE A4.1

LOAD CASE 1	JOINT NUMBER 1					
LOAD Kg/JOINT	X DEFLECTION (mm)			Y DEFLECTION (mm)		
	TH.	EXP.	ERROR	TH.	EXP.	ERROR
0.0	0.0	0.0	-	0.0	0.0	-
0.4	0.11	-0.49	-0.60	-0.95	-1.47	-0.52
0.8	0.25	-0.98	-1.23	-1.90	-2.45	-0.55
1.2	0.37	0.98	0.61	-2.88	-3.43	-0.55
1.6	0.50	-0.98	-1.48	-3.87	-3.92	-0.05
2.0	0.63	0.98	0.35	-4.87	-5.39	-0.52
	MEAN ERROR		0.85	MEAN ERROR		0.44

TABLE A4.2

LOAD CASE 1	JOINT NUMBER 2					
LOAD Kg/JOINT	X DEFLECTION (mm)			Y DEFLECTION (mm)		
	TH.	EXP.	ERROR	TH.	EXP.	ERROR
0.0	0.0	0.0	-	0.0	0.0	-
0.4	-0.10	0.0	0.10	-0.85	-0.98	-0.13
0.8	-0.21	0.0	0.21	-1.71	-1.96	-0.25
1.2	-0.33	-0.49	-0.16	-2.59	-2.94	-0.35
1.6	-0.44	-0.49	-0.05	-3.48	-3.92	-0.44
2.0	-0.56	-0.98	-0.38	-4.37	-4.90	-0.53
	MEAN ERROR		0.18	MEAN ERROR		0.34

TH. - THEORETICAL
EXP.- EXPERIMENTAL (ACCURACY $\pm$ 0.25 mm)

TABLE A4.3

LOAD CASE 1	JOINT NUMBER 3					
LOAD Kg/JOINT	X DEFLECTION (mm)			Y DEFLECTION (mm)		
	TH.	EXP.	ERROR	TH.	EXP.	ERROR
0.0	0.0	0.0	-	0.0	0.0	-
0.4	0.16	0.0	-0.16	-1.69	-1.47	0.22
0.8	0.31	0.0	-0.31	-3.12	-3.43	-0.31
1.2	0.47	0.0	-0.47	-4.69	-4.41	0.28
1.6	0.63	0.0	-0.63	-6.26	-5.88	0.38
2.0	0.79	0.0	-0.79	-7.83	-8.33	-0.50
	MEAN ERROR	0.47		MEAN ERROR	0.34	

TABLE A4.4

LOAD CASE 1	JOINT NUMBER 4					
LOAD Kg/JOINT	X DEFLECTION (mm)			Y DEFLECTION (mm)		
	TH.	EXP.	ERROR	TH.	EXP.	ERROR
0.0	0.0	0.0	-	0.0	0.0	-
0.4	-0.15	0.0	0.15	-1.62	-0.98	0.64
0.8	-0.29	-0.49	-0.20	-2.96	-2.45	0.51
1.2	-0.45	-0.49	-0.04	-4.45	-4.41	0.04
1.6	-0.60	-0.98	-0.38	-5.94	-6.37	0.43
2.0	-0.75	-0.98	-0.23	-7.43	-7.84	0.41
	MEAN ERROR	0.20		MEAN ERROR	0.41	

TABLE A4.5

LOAD CASE 1	JOINT NUMBER 5					
LOAD Kg/JOINT	X DEFLECTION (mm)			Y DEFLECTION (mm)		
	TH.	EXP.	ERROR	TH.	EXP.	ERROR
0.0	0.0	0.0	-	0.0	0.0	-
0.4	0.16	0.0	-0.16	-2.24	-1.96	0.28
0.8	0.29	0.49	0.20	-4.01	-4.41	0.40
1.2	0.43	0.49	0.06	-6.02	-6.37	0.35
1.6	0.58	0.98	0.40	-8.03	-8.33	0.30
2.0	0.72	0.98	0.26	-10.03	-10.78	0.75
	MEAN ERROR		0.22	MEAN ERROR		0.42

TABLE A4.6

LOAD CASE 1	JOINT NUMBER 6					
LOAD Kg/JOINT	X DEFLECTION (mm)			Y DEFLECTION (mm)		
	TH.	EXP.	ERROR	TH.	EXP.	ERROR
0.0	0.0	0.0	-	0.0	0.0	-
0.4	-0.14	0.0	0.14	-1.95	-1.96	-0.01
0.8	-0.28	-0.49	0.21	-3.88	-3.92	-0.04
1.2	-0.42	-0.49	0.07	-5.83	-5.88	-0.05
1.6	-0.56	-0.49	0.07	-7.76	-8.33	-0.57
2.0	-0.71	-0.98	0.27	-9.70	-10.29	-0.59
	MEAN ERROR		0.15	MEAN ERROR		0.25

TABLE A4.7

LOAD CASE 1	JOINT NUMBER 7					
LOAD Kg/JOINT	X DEFLECTION (mm)			Y DEFLECTION (mm)		
	TH.	EXP.	ERROR	TH.	EXP.	ERROR
0.0	0.0	0.0	-	0.0	0.0	-
0.4	0.10	0.0	-0.10	-2.34	-2.45	-0.11
0.8	0.20	0.0	-0.20	-4.66	-4.90	-0.24
1.2	0.30	0.49	0.19	-6.98	-6.86	0.12
1.6	0.40	0.49	0.09	-9.30	-9.31	-0.01
2.0	0.50	0.49	-0.01	-11.62	-12.74	-1.12
	MEAN ERROR		0.12	MEAN ERROR		0.32

TABLE A4.8

LOAD CASE 1	JOINT NUMBER 8					
LOAD Kg/JOINT	X DEFLECTION (mm)			Y DEFLECTION (mm)		
	TH.	EXP.	ERROR	TH.	EXP.	ERROR
0.0	0.0	0.0	-	0.0	0.0	-
0.4	-0.10	0.0	0.10	-2.28	-1.96	0.32
0.8	-0.20	0.0	0.20	-4.55	-4.41	0.14
1.2	-0.30	0.0	0.30	-6.82	-6.86	-0.04
1.6	-0.40	0.0	0.40	-9.08	-9.31	-0.23
2.0	-0.50	0.0	0.50	-11.33	-12.74	-1.41
	MEAN ERROR		0.30	MEAN ERROR		0.43

TABLE A4.9

LOAD CASE 1	JOINT NUMBER 9					
LOAD Kg/JOINT	X DEFLECTION (mm)			Y DEFLECTION (mm)		
	TH.	EXP.	ERROR	TH.	EXP.	ERROR
0.0	0.0	0.0	-	0.0	0.0	-
0.4	0.04	0.0	-0.04	-2.49	-2.45	0.04
0.8	0.07	0.0	-0.07	-4.97	-4.90	0.07
1.2	0.11	0.0	-0.11	-7.44	-7.35	0.09
1.6	0.14	0.0	-0.14	-9.91	-9.80	0.11
2.0	0.18	0.0	-0.18	-12.37	-13.23	-0.86
	MEAN ERROR		0.11	MEAN ERROR		0.23

TABLE A4.10

LOAD CASE 1	JOINT NUMBER 10					
LOAD Kg/JOINT	X DEFLECTION (mm)			Y DEFLECTION (mm)		
	TH.	EXP.	ERROR	TH.	EXP.	ERROR
0.0	0.0	0.0	-	0.0	0.0	-
0.4	-0.04	0.0	0.04	-2.44	-2.94	-0.50
0.8	-0.07	0.0	0.07	-4.87	-5.39	-0.52
1.2	-0.11	-0.49	-0.38	-7.29	-7.84	-0.55
1.6	-0.14	-0.49	-0.35	-9.70	-10.78	-1.08
2.0	-0.18	-0.49	-0.31	-12.11	-13.72	-1.61
	MEAN ERROR		0.23	MEAN ERROR		0.85

TABLE A4.11

LOAD CASE 1	JOINT NUMBER 11					
LOAD Kg/JOINT	X DEFLECTION (mm)			Y DEFLECTION (mm)		
	TH.	EXP.	ERROR	TH.	EXP.	ERROR
0.0	0.0	0.0	-	0.0	0.0	-
0.4	-0.04	0.0	0.04	-2.49	-2.45	0.04
0.8	-0.07	0.0	0.07	-4.97	-4.90	0.07
1.2	-0.11	0.0	0.11	-7.44	-7.35	0.09
1.6	-0.14	0.0	0.14	-9.91	-10.29	-0.38
2.0	-0.18	0.0	0.18	-12.37	-13.72	-1.35
	MEAN ERROR		0.11	MEAN ERROR		0.39

TABLE A4.12

LOAD CASE 1	JOINT NUMBER 12					
LOAD Kg/JOINT	X DEFLECTION (mm)			Y DEFLECTION (mm)		
	TH.	EXP.	ERROR	TH.	EXP.	ERROR
0.0	0.0	0.0	-	0.0	0.0	-
0.4	0.04	0.0	- 0.04	-2.44	-2.45	-0.01
0.8	0.07	0.0	-0.07	-4.87	-4.90	-0.03
1.2	0.11	0.0	-0.11	-7.29	-7.35	-0.06
1.6	0.14	0.0	-0.14	-9.70	-10.29	-0.59
2.0	0.18	0.0	-0.18	-12.11	-13.23	-1.12
	MEAN ERROR		0.11	MEAN ERROR		0.36

TABLE A4.13

LOAD CASE 1	JOINT NUMBER 14					
LOAD Kg/JOINT	X DEFLECTION (mm)			Y DEFLECTION (mm)		
	TH.	EXP.	ERROR	TH.	EXP.	ERROR
0.0	0.0	0.0	-	0.0	0.0	-
0.4	0.10	-0.49	-0.59	-2.28	-2.45	-0.17
0.8	0.20	-0.49	-0.69	-4.55	-4.90	-0.35
1.2	0.30	-0.49	-0.79	-6.82	-7.35	-0.53
1.6	0.40	0.0	-0.40	-9.08	-8.82	0.26
2.0	0.50	0.0	-0.50	-11.33	-12.74	-1.41
	MEAN ERROR		0.59	MEAN ERROR		0.34

TABLE A4.14

LOAD CASE 1	JOINT NUMBER 16					
LOAD Kg/JOINT	X DEFLECTION (mm)			Y DEFLECTION (mm)		
	TH.	EXP.	ERROR	TH.	EXP.	ERROR
0.0	0.0	0.0	-	0.0	0.0	-
0.4	0.14	0.0	-0.14	-1.95	-1.47	0.48
0.8	0.28	0.0	-0.28	-3.89	-3.92	-0.03
1.2	0.42	0.49	0.07	-5.83	-5.39	0.44
1.6	0.56	0.49	-0.07	-7.76	-7.35	0.41
2.0	0.71	0.98	0.27	-9.70	-9.80	-0.10
	MEAN ERROR		0.17	MEAN ERROR		0.29

TABLE A4.15

LOAD CASE 2	JOINT NUMBER 1					
LOAD Kg/JOINT	X DEFLECTION (mm)			Y DEFLECTION (mm)		
	TH.	EXP.	ERROR	TH.	EXP.	ERROR
0.0	0.0	0.0	-	0.0	0.0	-
0.4	1.05	1.47	0.42	-4.86	-4.90	-0.04
0.8	1.96	2.45	0.49	-9.24	-9.31	-0.07
1.2	2.72	3.43	0.71	-13.00	-12.74	0.26
1.6	3.36	3.92	0.56	-16.23	-15.19	1.04
2.0	3.90	4.90	1.00	-19.08	-19.11	-0.03
	MEAN ERROR	0.64		MEAN ERROR	0.29	

TABLE A4.16

LOAD CASE 2	JOINT NUMBER 2					
LOAD Kg/JOINT	X DEFLECTION (mm)			Y DEFLECTION (mm)		
	TH.	EXP.	ERROR	TH.	EXP.	ERROR
0.0	0.0	0.0	-	0.0	0.0	-
0.4	-1.05	-0.98	0.07	-4.75	-4.90	-0.15
0.8	-1.99	-1.96	0.03	-9.00	-8.82	0.08
1.2	-2.81	-2.94	-0.13	-12.61	-12.74	-0.13
1.6	-3.51	-3.92	-0.41	-15.70	-15.68	0.02
2.0	-4.12	-4.41	-0.29	-18.39	-18.62	-0.23
	MEAN ERROR	0.19		MEAN ERROR	0.12	

TABLE A4.17

LOAD CASE 2	JOINT NUMBER 3					
LOAD Kg/JOINT	X DEFLECTION (mm)			Y DEFLECTION (mm)		
	TH.	EXP.	ERROR	TH.	EXP.	ERROR
0.0	0.0	0.0	-	0.0	0.0	-
0.4	1.44	1.47	0.03	-7.25	-7.35	-0.10
0.8	2.72	2.94	0.22	-13.76	-13.72	0.04
1.2	3.78	3.92	0.14	-19.34	-19.60	-0.26
1.6	4.67	4.41	-0.26	-24.15	-23.52	0.63
2.0	5.43	5.88	0.45	-28.38	-28.91	-0.53
	MEAN ERROR		0.22	MEAN ERROR		0.31

TABLE A4.18

LOAD CASE 2	JOINT NUMBER 4					
LOAD Kg/JOINT	X DEFLECTION (mm)			Y DEFLECTION (mm)		
	TH.	EXP.	ERROR	TH.	EXP.	ERROR
0.0	0.0	0.0	-	0.0	0.0	-
0.4	-1.44	-1.47	-0.03	-7.17	-6.86	0.31
0.8	-2.74	-2.94	-0.20	-13.59	-13.23	0.36
1.2	-3.85	-3.92	-0.07	-19.06	-19.11	-0.05
1.6	-4.80	-4.90	-0.10	-23.77	-24.01	-0.24
2.0	-5.63	-5.39	0.24	-27.88	-27.93	-0.05
	MEAN ERROR		0.13	MEAN ERROR		0.20

TABLE A4.19

LOAD CASE 2	JOINT NUMBER 5					
LOAD Kg/JOINT	X DEFLECTION (mm)			Y DEFLECTION (mm)		
	TH.	EXP.	ERROR	TH.	EXP.	ERROR
0.0	0.0	0.0	-	0.0	0.0	-
0.4	1.50	1.47	-0.03	-7.88	-7.84	0.04
0.8	2.84	2.94	0.10	-14.97	-15.19	-0.22
1.2	3.96	4.41	0.45	-21.07	-21.56	-0.49
1.6	4.91	4.90	-0.01	-26.35	-26.95	-0.60
2.0	5.73	5.88	0.15	-31.01	-31.85	-0.84
	MEAN ERROR	0.15		MEAN ERROR		0.44

TABLE A4.20

LOAD CASE 2	JOINT NUMBER 6					
LOAD Kg/JOINT	X DEFLECTION (mm)			Y DEFLECTION (mm)		
	TH.	EXP.	ERROR	TH.	EXP.	ERROR
0.0	0.0	0.0	-	0.0	0.0	-
0.4	-1.49	-1.47	0.02	-7.81	-8.33	-0.52
0.8	-2.81	-2.94	-0.13	-14.83	-15.19	-0.36
1.2	-3.93	-3.92	0.01	-20.86	-21.56	-0.70
1.6	-4.88	-4.41	0.47	-26.07	-26.95	-0.88
2.0	-5.70	-5.39	0.31	-30.65	-31.85	-1.20
	MEAN ERROR	0.19		MEAN ERROR		0.73

TABLE A4.21

LOAD CASE 2	JOINT NUMBER 7					
LOAD Kg/JOINT	X DEFLECTION (mm)			Y DEFLECTION (mm)		
	TH.	EXP.	ERROR	TH.	EXP.	ERROR
0.0	0.0	0.0	-	0.0	0.0	-
0.4	1.37	1.47	0.10	-6.71	-6.86	-0.15
0.8	2.59	2.45	-0.14	-12.79	-13.23	-0.44
1.2	3.63	3.43	-0.20	-18.07	-18.62	-0.55
1.6	4.52	3.92	-0.60	-22.69	-23.52	-0.83
2.0	5.28	4.90	-0.38	-26.81	-27.44	-0.63
	MEAN ERROR	0.28		MEAN ERROR	0.52	

TABLE A4.22

LOAD CASE 2	JOINT NUMBER 8					
LOAD Kg/JOINT	X DEFLECTION (mm)			Y DEFLECTION (mm)		
	TH.	EXP.	ERROR	TH.	EXP.	ERROR
0.0	0.0	0.0	-	0.0	0.0	-
0.4	-1.34	-1.47	-0.13	-6.65	-6.86	-0.21
0.8	-2.52	-2.45	0.07	-12.68	-13.23	-0.55
1.2	-3.50	-3.43	0.07	-17.90	-18.13	-0.23
1.6	-4.33	-4.41	-0.08	-22.46	-23.03	-0.57
2.0	-5.04	-4.90	0.14	-26.52	-27.44	-0.92
	MEAN ERROR	0.10		MEAN ERROR	0.50	

TABLE A4.23

LOAD CASE 2	JOINT NUMBER 9					
LOAD Kg/JOINT	X DEFLECTION (mm)			Y DEFLECTION (mm)		
	TH.	EXP.	ERROR	TH.	EXP.	ERROR
0.0	0.0	0.0	-	0.0	0.0	-
0.4	1.19	1.47	0.28	-3.70	-3.92	-0.22
0.8	2.26	1.96	-0.30	-7.12	-7.35	-0.23
1.2	3.15	2.94	-0.21	-10.19	-10.29	-0.10
1.6	3.91	3.43	-0.48	-12.47	-13.72	-0.75
2.0	4.57	4.41	-0.16	-15.53	-16.17	-0.64
	MEAN ERROR	0.29		MEAN ERROR	0.39	

TABLE A4.24

LOAD CASE 2	JOINT NUMBER 10					
LOAD Kg/JOINT	X DEFLECTION (mm)			Y DEFLECTION (mm)		
	TH.	EXP.	ERROR	TH.	EXP.	ERROR
0.0	0.0	0.0	-	0.0	0.0	-
0.4	-1.17	-0.98	0.19	-3.64	-3.92	-0.28
0.8	-2.20	-1.96	0.24	-7.02	-7.35	-0.33
1.2	-3.05	-2.94	0.11	-10.03	-9.80	0.23
1.6	-3.77	-	-	-12.75	-	-
2.0	-4.38	-	-	-15.25	-	-
	MEAN ERROR	0.18		MEAN ERROR	0.28	

TABLE A4.25

LOAD CASE 2	JOINT NUMBER 11					
LOAD Kg/JOINT	X DEFLECTION (mm)			Y DEFLECTION (mm)		
	TH.	EXP.	ERROR	TH.	EXP.	ERROR
0.0	0.0	0.0	-	0.0	0.0	-
0.4	1.13	0.49	-0.64	1.21	0.98	-0.23
0.8	2.11	1.47	-0.64	2.13	1.96	-0.17
1.2	2.90	1.96	-0.94	2.72	2.45	-0.27
1.6	3.55	2.45	-1.10	3.02	2.45	-0.57
2.0	4.09	3.43	-0.66	3.11	2.45	-0.66
	MEAN ERROR	0.80		MEAN ERROR	0.38	

TABLE A4.26

LOAD CASE 2	JOINT NUMBER 12					
LOAD Kg/JOINT	X DEFLECTION (mm)			Y DEFLECTION (mm)		
	TH.	EXP.	ERROR	TH.	EXP.	ERROR
0.0	0.0	0.0	-	0.0	0.0	-
0.4	-1.15	-0.98	0.17	1.20	0.49	-0.71
0.8	-2.20	-1.96	0.24	2.12	0.98	-1.14
1.2	-3.09	-2.94	0.15	2.70	1.47	-1.23
1.6	-3.84	-	-	2.99	-	-
2.0	-4.50	-	-	3.06	-	-
	MEAN ERROR	0.19		MEAN ERROR	1.03	

TABLE A4.27

LOAD CASE 2	JOINT NUMBER 13					
LOAD Kg/JOINT	X DEFLECTION (mm)			Y DEFLECTION (mm)		
	TH.	EXP.	ERROR	TH.	EXP.	ERROR
0.0	0.0	0.0	-	0.0	0.0	-
0.4	1.24	0.98	-0.26	4.38	4.41	0.03
0.8	2.30	1.96	-0.34	8.13	8.33	0.20
1.2	3.15	2.70	-0.45	11.08	11.27	0.19
1.6	3.84	3.43	-0.41	13.40	13.72	0.32
2.0	4.41	3.92	-0.49	15.21	15.19	-0.02
	MEAN ERROR	0.39		MEAN ERROR	0.15	

TABLE A4.28

LOAD CASE 2	JOINT NUMBER 14					
LOAD Kg/JOINT	X DEFLECTION (mm)			Y DEFLECTION (mm)		
	TH.	EXP.	ERROR	TH.	EXP.	ERROR
0.0	0.0	0.0	-	0.0	0.0	-
0.4	-1.27	-1.47	-0.20	4.37	3.92	-0.45
0.8	-2.41	-2.45	-0.04	8.11	7.84	-0.27
1.2	-3.39	-3.43	-0.04	11.06	11.27	0.21
1.6	-4.21	-4.41	-0.20	13.36	13.23	-0.13
2.0	-4.93	-4.90	0.03	15.16	15.19	0.03
	MEAN ERROR	0.10		MEAN ERROR	0.22	

TABLE A4.29

LOAD CASE 2	JOINT NUMBER 15					
LOAD Kg/JOINT	X DEFLECTION (mm)			Y DEFLECTION (mm)		
	TH.	EXP.	ERROR	TH.	EXP.	ERROR
0.0	0.0	0.0	-	0.0	0.0	-
0.4	1.34	1.47	0.13	5.87	5.88	0.01
0.8	2.51	2.45	-0.06	10.96	11.27	0.31
1.2	3.45	3.43	-0.02	15.07	15.19	0.12
1.6	4.22	3.92	-0.30	18.37	18.62	0.25
2.0	4.85	4.41	-0.44	21.06	21.56	0.50
	MEAN ERROR		0.19	MEAN ERROR		0.24

TABLE A4.30

LOAD CASE 2	JOINT NUMBER 16					
LOAD Kg/JOINT	X DEFLECTION (mm)			Y DEFLECTION (mm)		
	TH.	EXP.	ERROR	TH.	EXP.	ERROR
0.0	0.0	0.0	-	0.0	0.0	-
0.4	-1.36	-1.47	-0.11	5.87	5.88	0.01
0.8	-2.58	-2.45	0.13	10.95	11.27	0.32
1.2	-3.60	-3.43	0.17	15.05	15.68	0.61
1.6	-4.46	-4.41	0.05	18.34	19.11	0.77
2.0	-5.20	-5.39	-0.19	21.02	21.56	0.54
	MEAN ERROR		0.13	MEAN ERROR		0.45

TABLE A4.31

LOAD CASE 2	JOINT NUMBER 17					
LOAD Kg/JOINT	X DEFLECTION (mm)			Y DEFLECTION (mm)		
	TH.	EXP.	ERROR	TH.	EXP.	ERROR
0.0	0.0	0.0	-	0.0	0.0	-
0.4	1.29	1.47	0.18	5.70	5.88	0.18
0.8	2.42	2.45	0.02	10.66	10.78	0.12
1.2	3.35	3.43	0.08	14.69	14.70	0.01
1.6	4.12	3.92	-0.20	17.97	18.13	0.16
2.0	4.76	4.41	-0.35	20.67	20.58	-0.09
	MEAN ERROR		0.17	MEAN ERROR		0.11

TABLE A4.32

LOAD CASE 2	JOINT NUMBER 18					
LOAD Kg/JOINT	X DEFLECTION (mm)			Y DEFLECTION (mm)		
	TH.	EXP.	ERROR	TH.	EXP.	ERROR
0.0	0.0	0.0	-	0.0	0.0	-
0.4	-1.29	-1.47	-0.18	5.69	5.39	-0.30
0.8	-2.43	-2.94	-0.51	10.66	10.29	-0.37
1.2	-3.38	-3.92	-0.54	14.69	14.70	0.01
1.6	-4.17	-4.90	-0.73	17.97	17.64	-0.33
2.0	-4.84	-5.39	-0.55	20.67	20.58	-0.09
	MEAN ERROR		0.50	MEAN ERROR		0.22

TABLE A4.33

LOAD CASE 2	JOINT NUMBER 19					
LOAD Kg/JOINT	X DEFLECTION (mm)			Y DEFLECTION (mm)		
	TH.	EXP.	ERROR	TH.	EXP.	ERROR
0.0	0.0	0.0	-	0.0	0.0	-
0.4	0.94	1.47	0.53	3.91	3.92	0.01
0.8	1.77	2.45	0.68	7.33	7.35	0.02
1.2	2.45	2.94	0.49	11.12	10.29	-0.83
1.6	3.02	3.43	0.41	12.39	12.25	-0.14
2.0	3.50	3.92	0.42	14.28	14.21	-0.07
	MEAN ERROR	0.51		MEAN ERROR	0.21	

TABLE A4.34

LOAD CASE 2	JOINT NUMBER 20					
LOAD Kg/JOINT	X DEFLECTION (mm)			Y DEFLECTION (mm)		
	TH.	EXP.	ERROR	TH.	EXP.	ERROR
0.0	0.0	0.0	-	0.0	0.0	-
0.4	-0.93	-1.47	-0.54	3.92	3.92	0.0
0.8	-1.74	-2.45	-0.71	7.35	6.86	-0.49
1.2	-2.41	-2.94	-0.53	10.15	9.80	-0.35
1.6	-2.96	-3.43	-0.47	12.44	12.25	-0.19
2.0	-3.42	-4.41	-0.99	14.33	13.72	-0.61
	MEAN ERROR	0.65		MEAN ERROR	0.33	

APPENDIX 4.2

TABULATED TENSION RESULTS FOR 2D CABLE TRUSS EXPERIMENT

TABLE 4.35

Variation of Member (No. 3) Force with Load for Load Case 1			
Applied Load (N/Joint)	MEMBER TENSION (N) Theoretical	Experimental	Error %
0.0	9.807	9.524	-2.88
1.961	10.757	10.455	-2.81
3.923	11.741	11.339	-3.42
5.884	12.713	12.335	-2.97
7.845	13.707	13.204	-3.67
9.807	14.716	14.340	-2.55
11.767	15.641	15.189	-2.89
13.729	16.784	16.266	-3.09
15.691	17.848	17.361	-2.73
17.652	18.910	18.548	-1.91
19.613	19.926	19.785	-0.71

TABLE 4.36

Variation of Member (No. 6) Force with Load for Load Case 1			
Applied Load (N/Joint)	MEMBER TENSION (N) Theoretical	Experimental	Error %
0.0	9.807	9.832	0.67
1.961	10.736	10.874	1.28
3.923	11.719	11.812	0.79
5.884	12.714	12.743	0.23
7.845	13.725	13.718	-0.05
9.807	14.741	14.614	-0.86
11.768	15.771	15.708	-0.40
13.729	16.814	16.625	-1.13
15.691	17.869	17.802	-0.37
17.652	18.934	18.944	0.05
19.613	20.012	20.238	1.13

TABLE 4.37

Variation of Member (No. 9) Force with Load for Load Case 1			
Applied Load (N/Joint)	MEMBER TENSION (N) Theoretical	Experimental	Error %
0.0	9.807	9.157	6.63
1.961	10.840	9.986	7.88
3.923	11.819	11.020	6.76
5.884	12.806	12.043	-5.96
7.845	13.806	13.023	-5.68
9.807	14.818	14.174	-4.35
11.768	15.840	15.071	-4.85
13.729	16.871	16.130	-4.39
15.691	17.911	17.315	-3.33
17.652	18.961	18.426	-2.82
19.613	20.021	19.883	-0.69

TABLE 4.38

Variation of Member (No. 12) Force with Load for Load Case 1			
Applied Load (N/Joint)	MEMBER TENSION (N) Theoretical	Experimental	Error %
0.0	9.807	9.805	-0.02
1.961	10.732	10.714	-0.17
3.923	11.716	11.604	-0.96
5.884	12.712	12.585	-1.00
7.845	13.721	13.626	0.69
9.807	14.742	14.489	1.71
11.768	15.774	15.434	2.16
13.729	16.818	16.425	2.34
15.691	17.873	17.419	2.5
17.652	18.941	18.573	0.69
19.613	20.020	19.882	0.69

TABLE 4.39

Variation of Member (No. 15) Force with Load for Load Case 1			
Applied Load (N/Joint)	MAMBER TENSION (N) Theoretical	Experimental	Error %
0.0	9.807	8.988	8.35
1.961	10.786	9.966	7.6
3.923	11.768	10.892	7.44
5.884	12.763	11.900	6.76
7.845	13.769	12.806	7.00
9.807	14.783	13.888	6.05
11.768	15.809	14.855	6.03
13.729	16.847	15.938	5.40
15.691	17.896	17.043	4.77
17.652	18.956	18.201	3.98
19.613	20.027	19.608	2.09

TABLE 4.40

Variation of Member (No. 6) Force with Load for Load Case 2			
Applied Load (N/Joint)	MEMBER TENSION (N) Theoretical	Experimental	Error %
0.0	9.807	9.853	0.47
1.961	10.832	10.949	1.08
3.923	12.070	12.131	0.51
5.884	13.445	13.514	0.51
7.845	14.921	14.750	-1.14
9.807	16.473	16.391	-0.50
11.768	18.094	17.953	-0.78
13.729	19.754	19.504	-1.27
15.691	21.445	21.111	-1.56
17.652	23.160	22.909	-1.09
19.613	24.893	24.452	-1.77

TABLE 4.41

variation of Member (No. 9) Force with Load for Load Case 2			
Applied Load (N/Joint)	MEMBER TENSION (N) Theoretical	Experimental	Error %
0.0	9.807	9.129	-6.91
1.961	10.939	10.183	-6.91
3.923	12.173	11.385	-6.47
5.884	13.547	12.657	-6.57
7.845	15.019	14.016	-6.67
9.807	16.577	15.460	-6.74
11.768	18.193	17.071	-6.17
13.729	19.850	18.726	-5.66
15.691	21.538	20.255	-5.96
17.652	23.250	21.870	-5.94
19.613	24.980	23.474	-6.02

TABLE 4.42

Variation of Member (No. 12) Force with Load for Load Case 2			
Applied Load (N/Joint)	MEMBER TENSION (N) Theoretical	Experimental	Error %
0.0	9.807	9.805	-0.02
1.961	10.831	10.816	-0.14
3.923	12.069	12.003	-0.55
5.884	13.437	13.359	-0.58
7.845	14.911	14.805	-0.71
9.807	16.460	16.257	-1.23
11.768	18.072	17.823	-1.38
13.729	19.724	19.399	-1.65
15.691	21.408	20.972	-2.04
17.652	23.116	22.654	-2.00
19.613	24.841	24.357	-1.95

APPENDIX 5.1

Boundary Shape of Orthogonal Net for Minimum Bending

(After Möllmann (1.8))

The projected shape of a boundary arch along the line of thrust of the projected boundary forces gives minimum bending in that projected plane. Consider an orthogonal net structure supported by two inclined arches, as in Fig. A5.1, with constant intensity of prestress in each direction

i.e. H_x = constant

H_y = constant

Again refering to Fig. A5.1 consider an element of boundary between point $Q_o(x_o, y_o)$ and some general point $Q(x, y)$. Let the horizontal components of the thrust at Q_o be F_{xo} and F_{yo}. Taking moments about a vertical line through point Q we have

$$H_y \frac{(x - x_o)^2}{2} + H_x \frac{(y - y_o)^2}{2} - F_{yo}(x - x_o) + F_{xo}(y - y_o) = 0 \quad (1)$$

Equation (1) is an equation of an ellipse with axes parallel to the coordinate axes. Defining "a" as the semi axis parallel to the x-axis and "b" as the semi axis parallel to the y-axis it can be shown from equation (1) that the ratio

$$\frac{a}{b} = \sqrt{\frac{H_x}{H_y}} \quad (2)$$

FIG A5.1

BOUNDARY SHAPE OF ORTHOGONAL NET

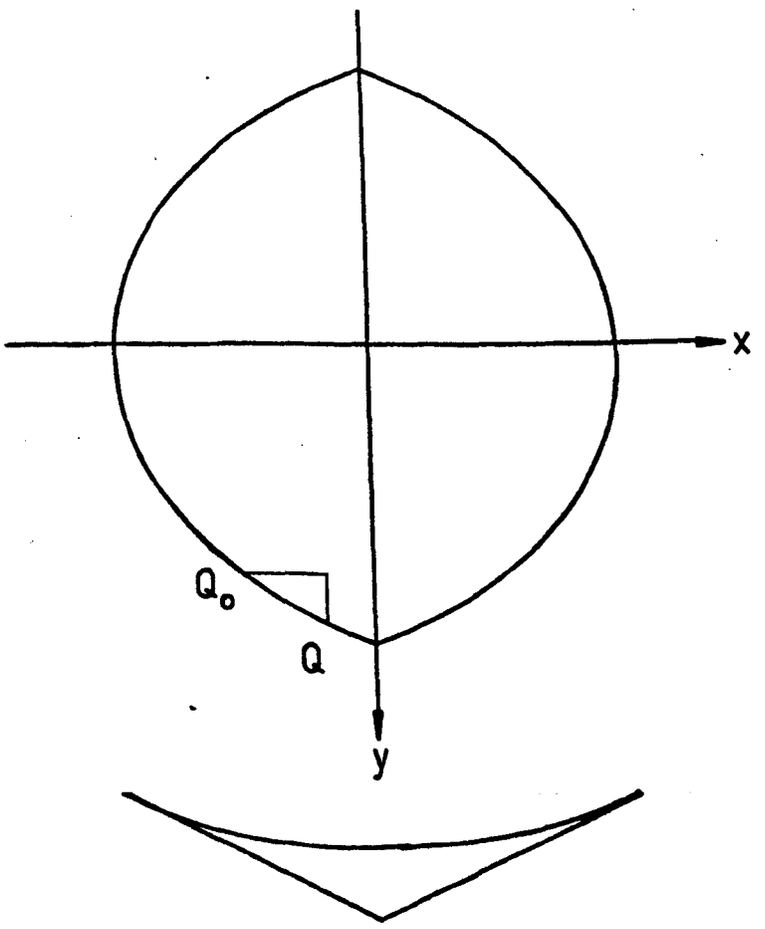

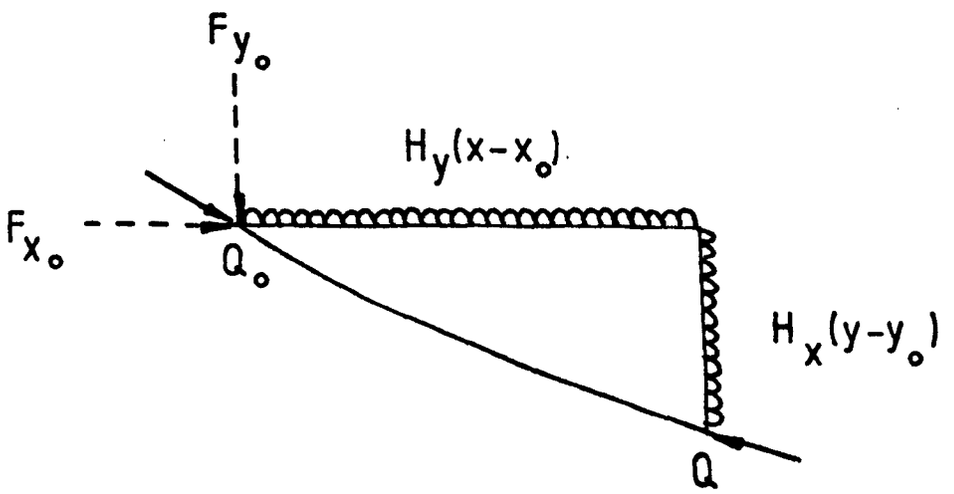

APPENDIX 5.2

TABULATED TENSION RESULTS FOR 3D CABLE NET EXPERIMENT

TABLE A5.1

LOAD CASE 1: CHANGE IN MEMBER TENSION (N)

LOAD N/JOINT	MEMBER NUMBER 1		MEMBER NUMBER 2		MEMBER NUMBER 3		MEMBER NUMBER 7		MEMBER NUMBER 20	
	Th.	Exp.	Th.	Exp.	Th.	Exp.	Th.	Exp.	Th.	Exp.
0.0	0.0	0.0	0.0	0.0	0.0	0.0	0.0	0.0	0.0	0.0
2.94	3.23	-	-12.40	-	-15.03	-	2.53	-	5.67	-
5.39	10.24	18.29	-21.23	-9.56	-26.01	-20.70	6.46	18.67	14.81	27.86
7.84	20.44	-	-29.16	-	-35.97	-	11.53	-	26.88	-
10.30	32.90	45.58	-35.58	-11.45	-45.26	-36.10	17.22	38.98	40.89	63.63
20.10	-	107.48	-	5.55	-	-45.06	-	108.08	-	151.97

TABLE A5.2

LOAD CASE 2: CHANGE IN MEMBER TENSION (N)

LOAD N/JOINT	MEMBER NUMBER 1		MEMBER NUMBER 2		MEMBER NUMBER 3		MEMBER NUMBER 4		MEMBER NUMBER 5	
	Th.	Exp.	Th.	Exp.	Th.	Exp.	Th.	Exp.	Th.	Exp.
0.0	0.0	0.0	0.0	0.0	0.0	0.0	0.0	0.0	0.0	0.0
2.94	1.39	-	-13.27	-	-15.19	-	0.16	-	0.97	-
5.39	5.31	13.30	-23.78	-17.31	-26.92	-23.96	0.99	4.88	2.55	7.67
7.84	11.60	-	-33.75	-	-37.89	-	2.31	-	4.81	-
10.30	19.87	31.36	-43.20	-28.51	-48.23	-42.83	3.93	9.84	7.56	17.22
15.20	-	55.80	-	-34.09	-	-47.65	-	13.38	-	31.43
20.10	-	81.59	-	-33.34	-	-48.37	-	15.70	-	47.00
25.01	-	119.31	-	-32.28	-	-47.16	-	17.61	-	62.85
29.91	-	125.11	-	-27.56	-	-46.40	-	19.15	-	77.47
34.81	-	145.42	-	-21.81	-	-46.77	-	18.29	-	91.86
39.72	-	164.49	-	-14.54	-	-46.72	-	16.74	-	105.66

TABLE A5.2 (cont.)

LOAD CASE 2: CHANGE IN MEMBER TENSION (N)

LOAD N/JOINT	MEMBER NUMBER 6		MEMBER NUMBER 7		MEMBER NUMBER 13		MEMBER NUMBER 20		MEMBER NUMBER 26	
	Th.	Exp.	Th.	Exp.	Th.	Exp.	Th.	Exp.	Th.	Exp.
0.0	0.0	0.0	0.0	0.0	0.0	0.0	0.0	0.0	0.0	0.0
2.94	1.63	-	1.75	-	0.88	-	3.03	-	2.52	-
5.39	4.37	7.53	4.20	10.57	2.63	9.33	7.90	15.88	6.85	13.74
7.84	8.22	-	7.42	-	5.11	-	14.60	-	12.92	-
10.30	12.94	18.22	11.16	23.63	8.10	21.08	22.71	37.87	20.32	34.33
15.20	-	30.67	-	45.35	-	41.00	-	65.72	-	59.30
20.10	-	41.40	-	69.92	-	63.77	-	94.03	-	83.45
25.01	-	54.65	-	93.19	-	85.35	-	112.28	-	111.22
29.91	-	66.38	-	116.07	-	106.74	-	149.07	-	136.08
34.81	-	77.61	-	139.36	-	126.37	-	175.30	-	160.15
39.72	-	87.84	-	158.20	-	146.86	-	200.32	-	183.44

TABLE A5.3

LOAD CASE 3: CHANGE IN MEMBER TENSION (N)

LOAD N/JOINT	MEMBER NUMBER 1			MEMBER NUMBER 2		
	Th.	Exp.	Error	Th.	Exp.	Error
0.0	0.0	0.0	0.0	0.0	0.0	0.0
5.39	5.82	9.11	3.29	-8.42	-2.97	5.45
10.30	18.12	22.16	4.04	-9.25	1.37	10.62
15.20	32.63	34.85	2.22	-6.89	6.31	13.20
20.10	47.59	45.71	-1.88	-3.03	13.93	16.96
25.01	62.47	62.41	-0.06	1.62	21.72	20.10
29.91	77.14	73.54	-3.6	6.73	30.01	23.28
34.81	92.77	91.27	-1.5	11.53	39.84	28.31
39.72	108.15	102.33	-5.82	16.31	48.10	31.79

LOAD CASE 3: CHANGE IN MEMBER TENSION (N)

LOAD N/JOINT	MEMBER NUMBER 3			MEMBER NUMBER 4		
	Th.	Exp.	Error	Th.	Exp.	Error
0.0	0.0	0.0	0.0	0.0	0.0	0.0
5.39	-13.87	-11.24	2.63	-8.63	-6.26	2.37
10.30	-22.60	-18.52	4.08	-12.27	-8.79	3.48
15.20	-30.43	-27.23	3.20	-14.82	-12.02	2.80
20.10	-38.28	-34.85	3.43	-17.27	-14.72	2.55
25.01	-46.33	-42.25	4.08	-19.87	-17.11	2.76
29.91	-54.58	-48.75	5.83	-22.63	-19.41	3.22
34.81	-56.23	-54.29	1.94	-23.22	-21.34	1.88
39.72	-56.23	-54.26	1.97	-23.67	-22.26	1.41

TABLE A5.3 (cont.)

LOAD CASE 3: CHANGE IN MEMBER TENSION (N)

LOAD N/JOINT	MEMBER NUMBER 5			MEMBER NUMBER 6		
	Th.	Exp.	Error	Th.	Exp.	Error
0.0	0.0	0.0	0.0	0.0	0.0	0.0
5.39	-6.66	-1.23	5.43	6.05	9.37	3.32
10.30	-6.03	3.90	9.93	18.23	23.79	5.56
15.20	-2.40	10.04	12.44	32.52	36.13	3.61
20.10	2.51	17.85	15.34	47.23	49.50	2.27
25.01	8.04	26.56	18.52	61.87	62.91	1.04
29.91	13.88	35.72	21.84	76.33	76.75	0.42
34.81	20.57	45.93	25.36	91.78	93.22	1.44
39.72	27.57	54.82	27.25	107.00	104.64	-2.36

LOAD CASE 3: CHANGE IN MEMBER TENSION (N)

LOAD N/JOINT	MEMBER NUMBER 7			MEMBER NUMBER 13		
	Th.	Exp.	Error	Th.	Exp.	Error
0.0	0.0	0.0	0.0	0.0	0.0	0.0
5.39	8.83	14.25	5.42	6.26	12.02	5.76
10.30	24.67	33.82	9.15	19.72	29.46	9.74
15.20	42.76	50.81	8.05	35.42	44.11	8.69
20.10	61.08	72.74	11.66	51.37	62.03	10.66
25.01	79.06	89.29	10.23	67.00	76.25	9.25
29.91	96.57	108.87	12.30	82.17	93.64	11.47
34.81	118.97	128.16	9.19	102.21	112.09	9.88
39.72	142.01	148.44	6.43	122.88	131.21	8.33

TABLE A5.3 (cont.)

LOAD CASE 3: CHANGE IN MEMBER TENSION (N)

LOAD N/JOINT	MEMBER NUMBER 20			MEMBER NUMBER 26		
	Th.	Exp.	Error	Th.	Exp.	Error
0.0	0.0	0.0	0.0	0.0	0.0	0.0
5.39	11.61	17.11	5.5	8.88	14.26	5.38
10.30	31.63	40.16	8.53	26.51	36.24	9.73
15.20	54.47	63.40	8.93	47.05	57.05	10.00
20.10	77.81	85.48	7.67	68.15	77.58	9.43
25.01	100.98	109.01	8.03	89.15	98.91	9.76
29.91	123.83	131.89	8.06	109.86	121.16	11.3
34.81	148.45	158.26	9.81	132.23	146.52	14.29
39.72	172.86	178.60	5.74	154.35	165.96	11.61

TABLE A5.4

LOAD CASE 4: CHANGE IN MEMBER TENSION (N)

LOAD N/JOINT	MEMBER NUMBER 1			MEMBER NUMBER 2		
	Th.	Exp.	Error	Th.	Exp.	Error
0.0	0.0	0.0	0.0	0.0	0.0	0.0
5.39	2.37	4.42	2.05	-9.90	-5.76	4.14
10.30	8.94	13.25	4.31	-13.40	-4.15	9.25
15.20	17.67	21.48	3.81	-12.76	0.0	12.76
20.10	27.21	31.74	4.53	-9.54	7.78	17.32
25.01	36.93	41.77	4.84	-4.74	16.88	21.62
29.91	46.57	51.08	4.51	1.08	25.27	24.19
34.81	56.03	56.67	0.64	7.60	34.98	27.38

LOAD CASE 4: CHANGE IN MEMBER TENSION (N)

LOAD N/JOINT	MEMBER NUMBER 3			MEMBER NUMBER 4		
	Th.	Exp.	Error	Th.	Exp.	Error
0.0	0.0	0.0	0.0	0.0	0.0	0.0
5.39	-14.06	-12.65	1.41	2.03	4.97	2.94
10.30	-23.47	-19.76	3.71	6.11	11.97	5.86
15.20	-30.74	-26.27	4.47	11.27	18.34	7.07
20.10	-36.79	-31.93	4.86	16.72	25.21	8.49
25.01	-42.16	-35.66	6.5	22.09	31.84	9.75
29.91	-47.08	-38.19	8.89	27.27	36.68	9.41
34.81	-51.69	-42.29	9.4	32.19	41.26	9.07

TABLE A5.4 (cont.)

LOAD CASE 4: CHANGE IN MEMBER TENSION (N)

LOAD N/JOINT	MEMBER NUMBER 5			MEMBER NUMBER 6		
	Th.	Exp.	Error	Th.	Exp.	Error
0.0	0.0	0.0	0.0	0.0	0.0	0.0
5.39	2.60	5.21	2.61	2.51	3.71	1.20
10.30	7.90	14.32	6.42	7.89	9.87	1.98
15.20	14.91	23.55	8.94	14.94	16.66	1.72
20.10	22.72	33.61	10.89	22.67	24.40	1.73
25.01	30.86	44.03	13.17	30.59	30.98	0.39
29.91	39.10	54.20	15.10	38.48	37.35	-1.13
34.81	47.35	64.26	16.91	46.26	43.29	-2.97

LOAD CASE 4: CHANGE IN MEMBER TENSION (N)

LOAD N/JOINT	MEMBER NUMBER 7			MEMBER NUMBER 13		
	Th.	Exp.	Error	Th.	Exp.	Error
0.0	0.0	0.0	0.0	0.0	0.0	0.0
5.39	9.26	12.44	3.18	7.05	9.32	2.27
10.30	23.02	28.22	5.2	18.55	24.07	5.52
15.20	39.74	45.26	5.52	32.80	38.83	6.03
20.10	57.64	61.56	3.92	48.12	53.58	5.46
25.01	75.86	78.91	3.05	63.66	69.25	5.59
29.91	94.01	94.90	0.89	79.08	83.74	4.66
34.81	111.96	110.26	-1.7	94.25	96.43	2.18

TABLE A5.4 (cont.)

LOAD CASE 4: CHANGE IN MEMBER TENSION (N)

LOAD N/JOINT	MEMBER NUMBER 20			MEMBER NUMBER 26		
	Th.	Exp.	Error	Th.	Exp.	Error
0.0	0.0	0.0	0.0	0.0	0.0	0.0
5.39	12.69	16.96	4.27	10.76	13.71	2.95
10.30	30.63	38.27	7.64	26.72	31.75	5.03
15.20	51.55	61.11	9.56	45.57	51.32	5.75
20.10	73.36	83.25	9.89	65.11	71.35	6.24
25.01	95.12	103.74	8.62	84.61	90.56	5.95
29.91	116.50	125.29	8.79	103.70	108.70	5.0
34.81	137.40	144.48	7.08	122.25	125.36	3.11

APPENDIX 6.1

Results comparing different analyses of a simple truss structure

The Figure below shows the initial tensile force in each of the cable truss members and the forces applied at each node. Table A 6.1 compares the member forces after the application of the nodal forces for the following cases:

(i) Linear analysis

(ii) Non-linear analysis developed by Buchholdt

(iii) Non-linear analysis using the consistent terms presented in Chapter 2.

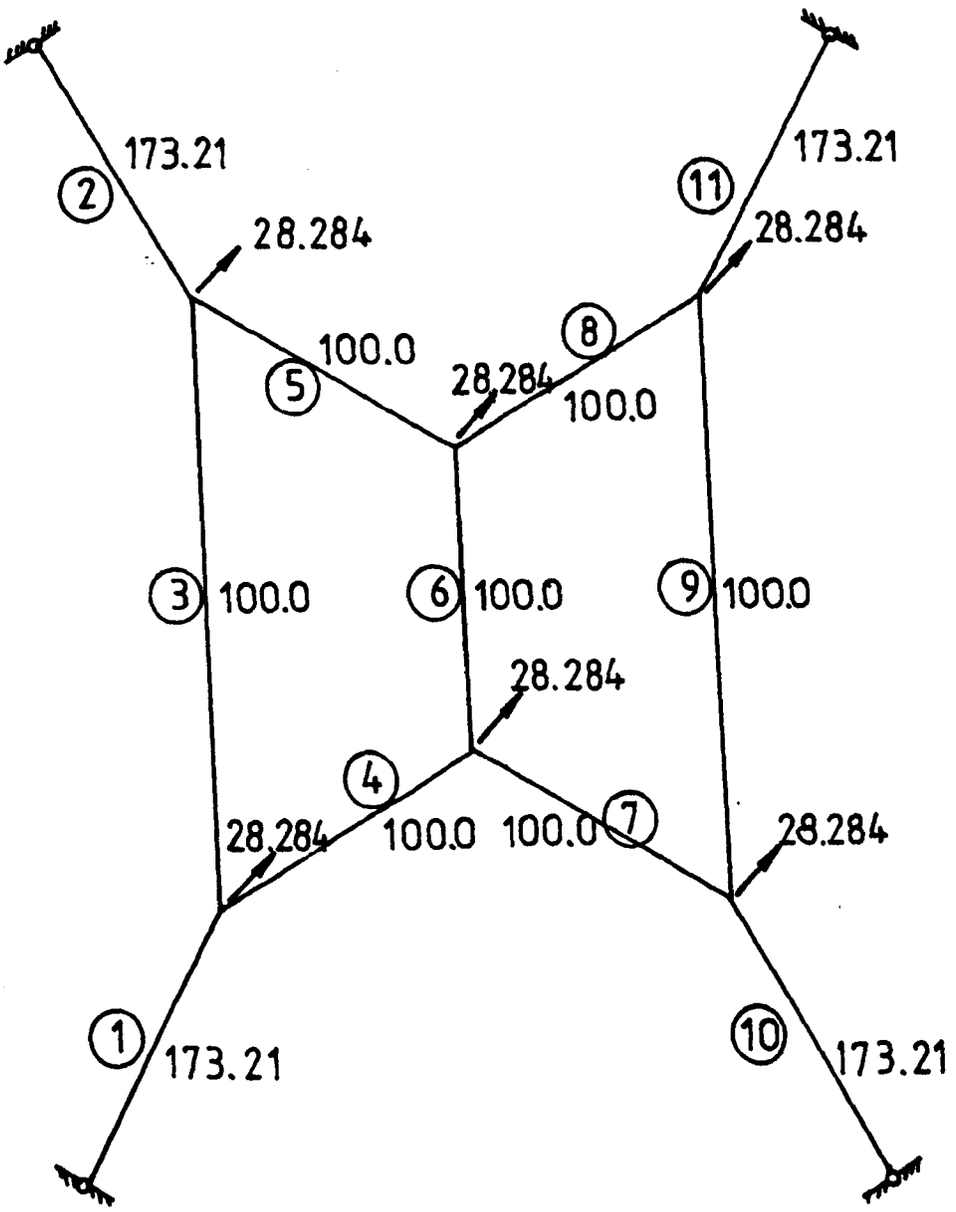

Table A 6.1

Member Number	Member Force (N)		
	Linear	Buchholdt	Thew
1	264.06	263.63	263.13
2	195.10	195.75	195.27
3	141.69	141.28	140.99
4	131.40	132.32	132.07
5	92.01	93.19	92.94
6	100.00	101.28	101.03
7	107.99	108.97	108.72
8	68.60	70.06	69.81
9	58.31	58.22	57.98
10	151.30	152.22	151.80
11	82.35	83.84	83.42